

**AN INVESTIGATION INTO INHIBITION OF
PRECIPITATION IN MIXED ANIONIC
SURFACTANT SYSTEMS**

Atthaphon Maneedaeng

**A Thesis Submitted in Partial Fulfillment of the Requirements for the
Degree of Doctor of Philosophy in Chemical Engineering**

Suranaree University of Technology

Academic Year 2010

การศึกษาการยับยั้งการตกตะกอนของสารลดแรงตึงผิวชนิดประจุลบแบบผสม

นายอรรถพล มณีแดง

วิทยานิพนธ์นี้เป็นส่วนหนึ่งของการศึกษาตามหลักสูตรปริญญาวิศวกรรมศาสตรดุษฎีบัณฑิต

สาขาวิชาวิศวกรรมเคมี

มหาวิทยาลัยเทคโนโลยีสุรนารี

ปีการศึกษา 2553

**AN INVESTIGATION INTO INHIBITION OF PRECIPITATION
IN MIXED ANIONIC SURFACTANT SYSTEMS**

Suranaree University of Technology has approved this thesis submitted in partial fulfillment of the requirements for the Degree of Doctor of Philosophy.

Thesis Examining Committee

(Dr. Terasut Sookkumnerd)

Chairperson

(Assoc. Prof. Dr. Adrian Flood)

Member (Thesis Advisor)

(Assoc. Prof. Dr. Chaiyot Tangsathitkulchai)

Member

(Prof. Dr. Brian Grady)

Member

(Asst. Prof. Dr. Sopark Sonwai)

Member

(Prof. Dr. Sukit Limpijumnong)

Vice Rector for Academic Affairs

(Assoc. Prof. Grp. Capt. Dr. Vorapot Khompis)

Dean of Institute of Engineering

อรรถพล มณีแดง : การศึกษาการยับยั้งการตกตะกอนของสารลดแรงตึงผิวชนิดประจุลบแบบผสม (AN INVESTIGATION INTO INHIBITION OF PRECIPITATION IN MIXED ANIONIC SURFACTANT SYSTEMS) อาจารย์ที่ปรึกษา : รศ. ดร.เอเดรียน ฟลัด, 224 หน้า.

การหลีกเลี่ยงการตกตะกอนของสารลดแรงตึงผิวในอุตสาหกรรมผงซักฟอกถือเป็นหัวใจสำคัญต่อผลลัพธ์ของการทำความสะอาด สมบัติสำคัญอย่างหนึ่งของสารลดแรงตึงผิวชนิดประจุลบที่สามารถยับยั้งประสิทธิภาพของตัวมันเองสำหรับการประยุกต์ใช้งานที่เกี่ยวข้องกับการซักล้างคือ สารลดแรงตึงผิวชนิดประจุลบมีแนวโน้มที่จะตกตะกอนในสารละลายที่มีน้ำเป็นตัวทำละลาย โดยเฉพาะอย่างยิ่งการใช้งานในสถานะน้ำกระด้างซึ่งทำให้เกิดตะกอนโคลสบู อย่างไรก็ตามตัวแปรในด้านความสัมพันธ์เชิงอุณหพลศาสตร์และจลนพลศาสตร์ที่เกี่ยวข้องกับการกระบวนการตกตะกอนของโคลสบู และโดยเฉพาะขอบเขตวิภาคของการตกตะกอนเมื่อใช้สารลดแรงตึงผิวชนิดประจุลบผสมในน้ำกระด้างยังคงมีความสำคัญอย่างมาก แต่ในขณะที่ข้อมูลที่เป็นระบบในด้านความสัมพันธ์เชิงอุณหพลศาสตร์และจลนพลศาสตร์ของการตกตะกอนค่อนข้างมีจำกัดในงานวิจัยทางวิทยาศาสตร์ ดังนั้นเพื่อเป็นการต่อยอดความรู้ความเข้าใจในเรื่องการตกตะกอนของสารลดแรงตึงผิวชนิดประจุลบทั้งในด้านความสัมพันธ์เชิงอุณหพลศาสตร์และจลนพลศาสตร์ ระบบของสารลดแรงตึงผิวชนิดประจุลบแบบผสมสองชนิด ได้ถูกใช้เพื่อศึกษาอย่างเป็นระบบถึงผลกระทบในเชิงเสริมกันของการเพิ่มขึ้นของระยะเวลาในการเหนี่ยวนำการตกตะกอนของสารลดแรงตึงผิวชนิดประจุลบและไอออนประจุสองบวก โดยระบบผสมแบบสองชนิดของโซเดียมโดเดซิลซัลเฟตกับโซเดียมโพร์อ็อกทิลเบนซีนซัลโฟเนต และโซเดียมโดเดซิลซัลเฟตกับโซเดียมเดคซิลซัลเฟต ถูกใช้ในการศึกษาทั้งในเชิงอุณหพลศาสตร์และจลนพลศาสตร์ โดยได้นำทฤษฎีสารละลายปกติ และสมมติฐานการแยกวิภาคเทียมมาใช้ในการหาปริมาณความเข้มข้นของสารลดแรงตึงผิวในวิภาคไมเซลล์และวิภาคมอนอเมอร์ จากผลของการศึกษาเชิงอุณหพลศาสตร์ของการเกิดไมเซลล์แบบผสมแสดงให้เห็นว่าระบบการผสมจะเป็นแบบอุดมคติในระบบผสมของโซเดียมโดเดซิลซัลเฟตกับโซเดียมโพร์อ็อกทิลเบนซีนซัลโฟเนต ในขณะที่ระบบการผสมจะค่อนข้างเป็นแบบไม่อุดมคติในระบบผสมของโซเดียมโดเดซิลซัลเฟตกับโซเดียมเดคซิลซัลเฟต สัดส่วนของการเกาะติดของไอออนประจุตรงข้ามบนพื้นผิวของไมเซลล์ได้ถูกศึกษาผ่านการวัดความเข้มข้นจริง โดยที่สมการสมดุลเคมีระหว่างไอออนประจุตรงข้ามที่เกาะติดและไอออนประจุตรงข้ามที่เป็นอิสระจากไมเซลล์สามารถใช้ในสร้างแบบจำลองสัดส่วนของการเกาะติดที่พื้นผิวของไมเซลล์ของไอออนประจุตรงข้ามได้เป็นอย่างดี นอกจากนี้ข้อมูลทั่วไปของตัวแปรทางอุณหพลศาสตร์ของเกลือแคลเซียมของสารลดแรงตึงผิวชนิดประจุลบได้ถูกศึกษาเพื่อให้เกิดความรู้ความ

เข้าใจที่ดียิ่งขึ้นในกระบวนการการตกตะกอนของสารลดแรงตึงผิวชนิดประจุลบโดยไอออนประจุตรงข้าม ข้อมูลในเชิงอุณหพลศาสตร์นี้สามารถช่วยในการทำนายขอบเขตวิกฤตการตกตะกอนของสารลดแรงตึงผิวชนิดประจุลบกับสารละลายแคลเซียมคลอไรด์ที่ใช้ศึกษาในงานวิจัยนี้ได้ อย่างถูกต้อง ผลของการศึกษาตัวแปรทางอุณหพลศาสตร์ของเกลือแคลเซียมของสารลดแรงตึงผิวชนิดประจุลบทำให้เกิดความเข้าใจที่ดียิ่งขึ้นของแบบจำลองทางอุณหพลศาสตร์ของขอบเขตวิกฤตการตกตะกอนในระบบของสารลดแรงตึงผิวชนิดประจุลบทั้งแบบเดี่ยวและแบบผสม

นอกจากนี้ระยะเวลาในการเหนี่ยวนำการตกตะกอนได้ถูกศึกษาทั้งในระบบของสารลดแรงตึงผิวชนิดประจุลบแบบเดี่ยวและแบบผสมเช่นกัน เพื่อเฝ้าติดตามการเพิ่มขึ้นของระยะเวลาในการเหนี่ยวนำการตกตะกอนในระบบสารลดแรงตึงผิวชนิดประจุลบแบบผสม จากผลการทดลองแสดงให้เห็นว่า การเกิดการยับยั้งการตกตะกอนของสารลดแรงตึงผิวชนิดประจุลบแบบผสม มีสาเหตุส่วนหนึ่งมาจากการลดลงของความเข้มข้นของสารที่จะเกิดการตกตะกอนจากการเปลี่ยนแปลงสัดส่วนความเข้มข้น โดยโมลของสารลดแรงตึงผิวชนิดประจุลบแบบผสม และมีสาเหตุส่วนหนึ่งมาจากการเปลี่ยนแปลงเชิงอุณหพลศาสตร์ของการเกิดไมเซลล์แบบผสมด้วย และระบบของสารลดแรงตึงผิวชนิดประจุลบแบบผสมยังแสดงให้เห็นถึงความสามารถในการเปลี่ยนแปลงของพลังงานบนพื้นผิวของการเกิดนิวคลีออยวิกฤตในทางที่เพิ่มขึ้นที่สัดส่วนส่วนความเข้มข้น โดยโมลช่วงหนึ่งของสารลดแรงตึงสารลดแรงตึงผิวชนิดประจุลบแบบผสม ดังนั้นจากผลการทดลองจะเห็นได้ว่า จะเกิดการยับยั้งการตกตะกอนในระบบสารลดแรงตึงสารลดแรงตึงผิวชนิดประจุลบแบบผสมอย่างชัดเจน โดยเห็นได้จากการเพิ่มขึ้นของระยะเวลาในการเหนี่ยวนำการตกตะกอน

ATTHAPHON MANEEDAENG : AN INVESTIGATION INTO
INHIBITION OF PRECIPITATION IN MIXED ANIONIC SURFACTANT
SYSTEMS. THESIS ADVISOR : ASSOC. PROF. ADRIAN FLOOD, Ph.D.,
224 PP.

SURFACTANT/MIXED ANIONIC SURFACTANTS/PRECIPITATION/
THERMODYNAMICS OF MIXED MICELLIZATION/KINETICS OF MIXD
ANIONIC SURFACTANT PRECIPITATION/INDUCTION TIME

Avoidance of precipitation of surfactants in the detergency industry is especially important for acceptable cleaning results. An important characteristic of anionic surfactants that is deleterious to their use in many detergency applications is their tendency to precipitate from solutions, especially when they are used in hard water, forming soap scum. The thermodynamic and kinetic parameters involved in the precipitation process of the soap scum, and in particular the precipitation boundary as the surfactant is mixed with hard water is still extremely important but these data are quite limited in the scientific literature. Consequently, to extend the understanding of surfactant precipitation, both in the aspects of thermodynamics and kinetics, binary anionic surfactants were used to systematically investigate the synergistic effect to delay the induction time of anionic surfactants precipitated by divalent ions.

The two binary systems; sodium dodecyl sulfate (NaDS)/sodium 4-octylbenzenesulfonate (NaOBS), and NaDS/sodium decyl sulfate (NaDeS) are investigated with respect to thermodynamics and kinetics. The regular solution theory and pseudophase separation assumptions are employed to quantify surfactant concentrations in the micellar and monomeric phases. The thermodynamic results of

mixed micellization show that ideal mixing is seen in the NaDS/NaOBS system while the NaDS/NaDeS system is relatively nonideal. The degree of counterion binding to the micelle is investigated by activity measurement. The chemical equilibrium of unbound and bound counterions during the micellization can be used to model the fraction of counterions binding to the micelle relatively well. The general thermodynamic properties of calcium surfactant salts are investigated to better understanding the anionic surfactant precipitation by counterions. These thermodynamic data will help to accurately predict the precipitation phase boundary of anionic surfactants used in this study, when precipitated by CaCl_2 . The results reveal more accurate thermodynamic data, which allows better thermodynamic modeling of the precipitation phase boundary of single and binary mixed anionic surfactant systems. The induction time was investigated in binary mixed anionic surfactant systems in order to monitor the delay of the induction time. The results show that the inhibition of anionic surfactant precipitation is due partly to the precipitating species change as mixed anionic surfactant molar ratios are changed, and partly due to the thermodynamics of mixed micellization change. Mixed anionic surfactant systems also show the ability to increase the surface energy required to create the critical nuclei at a particular range of molar ratio of binary mixed anionic surfactant systems.

School of Chemical Engineering

Academic Year 2010

Student's Signature _____

Advisor's Signature _____

ACKNOWLEDGEMENTS

First and foremost, I would like to express my sincere gratitude to my thesis advisor Assoc. Prof. Dr. Adrian E. Flood for his limitless patience, motivation, enthusiasm, and immense knowledge. It has always been a great honor to be his Ph.D. student. He has taught me, both consciously and unconsciously, of how good Ph.D. candidates should be. I appreciate his contributions of time, ideas, and funding in order to make my Ph.D. experience very productive and enormously stimulating. The joy and enthusiasm he has for research was contagious, and motivated to me even during tough times in my pursuit of the Ph.D. His supervision helped me throughout the times of research and writing of this thesis. I could not have imagined having any better advisor and mentor for my study for the Ph.D. His belief and trust in me has facilitated making this achievement possible.

I would also like to acknowledge my co-advisor Assoc. Prof. Dr. Kenneth J. Haller from the School of Chemistry, Suranaree University of Technology (SUT) for his guidance during my studies, and for being a part of my thesis proposal committee. Special appreciation goes to Prof. Dr. Brian P. Grady, in association with Prof. Dr. John F. Scamehorn from the University of Oklahoma (OU), Norman, Oklahoma, USA, for their valuable suggestions and guidance throughout my education. In addition, I would like to convey my gratitude to the rest of my thesis committee whose names are as follows: Dr. Terasut Sookkumnerd, Assoc. Prof. Dr. Chaiyot Tangsathitkulchai, and Asst. Prof. Dr. Sopark Sonwai for their encouragement, insightful

comments, and supportive questions. I am especially grateful to Asst. Prof. Dr. Ratanawan (Wibulswas) Kiattikomol for bestowing encouragement and mental support throughout the decade I have spent at SUT. I am also keen to thank all the academic members, lab technicians, and secretaries in School of Chemical Engineering, SUT.

I gratefully acknowledge the funding sources that made my Ph.D. work possible, especially the Thailand Research Fund (TRF) through the Royal Golden Jubilee (RGJ) Ph.D. program, grant number PHD/0177/2547 for sponsoring my study and support for research. Part of the financial support of this work was provided by the industrial sponsors of the Institute of Applied Surfactant Research, School of Chemical, Biological, and Materials Engineering, OU.

My time at SUT was made enjoyable in large part due to many friends and groups that have become a part of my life. My time at SUT was also enriched by the Chem. Eng. graduate and undergraduate students. Also I am grateful for time spent with my OU friends, for my backpacking buddies and our memorable trips during my stay in the USA, and for many other people and memories.

Last but not least, I am greatly indebted to my dear family for all their unconditional love and support, for my parents who raised me with love in lifelong education and supported me in the pursuit of success. Without these two most beloved people I could never have imagined achieving this goal.

Atthaphon Maneedaeng

TABLE OF CONTENTS

	Page
ABSTRACT (THAI).....	I
ABSTRACT (ENGLISH).	III
ACKNOWLEDGEMENTS	V
TABLE OF CONTENTS	VII
LIST OF TABLES	XIV
LIST OF FIGURES.....	XIX
SYMBOLS AND ABBREVIATIONS	XXVII
 CHAPTER	
I INTRODUCTION	1
1.1 Introduction to Surfactants	1
1.2 Significance of the Problem	4
1.3 Research Objectives	6
1.4 Scope and Limitations	7
1.4.1 Thermodynamic Properties of Anionic Surfactant Precipitation	7
1.4.2 Kinetic Properties of Anionic Surfactant Precipitation	8
1.5 References	8

TABLE OF CONTENTS (Continued)

	Page
II THERMODYNAMICS OF BINARY MIXED ANIONIC SURFACTANT SYSTEMS AND THE EFFECT OF COUNTERION BINDING TO THE MICELLE.....	11
2.1 Abstract	11
2.2 Introduction	13
2.3 Theory	15
2.3.1 Adsorption of Surfactants at Interfaces	15
2.3.2 Regular Solution Theory	16
2.4 Experimental Procedure	20
2.4.1 Materials	20
2.4.2 Determination of Critical Micelle Concentration of Surfactant Mixture (CMC _M)	20
2.4.2.1 Surface Tension Measurement	20
2.4.2.2 Conductivity Measurement	21
2.4.3 Activity of Counterion Measurement.....	22
2.5 Results and Discussion.....	25
2.5.1 Measurement of the CMC and Micelle Composition in Mixed Anionic Surfactant Systems	25

TABLE OF CONTENTS (Continued)

	Page
2.5.2 Fitting the Experimental CMCs with Regular Solution Theory and Prediction of Micelle Compositions	28
2.5.3 The Effect of Counterions in Solution on the CMC.....	35
2.5.4 Measurement and Modeling of Counterion Binding to the Micelle	39
2.5.5 A Model of Sodium and Calcium Ions Binding to the Micelle	50
2.6 Conclusions.....	53
2.7 References.....	54
III CALCIUM SALTS OF SURFACTANT AND PRECIPITATION PHASE BOUNDRIES	60
3.1 Abstract	60
3.2 Introduction	61
3.3 Theory.....	63
3.3.1 Driving Force of Reactive Crystallization	64
3.3.1.1 Solubility.....	64
3.3.1.2 Activity and Ionic Strength.....	66
3.3.1.3 Solubility Product	68

TABLE OF CONTENTS (Continued)

	Page
3.3.1.4 Supersolubility and Supersaturation	69
3.3.1.5 Dissolution of Anionic Surfactant in Water.....	71
3.3.2 Precipitation of Anionic Surfactant Systems with Calcium Chloride.....	72
3.3.2.1 Single Anionic Surfactant Systems.....	74
3.3.2.1 Binary Mixed Anionic Surfactant Systems	76
3.4 Experimental Procedure.....	78
3.4.1 Materials	78
3.4.2 Preparation of Calcium Surfactant Salts	78
3.4.3 Solubility Measurement.....	79
3.4.4 Determination of Precipitation Phase Boundaries	81
3.5 Results and Discussion	83
3.5.1 Thermodynamic Properties of Calcium Surfactant Salts	83
3.5.1.1 Calcium Dodecyl Sulfate	83
3.5.1.2 Calcium Decyl Sulfate	90

TABLE OF CONTENTS (Continued)

	Page
3.5.1.3 Calcium Octylbenzenesulfonate	95
3.5.2 Precipitation Phase Boundary	96
3.5.2.1 Single Anionic Surfactant	
Precipitation Phase Boundary	96
3.5.2.2 Binary Mixed Anionic Surfactant	
Precipitation Phase Boundary	103
3.6 Conclusions.....	107
3.7 References.....	110
IV THE INDUCTION TIME OF BINARY MIXED	
ANIONIC SURFACTANT PRECIPITATION.....	115
4.1 Abstract	115
4.2 Introduction	117
4.3 Theory	119
4.3.1 Surfactant Precipitation.....	119
4.3.2 Induction time to Precipitation.....	123
4.4 Experimental Procedure.....	126
4.4.1 Materials	126
4.4.2 Determination of Induction time.....	126

TABLE OF CONTENTS (Continued)

	Page
4.5 Results and Discussion	129
4.5.1 Precipitation of Single Anionic Surfactant Systems by CaCl_2	129
4.5.2 Precipitation of Binary Mixed Anionic Surfactant Systems by CaCl_2	137
4.5.2.1 Binary Mixed NaDS/NaDeS Systems	137
4.5.2.2 Binary Mixed NaDS/NaOBS Systems	142
4.5.2 The Estimation of Kinetic Parameters of Anionic Surfactant Precipitation	149
4.6 Conclusions.....	155
4.7 References.....	157
V CONCLUSIONS AND RECOMMENDATIONS	161
5.1 Conclusions.....	161
5.2 Recommendations.....	167
 APPENDICES	
APPENDIX A. Steps in Calculation of the Precipitating Species by Thermodynamic Models for Single Anionic Surfactant Systems.....	169

TABLE OF CONTENTS (Continued)

	Page
APPENDIX B. Steps in Calculation of the Precipitating Species by Thermodynamic Models for Binary Mixed Anionic Surfactant Systems	176
APPENDIX C. Raw Data of Induction Time.....	184
APPENDIX D. List of Publications and Conference Proceedings.....	199
BIOGRAPHY	224

LIST OF TABLES

Table	Page	
2.1	Typical thermodynamic data of micellization for two mixed anionic surfactant systems of NaDS: (a) with NaOBS; (b) with NaDeS in aqueous solution at 30°C.....	26
2.2	Thermodynamic parameters of mixed micellization obtained From regular solution theory for anionic/anionic surfactant systems in aqueous solution at 30°C.....	31
3.1	Total calcium ion concentration at saturation using the AAS Technique for Ca(DS) ₂ in aqueous solution	84
3.2	Total calcium ion concentration at saturation using the AAS Technique for Ca(DeS) ₂ in aqueous solution.....	90
3.3	Total calcium ion concentration at saturation temperature of 30°C using the AAS technique for Ca(DS) ₂ in aqueous solution	96
4.1	The summary of induction time of pure NaDS systems precipitating by CaCl ₂ corresponding to its supersaturation ratio at 30°C.....	135
4.2	Induction time vs. supersaturation ratio for binary mixed NaDS/NaDeS systems precipitated by CaCl ₂ at 30°C.....	139

LIST OF TABLES (Continued)

Table	Page
4.3 Induction time vs. supersaturation ratio for binary mixed NaDS/NaOBS systems precipitated by CaCl ₂ at 30°C. S ₀ is given for both possible sodium salts	145
4.4 The interfacial energy required for calcium surfactant salts precipitation at 30°C	152
A.1 The results of calculation of saturated points (precipitation phase boundary) from the improved models of anionic surfactant precipitation	175
B.1 The results of the iterative calculation of binary mixed NaDS/NaDeS system equimolar ratio where [NaS] = 0.012 M by the regular solution model at 30°C	178
B.2 The results of calculation of saturated points (precipitation phase boundary) from the improved models of binary mixed NaDS/NaDeS precipitation by CaCl ₂	183
C.1 The induction time of single NaDS systems precipitating by CaCl ₂ for for the systems <i>below</i> the CMC of NaDS (7.9 mM) corresponding to its supersaturation ratio at 30°C	185
C.2 The induction time of single NaDS systems precipitating by CaCl ₂ for the systems <i>above</i> the CMC of NaDS (7.9 mM) corresponding to its supersaturation ratio at 30°C	186

LIST OF TABLES (Continued)

Table	Page
C.3 The induction time of 75:25 NaDS/NaDeS molar ratio systems precipitating by CaCl ₂ for the systems <i>below</i> the CMC _M of NaDS/NaDeS mixtures (8.4 mM) corresponding to its supersaturation ratio at 30°C.....	187
C.4 The induction time of 75:25 NaDS/NaDeS molar ratio systems precipitating by CaCl ₂ for the systems <i>above</i> the CMC _M of NaDS/NaDeS mixtures (8.4 mM) corresponding to its supersaturation ratio at 30°C.....	188
C.5 The induction time of 50:50 NaDS/NaDeS molar ratio systems precipitating by CaCl ₂ for the systems <i>below</i> the CMC _M of NaDS/NaDeS mixtures (9.8 mM) corresponding to its supersaturation ratio at 30°C.....	189
C.6 The induction time of 50:50 NaDS/NaDeS molar ratio systems precipitating by CaCl ₂ for the systems <i>above</i> the CMC _M of NaDS/NaDeS mixtures (9.8 mM) corresponding to its supersaturation ratio at 30°C.....	190
C.7 The induction time of 25:75 NaDS/NaDeS molar ratio systems precipitating by CaCl ₂ for the systems <i>below</i> the CMC _M of NaDS/NaDeS mixtures (14.5 mM) corresponding to its supersaturation ratio at 30°C.....	191

LIST OF TABLES (Continued)

Table	Page
C.8 The induction time of 25:75 NaDS/NaDeS molar ratio systems precipitating by CaCl ₂ for the systems <i>above</i> the CMC _M of NaDS/NaDeS mixtures (14.5 mM) corresponding to its supersaturation ratio at 30°C.....	192
C.9 The induction time of 75:25 NaDS/NaOBS molar ratio systems precipitating by CaCl ₂ for the systems <i>below</i> the CMC _M of NaDS/NaOBS mixtures (8.5 mM) corresponding to its supersaturation ratio at 30°C.....	193
C.10 The induction time of 75:25 NaDS/NaOBS molar ratio systems precipitating by CaCl ₂ for the systems <i>above</i> the CMC _M of NaDS/NaOBS mixtures (8.5 mM) corresponding to its supersaturation ratio at 30°C.....	194
C.11 The induction time of 50:50 NaDS/NaOBS molar ratio systems precipitating by CaCl ₂ for the systems <i>below</i> the CMC _M of NaDS/NaOBS mixtures (10.0 mM) corresponding to its supersaturation ratio at 30°C.....	195
C.12 The induction time of 50:50 NaDS/NaOBS molar ratio systems precipitating by CaCl ₂ for the systems <i>above</i> the CMC _M of NaDS/NaOBS mixtures (10.0 mM) corresponding to its supersaturation ratio at 30°C.....	196

LIST OF TABLES (Continued)

Table	Page
C.13 The induction time of 25:75 NaDS/NaOBS molar ratio systems precipitating by CaCl ₂ for the systems <i>below</i> the CMC _M of NaDS/NaOBS mixtures (11.4 mM) corresponding to its supersaturation ratio at 30°C.....	197
C.14 The induction time of 25:75 NaDS/NaOBS molar ratio systems precipitating by CaCl ₂ for the systems <i>above</i> the CMC _M of NaDS/NaOBS mixtures (11.4 mM) corresponding to its supersaturation ratio at 30°C.....	198

LIST OF FIGURES

Figure	Page
1.1	Schematic illustration of a surfactant..... 2
2.1	Plots of surface tension (γ) as a function of logarithmic concentration ($\log C_i$) at 30°C. (a) represents the NaDS/NaOBS system and the two related pure systems; (b) represents the NaDS/NaDeS system and the two related pure systems 27
2.2	(a) The dependence of CMC on the mole fraction of NaDS in the monomeric phase (α_1) (b) Plot of the mole fraction of NaDS in the micellar phase (X_1) as a function of α_1 for the NaDS/NaOBS system at 30°C..... 29
2.3	(a) The dependence of CMC on the mole fraction of NaDS in the monomeric phase (α_1). (b) Plot of the mole fraction of NaDS in the micellar phase (X_1) as a function of α_1 for the NaDS/NaDeS system at 30°C..... 30
2.4	Plots of evolution of conductivity of NaDS solution as a function of concentration at 30°C..... 34
2.5	Plots of evolution of conductivity of NaOBS solution as a function of concentration at 30°C 34

LIST OF FIGURES (Continued)

Figure	Page
2.6	Plots of evolution of conductivity of NaDeS solution as a function of concentration at 30°C..... 35
2.7	Plots of the critical micelle concentration of NaDS as a function of unbound sodium ion concentration at different temperatures 36
2.8	The effect of calcium ion present in the solution on the CMC of NaDS at 30°C. The CMC for calcium-free NaDS solutions is at 7.9 mM at 30°C..... 36
2.9	Plots of dissociated species concentration of NaDS in aqueous solution at 30°C predicted by several proposed data..... 37
2.10	Critical micelle concentration and K_1 parameter as a function of temperature for NaDS in aqueous solution..... 38
2.11	Extrapolation of the Δ_i function to obtain $E_{i,0}$ based on equation (2.16). (a) Na-ISE (b) Ca-ISE 41
2.12	The activity of sodium ion, and dodecyl sulfate monomer (Sasaki, <i>et al.</i> , 1975) present in the system studied as a function of the NaDS concentration at 30°C 42
2.13	The activity of calcium ion present as a function of the NaDS concentration with varying CaCl_2 concentration at 30°C..... 43

LIST OF FIGURES (Continued)

Figure	Page
2.14	Variation of the degree of sodium ion binding to micelle parameter (β_{Na^+}) as a function of NaDS concentration at 30°C..... 45
2.15	Variation of the degree of calcium ion binding to micelle parameter ($\beta_{Ca^{2+}}$) as a function of NaDS concentration at 30°C at different CaCl ₂ concentrations in the solution 46
2.16	Variation of the counterion binding parameters as a function of NaDS concentration at 30°C for several systems. All lines fitting the experimental data in this figure are obtained from the chemical equilibrium model; equation (2.25), with constants $K = 0.015$ and $\beta_T = 0.65$ 48
2.17	Total degree of counterion binding to micelle as a function of CaCl ₂ concentration in NaDS solution at 30°C 49
3.1	An illustration of micelle-monomer-precipitate co-existence in equilibrium for anionic surfactant in the presence of counterions..... 73
3.2	Saturation point determination via the conductivity measurement of Ca(DS) ₂ solution at various concentrations..... 84
3.3	Solubility product of Ca(DS) ₂ in aqueous solution as a function of temperature..... 85

LIST OF FIGURES (Continued)

Figure	Page
3.4	The CMC of Ca(DS) ₂ in aqueous solution at 60°C determination via conductivity measurement 87
3.5	Solubility data of Ca(DS) ₂ in aqueous solution for below and above the Krafft temperature on a van't Hoff plot 88
3.6	Gibbs free energy change for Ca(DS) ₂ dissolution in water as a function of temperature..... 89
3.7	Saturation point determination via the conductivity measurement of Ca(DeS) ₂ solution at various concentrations 90
3.8	Solubility product of Ca(DeS) ₂ in aqueous solution as a function of temperature..... 91
3.9	The CMC of Ca(DeS) ₂ in aqueous solution at 30°C determination via conductivity measurement 92
3.10	Solubility data of Ca(DeS) ₂ in aqueous solution for below and above the Krafft temperature on a van't Hoff plot 93
3.11	Gibbs free energy change for Ca(DeS) ₂ dissolution in water as a function of saturated temperature 94
3.12	Theoretical precipitation phase boundaries estimated by the improved models for NaDS and CaCl ₂ systems as a function of temperature corresponding with the experimental data..... 97

LIST OF FIGURES (Continued)

Figure	Page
3.13 Theoretical precipitation phase boundaries estimated by the previous model (Stellner and Scamehorn, 1989a) for NaDS and CaCl ₂ systems as a function of temperature corresponding with the experimental data.	99
3.14 Comparison of prediction of the precipitation phase boundaries where the ionic strength, <i>I</i> , used in the Debye-Hückel equation is either based on, or discarding the counterion binding to the micelle effect for the NaDS and CaCl ₂ systems, corresponding with the experimental data at 30°C	102
3.15 Theoretical precipitation phase boundaries from the improved models for binary mixed NaDS/NaOBS and CaCl ₂ systems corresponding to the experimental data at pure NaDS and equimolar surfactant concentration at 30°C	105
3.16 Theoretical precipitation phase boundaries from the improved models for binary mixed NaDS/NaDeS and CaCl ₂ systems corresponding to the experimental data at pure NaDS systems at 30°C	106

LIST OF FIGURES (Continued)

Figure	Page
4.1	The design of a turbidity device to study the kinetics of anionic surfactant precipitation..... 127
4.2	Supersaturation ratio curves as a function of CaCl_2 with varying NaDS concentration at 30°C below and above the CMC of NaDS 129
4.3	Supersaturation ratio regions over the theoretical precipitation phase boundary (PPB) for NaDS precipitating by CaCl_2 at 30°C 131
4.4	Some selected turbidity curves by precipitation of NaDS with CaCl_2 (a) below and (b) above the CMC at 30°C with varying supersaturation ratio, S_0 132
4.5	Dependence of the induction time on the supersaturation ratio for NaDS precipitating by CaCl_2 at 30°C 135
4.6	The theoretical precipitation phase boundary of NaDS precipitating by CaCl_2 and the corresponding induction time at 30°C 136
4.7	Dependence of the induction time on the supersaturation ratio for binary mixed NaDS/NaDeS systems precipitating by CaCl_2 at 30°C 138

LIST OF FIGURES (Continued)

Figure	Page
4.8 Dependence of the induction time on the supersaturation ratio for binary mixed NaDS/NaOBS systems precipitating by CaCl_2 for 25% and 50% NaDS molar ratios and supersaturation ratio based on Ca(OBS)_2 , at 30°C	143
4.9 Dependence of the induction time on the supersaturation ratio for binary mixed NaDS/NaOBS systems precipitating by CaCl_2 for 50%, 75%, and 100% NaDS molar ratios, and supersaturation ratio based on Ca(DS)_2 , at 30°C	144
4.10 Precipitation phase boundaries for an equimolar ratio of NaDS/NaOBS mixtures precipitating by CaCl_2 at 30°C , and the experimental data corresponding to the precipitation system.	147
4.11 Variation in the induction time as a function of supersaturation ratio for the binary mixed NaDS/NaDeS systems precipitating by CaCl_2 at 30°C	149
4.12 Variation in the induction time as a function of supersaturation ratio for the binary mixed NaDS/NaOBS systems precipitating by CaCl_2 at 30°C where S_0 is based on Ca(OBS)_2	150

LIST OF FIGURES (Continued)

Figure		Page
4.13	Variation in the induction time as a function of supersaturation ratio for the binary mixed NaDS/NaOBS systems precipitating by CaCl_2 at 30°C where S_0 is based on $\text{Ca}(\text{DS})_2$	151
4.14	Dependence of the nucleation rate and the excess Gibbs free energy change of formation of critical nuclei as a function of supersaturation ratio for the binary mixed NaDS/NaOBS systems precipitating by CaCl_2 at 30°C	153
4.15	Variation of radius of critical nucleus of calcium surfactant salts as a function of supersaturation ratio at 30°C	154

SYMBOLS AND ABBREVIATIONS

a_c	=	the solute activity, mol/L
a_i	=	The activity of ion i , mole/L
	=	the an empirical value based on diameter of the ion, m
a_m	=	the value of the mean molecular area, \AA^2
C	=	the molar concentration, mole/L
$[Ca^{2+}]_b$	=	the bound calcium ion concentration, mole/L
$[Ca^{2+}]_{tot}$	=	the total calcium ion concentration, mole/L
$[Ca^{2+}]_{unb}$	=	the unbound calcium ion concentration, mole/L
C_i	=	the concentration of cation of interest, mole/L
C_t	=	the total concentration of surfactant in the bulk solution, mole/L
c	=	the solute composition, mole/L
c^*	=	the equilibrium saturation at the given temperature, mole/L
c_i	=	the concentration of ionic species, mole/L
$[DS^-]_{mic}$	=	the dodecyl sulfate ion concentration in micellar phase, mole/L
$[DS^-]_{mon}$	=	the dodecyl sulfate ion concentration in monomeric phase, mole/L
E_i	=	the EMF of the solution at any moment, mV
$E_{i,0}$	=	the EMF constant depending on the type of reference electrode and the filling solution, mV

SYMBOLS AND ABBRVIATIONS (Continued)

F	=	the Faraday constant, C/mole
	=	the force balance, -
$f(\theta)$	=	the correction factor, -
f_{\pm}	=	the mean activity coefficient of the ion, -
f_c	=	the activity coefficient corresponding to the composition c , -
f_i	=	the activity coefficient corresponding to the ion i , -
$G_{\min}^{(S)}$	=	the surface free energy, kJ/mole
I	=	the intensity of light, candela
	=	the ionic strength of the electrolyte solution, mole/L
I_0	=	the intensity of light detected with the isotropic sample (blank), candela
J	=	the nucleation rate, #/m ³ /sec
K	=	the ratio of the activity based equilibrium constant of counterions binding to the micelle, -
K_I	=	the Corrin-Harkins constant determining the CMC in solutions having an unbound sodium ion concentration of 1 mole/L, -
$K_{Ca^{2+}}$	=	the activity based equilibrium constant of calcium ions binding to the micelle, -
K_g	=	the Corrin-Harkins constant determining the effect of the unbound sodium ion on the CMC, -

SYMBOLS AND ABBRVIATIONS (Continued)

K_{Na^+}	=	the activity based equilibrium constant of sodium ions binding to the micelle, -
K_{SP}	=	the solubility product, -
k_B	=	the Boltzmann constant, J/K
L	=	the light path length, cm
N	=	the Avogadro's number, mole ⁻¹
$[Na^+]_b$	=	the bound sodium ion concentration, mole/L
$[Na^+]_{tot}$	=	The total sodium ion concentration, mole/L
$[Na^+]_{unb}$	=	the unbound sodium ion concentration, mole/L
n	=	the number of moles of the solute species, mole
n_1	=	the number of mole for individual surfactants 1 in the mixture, mole
n_2	=	the number of mole for individual surfactants 2 in the mixture, mole
R	=	the universal gas constant, J/mole·K
rc	=	the radius of the critical nucleus, Å
$[S-]_{mic}$	=	the anionic surfactant ion concentration in micellar phase, mole/L
$[S-]_{mon}$	=	the anionic surfactant ion concentration in monomeric phase, mole/L
S_0	=	the degree of supersaturation or supersaturation ratio, -
T	=	the absolute temperature, K
T_f	=	the fusion temperature (melting point) of the solute, K

SYMBOLS AND ABBRVIATIONS (Continued)

T_{sat}	=	the saturation temperature, K
t_{ind}	=	the induction time, sec
V	=	the voltage, mV
V_0	=	the voltage corresponding to the isotropic sample (blank), mV
V_m	=	the molecular volume, \AA^3
X_1	=	the mole fraction of the surfactant 1 in micellar phase, -
X_2	=	the mole fraction of the surfactant 2 in micellar phase, -
x	=	the mole fraction of solute, -
x_1	=	the mole fraction of the surfactant 1 at the interface, -
x_2	=	the mole fraction of the surfactant 2 at the interface, -
z_-	=	the valencies of the anion, -
z_+	=	the valencies of the cation, -
z_i	=	the ion valance of the ion i , -
α_1	=	the mole fraction of the surfactant 1 in monomeric phase, -
α_2	=	the mole fraction of the surfactant 2 in monomeric phase, -
β	=	the geometric factor, -
$\beta_{Ca^{2+}}$	=	the fractional bindings of calcium ion to the anionic surfactant micelle, -
β_i	=	the fractional bindings of ion i to the anionic surfactant micelle, -
β_M	=	the regular solution theory interaction parameter, -

SYMBOLS AND ABBRVIATIONS (Continued)

β_{Na^+}	=	the fractional bindings of sodium ion to the anionic surfactant micelle, -
β_T	=	the total bindings of counterion to the anionic surfactant micelle, -
ΔG	=	the Gibbs free energy, J/mole
ΔG_{crit}	=	the critical Gibbs free energy, J/mole
ΔH	=	the enthalpy change, J/mole
Δ_i	=	the function in order to find $E_{i,0}$ for ion i , mole/L
ΔS	=	the entropy change, J/mole·K
Γ_t	=	the surface excess concentration, mole/m ²
γ	=	the surface (interfacial) tension, mN/m
γ	=	the surface energy, J/m ²
$\gamma_{1,m}$	=	the activity coefficients of surfactant 1 in the monomeric solution, -
$\gamma_{1,M}$	=	the activity coefficients of surfactant 1 in the micellar solution, -
$\gamma_{2,m}$	=	the activity coefficients of surfactant 2 in the monomeric solution, -
$\gamma_{2,M}$	=	the activity coefficients of surfactant 2 in the micellar solution, -
γ_{CMC}	=	the surface (interfacial) tension at the CMC, mN/m
$\gamma_{i,m}$	=	the activity coefficients of surfactant i in the monomeric solution, -
$\gamma_{i,M}$	=	the activity coefficients of surfactant i in the micellar solution, -
κ	=	the conductivity of the solution, $\mu\text{S/cm}$
μ	=	the chemical potential, J/mole

SYMBOLS AND ABBRVIATIONS (Continued)

μ_{0C}	=	the standard chemical potential, J/mole
σ	=	the relative supersaturation, -
τ	=	the turbidity with units of inverse length, cm^{-1}
AAS	=	the atomic adsorption spectroscopy
ATC	=	the automatic temperature control
Ca(DeS)_2	=	calcium decyl sulfate
Ca(DS)_2	=	calcium dodecyl sulfate
Ca(OBS)_2	=	calcium octylbenzenesulfonate
Ca-ISE	=	the calcium ion specific electrode
CMC	=	the critical micelle concentration
EMF	=	the electromotive force
ISE	=	the ion-specific electrode
mM	=	millimolar
μS	=	microsiemenscc
NaDeS	=	sodium decyl sulfate
NaDS	=	sodium dodecyl sulfate
Na-ISE	=	the sodium ion specific electrode
NaOBS	=	sodium octylbenzenesulfonate
RST	=	the regular solution theory

CHAPTER I

INTRODUCTION

1.1 Introduction to Surfactants

Surfactant is short form of surface active agent, which indicates a chemical species which is active at a surface. Surfactants can be found in many detergency products and various other applications. It is less well known that they can be used as an anti-caking agent for products as diverse as cement and flour (Kamoun, Jelidi, and Chaabouni, 2003), as well as species such as lecithin, a natural surfactant which can be used to promote the dispersion of a variety of substance powder in food products (Schubert, 1993). Further, surfactants can increase the yield in mineral oil extraction, stabilize cosmetic emulsions, give washed fabrics a soft feel, disinfect swimming pods, and are the active substances in contraceptive devices (Hummel, 2000; Myers, 2006). Of course, these numerous properties cannot be achieved by just a few chemical structures, and specific methods are required for their identification because of the very wide range of possible surfactants.

All surfactant molecules are composed of at least two parts, one of which is soluble in a specific fluid (the lyophilic part) and one which is insoluble (the lyophobic part). When the fluid is water, these are generally called the hydrophilic and hydrophobic parts, respectively. The hydrophilic part is referred to as the head group and the hydrophobic part as the tail, as shown in Figure 1.1.

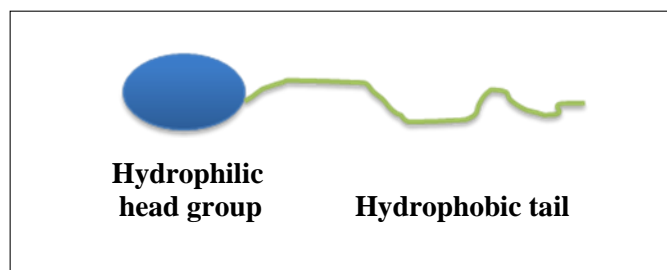


Figure 1.1 Schematic illustration of a surfactant molecule.

One characteristic feature of surfactants is their ability to adsorb at interfaces (solid-liquid, liquid-liquid, and liquid-vapor). Another fundamental property of surfactants is that the molecules in solution can form aggregates, so-called micelles. The unassociated surfactant is referred to in the literature either as *monomer* or *unimer*. Micelle formation or micellization can be considered as an alternative mechanism to adsorption at interfaces for removing hydrophobic groups from contact with water, thereby reducing the free energy of the system. Micellization is an important phenomenon since surfactant molecules behave very differently when present in micelles rather than as free monomers in the solution. Only surfactant monomers contribute to the lowering of surface and interfacial tension, and dynamic phenomena such as wetting and forming. The micelles may be seen as a reservoir for surfactant monomers. The exchange rate of a surfactant molecule between micelle and bulk solution may vary by many orders of magnitude depending on the size and structure of the surfactant. Micelles are generally formed at a very low concentration of surfactant in aqueous solution. The concentration at which micelles starts to form is called the critical micelle concentration, or CMC, and it is an important characteristic of a surfactant.

The most useful chemical classification of surfactants is made on the basis of the charge of the polar head group with subgroups based on the nature of hydrophobe or tail. It is common practice to divide surfactants into the four classes as follows:

- **Anionic:** the hydrophile is a negatively charged group such as carboxyl (RCOO^-M^+), sulfonate (RSO_3^-M^+), sulfate (RSO_4^-M^+), or phosphate ($\text{ROPO}_3^-\text{M}^+$).
- **Cationic:** the hydrophile bears a positive charge, as for example the quaternary ammonium halides ($\text{R}_4\text{N}^+\text{X}^-$), where the four R -groups, may or may not be all the same (they seldom are), but will usually be of the same general family.
- **Nonionic:** the hydrophile has no charge, but derives its water solubility from highly polar groups such as polyoxyethylene (POE or $\text{R-OCH}_2\text{CH}_2\text{O-}$) or R-polyol groups, including sugars.
- **Amphoteric (and zwitterionic):** the molecule contains, or can potentially contain, both a negative charge and a positive charge, such as the sulfobetaines $\text{RN}^+(\text{CH}_3)_2\text{CH}_2\text{CH}_2\text{SO}_3^-$

Most ionic surfactants are monovalent but there are also important examples of divalent anionic amphiphiles. For ionic surfactants the choice of counterion plays a significant role in physicochemical properties. Most anionic surfactants have sodium as a counterion but other cations, such as lithium, potassium, calcium, and protonated amines, are used as surfactant counterions for speciality objectives. The counterion of cationic surfactants is usually a halide or methyl sulfate.

1.2 Significance of the Problem

A significant characteristic of anionic surfactants which can be deleterious to their use is the tendency to precipitate from aqueous solutions by counterions. Avoidance of anionic surfactant precipitation by counterions is crucial in many applications of surfactants especially in the detergency industry. One condition that can cause anionic surfactant to precipitate is hard water (water containing multivalent cations) since divalent cation salts of surfactants tend to have very low solubility products (K_{SP}). Precipitation of surfactants due to hard water can be unfavorable in laundry detergency applications, where precipitated surfactant is not available for participation in the cleaning cycle. Conversely, precipitation of surfactant can be advantageous in other applications, such as enhanced crude oil recovery in oil reservoirs, as it is the basis of a waterflooding technology (Gale, Saunders, and Ashcraft Jr, 1976) and surfactant recovery from surfactant-based separations (Vanjara and Dixit, 1996; Wu, Christian, and Scamehorn, 1998). Due to the precipitation behavior of anionic surfactants, the ability to manipulate this behavior is greatly significant.

Nevertheless, precipitation behavior can be manipulated most when not dealing with an individual surfactant system but with a mixture of surfactants. There have been many studies suggesting that using mixed surfactants will cause a delay in surfactant precipitation (Rodriguez and Scamehorn, 1999, 2001; Soontravanich S., and Scamehorn, 2010; Soontravanich S., Walsh, Scamehorn, Harwell, and Sabatini, 2008; Stellner and Scamehorn, 1989), and that the use of surfactant mixtures generally can have more synergism than the use of a single surfactant (Holland and Rubingh, 1992; Jost, Leiter, and Schwuger, 1988; Kume, Gallotti, and Nunes, 2008;

Li F., Li G.-Z., and Chen, 1998; Rosen, 1991). Consequently, the understanding of precipitation phenomena which involves thermodynamics of mixed surfactants and kinetics of mixed surfactant precipitation is of great importance to practical applications of surfactants.

There has been considerable research on the thermodynamics of mixed surfactant systems, but only a few investigations of the kinetics of mixed surfactant precipitation in spite of the fact that several practical surfactant applications may be away from the equilibrium. Because the enormous majority of surfactants applied in industry or consumer products are mixtures of surfactants, the effect of mixed surfactant composition on precipitation kinetics has essential consequences for their applications.

Previously, measurements of the kinetics of surfactant precipitation for both single and mixed systems was performed through calorimetry (Rodriguez, Lowery, Scamehorn, and Harwell, 2001; Rodriguez and Scamehorn, 2001), stopped-flow spectrometry (Clarke, Lee, and Robb, 1976), and conductivity (Lee and Robb, 1979) but that only gave the mass crystallization rate, not the nucleation rate or growth rate. Hence, it is beneficial to measure kinetic and thermodynamic properties of crystallization directly, as these are quite limited in the surfactant precipitation area currently. It has been noted that there is precipitation inhibition in mixed systems, but it is not clear whether this inhibition is due to (i) changes in precipitation phase boundaries, (ii) changes in concentrations of the individual surfactants with the phase boundaries staying the same, or (iii) inhibition of nucleation. The main part of the thesis is to determine which mechanism is responsible for the inhibition. These rationales raise the author to address the fundamental significance and practical

importance in studying kinetics and thermodynamics of precipitation of anionic surfactants by divalent counterions as the research objectives proposed here.

1.3 Research Objectives

This thesis research will use experimental and modeling work to thermodynamically and kinetically investigate this inhibition of precipitation using both individual and mixed systems of anionic surfactants as follows:

1.3.1 To investigate thermodynamics of binary mixed anionic surfactant systems in the intermicellar solutions. The nonideality models known as regular solution theory and the assumption of pseudophase separation theory will be used to thermodynamically treat the binary mixed micellization of anionic surfactants employed in this research.

1.3.2 To investigate the effect of mono- and divalent counterions on the thermodynamics and kinetics of precipitation of single and binary mixed anionic surfactant systems. The experimental measurement of activity of counterion species in the intermicellar solution will be directly probed by the activity measurement via ion-specific electrodes. Modeling work will be also introduced in order to improve the earlier models of the thermodynamics and kinetics of anionic surfactant precipitation both for single and binary mixed anionic surfactant systems.

1.3.3 To investigate the thermodynamic properties of calcium surfactant salts such as, solubility, CMC, Krafft temperature, and energy required for dissolution. As well, this research will provide improved thermodynamic models of the precipitation phase boundary for anionic surfactants with divalent ions both in single anionic surfactant systems and in binary mixed anionic surfactant systems. The

models will be applied to investigate the induction time for precipitation of anionic surfactants used with the addition of calcium ions, and also the prediction of nucleation rate and other related kinetic parameters to investigate the causes of inhibition of precipitation in mixed anionic surfactants.

1.3.4 To address the mechanisms of inhibition in precipitation of mixtures of anionic surfactants; whether this inhibition is due to (i) changes in precipitation phase boundaries, (ii) changes in concentrations of the individual surfactants with the phase boundaries staying the same, or (iii) inhibition of nucleation, by the use of thermodynamic and kinetic experimental studies.

1.4 Scope and Limitations

1.4.1 Thermodynamic Properties of Anionic Surfactant Precipitation

Thermodynamic properties of calcium salts of surfactant are required in order to model the precipitation phase boundaries of anionic surfactant precipitation with calcium chloride. The model accuracy is verified by the quantitative elemental analysis using spectroscopy instruments. The thermodynamic models from earlier studies will be improved by additional experiments here, possibly relating to modeling of the micelle formation and composition. Together with the experimental work, modeling will be used to investigate the effect of counterions on the micellization by using the activity measurement.

1.4.2 Kinetic Properties of Anionic Surfactant Precipitation

The investigation of induction time for anionic surfactant precipitation will be performed to study the inhibition in mixed anionic surfactants system at specific temperatures by a turbidity device using the change of light intensity during the precipitation phenomenon. The estimation of nucleation rate and other kinetic parameters will be only predicted through the relationship with induction time and the degree of supersaturation from classical homogeneous nucleation theory. This is because there is some difficulty to experimentally measure the nucleation rate in a conventional laboratory as the induction time is relatively fast and the nucleation rate is extremely high in single anionic surfactant systems and mixed anionic surfactant systems at some specific molar ratios of surfactant compositions.

1.5 References

- Clarke, D. E., Lee, R. S., and Robb, I. D. (1976). Precipitation of calcium salts of surfactants. **Faraday Discussions of the Chemical Society** 61: 165-174.
- Gale, W. W., Saunders, R. K., and Ashcraft Jr, T. L. (1976). **Oil recovery method using a surfactant**. US Patent no. 3,977,471.
- Holland, P. M. and Rubingh, D. N. (1992). Mixed surfactant systems. In P. M. Holland and D. N. Rubingh (Eds.). **Mixed surfactant systems** (pp. 2-30). Washington, DC: American Chemical Society.
- Hummel, D. O. (2000). **Handbook of surfactant analysis: Chemical, physico-chemical and physical methods**. London: John Wiley & Sons.
- Jost, F., Leiter, H., and Schwuger, M. J. (1988). Synergisms in binary surfactant mixtures. **Colloid & Polymer Science** 266(6): 554-561.

- Kamoun, A., Jelidi, A., and Chaabouni, M. (2003). Evaluation of the performance of sulfonated esparto grass lignin as a plasticizer-water reducer for cement. **Cement and Concrete Research** 33(7): 995-1003.
- Kume, G., Gallotti, M., and Nunes, G. (2008). Review on anionic/cationic surfactant mixtures. **Journal of Surfactants and Detergents** 11(1): 1-11.
- Lee, R. S. and Robb, I. D. (1979). Precipitation of calcium surfactants. Part 3. **Journal of the Chemical Society, Faraday Transactions** 1 75: 2126-2136.
- Li, F., Li, G.-Z., and Chen, J.-B. (1998). Synergism in mixed zwitterionic-anionic surfactant solutions and the aggregation numbers of the mixed micelles. **Colloids and Surfaces A: Physicochemical and Engineering Aspects** 145(1-3): 167-174.
- Myers, D. (2006). **Surfactant science and technology**. New Jersey: John Wiley & Sons.
- Rodriguez, C. H., Lowery, L. H., Scamehorn, J. F., and Harwell, J. H. (2001). Kinetics of precipitation of surfactants. I. Anionic surfactants with calcium and with cationic surfactants. **Journal of Surfactants and Detergents** 4(1): 1-14.
- Rodriguez, C. H. and Scamehorn, J. F. (1999). Modification of Krafft temperature or solubility of surfactants using surfactant mixtures. **Journal of Surfactants and Detergents** 2: 17.
- Rodriguez, C. H. and Scamehorn, J. F. (2001). Kinetics of precipitation of surfactants. II. Anionic surfactant mixtures. **Journal of Surfactants and Detergents** 4(1): 15-26.

- Rosen, M. J. (1991). Synergism in mixtures containing zwitterionic surfactants. **Langmuir** 7(5): 885-888.
- Schubert, H. (1993). Instantization of powdered food products. **International Chemical Engineering** 33(1): 28-45.
- Soontravanich, S. and Scamehorn, J. F. (2010). Use of a nonionic surfactant to inhibit precipitation of anionic surfactants by calcium. **Journal of Surfactants and Detergents** 13(1): 13-18.
- Soontravanich, S., Walsh, S., Scamehorn, J., Harwell, J., and Sabatini, D. (2008). Interaction Between an Anionic and an Amphoteric Surfactant. Part II: Precipitation. **Journal of Surfactants and Detergents**.
- Stellner, K. L. and Scamehorn, J. F. (1989). Hardness tolerance of anionic surfactant solutions. 2. Effect of added nonionic surfactant. **Langmuir** 5(1): 77-84.
- Vanjara, A. K. and Dixit, S. G. (1996). Recovery of cationic surfactant by using precipitation method. **Separations Technology** 6(1): 91-93.
- Wu, B., Christian, S. D., and Scamehorn, J. F. (1998). Recovery of surfactant from micellar-enhanced ultrafiltration using a precipitation process. In F. Kremer and G. Lagaly (Eds.). **Progress in colloid & polymer science** (pp. 60-73). New York: Springer Berlin/Heidelberg.

CHAPTER II

THERMODYNAMICS OF BINARY MIXED ANIONIC SURFACTANT SYSTEMS AND THE EFFECT OF COUNTERION BINDING TO THE MICELLE

2.1 Abstract

Properties of the anionic surfactants sodium decyl sulfate (NaDeS), sodium dodecyl sulfate (NaDS), and sodium 4-octylbenzenesulfonate (NaOBS) have been determined in both single and binary aqueous systems. Regular solution theory has been used to thermodynamically treat the micellization of mixed anionic surfactants. The model shows a satisfactory prediction of the critical micelle concentration (CMC) of surfactant mixtures together with providing equilibrium compositions in monomeric and micellar phases. The mixed micelle is ideal for the NaDS/NaOBS mixture, not surprising given the similarity in structure. The NaDS/NaDeS mixture is slightly nonideal (having attractive interactions in the micelle) with the nonideality probably being due to the difference in the number of carbon atoms in the backbone of the surfactant molecule. The effect of the counterion on the CMC of anionic surfactants has been measured for the pure surfactants. Experimentally, the CMC of the anionic surfactant depends on the concentration of the monovalent cations present in the solution, and can be described by the Corrin-Harkins relationship, while the dependence of the CMC on the concentration of the trace divalent cations is far less

significant. Moreover, the behavior of counterion binding to micelle of anionic surfactant system is investigated quantitatively. Experimentally, the counterion binding of sodium to the micelle is influenced by the calcium ion concentration, and vice versa. However the total degree of counterion binding is essentially constant at approximately 0.65 charge negation at the micelle's surface. The counterion binding coefficients can be quantitatively modeled using a simple equilibrium model relating concentrations of bound and unbound counterions.

2.2 Introduction

Practical applications of surfactants such as their use in cleaning and household products usually involve surfactant mixtures. Surfactants used in commercial applications, for instance sodium alkyl sulfates, are mixtures of homologous anionic surfactants, unreacted raw materials, and by-products. In addition, in many applications surface-active materials are mixed to create synergism due to the presence of the second surfactant (Stellner and Scamehorn, 1989b). The largest synergies appear to be in mixtures of ionic and nonionic surfactants (Haque, Das, Rakshit, and Mouliks, 1996; Soontravanich S., Munoz, Scamehorn, Harwell, and Sabatini, 2008; Vora, George, Desai, and Bahadur, 1999) rather than in mixed ionic surfactant systems, however a number of researchers have investigated interactions between surfactants in the micellar phase for ionic/ionic systems (Bakshi, *et al.*, 2002; Cui and Canselier, 2001; López-Fontán, Suárez, Mosquera, and Sarmiento, 2000; Tsubone, 2003; Vora, *et al.*, 1999). Regular solution theory has been shown to be a reasonable model to predict the interactions between binary and multicomponent surfactant mixtures (Holland and Rubingh, 1983; Rubingh, 1979). The regular solution model does not provide a means to deal with the effect of counterion binding to the micelle, however the model shows a satisfactory ability to model the critical micelle concentration (CMC) of surfactant mixtures together with their compositions in the micelle (Haque, *et al.*, 1996; Hoffmann and Pössneck, 1994; López-Fontán, *et al.*, 2000; Schulz, Rodríguez, Minardi, Sierra, and Morini, 2006). Only a few studies have reported the degree of dissociation and/or binding of counterions to the micelle (Bandyopadhyay and Moulik, 1988; Podchasskaya and Us' yarov, 2005; Rathman and Scamehorn, 1984, 1987; Sasaki, Hattori, Sasaki, and Nukina, 1975; Srinivasan and

Blankschtein, 2003; Talens-Alesson, 2007). However, there are still no definitive results due to differences in values measured by different experimental techniques, and the exact theoretical definition of counterion binding is not uniform. Thus, this work aims to provide experimental data and modeling of the data with the regular solution model to thermodynamically predict the micellization behavior of systems with the mixed binary anionic surfactants used. The effect of the counterion on the micelle and the counterion binding to the micelle are investigated by the use of ion-selective electrodes to directly measure the activity of the ionic species present in the bulk solution; these results can then be used with the micellization model to predict the degree of counterion binding.

Furthermore, the work presented here can be used to improve the thermodynamic modeling of micellar systems so as to better understand the activities of the monomer surfactant in the solution phase (which requires accurate modeling of the CMC as a function of the state of the solution, and the composition of the micelle), and the activity of the counterions in the solution phase (which requires accurate knowledge of counterion binding to the micelle). One example use would be for modeling both solubility and degree of supersaturation in surfactant systems.

2.3 Theory

2.3.1 Adsorption of Surfactants at Interfaces

The amount of surfactant absorbed per unit area of interface for a binary surfactant mixture can be calculated using the Gibbs adsorption equation (Rosen, 2004):

$$\Gamma_t = -\frac{1}{2.303nRT} \left(\frac{d\gamma}{d \log C_t} \right)_{T, x_i} \quad (2.1)$$

where Γ_t is the surface excess concentration, defined as the excess amount of surfactant (i.e. surfactant 1 + surfactant 2) per unit area of interface, compared to that present in a reference system in which the bulk concentrations of the two surfactants remain uniform up to the hypothetical interface. The parameter n is the number of moles of the solute species; for mixtures of two different surfactants, the value of n is equal to $n_{\text{mix}} = n_1x_1 + n_2x_2$, where n_1 and n_2 are the n values for individual surfactants 1 and 2 of the mixture and x_1 and x_2 are the mole fraction of the surfactant at the interface. R is the gas constant and T is the absolute temperature. γ is the surface (interfacial) tension, and C_t is the total concentration of surfactant in the bulk solution.

The area per molecule at the interface gives qualitative information on the degree of packing and the orientation of the absorbed surfactant molecules when compared with the dimensions of the molecule obtained with molecular models. The value of the mean molecular area a_m (\AA^2), can be calculated from the equation:

$$a_m = \frac{10^{16}}{N\Gamma_t} \quad (2.2)$$

where N is Avogadro's number and Γ_t is the surface excess concentration (mole/cm²). Moreover, the surface free energy ($G_{\min}^{(S)}$) can be calculated from the parameters determined above; the equation, proposed by Sugihara *et al.* (2003), has been described as the thermodynamic quantity for the evaluation of synergism upon mixing.

$$G_{\min}^{(S)} = a_m \gamma_{CMC} N \quad (2.3)$$

Sugihara defines $G_{\min}^{(S)}$ as the minimum free energy of the surface assuming full adsorption of the surfactant molecules.

2.3.2 Regular Solution Theory

For several decades, regular solution theory has been employed to model the thermodynamic nonidealities of mixed surfactant systems in both ionic/ionic systems (Haque, *et al.*, 1996; Hoffmann and Pössneck, 1994; López-Fontán, *et al.*, 2000; Schulz, *et al.*, 2006) and ionic/nonionic systems (Haque, *et al.*, 1996; Soontravanich S., *et al.*, 2008; Vora, *et al.*, 1999) of surfactants and it has been shown to be able to accurately model CMC values (Kakehashi, Shizuma, Yamamura, and Takeda, 2004) and the micelle-monomer equilibrium compositions (Soontravanich S., *et al.*, 2008; Vora, *et al.*, 1999). Regular solution theory was first introduced to binary and multicomponent amphiphile systems by Rubingh (1983; 1979). When the effect of counterion binding to the micelle on the micelle composition is negligible (Nishikido, 1993) the pseudo phase separation model and

regular solution theory has been widely used for the analysis of this type of experimental data.

The pseudophase separation model assumes that micelles are a separate phase that forms at concentrations above the CMC, which represents the saturation concentration for monomeric surfactants. A mixture of two different surfactants can be in the monomeric form at the compositions α_1 and α_2 , in equilibrium with micelles that have composition X_1 and X_2 . Mole fractions are on a surfactant-only basis, consequently:

$$X_1 + X_2 = 1 \quad (2.4)$$

$$\alpha_1 + \alpha_2 = 1 \quad (2.5)$$

At the CMC:

$$\alpha_1 \gamma_{1,m} CMC_1 = X_1 \gamma_{1,M} CMC_M \quad (2.6)$$

$$\alpha_2 \gamma_{2,m} CMC_2 = X_2 \gamma_{2,M} CMC_M \quad (2.7)$$

where $\gamma_{i,m}$ and $\gamma_{i,M}$ are activity coefficients of surfactant i in the monomeric and micellar solutions respectively, CMC_i is the CMC of the pure surfactant ($i = 1, 2$) and CMC_M is the CMC of the mixed system. In the case of binary nonideal mixtures of components modeled using regular solution theory, a molecular interaction parameter (β_M) is introduced and the activity coefficients in the mixed micelles are given by:

$$\gamma_{1,M} = \exp(\beta_M X_2^2) \quad (2.8)$$

$$\gamma_{2,M} = \exp(\beta_M X_1^2) \quad (2.9)$$

The parameter β_M is known as the regular solution theory interaction parameter in $k_B T$ units, where k_B is the Boltzmann constant and T is the temperature in units of Kelvin. The interaction parameter is a measure of the interaction between two different surfactants in the mixed micelle, which is a measure of degree of nonrandomness or nonideality in the mixing of the components within the micelle. A high negative value of β_M indicates a strong attractive interaction between the two different surfactants in the micelle (Vora, *et al.*, 1999), while a positive value of β_M indicates repulsive interactions, whereas $\beta_M = 0$ indicates an ideal mixture in the micelle. In other words, a high negative value of β_M favors the formation of mixed micelles in a mixed surfactant system. The value of the interaction parameter can be estimated from following equation:

$$F = \frac{X_1^2 \ln(\alpha_1 CMC_M / X_1 CMC_1)}{(1 - X_1)^2 \ln((1 - \alpha_1) CMC_M / (1 - X_1) CMC_2)} - 1 = 0 \quad (2.10)$$

This requires solving iteratively for X_1 at the CMC and β_M can be then calculated directly by the following expression:

$$\beta_M = \frac{\ln(\alpha_1 CMC_M / X_1 CMC_1)}{(1 - X_1)} \quad (2.11)$$

In the regular solution treatment of mixed micelle formation, the CMC value of a binary surfactant mixture is related to those of pure components by:

$$CMC_M = \left[\frac{\alpha_1}{\gamma_{1,M} CMC_1} + \frac{\alpha_2}{\gamma_{2,M} CMC_2} \right]^{-1} \quad (2.12)$$

For the ideal behavior, the activity coefficients $\gamma_{1,M} = \gamma_{2,M} = 1$ and equation (2.12) becomes:

$$CMC_M = \left[\frac{\alpha_1}{CMC_1} + \frac{\alpha_2}{CMC_2} \right]^{-1} \quad (2.13)$$

2.4 Experimental Procedure

2.4.1 Materials

Sodium dodecyl sulfate (NaDS) was purchased from Carlo Erba with purity greater than 92%. Sodium 4-octylbenzene sulfonate (NaOBS) was purchased from Aldrich with purity greater than 97%. These two anionic surfactants were further purified by twice recrystallizing using deionized water and methanol, respectively. They were dried over silica gel at room temperature for 24 hours. Sodium decyl sulfate (NaDeS) was purchased from Fluka with purity greater than 99% and was used as received without further purification. Reagent grade sodium chloride (NaCl), with purity greater than 99.5%, was purchased from Merck and was used as received. Calcium chloride dihydrate ($\text{CaCl}_2 \cdot 2\text{H}_2\text{O}$), analytical reagent grade with purity greater than 98.0%, was purchased from Sigma-Aldrich and was used as received. Deionized water ($18 \text{ M}\Omega \cdot \text{cm}$) was used to prepare all aqueous samples throughout the experiments.

2.4.2 Determination of Critical Micelle Concentration of Surfactant

Mixture (CMC_M)

2.4.2.1 Surface Tension Measurement

Measurements of the effect of binary anionic surfactant on the CMC of surfactant mixtures were carried out by surface tension measurement using a Wilhelmy plate type tensiometer. Pure NaDS solutions were prepared covering a range both below and above the CMC. In addition, mixed anionic surfactant solutions were prepared for NaDS/NaOBS and NaDS/NaDeS at different molar ratios. Surface tension was measured at 30°C for the systems NaDS(1)/NaOBS(2) and NaDS(1)/NaDeS(2) at compositions of $x_1 = 0.25, 0.50, \text{ and } 0.75$ (on a solvent-free

basis). The surface tensions of the pure NaDS, NaOBS and NaDeS systems are already well characterized in the literature. Surface tension measurements were used to determine the CMC at a break in the surface tension versus surfactant concentration plot. The surface tension was performed by a Krüss (K10ST model) tensiometer equipped with a platinum plate. Equilibration times in the case of surfactant mixtures can be quite long as noted in an earlier study (Lunkenheimer and Wantke, 1981). Samples were held to equilibrate at 30°C until the surface tension on the digital reading display stabilized and measurements were taken every 15 minutes until three subsequent readings matched. The value of the final reading at three hours after the mixing would be used in the case that the reading shown on the display has not stabilized by that time.

2.4.2.2 Conductivity Measurement

The effect of counterions on the CMC of NaDS was investigated by a conductimetry technique. Conductivity was used to monitor the effect of counterion presence on the CMC in the intermicellar solution and also the CMC of pure NaDS, NaOBS, and NaDeS solutions. For the effect of the sodium ion on the CMC, a fresh (to avoid NaDS hydrolysis) stock NaDS solution above the CMC was prepared. Conductivity was measured by an inoLab Cond Level 2 conductivity meter with a 4-cell conductivity epoxy probe, both with and without NaCl, at 10, 30, and 50°C. Measurements were performed in a 300-mL vessel with jacket, the system temperature was maintained by a temperature-controlled water bath. For the effect of calcium ions on the CMC, a fresh stock NaDS solution above the CMC was prepared with varying CaCl₂ concentration, with NaDS and CaCl₂ concentrations being such that the system always lies below the precipitation phase boundary. The

concentration at the point that the slope is discontinuous in the evolution of conductivity as a function of NaDS concentration is the CMC of the system. The relationship between CMC and unbound sodium ion concentration can be demonstrated on logarithmic scale at specific temperature as proposed by Corrin and Harkins (1947):

$$\ln[CMC] = -K_1 - K_g \ln[Na^+]_{unb} \quad (2.14)$$

where K_1 is a constant determining the CMC in solutions having an unbound sodium ion concentration of 1 molar (a reference state) and K_g which determines the effect of the unbound sodium ion on the CMC. This expression provides a correction for the monomer surfactant concentration at the CMC as the concentration of the counterion in the solution varies. The unbound sodium ion concentration, $[Na^+]_{unb}$, in the Corrin–Harkins plot is defined as the amount of $[Na^+]$ dissociated from NaDS molecules at the CMC plus $[Na^+]$ present due to NaCl and other sodium salts present in the system.

2.4.3 Activity of Counterion Measurement

Activity measurements were carried out by ion selective electrodes (ISE) at 30°C. Sodium- and calcium-specific electrodes were used to measure the response in intermicellar solutions containing dissociated sodium ions and dissolved calcium ions. Electrodes were checked periodically by measurement of solutions of NaCl and CaCl₂ of known ion activities before their use to test the electrode reliability with regards to the Nernst equation. The response of the sodium-specific electrode was obtained by the VWR symPHony sodium ion selective glass combination

electrode (Na-ISE) where mercury(I) chloride (calomel, Hg_2Cl_2) solution was the internal reference solution. Mercury (I) chloride was purchased from VWR Scientific International (UK). The response of the calcium-specific electrode (Ca-ISE) was obtained by a Cole-Parmer calcium ISE electrode double-junction, where a potassium chloride solution was the internal reference solution and was purchased from Cole-Parmer Instrument Company (USA). The electromotive force (EMF) from the electrodes were registered by an Accumet AB15+ pH/mV benchtop meter with an ATC probe purchased from Cole-Parmer (USA). A fresh stock solution of NaDS above the CMC was prepared to avoid hydrolysis of the NaDS. Specific concentrations of NaDS solutions without the presence of CaCl_2 were prepared by addition of deionized water. The sodium ion in the intermicellar solution was monitored by a sodium electrode. For NaDS solutions containing CaCl_2 , the solution was diluted using a CaCl_2 solution at the same concentration level as present in the NaDS solution to maintain a constant divalent ion concentration as the solution background while the NaDS was diluted continuously. The response from the calcium electrode was registered by an ion meter until the solution passed below the CMC as the solution concentration decreased. The activity measurement was performed in a 300-mL jacketed vessel with the system temperature being held constant at 30°C by a temperature-controlled water bath and monitored by an ATC probe. The solution was agitated by a magnetic stirrer with a constant rotational speed. EMF can be used to calculate the activity of ion species of interest through the use of the Nernst equation. The activity of sodium and calcium ions (a_i) was calculated using the following equation (Bockris and Reddy, 1970):

$$\log a_i = \frac{0.4343F}{RT} (E_i - E_{i,0}) \quad (2.15)$$

where F is the Faraday constant, R is the universal gas constant and T is the absolute temperature. E_i is the EMF of the solution at any moment and $E_{i,0}$ is a constant depending on the type of reference electrode and the filling solution. The value of $E_{i,0}$ can be determined by projecting the following equation backward to the intercept (Robinson and Stokes, 1959):

$$\Delta_i = \frac{0.4343F}{RT} E_i - \log[C_i] \quad (2.16)$$

where C_i is the concentration of cation of interest, so at the intercept ($C_i = 0$),

$$E_{i,0} = \frac{RT}{0.4343F} \lim_{C \rightarrow 0} \Delta_i \quad (2.17)$$

The plot of activity of sodium ions in the intermicellar solution as a function of surfactant concentration can be used to predict the degree of counterion binding to the charged surface of the micelle surface. Also, the activity of calcium ions in the intermicellar solution at different CaCl_2 concentrations in solution can be used to predict the degree of calcium ion binding to micelle.

2.5 Results and Discussion

2.5.1 Measurement of CMC and Micelle Composition in Mixed Surfactant Systems

Typical plots of surface tension vs. logarithmic total surfactant concentration ($\log C_t$) are shown in Figure 2.1 at 30°C and varying mole fractions; NaDS(1)-NaOBS(2) mixtures are shown in Figure 2.1(a) and NaDS(1)-NaDeS(2) mixtures in Figure 2.1(b). It is seen that the surface tension decreases monotonically with increasing surfactant concentration in all pure and mixed systems at low concentrations. At the CMC there is a discontinuous change in slope in the surface tension curve due to the formation of micelles. It should be noted that the slope above the CMC for the mixed systems shows a slight increase in surface tension, which indicates a change in composition and possibly excess surface concentration at the air-liquid interface (Takehashi, *et al.*, 2004; Sugihara, Nagadome, Oh, and Ko, 2008). The surface tension of the pure NaDeS solution is higher than that of NaDS because efficiency in the surface tension reduction increases as the number of carbon atoms in the hydrophobic group decreases (Rosen, 2004).

The surface excess according to the Gibbs adsorption isotherm can be estimated from the slope of the relationship between surface tension and the total surfactant concentration at concentrations just below the CMC. Data related to the surface energy, mean molecular area, and minimum surface free energy are tabulated in Table 2.1. The surface excess changes slightly with variations in the mole fraction. In addition, the value of the mean molecular area, a_m has been calculated in this work. The lower the value of surface energy, the more thermodynamically stable the surface which is formed (Sugihara, *et al.*, 2003).

Table 2.1 Typical thermodynamic data of micellization for two mixed systems of NaDS: (a) with NaOBS; (b) with NaDeS in aqueous solution at 30°C.

System	α_1	CMC (mM)	γ_{CMC} (mN/m)	Γ_t (10^{-6} mole/m ²)	a_m (\AA^2 /molecule)	$G_{\min}^{(S)}$ (kJ/mole)
NaDS/NaOBS	0.00	12.6*	40.9	3.45	48.2	1.19
	0.25	10.7	31.5	4.05	41.0	0.78
	0.50	9.70	34.3	2.58	64.4	1.33
	0.75	8.50	36.3	2.87	57.9	1.27
	1.00	7.83*	38.7	3.02	55.0	1.28
NaDS/NaDeS	0.00	31.6*	36.0	3.14	52.9	1.15
	0.25	14.5	33.2	5.56	29.9	0.60
	0.50	9.80	32.8	5.55	29.9	0.59
	0.75	8.40	34.9	4.43	37.5	0.79
	1.00	7.83*	38.7	3.02	55.0	1.28

Remark: * Data for the pure systems (Dao, Bee, and Treiner, 1998; Hines, 1996; Tsunoda and Sasaki, 1963).

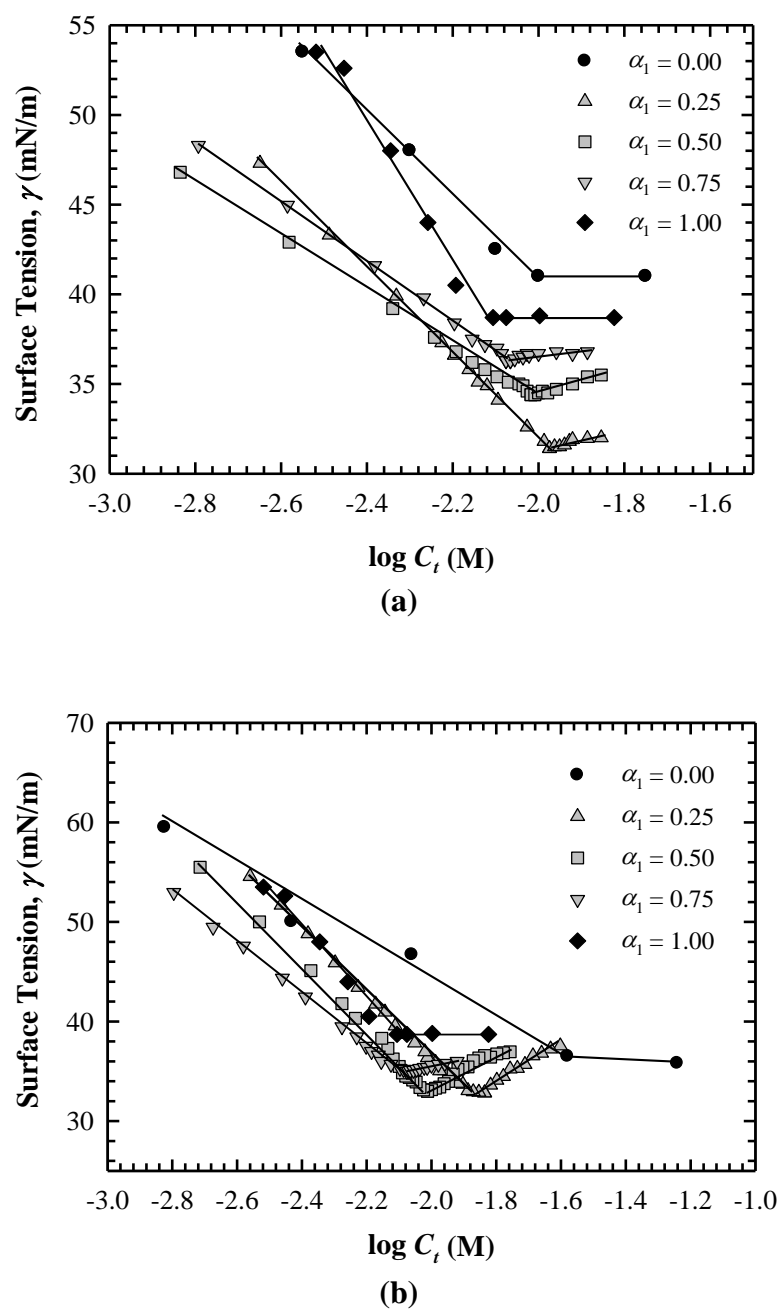
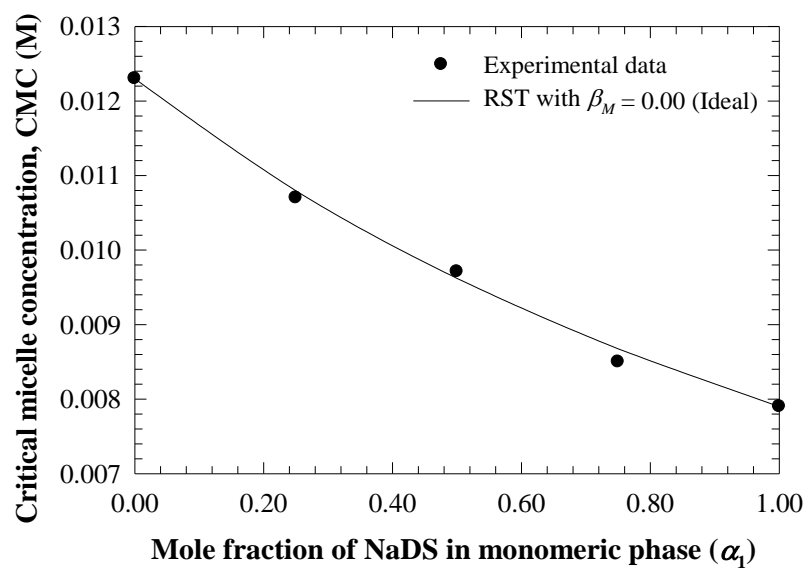


Figure 2.1 Plots of surface tension (γ) as a function of logarithmic concentration ($\log C_t$) at 30°C. (a) represents the NaDS/NaOBS system and the two related pure systems; (b) represents the NaDS/NaDeS system and the two related pure systems.

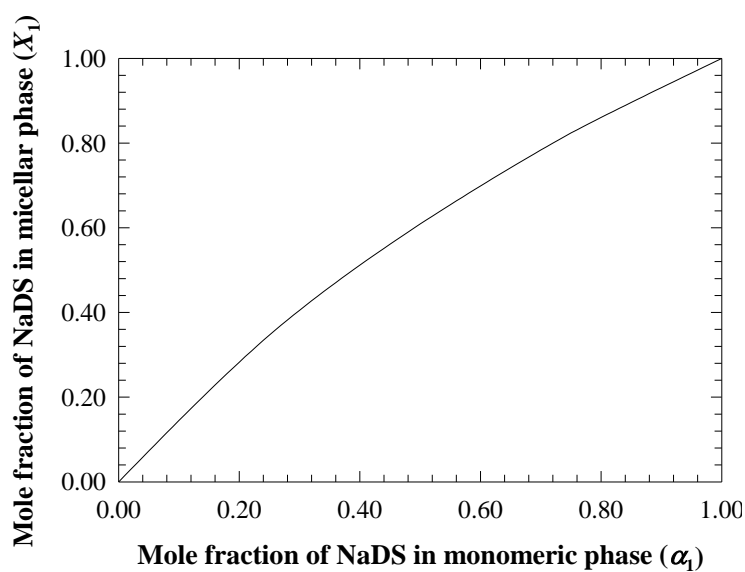
2.5.2 Fitting of Experimental CMCs with Regular Solution Theory and Prediction of Micelle Compositions

Experimental data for the CMC as a function of the surfactant composition of the mixtures are shown in Figure 2.2(a) for NaDS/NaOBS, and 2.3(a) for NaDS/NaDeS. Figures 2.2(b) and 2.3(b) show the mole fraction of NaDS in the micellar phase (X_1) as a function of the mole fraction of NaDS in the liquid phase on a solvent-free basis (α_1) at 30°C for the systems NaDS/NaOBS and NaDS/NaDeS respectively. Thermodynamic parameters for the binary mixed anionic surfactant systems are tabulated in Table 2.2.

Regular solution theory provides a powerful tool to treat nonideal binary anionic surfactant mixtures resulting in a good model for the CMC values in both systems studied here. The regular solution interaction parameter is normally assumed to be constant over the entire range of composition (Holland and Rubingh, 1983) but may have a dependence on temperature (Treiner, Khodja, and Fromon, 1987). In some instances, the interaction parameter has been dependent on micellar composition (Crisantino, Lisi, and Milioto, 1994; Holland and Rubingh, 1983; M.J. Rosen and Zhao, 1983; Shiloach and Blankschtein, 1998; Treiner, *et al.*, 1987). Thus, the interaction parameter is normally determined as the mean value across a range of composition (Schulz, *et al.*, 2006). The interaction parameters can be approximated from a series of equations by Rubingh's approach, which is described earlier in the theoretical section. The best fit for the interaction parameters are 0.00 ± 0.1 and -1.05 ± 0.2 for the NaDS/NaOBS and NaDS/NaDeS systems respectively. Given the uncertainty in interaction parameter, the NaDS/NaOBS system acts as an ideal mixture.

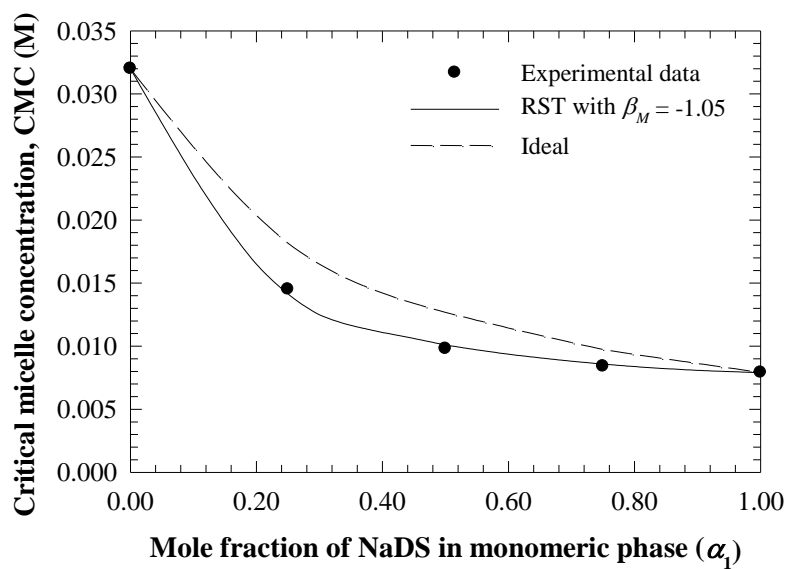


(a)

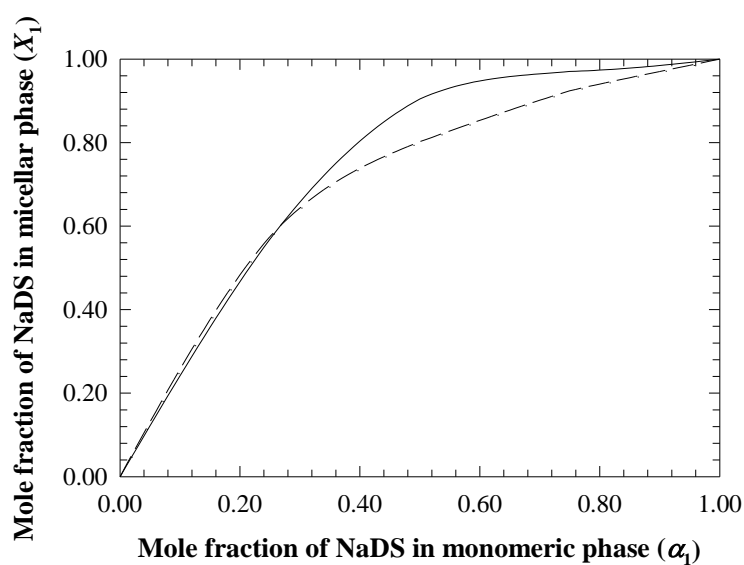


(b)

Figure 2.2 (a) The dependence of CMC on the mole fraction of NaDS in the monomeric phase (α_1) (b) Plot of the mole fraction of NaDS in the micellar phase (X_1) as a function of α_1 for the NaDS/NaOBS system at 30°C.



(a)



(b)

Figure 2.3 (a) The dependence of CMC on the mole fraction of NaDS in the monomeric phase (α_1). (b) Plot of the mole fraction of NaDS in the micellar phase (X_1) as a function of α_1 for the NaDS/NaDeS system at 30°C.

Table 2.2 Thermodynamic parameters of mixed micellization obtained from regular solution theory for anionic/anionic surfactant systems in aqueous solution at 30°C

System	α_1	X_1	$\gamma_{1,M}$	$\gamma_{2,M}$	β_M	Fitted β_M
NaDS/NaOBS	0.00	0.0000	-	1.0000	-	0.00 ± 0.1
	0.25	0.3467	1.0000	1.0000	-0.0815	
	0.50	0.6089	1.0000	1.0000	+0.1207	
	0.75	0.8237	1.0000	1.0000	-0.1397	
	1.00	1.0000	1.0000	-	-	
NaDS/NaDeS	0.00	0.0000	-	1.0000	-	-1.05 ± 0.2
	0.25	0.5688	0.8226	0.7120	-0.9129	
	0.50	0.9045	0.9905	0.4238	-1.3639	
	0.75	0.9703	0.9991	0.3506	-1.3835	
	1.00	1.0000	1.0000	-	-	

A negative interaction parameter indicates attractive interactions in the mixed micelle in the NaDS/NaDeS system, and with no interaction between the DS⁻ and OBS⁻ ions in the mixed micelle since the interaction parameter is essentially zero. The latter result has been reported elsewhere (Soontravanich S., and Scamehorn, 2010). DS⁻ and OBS⁻ tails have similar size; although the former is totally aliphatic while the latter has an aromatic portion. In this case, this aliphatic-aromatic difference does not affect the ideality of the mixture with respect to micelle formation. Although the only difference between DS⁻ and DeS⁻ is a difference in length of two carbon atoms in their tail, mixtures of homologous surfactants have been proven to be nonideal (Schulz, *et al.*, 2006) and so the non-ideality in the NaDS/NaDeS system is not surprising. The in-depth study and literature review reported by Schulz, *et al.* (2006)

shows that the interaction parameter is always negative, i.e. introducing disorder into the micelle by varying chain length of the surfactant improves the ability to form micelles. However, the absolute value of the interaction parameter found here is rather large, about a factor of 2 larger than for typical homologous anionic surfactants differing only by two carbon units. We do not have a good explanation for this large negative interaction parameter.

Regular solution theory also can be used to calculate equilibrium surfactant compositions in the monomeric and micellar phases. The compositions of the mixed micelle as a function of the singly dispersed molecules for the two systems are shown in Figure 2.2(b) and 2.3(b). In systems with a negative value of the interaction parameter the phase equilibrium diagram will have a positive deviation from the ideal line due to the cohesive forces of like molecules.

However the CMC values vary over a wide concentration range at a specific temperature when electrolyte concentration is varied. Further, determination of the CMC is not without uncertainty, and the uncertainty differs depending on the method used. Further, small amounts of impurities can alter the CMC as well by inducing micellization. The CMC value of NaDS in aqueous solution at 30°C has been given in the range of 0.0067-0.0082 M depending on the method used, including values of 0.0071 M by calorimetry (da Silva, Loh, and Olofsson, 2004), 0.0076-0.0079 M by activity measurement via ISE (Sasaki, *et al.*, 1975; Umlong and Ismail, 2007), 0.0067-0.0078 M by tensiometer (Rodriguez, Lowery, Scamehorn, and Harwell, 2001; Umlong and Ismail, 2007), 0.0080 M by a light scattering technique (Winnik, Bystryak, Chassenieux, Strashko, Macdonald, and Siddiqui, 2000), and 0.0078-0.0081 M by conductimetry (Dutkiewicz and Jakubowska, 2002; Umlong and

Ismail, 2007) at 25-30°C. The range of measured CMC values for the NaDS system is partly due to the problem of hydrolysis of NaDS (Hines, 1996; Lunkenheimer and Czichocki, 1993; Mysels, 1986).

The plots of the evolution of solution conductivity as a function of total surfactant concentration for NaDS, NaOBS and NaDeS at 30°C are shown in Figure 2.4 to Figure 2.6. If the conductivity is plotted against the surfactant concentration, the point that the slope is discontinuous is the CMC for the measured surfactant system. The break in the curve is due to the reduction in the conductivity of the solution due to a fraction of the dissociated ionic species being neutralized after the commencement of micellization. The CMC values for aqueous solutions of NaDS, NaOBS, and NaDeS are 0.0079, 0.0122, and 0.0320 M respectively at 30°C. The experimental CMC values by conductivity method are consistent with other values in the literature (Dao, *et al.*, 1998; Hines, 1996; Tsunoda and Sasaki, 1963).

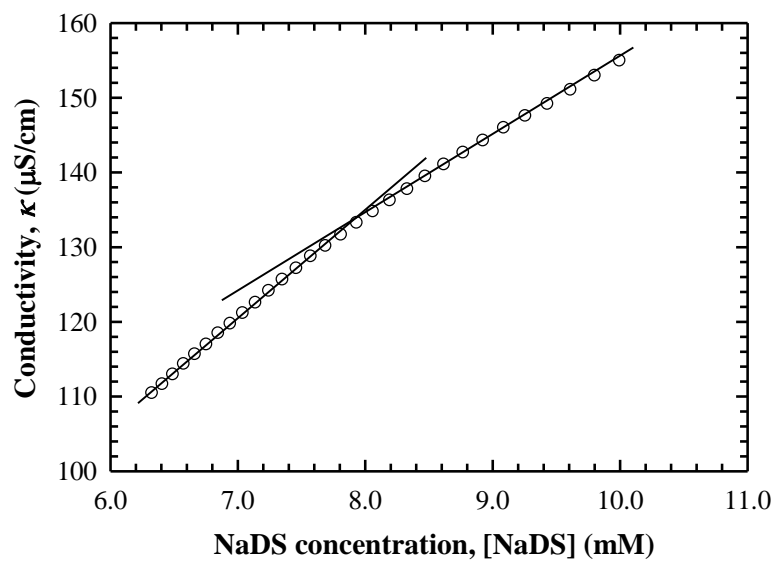


Figure 2.4 Plots of evolution of conductivity of NaDS solution as a function of concentration at 30°C.

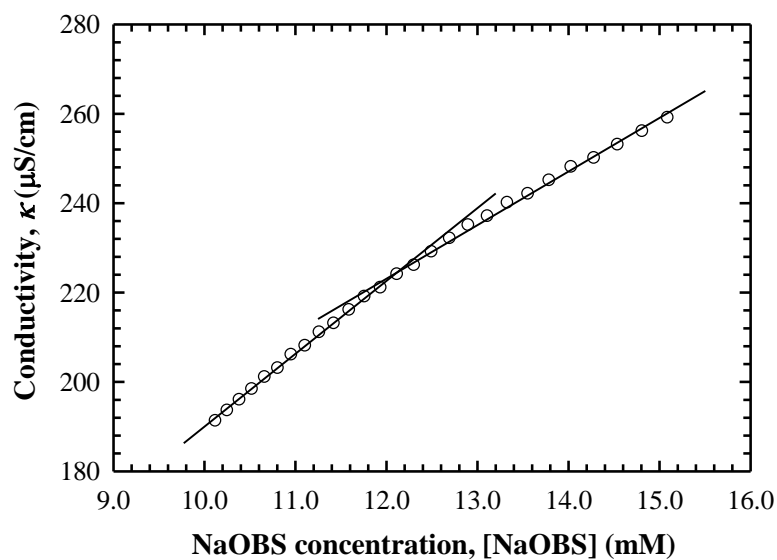


Figure 2.5 Plots of evolution of conductivity of NaOBS solution as a function of concentration at 30°C.

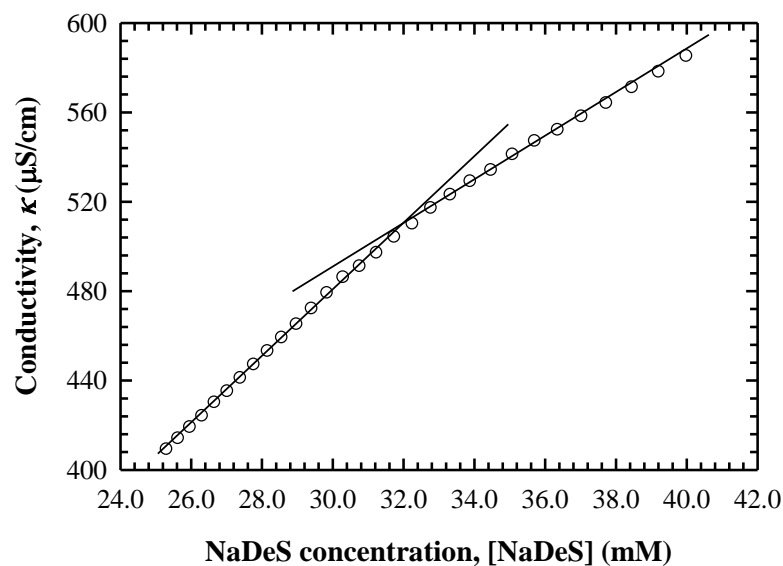


Figure 2.6 Plots of evolution of conductivity of NaDeS solution as a function of concentration at 30°C.

2.5.3 The Effect of Counterions in Solution on the CMC

Previous studies have shown that the CMC of anionic surfactants depends strongly on the concentration of monovalent counterion present in the bulk solution (Bockris and Reddy, 1970; Dutkiewicz and Jakubowska, 2002; Stellner and Scamehorn, 1989a), but trace divalent cations by experiment were assumed to have no significant effect on the CMC (Rodriguez and Scamehorn, 1999; Shinoda, Nakagawa, K., and Shinoda, 1963; Stellner and Scamehorn, 1989a). The effect of the unbound sodium ion concentration on the CMC of NaDS at different temperatures is shown in Figure 2.7, and the effect of the calcium ion on the CMC is shown in Figure 2.8.

The plots show that the CMC depends strongly on the unbound sodium ion concentration as described by the Corrin-Harkins relationship, but depends only slightly on the calcium ion concentration at the low to moderate concentrations used in the present study, as also noted in a previous study (Shinoda, *et al.*, 1963).

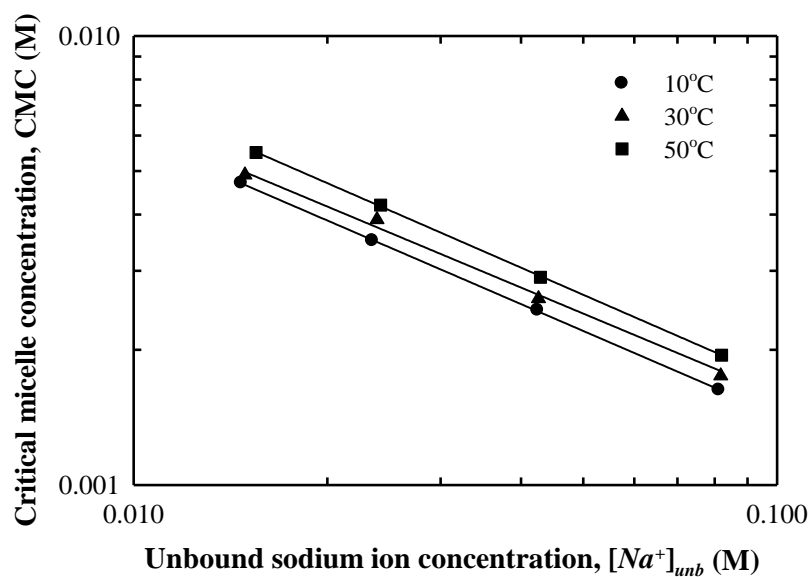


Figure 2.7 Plots of the critical micelle concentration of NaDS as a function of unbound sodium ion concentration at different temperatures.

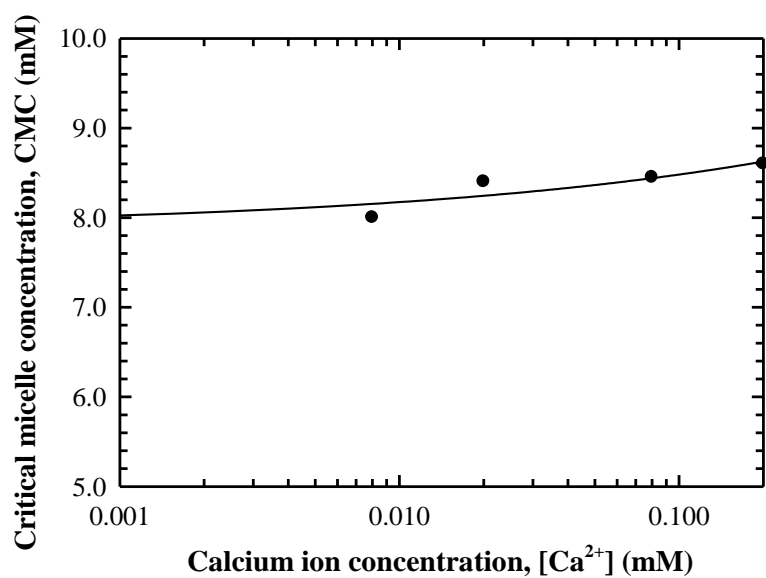


Figure 2.8 The effect of calcium ion present in the solution on the CMC of NaDS at 30°C. The CMC for calcium-free NaDS solutions is at 7.9 mM at 30°C.

The Corrin-Harkins parameters for the dependence of the CMC on the sodium ion concentration can be estimated from the intercept and slope of the plots in Figure 2.7. K_g is equal to 0.618, 0.599, and 0.625 for 10, 30, and 50°C, respectively. Previously, this parameter is only available in the literature at 30°C, thus this study has increased the range of knowledge about this parameter. Stellner and Scamehorn (1989a) reported $K_1 = -8.513$ and $K_g = 0.698$ while Rodriguez and Scamehorn (1999) reported $K_1 = -8.317$ and $K_g = 0.704$. It should, however, be noted that K_g is relatively constant throughout the range of temperature examined: thus, an average value is commonly used. Our average K_g value is slightly lower than in the literature; however, it does not make a significant difference in surfactant partitioning between monomer and micelle, as shown by Figure 2.9.

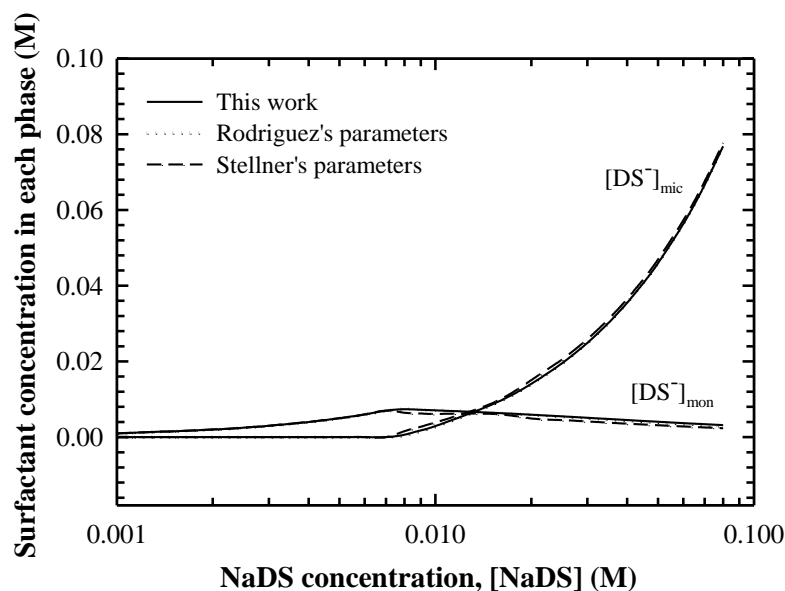


Figure 2.9 Plots of dissociated species concentration of NaDS in aqueous solution at 30°C predicted by several proposed data.

Plots such as that shown in Figure 2.7 can be used to determine the K_1 parameter in the Corrin-Harkins equation as a function of temperature. The plots of K_1 and the CMC (determined by the conductivity method) of NaDS as a function of temperature are shown in Figure 2.10. Consequently, the CMC value can be predicted over a range of temperature and are relatively consistent with the previous study (Shah, Jamroz, and Sharif, 2001).

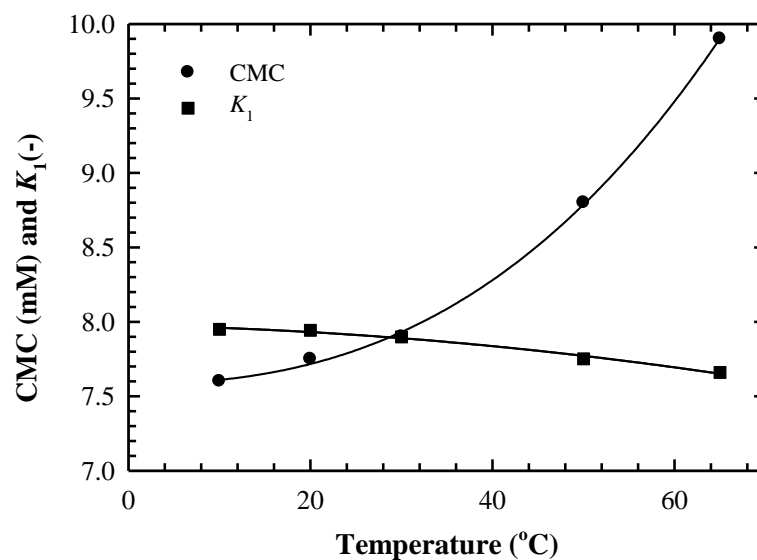


Figure 2.10 Critical micelle concentration and K_1 parameter as a function of temperature for NaDS in aqueous solution.

2.5.4 Measurement and Modeling of Counterion Binding to the Micelle

The degree of counterion binding to the micelle is defined as the ratio of amount of neutralized charges in a micelle to the total amount of surfactant molecules in the micellar phase (Stellner and Scamehorn, 1989a). Hence the fractional bindings of sodium and calcium ions to the anionic surfactant micelle are defined as follows:

$$\beta_{Na^+} = \frac{[Na^+]_{tot} - [Na^+]_{unb}}{[NaS]_{tot} - [S^-]_{mon}} = \frac{[Na^+]_b}{[S^-]_{mic}} \quad (2.18)$$

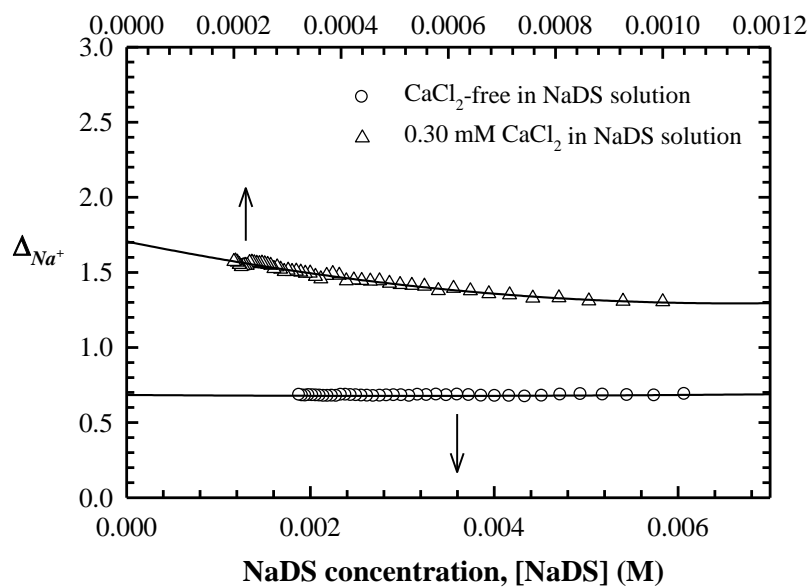
$$\beta_{Ca^{2+}} = \frac{2([Ca^{2+}]_{tot} - [Ca^{2+}]_{unb})}{[NaS]_{tot} - [S^-]_{mon}} = \frac{2[Ca^{2+}]_b}{[S^-]_{mic}} \quad (2.19)$$

where $[Na^+]_b$ and $[Ca^{2+}]_b$ are the bound counterion concentrations, $[Na^+]_{unb}$ and $[Ca^{2+}]_{unb}$ are the unbound counterion concentrations, $[NaS]_{tot}$, $[S^-]_{mon}$, and $[S^-]_{mic}$ are the total anionic surfactant, anionic surfactant concentration in the solution phase (as monomers), and in the micellar phase, respectively. The fraction of charge negation due to the calcium ion binding to the micelle is twice that of the sodium ion according to the charges neutralized by the calcium ion, and this is taken into account in the definition of the counterion binding parameter.

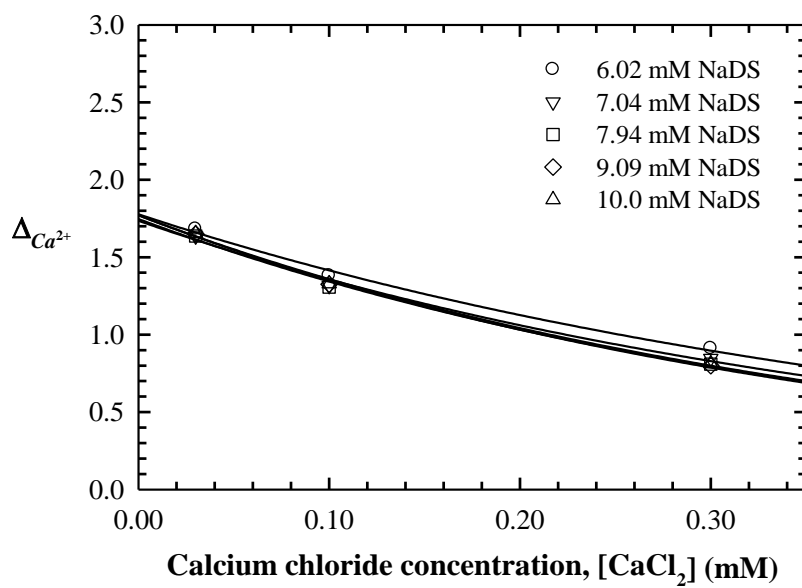
The activity of the sodium and calcium ions is obtained from equations (2.15) - (2.17). The extrapolations to obtain the parameter $E_{i,0}$, required for the application of the Nernst equation, are shown in Figure 2.11. The value of $E_{i,0}$ depends on the type of reference solution and the electrode. Figure 2.11(a) shows the value of Δ_{Na^+} for the sodium-ion specific electrode as the background solution varies

with respect to the NaDS concentration for pure NaDS and 0.30 mM CaCl_2 in NaDS solution, and can be used to estimate $E_{i,0}$ for the sodium measurement. Figure 2.11(b) shows the value of $\Delta_{\text{Ca}^{2+}}$ for the calcium-ion specific electrode as the background solution varies with respect to the CaCl_2 concentration for several NaDS contents, which can be used to estimate $E_{i,0}$ for the calcium measurement.

The unbound counterion concentrations ($[\text{Na}^+]_{\text{unb}}$ and $[\text{Ca}^{2+}]_{\text{unb}}$) can be estimated by the Nernst equation, and a mass balance was used to calculate the bound counterion concentrations ($[\text{Na}^+]_b$ and $[\text{Ca}^{2+}]_b$) from the total ion concentrations. An accurate value of the dodecyl sulfate concentration in the monomeric phase ($[\text{DS}^-]_{\text{mon}}$) can be predicted by use of the Corrin-Harkins expression; the dodecyl sulfate concentration in micellar phase ($[\text{DS}^-]_{\text{mic}}$) can be obtained from a mass balance. Once the ion contents of the micelles have been determined, counterion binding parameters can be calculated using equations (2.18) and (2.19).



(a)



(b)

Figure 2.11 Extrapolation of the Δ_i function to obtain $E_{i,0}$ based on equation (2.16). (a) Na-ISE (b) Ca-ISE

The plots of the activity of the species present in the systems studied as a function of NaDS concentration are shown in Figure 2.12 - 2.13. The break in the plots of logarithm of the activity of counterion against the logarithm of the NaDS concentration indicates the formation of micelle. The activity of sodium and calcium ions changes due to the micellization as the counterion binding to the micelle. The concentration of the free molecules decreases above the CMC resulting in a curve with a discontinuous value of the slope.

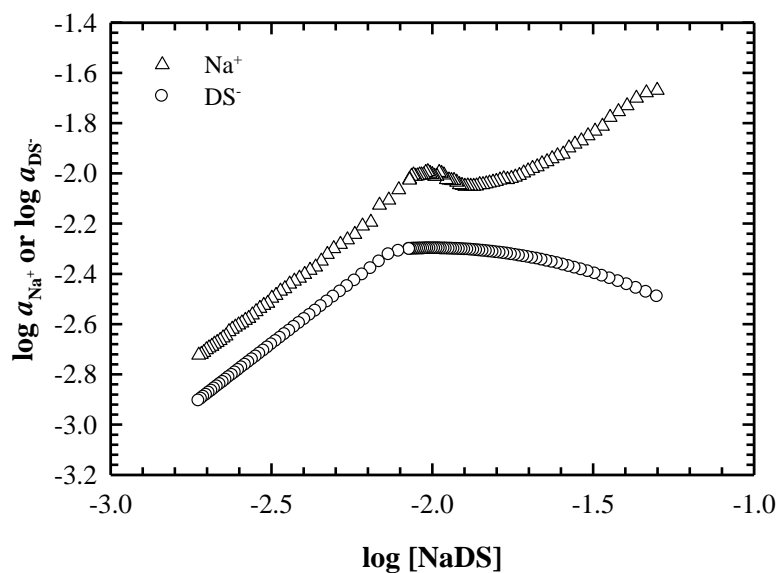


Figure 2.12 The activity of sodium ion, and dodecyl sulfate monomer (Sasaki, *et al.*, 1975) present in the system studied as a function of the NaDS concentration at 30°C.

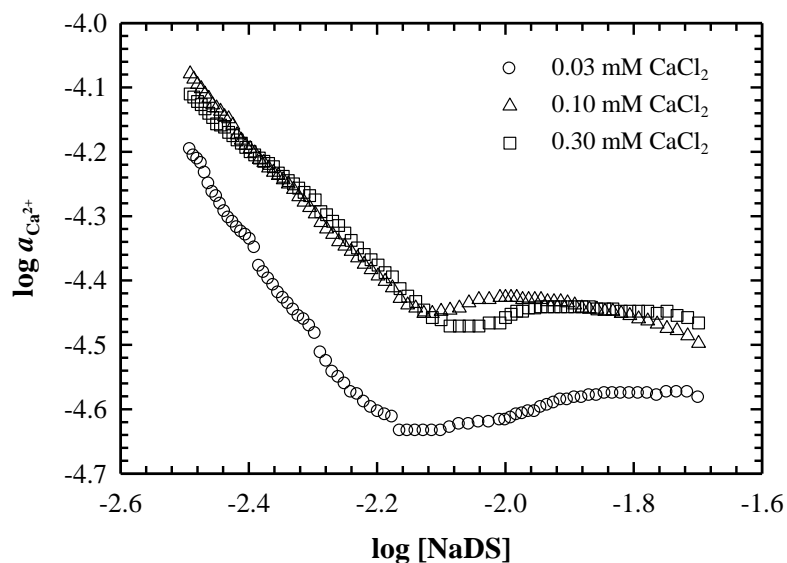


Figure 2.13 The activity of calcium ion present as a function of the NaDS concentration with varying CaCl_2 concentration at 30°C .

Curves of fractional counterion binding to the micelle based on the ISE results are shown in Figure 2.14. The plots can be used to determine whether the sodium ion binding to micelle is constant or not, as discussed in earlier studies (Rathman and Scamehorn, 1984; Stellner and Scamehorn, 1989a). The parameter has been reported as constant, approximately 0.67, when measured at a concentration of approximately 30 mM NaDS, which is far above the CMC. The counterion binding to the micelle results for pure NaDS solutions in Figure 2.14 reveal that the change in the counterion binding is relatively strong at the commencement of the micellization phenomenon, resulting in a steep curve up to a binding parameter of 0.80 at 10 mM. The average value of the counterion binding parameter from the plots is 0.65 and 0.67 for the EMF method and the Corrin-Harkins relationship, respectively, which is in good quantitative agreement with the value given at 30 mM. The review by Sasaki *et al.* (1975) reported that data from a literature survey on sodium ion binding to the micelle

was quite scattered, ranging between 0.46-0.86. This is likely due to differences in the technique and the purity of NaDS used, a problem also seen in CMC measurements for instance (Hines, 1996; Lunkenheimer and Czichocki, 1993; Mysels, 1986). Moreover, earlier studies proposed that the existence of the linearity in Corrin-Harkins plot can be reconciled using a model to directly estimate the *apparent* counterion binding onto the micelle parameter as the slope K_g is equivalent to β_{Na^+} (Evans, Mitchell, and Ninham, 1984). In this study, the value of K_g (0.59-0.63) is roughly equivalent to the equilibrium value of β_{Na^+} , 0.67. Recently, the effects of self-assembly process of ionic surfactants into micelles was also investigated by the atomistic simulations, it showed the total degree of counterion binding in NaDS solution is around 67% in the absence of salt (Jusufi, Hynninen, Haataja, and Panagiotopoulos, 2009).

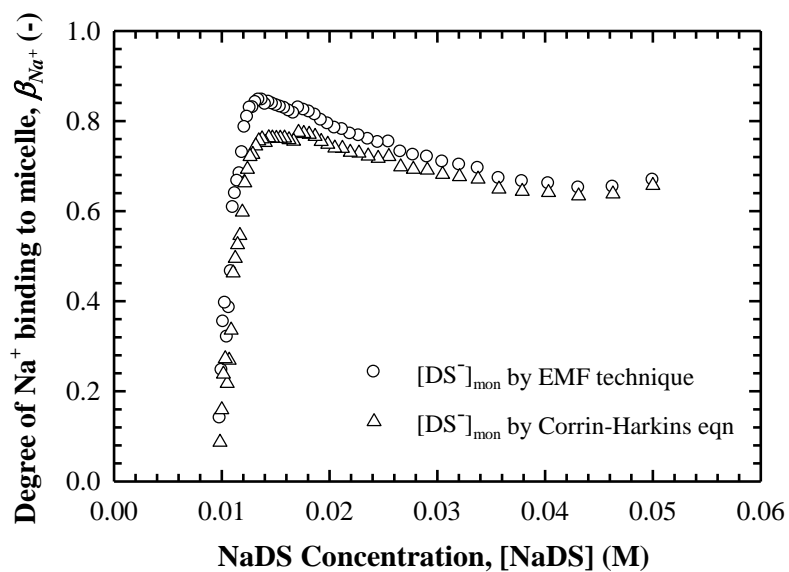


Figure 2.14 Variation of the degree of sodium ion binding to micelle parameter (β_{Na^+}) as a function of NaDS concentration at 30°C.

The degree of calcium ion binding onto the micelle at 30°C, as a function of the NaDS concentration and for different $CaCl_2$ concentrations is shown in Figure 2.15. As the NaDS concentration increases, the calcium ion binding coefficient decreases while the total counterion binding remains approximately constant.

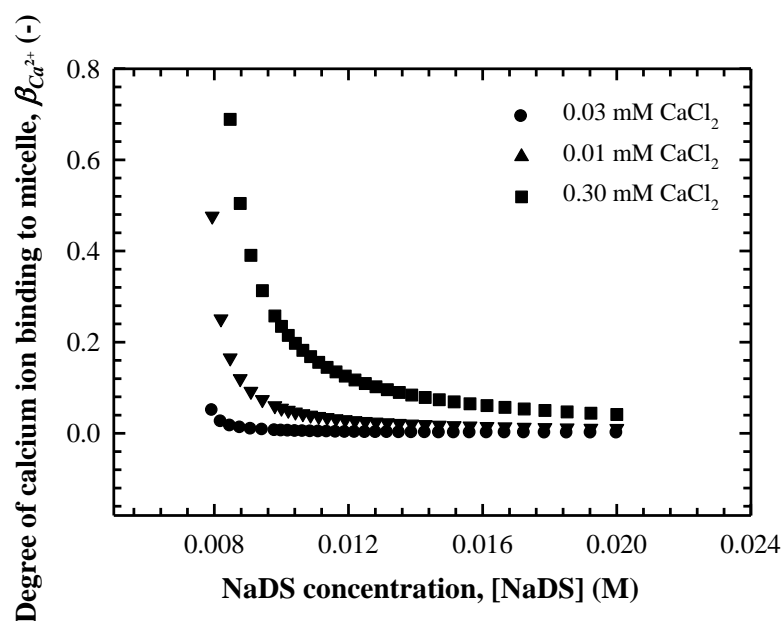


Figure 2.15 Variation of the degree of calcium ion binding to micelle parameter ($\beta_{Ca^{2+}}$) as a function of NaDS concentration at 30°C at different CaCl₂ concentrations in the solution.

This behavior has previously been described by a competitive adsorption to the micelle surface between the different cations (Paton-Morales and Talens-Alesson, 2002). The authors of this study have suggested that at the commencement of the micellization phenomenon, dissociated sodium ions do not occupy much of the surface of the micelle compared to calcium ions. When the NaDS is added continuously, the binding is dominated by sodium ions as the nature of a monovalent species allows it to occupy the micelle surface of the monovalent anionic surfactant more effectively (Paton-Morales and Talens-Alesson, 2002); hence, the binding of the divalent cation to the micelle decreases as the NaDS concentration increases.

Binding is dependent on the concentration of CaCl_2 , as well as on the total NaDS concentration. In practice, some previous studies have assumed that the calcium ion binding remains constant at about 0.20 and the total counterion binding ($\beta_T = \beta_{\text{Ca}^{2+}} + \beta_{\text{Na}^+}$) is constant at 0.65 independent of changes in NaDS concentration (Rodriguez, *et al.*, 2001; Stellner and Scamehorn, 1989a). The current work shows that the counterion binding is not constant as a function of the NaDS concentration.

For further evidence about the competitiveness of the monovalent and divalent cation binding to micelle, Figure 2.16 shows the fraction of counterion binding to the micelle for both sodium and calcium ions with respect to the chemical equilibrium model which will be discussed in the next topic. For 0.30 mM CaCl_2 present in NaDS solution system, the degree of sodium ion binding to micelle (β_{Na^+}) is approximately equal to 0.56 which is near the average value. The total degree of counterion binding to the micelle for NaDS with 0.30 mM CaCl_2 can be determined by the combined sodium and calcium counterion binding, $\beta_T = 0.56 + 0.16 = 0.72$, which is close to the assumed total counterion binding of 0.65. Note that the concentration of bound calcium ions is 0.08 times that of the total surfactant content of the micelle, but this negates a fraction of 0.16 of the charge of the surfactant in the micelle. Consequently, this data suggests that the total fraction of negative charges from the surfactant molecule in the micelle neutralized by counterion binding to the micelle is approximately constant.

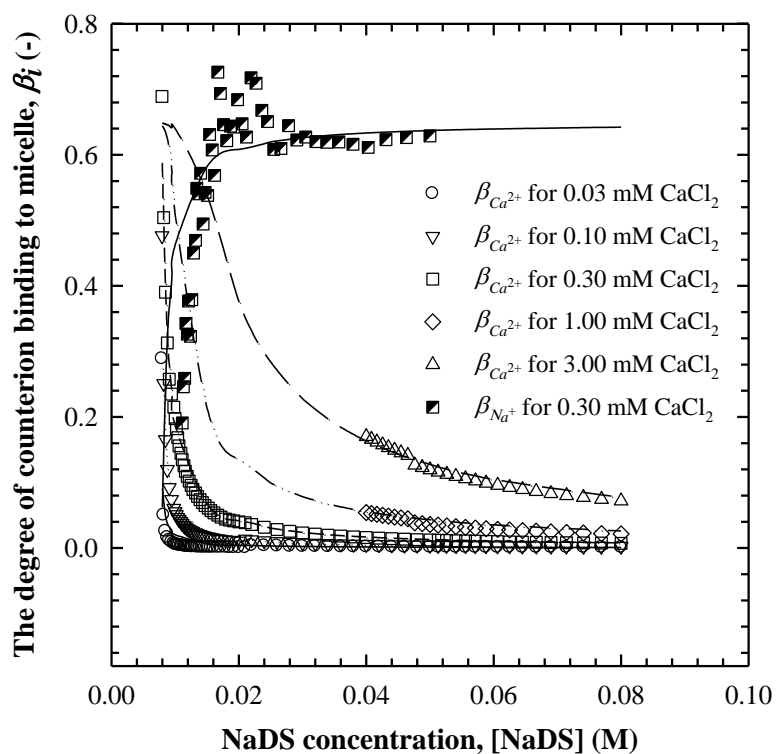


Figure 2.16 Variation of the counterion binding parameters as a function of NaDS concentration at 30°C for several systems. All lines fitting the experimental data in this figure are obtained from the chemical equilibrium model; equation (2.25), with constants $K = 0.015$ and $\beta_T = 0.65$.

To determine whether the total counterion binding was constant with respect to changes in counterion compositions a study was performed to determine total counterion binding over a range of CaCl_2 concentrations using conductivity. The degree of counterion binding was obtained from the ratio of the slopes of the conductivity as a function of NaDS concentration. Figure 2.17 shows experimental data of the total fraction of counterion binding for NaDS solution as the CaCl_2 concentration increases. Due to a difference in the fundamental treatment of

micellization, the results obtained by the conductivity technique are slightly lower than those from the EMF technique. However the results show that the total counterion binding to the micelle can be assumed to be constant, as found experimentally using two different techniques and theoretical treatments.

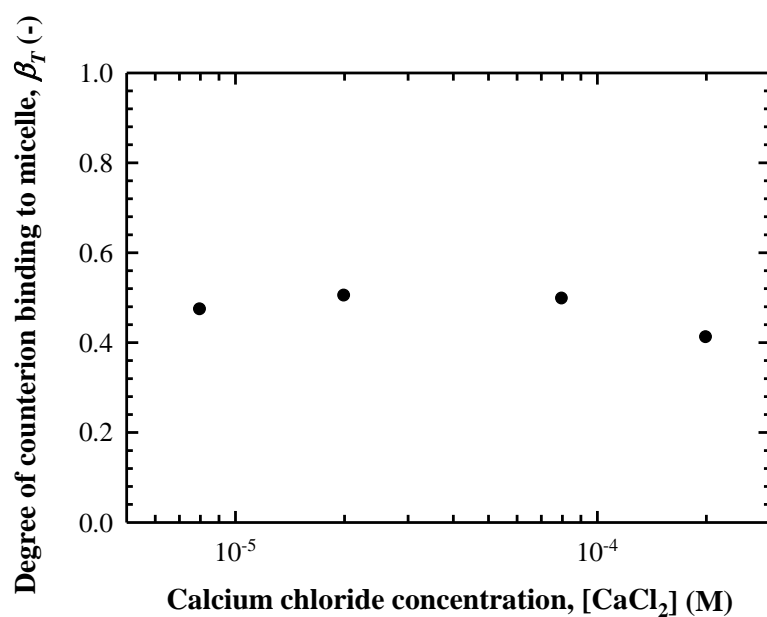
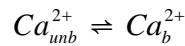


Figure 2.17 Total degree of counterion binding to micelle as a function of CaCl_2 concentration in NaDS solution at 30°C.

2.5.5 A Model of Sodium and Calcium Ions Binding to the Micelle

The competitive counterion binding to the micelle can be modeled using a chemical equilibrium model. The model considers only two factors, a chemical equilibrium between unbound counterion and counterion which is bound to the surface of the micelle, and a saturation level of counterion binding, β_T , beyond which level extra charge negation of the surface of the micelle is not possible. Initially, consider the system where the unbound calcium ions in solution are in equilibrium with the counterions bound to the surface of the micelle:



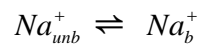
This chemical reaction can be thermodynamically modeled via the activity based equilibrium constant:

$$K_{Ca^{2+}} = \frac{a_{Ca^{2+},b}}{a_{Ca^{2+},unb}} \quad (2.20)$$

In the absence of further knowledge, and since the solution is relatively dilute we can assume that the activity of each species is equal to its concentration, or that the ratio of the activities is equal to the ratio of the concentrations:

$$K_{Ca^{2+}} = \frac{[Ca^{2+}]_b}{[Ca^{2+}]_{unb}} \quad (2.21)$$

A similar set of equations can be written for the sodium ion:



and

$$K_{Na^+} = \frac{a_{Na^+,b}}{a_{Na^+,umb}} \quad (2.22)$$

In this case it is evidently not suitable to assume that the concentration of the unbound sodium ions is equal to their activity. This would suggest that the counterion binding of sodium is finite at the CMC, where there should be a significant amount of sodium ions in solution, due to NaDS monomer at the CMC. In fact, experimentally the results show almost zero sodium binding to the micelle at the CMC. Zero binding can be rationalized if surfactant ions in solution significantly more strongly associate with the sodium ions than the calcium ions, thus lowering the activity of the sodium in solution. The surfactant appears to preferentially associate with sodium ions in solution, perhaps because they are both monovalent ions. Since sodium binding is essentially zero at the CMC, we should define the unbound sodium activity as:

$$a_{Na^+,umb} = [Na^+]_{umb} - [DS^-]_{mon} \quad (2.23)$$

Thus, the sodium binding equilibrium is:

$$K_{Na^+} = \frac{[Na^+]_b}{[Na^+]_{umb} - [DS^-]_{mon}} \quad (2.24)$$

Dividing the two equilibrium relations and rearranging gives:

$$\frac{[Na^+]_b}{[Na^+]_{umb} - [DS^-]_{mon}} = K \frac{[Ca^{2+}]_b}{[Ca^{2+}]_{umb}} \quad (2.25)$$

where $K = K_{Na^+} / K_{Ca^{2+}}$

A second equation is needed to fully describe the system, and that is the total counterion binding equation as seen as equation (2.18) + (2.19), which we have measured to be approximately constant at a value of 0.65. This gives:

$$\beta_T = \beta_{Ca^{2+}} + \beta_{Na^+} = 0.65 \quad (2.26)$$

Fitting the data gives an equilibrium constant of 0.015, and this fits all the counterion binding data measured very well, as shown in Figure 2.16. Application of this equilibrium model fitted to our data calls into question the validity of the assumption that the monovalent ion is more effectively able to bind to the micelle. This can be explained by the higher unbound sodium ion concentration as the NaDS concentration increases above the CMC which is due to dissociation of sodium from the surfactant. Even at $CaCl_2$ concentrations of 0.3 mM the concentration of sodium ions in the solution exceeds that of calcium ions in solution by more than an order of magnitude for concentrations of NaDS above the CMC. Where the bound sodium ion concentration exceeds the bound calcium ion concentration, the difference is much smaller than an order of magnitude. This indicates that calcium ions more strongly partition onto the surface of the micelle than sodium ions. This conclusion is verified

by the magnitude of the equilibrium constant ratio ($K = K_{Na^+} / K_{Ca^{2+}} = 0.015$) determined in the current study, which shows the calcium partitioning onto the micelle is much stronger than that of sodium.

2.6 Conclusions

This research has provided experimental data and thermodynamic parameters for two binary anionic surfactant systems. The regular solution model appears to be a good model to treat thermodynamically the mixed micellization of anionic surfactants used in this work. The attractive interaction has been noted in NaDS/NaDeS in aqueous solution at 30°C; however, the NaDS/NaOBS mixture is relatively ideal. The value of the interaction parameter is much more negative for the homologous NaDS/NaDeS than has been previously found for surfactants differing only by two carbon units.

The CMC of NaDS is affected more by the concentration of the monovalent cation than that of the divalent cation, and the effect of the monovalent ion can be described by the Corrin-Harkins equation. The Corrin-Harkins parameter K_g is relatively constant throughout the range of temperature examined (10 - 50°C) at 0.61, while the parameter K_1 is a strong function of temperature.

The total fraction of counterion binding to the micelle has been investigated quantitatively and qualitatively to determine how the counterions distribute between the solution phase and the micelles. The degree of counterion binding to the micelle cannot be assumed to be constant as either the total surfactant concentration or the composition of the counterions in solution changes. In addition, mono- and divalent cations compete for the negative charges of the micelle, but the total fraction of

charges negated per micelle is approximately constant independent of the identity of the cation at high surfactant concentrations and is equal to about 0.65 at 30°C. The relative amounts of this total binding that are taken up by sodium and calcium ions can be modeled very well using a simple equilibrium model relating to unbound and bound sodium and calcium counterion activities. It is likely that the improved model of counterion binding can greatly improve the modeling of the phase precipitation boundary of the surfactants near the CMC, where currently the models under-predict the amount of CaCl_2 required to reach the precipitation phase boundary (Soontravanich S., and Scamehorn, 2010).

2.7 References

- Bakshi, M., *et al.* (2002). Mixed-micelle formation by strongly interacting surfactant binary mixtures: effect of head-group modification. **Colloid & Polymer Science** 280(11): 990-1000.
- Bandyopadhyay, A. and Moulik, S. P. (1988). Counterion binding behaviour of micelles of sodium dodecyl sulphate and bile salts in the pure state, in mutually mixed states and mixed with a nonionic surfactant. **Colloid & Polymer Science** 266(5): 455-461.
- Bockris, J. O. M. and Reddy, A. K. N. (1970). **Modern electrochemistry: An introduction to an interdisciplinary area**. New York: Plenum.
- Corrin, M. and Harkins, W. (1947). The effect of salts on the critical concentration for the formation of micelles in colloidal electrolytes¹. **Journal of the American Chemical Society** 69(3): 683-688.

- Crisantino, R., Lisi, R. D., and Milioto, S. (1994). Energetics of sodium dodecylsulfate-dodecyldimethylamine oxide mixed micelle formation. **Journal of Solution Chemistry** 23(6): 639-662.
- Cui, Z. G. and Canselier, J. P. (2001). Interfacial and aggregation properties of some anionic/cationic surfactant binary systems II. Mixed micelle formation and surface tension reduction effectiveness. **Colloid & Polymer Science** 279(3): 259-267.
- da Silva, R. C., Loh, W., and Olofsson, G. (2004). Calorimetric investigation of temperature effect on the interaction between poly (ethylene oxide) and sodium dodecylsulfate in water. **Thermochimica Acta** 417(2): 295-300.
- Dao, K., Bee, A., and Treiner, C. (1998). Adsorption isotherm of sodium octylbenzenesulfonate on iron oxide particles in aqueous solutions. **Journal of Colloid and Interface Science** 204(1): 61-65.
- Dutkiewicz, E. and Jakubowska, A. (2002). Effect of electrolytes on the physicochemical behaviour of sodium dodecyl sulphate micelles. **Colloid & Polymer Science** 280(11): 1009-1014.
- Evans, D. F., Mitchell, D. J., and Ninham, B. W. (1984). Ion binding and dressed micelles. **The Journal of Physical Chemistry** 88(25): 6344-6348.
- Haque, M. E., Das, A. R., Rakshit, A. K., and Mouliks, S. P. (1996). Properties of mixed micelles of binary surfactant combinations. **Langmuir** 12(17): 4084-4089.
- Hines, J. D. (1996). The preparation of surface chemically pure sodium n -dodecyl sulfate by foam fractionation **Journal of Colloid and Interface Science** 180(2): 488-492.

- Hoffmann, H. and Pössneck, G. (1994). The mixing behavior of surfactants. **Langmuir** 10(2): 381-389.
- Holland, P. and Rubingh, D. (1983). Nonideal multicomponent mixed micelle model. **The Journal of Physical Chemistry** 87(11): 1984-1990.
- Jusufi, A., Hynninen, A.-P., Haataja, M., and Panagiotopoulos, A. Z. (2009). Electrostatic screening and charge correlation effects in micellization of ionic surfactants. **Journal of Physical Chemistry B** 113: 6314-6320.
- Kakehashi, R., Shizuma, M., Yamamura, S., and Takeda, T. (2004). Mixed micelles containing sodium oleate: the effect of the chain length and the polar head group. **Journal of Colloid and Interface Science** 279(1): 253-258.
- López-Fontán, J. L., Suárez, M. J., Mosquera, V., and Sarmiento, F. (2000). Micellar behavior of n-alkyl sulfates in binary mixed systems. **Journal of Colloid and Interface Science** 223(2): 185-189.
- Lunkenheimer, K. and Czichocki, G. (1993). On the stability of aqueous sodium dodecyl sulfate solutions. **Journal of Colloid and Interface Science** 160(2): 509-510.
- Lunkenheimer, K. and Wantke, K. (1981). Determination of the surface tension of surfactant solutions applying the method of Lecomte du Noüy (ring tensiometer). **Colloid & Polymer Science** 259(3): 354-366.
- Mysels, K. J. (1986). Surface tension of solutions of pure sodium dodecyl sulfate. **Langmuir** 2(4): 423-428.
- Nishikido, N. (1993). Thermodynamic models for mixed micellization. In K. Ogino and M. Abe (Eds.). **Mixed surfactant systems** (pp. 32). New York: Marcel Dekker.

- Paton-Morales, P. and Talens-Alession, F. I. (2002). Effect of competitive adsorption of Zn^{2+} on the flocculation of lauryl sulfate micelles by Al^{3+} . **Langmuir** 18(22): 8295-8301.
- Podchasskaya, E. S. and Us' yarov, O. G. (2005). Binding of counterions by micelles of ionic surfactants. **Colloid Journal** 67(2): 184-188.
- Rathman, J. F. and Scamehorn, J. F. (1984). Counterion binding on mixed micelles. **The Journal of Physical Chemistry** 88(24): 5807-5816.
- Rathman, J. F. and Scamehorn, J. F. (1987). Counterion binding on mixed micelles: effect of surfactant structure. **Langmuir** 3(3): 372-377.
- Robinson, R. A. and Stokes, R. H. (1959). **Electrolyte solutions**. London: Butterworths.
- Rodriguez, C. H., Lowery, L. H., Scamehorn, J. F., and Harwell, J. H. (2001). Kinetics of precipitation of surfactants. I. Anionic surfactants with calcium and with cationic surfactants. **Journal of Surfactants and Detergents** 4(1): 1-14.
- Rodriguez, C. H. and Scamehorn, J. F. (1999). Modification of Krafft temperature or solubility of surfactants using surfactant mixtures. **Journal of Surfactants and Detergents** 2: 17.
- Rosen, M. J. (2004). **Surfactants and interfacial phenomena**: New Jersey: John Wiley and Sons.
- Rosen, M. J. and Zhao, F. (1983). Binary mixtures of surfactants. The effect of structural and microenvironmental factors on molecular interaction at the aqueous solution/air interface. **Journal of Colloid and Interface Science** 95(2): 443-452.

- Rubingh, D. N. (1979). Mixed micelle solutions. In K. L. Mittal (Ed.), **Solution chemistry of surfactants** (pp. 337-354). New York: Plenum.
- Sasaki, T., Hattori, M., Sasaki, J., and Nukina, K. (1975). Studies of aqueous sodium dodecyl sulfate solutions by activity measurements. **Bulletin of the Chemical Society of Japan** 48(5): 1397-1403.
- Schulz, P. C., Rodríguez, J. L., Minardi, R. M., Sierra, M. B., and Morini, M. A. (2006). Are the mixtures of homologous surfactants ideal? **Journal of Colloid and Interface Science** 303(1): 264-271.
- Shah, S. S., Jamroz, N. U., and Sharif, Q. M. (2001). Micellization parameters and electrostatic interactions in micellar solution of sodium dodecyl sulfate (SDS) at different temperatures. **Colloids and Surfaces A: Physicochemical and Engineering Aspects** 178: 199-206.
- Shiloach, A. and Blankschtein, D. (1998). Predicting micellar solution properties of binary surfactant mixtures. **Langmuir** 14(7): 1618-1636.
- Shinoda, K., Nakagawa, T., K., and Shinoda, N. (1963). **Colloidal surfactants: Some physicochemical properties**. New York: Academic.
- Soontravanich, S., Munoz, J. A., Scamehorn, J. F., Harwell, J. H., and Sabatini, D. A. (2008). Interaction between an anionic and an amphoteric surfactant. Part I: Monomer–micelle equilibrium. **Journal of Surfactants and Detergents** 11(4): 251-261.
- Soontravanich, S. and Scamehorn, J. F. (2010). Relation of supersaturation ratio in mixed anionic surfactant solutions to kinetics of precipitation with calcium. **Journal of Surfactants and Detergents** 13(1): 1-11.

- Srinivasan, V. and Blankschtein, D. (2003). Effect of counterion binding on micellar solution behavior: 1. Molecular thermodynamic theory of micellization of ionic surfactants. **Langmuir** 19(23): 9932-9945.
- Stellner, K. L. and Scamehorn, J. F. (1989a). Hardness tolerance of anionic surfactant solutions. 1. Anionic surfactant with added monovalent electrolyte. **Langmuir** 5(1): 70-77.
- Stellner, K. L. and Scamehorn, J. F. (1989b). Hardness tolerance of anionic surfactant solutions. 2. Effect of added nonionic surfactant. **Langmuir** 5(1): 77-84.
- Sugihara, G., *et al.* (2003). Adsorption and micelle formation of mixed surfactant systems in water II: A combination of cationic gemini-type surfactant with MEGA-10. **Journal of Oleo Science** 52(9): 449-461.
- Sugihara, G., Nagadome, S., Oh, S. W., and Ko, J. S. (2008). A review of recent studies on aqueous binary mixed surfactant systems. **Journal of Oleo Science** 57(2): 61-92.
- Talens-Alesson, F. I. (2007). Behaviour of SDS micelles bound to mixtures of divalent and trivalent cations during ultrafiltration. **Colloids and Surfaces A: Physicochemical and Engineering Aspects** 299(1-3): 169-179.
- Treiner, C., Khodja, A. A., and Fromon, M. (1987). Micellar solubilization of 1-pentanol in binary surfactant solutions: a regular solution approach. **Langmuir** 3(5): 729-735.
- Tsubone, K. (2003). The interaction of an anionic gemini surfactant with conventional anionic surfactants. **Journal of Colloid and Interface Science** 261(2): 524-528.

CHAPTER III

CALCIUM SALTS OF SURFACTANT AND PRECIPITATION PHASE BOUNDARIES

3.1 Abstract

In hard water, single anionic surfactants, types commonly used in household products and the detergency industry tend to precipitate with counterions, for example calcium and magnesium ions, forming soap scum and are thus no longer available to participate in the cleaning action. General thermodynamic properties of calcium surfactant salts, for instance solubility data, Krafft temperature, CMC, and energy changes upon dissolution, are required to better understand anionic surfactant precipitation by counterions, but these properties are quite limited in the literature. These thermodynamic data will help to accurately predict the precipitation phase boundary of the anionic surfactant used in this study when precipitated by CaCl_2 . Hence, this work aims to investigate the activity-based solubility product of calcium surfactant salts in aqueous solutions as a function of temperature, with thermodynamic modeling of the precipitation phase boundary. The results reveal more accurately thermodynamic data from the experiments, which allows better thermodynamic modeling of the precipitation phase boundary of single and binary mixed anionic surfactant systems.

3.2 Introduction

Precipitation of surfactants by oppositely charged ions from aqueous solution can inhibit their use in many applications such as in the detergency industry, where an essential fraction of a laundry detergent can be composed of builder to separate multivalent cations, preventing these ions from precipitating anionic surfactants by their large affinity to hardness ions (Hollingsworth, 1978). On the other hand, crude oil recovery can be enhanced by anionic or cationic surfactant precipitation in oil reservoirs as it is the basis of the waterflooding technology (Gale, Saunders, and Ashcraft Jr, 1976). In addition, surfactant from surfactant-based separation processes can be recovered by precipitation methods (Vanjara and Dixit, 1996; Wu, Christian, and Scamehorn, 1998). Hence, understanding and manipulating surfactant precipitation has great importance for industrial applications.

For many decades, the use of surfactant mixtures has enabled considerable manipulation of precipitation behavior. Surfactant mixtures can have synergistic advantages over the use of single surfactants (Li, Li, and Chen, 1998; Rosen, 1991; Soontravanich S., Munoz, Scamehorn, Harwell, and Sabatini, 2008; Stellner and Scamehorn, 1989b). The different levels of synergistic advantages in the mixtures of surfactants are dependent on the molecular structure and the charge of the individual surfactant components. Although, surfactants have been used in several applications because of their unique characteristics, they have some disadvantageous properties. For instance, anionic surfactants can form insoluble salt as soap scum in hard water, water containing a high concentration of calcium and/or magnesium ions. In addition, their solubility is poor in cold water below the Krafft temperature.

This chapter will focus on thermodynamic properties of precipitation of single and mixed anionic surfactant systems. However, it is also necessary to have an understanding of the basic principles of the precipitation of single anionic surfactants by counterions. There are two general approaches to thermodynamically describe surfactant precipitation data in the literature; precipitation phase boundaries, and Krafft temperatures (sometimes called the Krafft point or micellization temperature). A precipitation phase boundary represents the lowest or highest amount of a species required to cause the precipitation of an infinitesimal amount of surfactant salt in an aqueous surfactant solution at a given temperature at various surfactant concentrations.

Consequently, the aim of this chapter is to thermodynamically study the precipitation of single and mixed anionic surfactants by calcium ions. This chapter will also illustrate anionic surfactant precipitation boundaries together with the use of improved models, as discussed in the previous chapter, to predict the theoretical precipitation phase boundaries as a function of temperature for NaDS precipitating by CaCl_2 , and for binary mixed NaDS/NaDeS and NaDS/NaOBS systems, which requires many thermodynamic properties of the anionic surfactants used and the activity of counterions in the intermicellar solution.

3.3 Theory

Precipitation, also called reactive crystallization, is an area for which crystallization as well as reaction engineering aspects are important. Classically, crystals are obtained from a solution by (1) increasing the solute concentration through solvent evaporation, (2) cooling, (3) combining these two processes when the solvent evaporation is used both cooling and for concentrating, or (4) by salting-out with the help of a cosolvent.

Precipitation differs from these classical processes in that the supersaturation, which is required for the crystallization, no longer results from an action on the physical properties of the solution. It is obtained by chemical reaction between two solute components leading to a less soluble product which crystallizes. The reactants can be ions or molecules. Alternatively, the reactants can directly lead to a very sparingly soluble precipitate. The generated particles can be amorphous or crystalline.

The reaction and crystallization occur simultaneously and have their own kinetics. Mixing effects also need to be taken into account. In the case of fast reaction kinetics, the supersaturation may be very high and thus high nucleation rates can be observed. Then, reaction and crystallization kinetic rates may be faster or in the same order of magnitude as the mixing process rates, resulting in competition between mixing, reaction, and nucleation. The mixing kinetics will have a high effect on the product crystals, especially on the number concentration of crystals formed, and on their size.

3.3.1 Driving Force of Reactive Crystallization

3.3.1.1 Solubility

One important property of the crystals, in order to study the precipitation or reactive crystallization, is the ability to dissolve in a given solvent at a specific temperature. These solubility characteristics have a considerable influence on the choice of the method of crystallization. It will also allow evaluation of the supersaturated region (the precipitation region), and the isotropic region where all solution is clear. In the majority of cases the solubility increases with temperature but solubility may also be a function of pressure at low to moderate pressure. Generally, the effect can be negligible in the systems normally encountered in crystallization from solution.

One of the most important expressions of the influence of temperature on solubility is the polynomial:

$$c = A + BT + CT^2 + \dots \quad (3.1)$$

where c is the solution composition expressed in any convenient units and T is the temperature. In addition to equation (3.1), a number of semi-empirical equations have been proposed for solubility correlation purposes, some of which are based on thermodynamic relationships relating to phase equilibria. Some of the expressions that have been used at one time or another are:

$$\log x = A + BT \quad (3.2)$$

$$\log x = A + BT + CT^2 \quad (3.3)$$

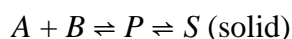
$$\log x = A + BT^{-1} \quad (3.4)$$

$$\log x = A + BT^{-1} + CT^{-2} \quad (3.5)$$

$$\log x = A + BT^{-1} + C \log T \quad (3.6)$$

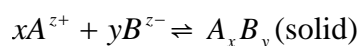
In all the relationships shown above, the solution composition x is expressed as mole fraction of solute and the temperature T is in units of Kelvin (K). However, the constants A , B , and C in equations (3.1) to (3.6) are not necessarily related to one another. Two possibilities can be considered in order to understand the driving force of reactive crystallization:

1) The chemical reaction leads to a more or less soluble molecule (P) which then crystallizes.



where A and B are reactants, and S is the solid of P . In this case, the solubility of component P can be described as the molar concentration of P in the solution at the thermodynamic solid-liquid equilibrium. This concentration is a function of temperature as mentioned above.

2) The chemical reaction does not lead to any intermediate soluble species, and the solid crystallizes directly from the reactants. It is the case of many ionic reactions, leading to sparingly soluble salts between anion and cation.



with the electroneutrality condition:

$$xz_+ = yz_- \quad (3.7)$$

where z_- and z_+ are the valencies of the anion and cation, respectively. In this case, the thermodynamic equilibrium will be described by the solubility product, which is a function of temperature.

3.3.1.2 Activity and Ionic Strength

The colligative properties of solutions depend on the effect of solute concentration on the solvent activity. The chemical potential (μ) of a non-electrolyte in dilute solution can be expressed by (Mullin, 1992; Myerson, 1993):

$$\mu = \mu_{0c} + RT \ln c \quad (3.8)$$

where c is the solute concentration in molar units (M) and μ_{0c} is the standard chemical potential in units of Joules per mole (J/mol). R is the universal gas constant and T is the temperature in Kelvin. Nevertheless, equation (3.8) cannot be applied to solutions of electrolytes for concentrations greater than about 10^{-3} M. In these cases, an expression based on activity rather than concentration should be applied:

$$\mu = \mu_{0c} + RT \ln a_c \quad (3.9)$$

where a_c is the solute activity as a molar basis, which is related to composition c via the corresponding activity coefficient (f_c) by:

$$a_c = cf_c \quad (3.10)$$

The activity coefficient becomes unity at infinite dilution, i.e. when ideality may be assumed (when using an asymmetric definition of the activity coefficients)

From the Debye-Hückel theory of electrolytes (Klotz and Rosenberg, 2008), the limiting (infinite dilution) law gives the mean activity coefficient of the ion as:

$$\log f_{\pm} = -A|z_+z_-|I^{1/2} \quad (3.11)$$

where I is the ionic strength in units of mole per liter (M), and is defined by:

$$I = \frac{1}{2} \sum c_i z_i^2 \quad (3.12)$$

where c_i is the concentration of the ionic species in molar units, z_i is the ion valency, and z_- and z_+ are the valencies of the anion and cation, respectively. The Debye-Hückel constant A , is dependent on the solvent and temperature of the solution.

The Debye-Hückel limiting law (equation 3.11) has to be modified for all but the most dilute solution, and many modifications have been proposed, for example the Güntelberg equation (Klotz and Rosenberg, 2008; Mullin, 1992):

$$\log f_{\pm} = -A|z_+z_-| \left[\frac{I^{1/2}}{I + I^{1/2}} \right] \quad (3.13)$$

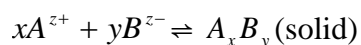
Equation (3.13) is useful for solutions of sparingly soluble electrolytes. The Davies equation (also known as the extended Debye-Hückel equation) (Davies and Shedlovsky, 1964) is also commonly used:

$$\log f_i = \frac{-A(z_i)^2 I^{1/2}}{1 + B a_i I^{1/2}} - 0.3I \quad (3.14)$$

where B is the Debye-Hückel constant, and is dependent on the solvent and temperature of the solution. a_i is the an empirical value based on diameter of the ion. The values of A and B have been tabulated elsewhere (Klotz and Rosenberg, 2008). Equation (3.14) is expected to be generally valid for values of I up to about 2 mol/L (Davies and Shedlovsky, 1964; Nancollas and Butler, 1967).

3.3.1.3 Solubility Product

The solubility of a sparingly soluble electrolyte in water is often expressed in terms of the concentration solubility product (K_c). For instance, if one molecule of such an electrolyte dissociates in solution into A^{z^+} cations and B^{z^-} anions according to the equation :



where z^+ and z^- are the valencies of the ions, then for a saturated solution the solubility product can be written as (Mullin, 1992; Myerson, 1993):

$$K_c = ([A^{z^+}]^x [B^{z^-}]^y) = \text{constant} \quad (3.15)$$

$[A^{z+}]$ and $[B^{z-}]$ are the molar concentrations of the two ions at equilibrium conditions. However, the simple solubility product (concentration-based) principle has extremely limited use. It should be valid only in solutions of very sparingly soluble salts ($< 10^{-3}$ M). For more concentrated solution, it is better to adopt a more fundamental approach relating to the use of activity concepts. The activity based solubility product is defined as (Mullin, 1992; Myerson, 1993):

$$K_{SP} = (a_{A^{z+}}^*)^x (a_{B^{z-}}^*)^y = \text{constant} \quad (3.16)$$

where $a_{A^{z+}}^*$ and $a_{B^{z-}}^*$ are the ionic activities at equilibrium. As the activity of an ion may be expressed in terms of the ionic concentration and the ionic activity coefficient (f), equation (3.16) becomes:

$$K_{SP} = ([A^{z+}]^* f_{z+}^*)^x ([B^{z-}]^* f_{z-}^*)^y = \text{constant} \quad (3.17)$$

where f_{z+}^* and f_{z-}^* are the activity coefficients of ions A^{z+} and B^{z-} at equilibrium, respectively.

3.3.1.4 Supersolubility and Supersaturation

A saturated solution is in thermodynamic equilibrium with the solid phase at a given temperature. However, it is often easy to prepare solutions (by cooling a hot concentrated solution slowly without agitation) containing more dissolved solid than that represented by the equilibrium saturation. Such solutions are said to be supersaturated. Crystallization processes can take place only in supersaturated phases, and the rate of crystallization is often determined by the degree

of supersaturation (also called the supersaturation ratio, S_0). The supersaturation of a system may be expressed in many different ways, and considerable confusion can arise if the basic units of concentration are not clearly defined. The temperature must also be specified.

Among the most common expressions of supersaturation are the concentration driving force (c), the supersaturation ratio (S), and a quantity sometimes referred to as the relative supersaturation (σ). These quantities are defined by (Mullin, 1992; Myerson, 1993):

$$\Delta c = c - c^* \quad (3.18)$$

$$S = \frac{c}{c^*} \quad (3.19)$$

$$\sigma = \frac{\Delta c}{c^*} = S - 1 \quad (3.20)$$

where c is the molar concentration and c^* is the equilibrium saturation at the given temperature.

It is important to consider reactive crystallization or precipitation when a component crystallizes out of an electrolytic solution composed of ions. In this case, the supersaturation can reach very high local values, particularly at the introduction points of reactants if the kinetics of reaction is fast. Hence, the treatment of classical crystallization processes cannot then be applied. The following equations should be used in the expressions of the kinetic rates of primary nucleation

of the nuclei formed. Regarding equations (3.16) and (3.17), the activity-based supersaturation ratio can be written as:

$$S_0 = \left(\frac{(a_{A^{z+}})^x (a_{B^{z-}})^y}{K_{SP}} \right)^{1/(x+y)} \quad (3.21)$$

3.3.1.5 Dissolution of Anionic Surfactant in Water

Dissolution of surfactants in water generally results in significant changes in thermodynamic properties, for instance the enthalpy and the entropy of dissolution, which are both temperature dependent. Both effects are partly due to a significant heat capacity change. This phenomenon is common for all nonpolar solute molecules. The reason for such behavior is the special character of water as a solvent. It is thought that the tetrahedrally coordinated hydrogen bonds of water molecules cause ordering around the nonpolar solute molecules (tails), forming so-called “icelikeness”, thus increasing the heat capacity of the system (Frank and Evans, 1945; Mancera and Buckingham, 1995). A study of material solubility is essential as it reflects molecular orientation in the precursor solution. Transformations from solution to solute molecules are controlled by intermolecular coordination with solvent molecules to the solid-solid bonds where strong solute-solute interactions lead to molecular self-assembly and crystallographic structure. An ideal solubility can be described by the van't Hoff equation (on a mole fraction basis) (Mullin, 1992) :

$$\ln(x) = \frac{\Delta H}{R} \left[\frac{1}{T_f} - \frac{1}{T} \right] \quad (3.22)$$

where x is the mole fraction of solute in the solution, T is the solution absolute temperature, T_f is the fusion temperature (melting point) of the solute, ΔH is the molal enthalpy of fusion, and R is the gas constant (8.314 J/mol·K). This ideal equation involves perfect mixing on the molecular scale of solute and solvent. In reality, solubility is solvent-dependent, and can be described by the chemical equilibrium basis of the van't Hoff equation (Atkins and De Paula, 2009; Dykstra, 1997):

$$\ln K_{sp} = \frac{\Delta S}{R} - \frac{\Delta H}{RT_{sat}} \quad (3.23)$$

where ΔH and ΔS are the enthalpy of dissolution, respectively, and T_{sat} is the saturation temperature, which is defined as the temperature of dissolution at an infinitely slow rate. Therefore, a plot of the natural logarithm of the equilibrium constant versus the reciprocal temperature gives a straight line. The slope of the line is equal to minus the standard enthalpy change divided by the gas constant, and the intercept is equal to the standard entropy change divided by the gas constant. The known ΔH , ΔS , and T_{sat} can then be used to calculate the Gibbs free energy; ΔG for this process was calculated using the equation:

$$\Delta G = \Delta H - T\Delta S \quad (3.24)$$

3.3.2 Precipitation of Anionic Surfactant Systems with Calcium Chloride

The precipitation phase boundary not only determines the region where precipitation will occur, but it can also indicate the hardness tolerance for each surfactant system. The hardness tolerance of anionic surfactants is defined as the

lowest concentration of multivalent cation necessary to cause surfactant precipitation. Hardness tolerance of a detergent mixture can limit effective cleaning using anionic surfactants in hard water, often requiring the addition of builder to a detergent formulation. Consider a completely dissociated monovalent anionic surfactant such as dodecyl sulfate as in Figure 3.1: if a divalent cation (e.g., a calcium ion) were added into the solution, the lowest calcium concentration required to cause the surfactant to precipitate as calcium dodecyl sulfate ($\text{Ca}(\text{DS})_2$) is the hardness tolerance.

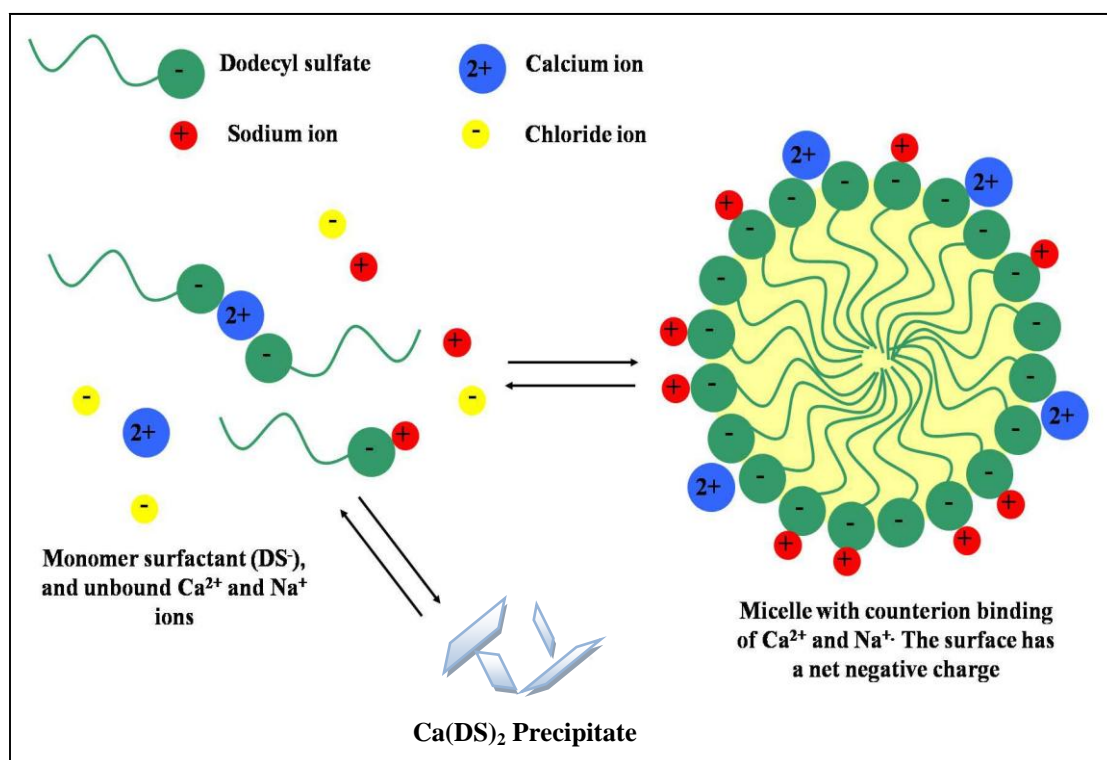


Figure 3.1 An illustration of micelle-monomer-precipitate co-existence in equilibrium for anionic surfactant in the presence of counterions.

Another aspect of Figure 3.1 is anionic surfactant can be in the form of monomers, micelles, and as precipitate. The divalent or hardness cation may be present in the unbound state, as bound counterions on the surface of micelles, or in the precipitate. Any monovalent cation present in solution is either unbound or bound onto micelles. Surfactant precipitation will occur if the product of the surfactant anion activity squared and the divalent counterion activity is greater than the solubility product of the surfactant salt. (Equilibrium occurs where these two variables are equal). Whether precipitation occurs or not also depends on the monomer-micelle equilibrium since the surfactant present as micelles does not contribute to surfactant activity and the bound counterion does not contribute to counterion activity (Rodriguez, Lowery, Scamehorn, and Harwell, 2001; Soontravanich S., and Scamehorn; Stellner and Scamehorn, 1989a).

3.3.2.1 Single Anionic Surfactant Systems

Along the precipitation phase boundary, an infinitesimal amount of precipitate is present. It is well known that hardness tolerance reaches a minimum at the CMC. Below the CMC, as the total anionic surfactant concentration increases, the calcium ion concentration required for precipitation to occur decreases. The solubility product relationship for a monovalent anionic surfactant is described by:

$$K_{SP} = [Ca^{2+}][S^{-}]^2 f_{Ca^{2+}} f_{S^{-}}^2 \quad (3.25)$$

where K_{SP} is the activity-based solubility product, $[Ca^{2+}]$ is the total calcium ion concentration in solution, and $[S^{-}]$ is the total surfactant concentration of the anionic

surfactant. It should be noted that total concentrations used are below the CMC and all of the surfactant is in the monomeric form. The parameters $f_{Ca^{2+}}$ and f_{S^-} are the activity coefficients of the calcium and anionic surfactant, respectively.

Along the precipitation phase boundary above the CMC, a simultaneous equilibrium exists between the surfactant as monomer, in micelle, and in precipitate as illustrated earlier in Figure 3.1. The solubility product relationship that describes surfactant precipitation above the CMC can be expressed by:

$$K_{SP} = [Ca^{2+}]_{unb} [S^-]_{mon}^2 f_{Ca^{2+}} f_{S^-}^2 \quad (3.26)$$

where $[Ca^{2+}]_{unb}$ is the unbound calcium concentration and $[S^-]_{mon}$ is the monomeric concentration of the anionic surfactant. The activity coefficients for insertion into above two equations are found using an extended Debye-Hückel expression as discussed in section 3.3.1.2. However, the parameter a_i is an empirical value based on the diameter of the ion, and is equal to $6 \times 10^{-8} \text{ cm}^{-1}$ for calcium (Klotz *et al.*, 2000) and is estimated as $7 \times 10^{-8} \text{ cm}^{-1}$ for NaDS, NaOBS, (Rodriguez *et al.*, 2001) and NaDeS. The difference between the molecules in two carbon atoms in the surfactant backbone of NaDS and NaDeS will be assumed to not have an effect on the diameter of the ion in this work, thus NaDeS is also assumed to be $7 \times 10^{-8} \text{ cm}^{-1}$.

If solution concentrations are not large enough to satisfy the solubility product even when the surfactant lies above the CMC, the intermicellar solution will contain only monomers and micelles, but will not precipitate at equilibrium. If the solubility product is not satisfied and the surfactant concentration is below the CMC, the surfactant will be present only as monomers. If a solution

contains a concentration of monomer surfactant ions and unbound calcium ions that exceeds the solubility product, then that solution is supersaturated and, theoretically, will precipitate until the solution concentration lies somewhere along the precipitation phase boundary.

In order to study the precipitation region, the initial conditions of a supersaturated solution are necessary. Supersaturation is a measure of the excess concentration of the reactants above the equilibrium solubility concentration (Lieser, 2003) . The degree of supersaturation and the presence of the foreign materials, or seed crystals, affect the ability of the supersaturated solution both to form nuclei and to grow crystals. In this thesis chapter, a supersaturation ratio (S_0) is used to describe the excess concentration of reactants above the precipitation phase boundary for an anionic surfactant precipitating with calcium ions, as follows:

$$S_0 = \left(\frac{[Ca^{2+}]_{unb} [S^-]_{mon}^2 f_{Ca^{2+}} f_{S^-}^2}{K_{SP}} \right)^{1/3} \quad (3.27)$$

Equation (3.27) only takes into consideration the monomer surfactant concentration and the unbound calcium concentration. If the initial solution condition exactly satisfies the solubility product, then $S_0 = 1$. Therefore, the more that S_0 exceeds unity, the more supersaturated the solution becomes.

3.3.2.2 Binary Mixed Anionic Surfactant Systems

There are few studies about the precipitation phase boundaries of single (Baviere, Bazin, and Aude, 1983; Gerbacia, 1983; Noïk, Bavière, and Defives, 1987; Rodriguez, *et al.*, 2001) and mixed anionic surfactant systems

(Rodriguez and Scamehorn, 1999, 2001), and few studies focusing on qualitative investigation on kinetics of precipitation to help explain the phenomena occurring during the precipitation process (Rodriguez and Scamehorn, 2001; Soontravanich S., and Scamehorn, 2010). Also there are only a few experimental determinations to verify the accuracy of the model for NaDS/NaOBS mixtures (Rodriguez and Scamehorn, 2001). Along a precipitation phase boundary, an infinitesimal amount of precipitate is present as in a single surfactant system, but it normally consists of only one ionic surfactant. Precipitation occurs below the CMC when the solubility product relationship for the less soluble surfactant is reached. The solubility product relationship for anionic surfactant with calcium ion below the CMC is described by equation (3.25) where $[S^-]$ is still the total surfactant concentration of the precipitating anionic surfactant. Total surfactant concentrations used are below the CMC because all of the surfactant is only in its monomeric form.

Precipitation occurs above the CMC when the monomeric concentration of the less soluble surfactant ionic surfactant, and the unbound counterion concentration exceed the equilibrium solubility product. This can be described by equation (3.26) except that $[S^-]_{mon}$ is the monomeric concentration of the precipitating anionic surfactant. Mixed precipitate is not generally observed along the precipitation boundary of anionic surfactant mixtures unless the K_{SP} values of the two precipitating surfactants are very similar (Tsujii, Saito, and Takeuchi, 1980). The improved models to thermodynamically treat the mixed micellization and activity of counterions in the intermicellar solution have been discussed in the previous chapter for both single and binary mixed anionic surfactant systems.

The improved models can be used to quantify the amount of precipitating species in the intermicellar solution and also to predict the hardness tolerance of a mixture and the equilibrium precipitating or nonprecipitating compositions in the mixed micellization solution.

3.4 Experimental Procedure

3.4.1 Materials

Sodium dodecyl sulfate (NaDS) was purchased from Carlo Erba with purity greater than 92%. Sodium 4-octylbenzene sulfonate (NaOBS) was purchased from Aldrich with purity greater than 97%. These two anionic surfactants were further purified by twice recrystallizing using deionized water and methanol, respectively. They were dried over silica gel at room temperature for 24 hours. Sodium decyl sulfate (NaDeS) was purchased from Fluka with purity greater than 99% and was used as received without further purification. Calcium chloride dihydrate ($\text{CaCl}_2 \cdot 2\text{H}_2\text{O}$), analytical reagent grade with purity greater than 98.0%, was purchased from Sigma-Aldrich and was used as received. Deionized water ($18 \text{ M}\Omega \cdot \text{cm}$) was used to prepare all aqueous samples through out the experiments.

3.4.2 Preparation of Calcium Surfactant Salts

The powdered calcium surfactant salts of calcium dodecyl sulfate ($\text{Ca}(\text{DS})_2$), calcium octylbenzenesulfonate ($\text{Ca}(\text{OBS})_2$), and calcium decyl sulfate ($\text{Ca}(\text{DeS})_2$) were prepared from the precipitation of NaDS, NaOBS, and NaDeS respectively with an excess concentration of calcium chloride solution. The crystals were separated by a $0.45 \mu\text{m}$ cellulose nitrate membrane and rinsed with cold deionized water. After drying by silica gel under room temperature overnight,

$\text{Ca}(\text{DS})_2$, $\text{Ca}(\text{OBS})_2$, and $\text{Ca}(\text{DeS})_2$ were then recrystallized twice in deionized water. The pure crystals were separated by paper filtration (Whatman 42) and dried over silica gel at room temperature for at least 24 hours. Dry crystals were used to prepare solutions in deionized water.

3.4.3 Solubility Measurements

Pure calcium surfactant salts were used to prepare the saturated solutions at different temperatures depending on the Krafft temperature. Calcium surfactant salts behave like a conventional anionic surfactant but have very low solubility at room temperature. Thus, the investigation of calcium surfactant salt solubility is divided into two techniques of measuring the solubility; measuring concentrations by Atomic Adsorption Spectroscopy (AAS) for saturated solutions at fixed temperatures, or measuring the conductivity of fixed concentration solutions as the temperature is varied to search for the saturation temperature. Which method is more convenient depends on whether the system is above or below the Krafft temperature, the minimum temperature at which surfactants form micelles. The Krafft temperature of $\text{Ca}(\text{DS})_2$ has been reported at 50°C (Lee and Robb, 1979; Moroi, Oyama, and Matuura, 1977).

For the $\text{Ca}(\text{DS})_2$ saturated solutions, an AAS method was used to measure the solubility below the Krafft temperature. A series of $\text{Ca}(\text{DS})_2$ solutions were prepared at varying saturation temperatures ranging from 10 to 50°C. Additional solutions at 51, 53, and 55°C were prepared to verify the consistency of the two techniques. AAS was used to measure the concentration of calcium ions in the solutions; the total amount of surfactant can be estimated using the stoichiometric

ratio of calcium ion to surfactant monomer. Solubilities were reported at the saturation temperature. The concentration was determined three times for each batch and three batches were performed per saturation temperature. The replicates show that the experimental data are highly reproducible, within 95% confident intervals of ± 0.005 mM. Conductimetry was used to measure the solubility above the Krafft temperature by determining the saturation temperature of known concentration solutions at 0.5, 3.0, 4.0, 6.0, 8.0, and 10.0 mM. The equilibrium temperature was determined by measuring the conductivity of a surfactant solution as a function of temperature. The concentration at the point that the slope is discontinuous is the saturation temperature for the concentration measured, since this is the point at which additional ions are removed from solution by precipitation.

To investigate the solubility of $\text{Ca}(\text{DeS})_2$ saturated solutions, the AAS method was used to measure the solubility below the Krafft temperature. A series of $\text{Ca}(\text{DeS})_2$ solutions at different concentrations were prepared at varying saturation temperatures ranging from 20 to 30°C. Solubilities were reported at the saturation temperature. The concentration was determined three times for each batch and three batches were performed per saturation temperature. The replicates show that the experimental data are highly reproducible within 95% confident intervals of ± 0.005 mM. Conductimetry was used to measure the solubility above the Krafft temperature by determining the saturation temperature of known concentration solutions at 5.0 – 30.0 mM. The equilibrium temperature was determined by measuring the conductivity of a surfactant solution as a function of temperature. The concentration at the point that the slope is discontinuous is the saturation temperature for the concentration measured.

However, for the measurement of the solubility of Ca(OBS)_2 in aqueous solution, only the AAS method was used to measure the solubility at only a saturation temperature of 30°C . This is because the Krafft temperature for Ca(OBS)_2 is very high in aqueous solution. As for the previous investigation of calcium surfactant salts, the concentration was determined three times for each batch and three batches were performed at 30°C . The replicates show that the experimental data are highly reproducible, within 95% confident intervals of ± 0.004 mM.

3.4.4 Determination of Precipitation Phase Boundaries

A series of solutions were prepared each with same concentration of NaDS ranging over surfactant concentrations both below and above the CMC, but with varying CaCl_2 concentrations. An equal volume of NaDS and CaCl_2 solutions for each system were reacted in a 25-mL test tube with a screw cap. The experiment was carried out at constant temperature at either 10, 30, or 50°C ; the system temperature was maintained by a temperature-controlled water bath. Since the surfactant solutions can remain supersaturated for long periods of time before precipitation starts to occur, the solutions were cooled down to near 0°C for 24 hours to force precipitation. The samples were then placed and held at the desired temperature in a shaking bath for two weeks to ensure all solutions reached equilibrium. The test tubes were visually observed at daily intervals to monitor the precipitate until a last observation was taken on day 14.

The crystals from the precipitation were tiny amounts of very fine crystals. For high supersaturation concentrations, the crystals from precipitation are detectable by visual observation. For low supersaturation concentrations (near the precipitation phase boundary), a tiny amount of nuclei was observed under a microscope. If the crystals can be detected in 5-10% of the area under the microscope, the observation was recorded that precipitation had occurred in the system. The precipitation phase boundary was judged by this criteria: at each surfactant concentration, the highest CaCl_2 concentration below the precipitation phase boundary (supersaturation ratio < 1) that had not nucleated, and the lowest CaCl_2 concentration above the precipitation phase boundary that (supersaturation ratio > 1) had nucleated defined the region that contained the phase boundary.

3.5 Results and Discussion

3.5.1 Thermodynamic Properties of Calcium Surfactant Salts

3.5.1.1 Calcium Dodecyl Sulfate

The results of the solubility study using AAS to measure saturation concentrations at fixed temperatures are shown in Table 3.1. Further experiments were performed on solutions from 0.5 to 10.0 mM $\text{Ca}(\text{DS})_2$ to determine the saturation temperature using measurements of conductivity as shown in Figure 3.2. The K_{SP} values as a function of temperature were calculated using the results of the two methods, and the results are shown in Figure 3.3. The agreement between the two techniques is excellent except for one value predicted using the conductivity technique at 42°C. At this point (which is well below the Krafft temperature) the change in the slope at the saturation point is very small, and therefore the relative error is quite large. However, it should be noted in Table 3.1 that the dilution ratio for the AAS technique increases as the saturated temperature increases, especially when the ratio is very large at 55°C. This is because the solubility of $\text{Ca}(\text{DS})_2$ increases extremely quickly above the Krafft temperature. The main improvements to the knowledge of the system gained from this study are that (a) it can be seen that two totally independent measurements can give consistent results for the K_{SP} ; (b) the K_{SP} value is now known over a wide range of temperature; (c) the K_{SP} value has been measured in pure $\text{Ca}(\text{DS})_2$ solutions where the effects of other ions have been removed (which will lower the ionic strength of the solution and therefore increase the accuracy of the activity coefficient model); (d) the K_{SP} predicted here is a measured property rather than a property determined by fitting to a boundary (Stellner and Scamehorn, 1989a).

Table 3.1 Total calcium ion concentration at saturation using the AAS technique for $\text{Ca}(\text{DS})_2$ in aqueous solution.

Temperature (°C)	Dilution ratio for AAS	Saturated concentration of calcium ion (mM)
10.0	1:10	0.253
15.0	1:10	0.255
20.0	1:10	0.318
25.0	1:10	0.352
30.0	1:10	0.441
35.0	1:10	0.523
40.0	1:25	0.576
45.0	1:25	0.712
50.0	1:25	0.922
51.0	1:25	1.079
53.0	1:25	1.129
55.0	1:2000	19.462

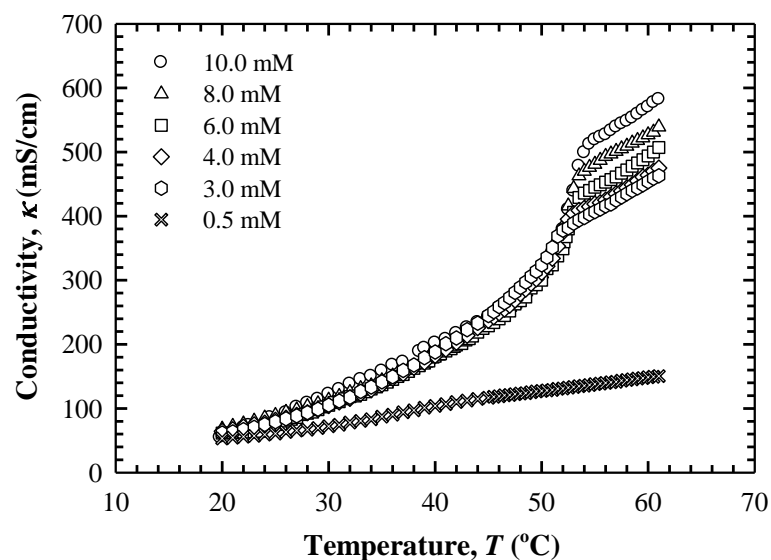


Figure 3.2 Saturation point determination via the conductivity measurement of $\text{Ca}(\text{DS})_2$ solution at various concentrations.

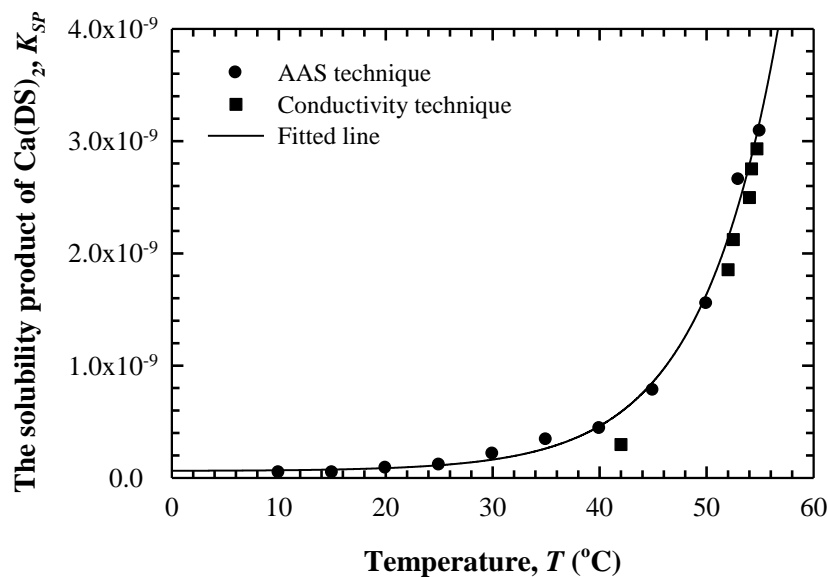


Figure 3.3 Solubility product of $\text{Ca}(\text{DS})_2$ in aqueous solution as a function of temperature.

The data in Figure 3.3 gives the solubility product of $\text{Ca}(\text{DS})_2$ in aqueous solution as a function of temperature, which can be used with the model discussed in the theoretical section (section 3.3.2) to model the precipitation phase boundary for solutions containing NaDS and CaCl_2 (section 3.5.2.1). This calculation has already been performed at 30°C (Stellner and Scamehorn, 1989a), however in this previous study the K_{SP} value was determined by regression over all of the data below the CMC in order to minimize the error between the experimental precipitation boundary and the model. While this is a reasonable approach to obtain an accurate empirical model of the system, it is useful to determine the most accurate possible value of K_{SP} to determine the fundamental accuracy of the model, and this can be achieved conveniently through determination of the solubility of pure $\text{Ca}(\text{DS})_2$ in water, as described earlier. The solubility product of $\text{Ca}(\text{DS})_2$ in aqueous solution is

approximately equal to 2.122×10^{-10} at 30°C and this is in the same order of magnitude as the K_{SP} value at the given temperature reported elsewhere. For instance, Kallay, Pastuovic, and Matijevic (1985) reported 2.137×10^{-10} at 20°C ; Lee and Robb (1979) reported 3.72×10^{-10} at 25°C . The lower value obtained here may be due to better treatment of activity coefficients compared to these older studies. The dependence of the solubility product of $\text{Ca}(\text{DS})_2$ on temperature (in degrees Celsius) can be described by an exponential growth function:

$$K_{SP} = 6.122 \times 10^{-11} + 1.664 \times 10^{-12} \exp(0.1371 T), \text{ where } T \text{ in } ^\circ\text{C} \quad (3.25)$$

Calcium dodecyl sulfate still behaves like a conventional anionic surfactant showing the co-existence between monomers and micelles above the CMC, however, the solubility of calcium surfactant salt is fairly poor below the Krafft temperature or micellization temperature. In other words, micellization cannot occur below the Krafft temperature. Thus, the CMC of $\text{Ca}(\text{DS})_2$ is approximately equal to 2.2 mM at 60°C as shown in Figure 3.4.

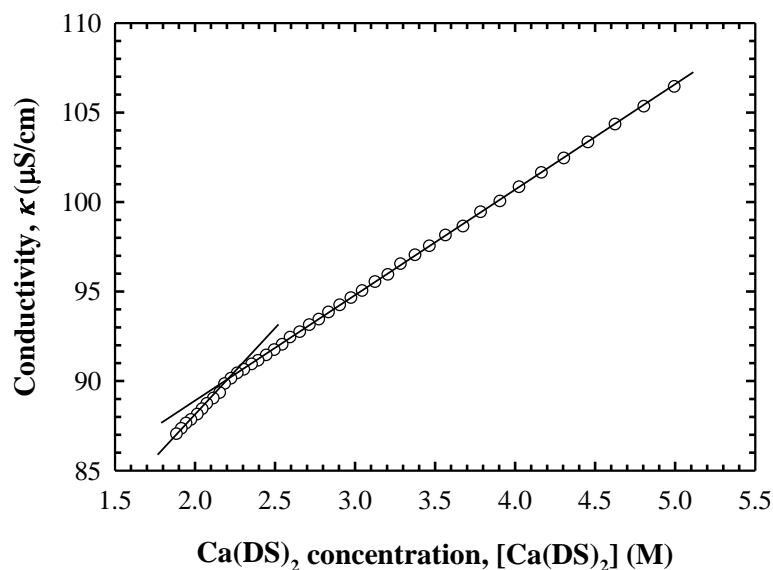


Figure 3.4 The CMC of $\text{Ca}(\text{DS})_2$ in aqueous solution at 60°C determination via conductivity measurement.

The van't Hoff plot of $\text{Ca}(\text{DS})_2$ using equation (3.23) is shown in Figure 3.5. Even though the plot is divided into two sections based on the Krafft temperature, or micellization temperature, of $\text{Ca}(\text{DS})_2$ in water (which is at 50°C), the enthalpy of dissolution is estimated only for temperature below the Krafft temperature, where the anionic surfactant going to the solution as monomers. From the slopes in the plot the enthalpy change of dissolution of $\text{Ca}(\text{DS})_2$ below the Krafft temperature is equal to 64.4 kJ/mole . The calculation of the enthalpy change of dissolution here is not valid above the CMC. Dissolution of several types of anionic surfactants dissolved in water was also found to be an endothermic process revealed by the positive value of the enthalpy change (Hrust, Skurić, Šošić, and Kallay, 1999). However, we do not have a good explanation for the higher the enthalpy change

above the Krafft temperature, but it probably involves phenomena related to the micellization.

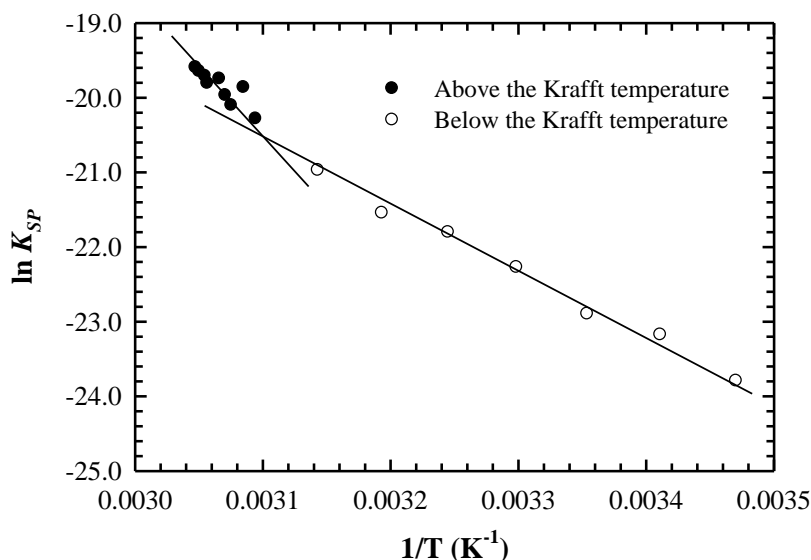


Figure 3.5 Solubility data of $\text{Ca}(\text{DS})_2$ in aqueous solution for below and above the Krafft temperature on a van't Hoff plot.

The entropy change of dissolution, ΔS , is also estimated from the intercept of the plot but only for the data below the Krafft temperature in Figure 3.5. The entropy change is equal to $27.1 \text{ J/mol}\cdot\text{K}$. The enthalpy change of dissolution appears to be an endothermic process, and also the entropy change of dissolution shows a positive value; therefore the process will occur spontaneously at high temperature. The positive value of ΔH comes from the endothermic reaction of breaking the hydrogen bonds to create a cavity for the solutes within the aqueous solution (Anuar, Daud, Roberts, Kamarudin, and Tasirin, 2009). Figure 3.6 shows the plot of Gibbs free energy as a function of temperature. The positive ΔH and ΔG

values are presumably because of the water ordering effect in the presence of a nonpolar material in water (the polar molecules) (Privalov and Gill, 1989).

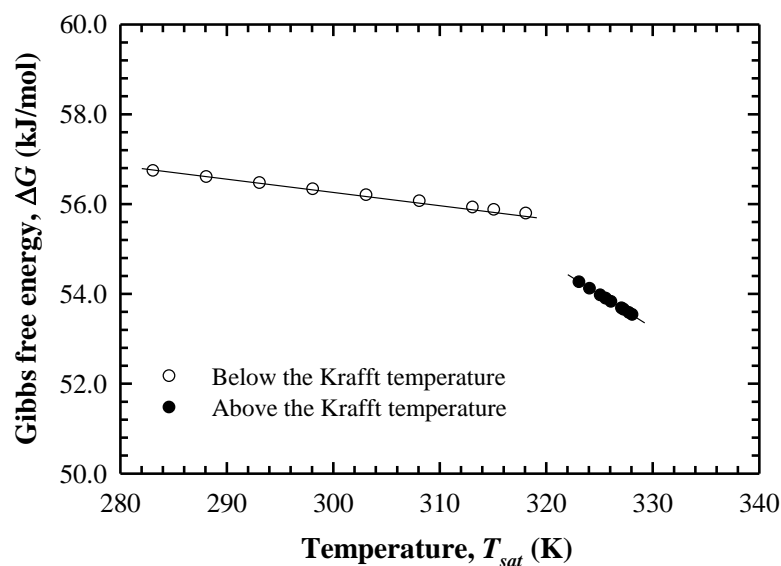


Figure 3.6 Gibbs free energy change for $\text{Ca}(\text{DS})_2$ dissolution in water as a function of temperature.

It should be noted that the Gibbs free energy slightly decreases as the temperature increases for temperature below the Krafft temperature, but it decreases more rapidly above the Krafft temperature. The lower Gibbs free energy above the Krafft temperature indicates a more stable micelle.

3.5.1.2 Calcium Decyl Sulfate

The results of the solubility study using AAS to measure saturation concentrations at fixed temperature are shown in Table 3.2. Further experiments were performed on solutions from 5.0 - 30.0 mM $\text{Ca}(\text{DeS})_2$ to determine the saturation temperature using measurements of conductivity as shown in Figure 3.7.

Table 3.2 Total calcium ion concentration at saturation using the AAS technique for $\text{Ca}(\text{DeS})_2$ in aqueous solution.

Temperature (°C)	Dilution ratio for AAS	Saturated concentration of calcium ion (mM)
20.0	1:50	5.203
25.0	1:50	6.415
30.0	1:200	66.104

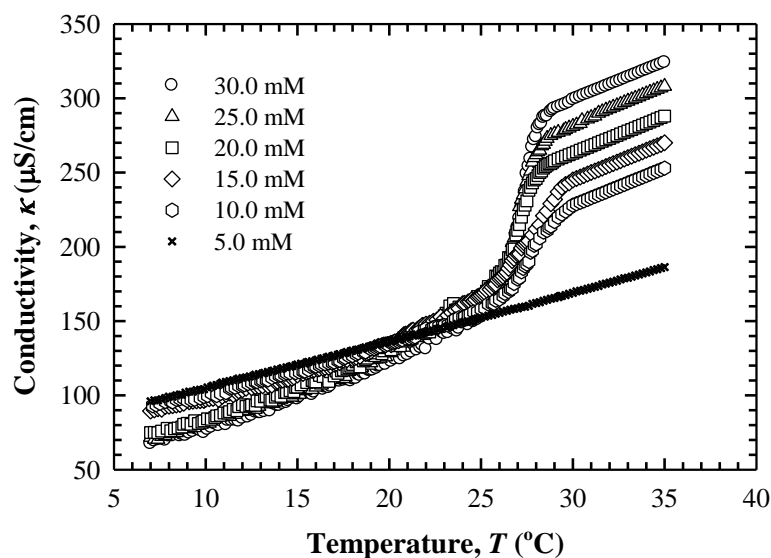


Figure 3.7 Saturation point determination via the conductivity measurement of $\text{Ca}(\text{DeS})_2$ solution at various concentrations.

The K_{SP} values as a function of temperature were calculated using the results of the two methods, and the results are shown in Figure 3.8. The agreement between the two techniques is also excellent. The K_{SP} of $\text{Ca}(\text{DeS})_2$ is much higher than that of $\text{Ca}(\text{DS})_2$ at a specific temperature, even though the only difference between the molecules is two carbon atoms in the surfactant backbone.

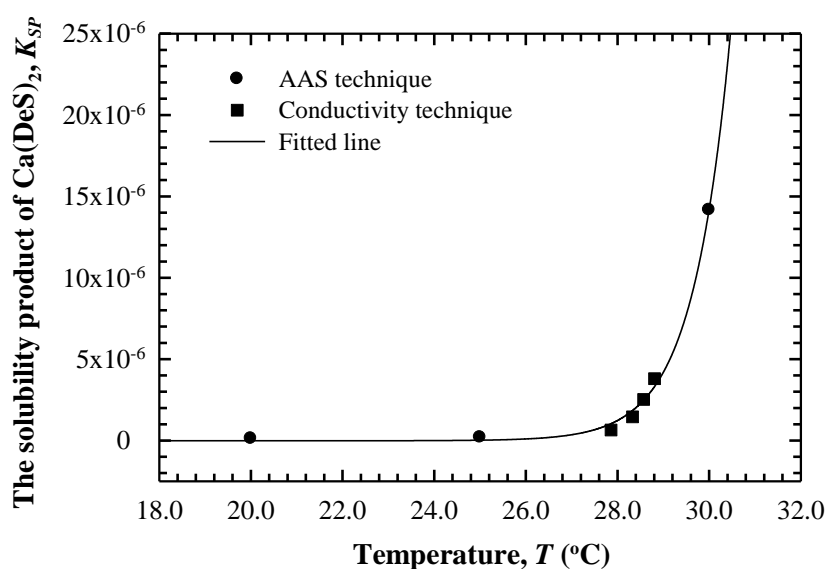


Figure 3.8 Solubility product of $\text{Ca}(\text{DeS})_2$ in aqueous solution as a function of temperature.

As with the solubility behavior of $\text{Ca}(\text{DS})_2$, when analyzing the $\text{Ca}(\text{DeS})_2$ solubility by the AAS technique the dilution ratio increases as the saturated temperature increases; especially when the ratio is much larger at 30°C . This is because the solubility of $\text{Ca}(\text{DeS})_2$ increases extremely rapidly above the Krafft temperature. The Krafft temperature of $\text{Ca}(\text{DeS})_2$ can be determined directly from the solubility curve and is approximately equal to 28.5°C , thus micellization cannot occur below this temperature.

Figure 3.9 shows the plot of conductivity as a function of $\text{Ca}(\text{DeS})_2$ concentration at 30°C . The CMC of $\text{Ca}(\text{DeS})_2$ is approximately equal to 7.0 mM as determined at the point of the change of the slope.

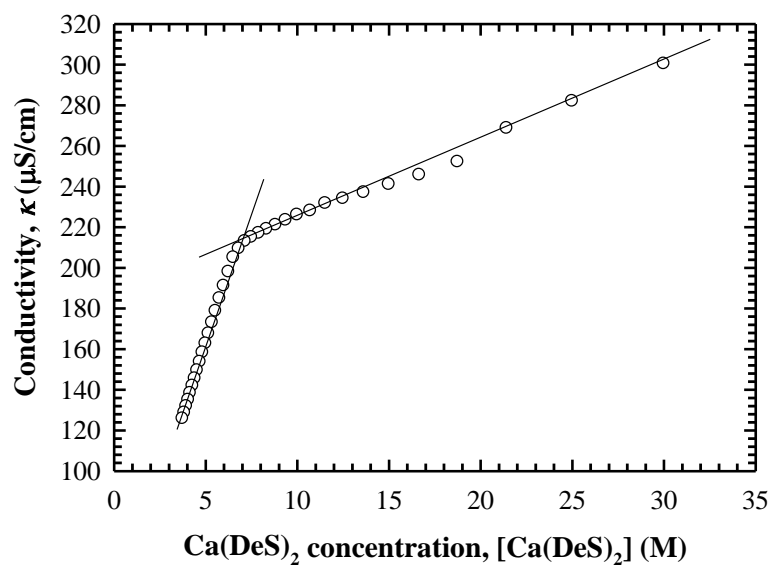


Figure 3.9 The CMC of $\text{Ca}(\text{DeS})_2$ in aqueous solution at 30°C determination via conductivity measurement.

The solubility product of $\text{Ca}(\text{DeS})_2$ as a function of temperature (in degrees Celsius) can be described by an exponential growth function:

$$K_{SP} = -2.194 \times 10^{-8} + 3.806 \times 10^{-21} \exp(1.218 T), \text{ where } T \text{ in } ^\circ\text{C} \quad (3.26)$$

The van't Hoff plot of $\text{Ca}(\text{DeS})_2$ using equation (3.23) is also shown in Figure 3.10. The plot is also divided into two sections based on the Krafft temperature, or micellization temperature of $\text{Ca}(\text{DeS})_2$ in water at 28°C due to the same reason described earlier for $\text{Ca}(\text{DS})_2$. From the slopes in the plot the enthalpy change of dissolution of $\text{Ca}(\text{DeS})_2$ below the Krafft temperature is equal to 40.8 kJ/mole.

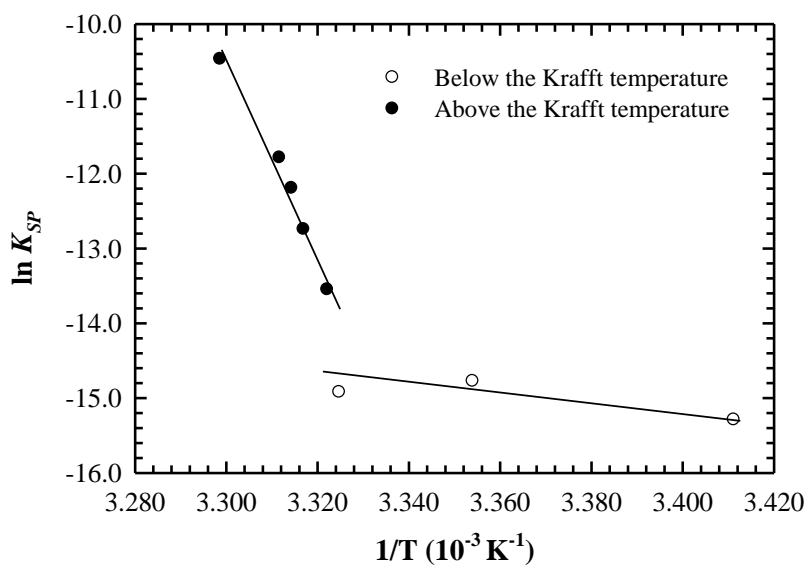


Figure 3.10 Solubility data of $\text{Ca}(\text{DeS})_2$ in aqueous solution for below and above the Krafft temperature on a van't Hoff plot.

The entropy change of dissolution is also estimated from the intercept of the plot but only for the data below the Krafft temperature in Figure 3.10. The entropy change is equal to 12.6 J/mol·K. Figure 3.11 shows the plot of Gibbs free energy as a function of temperature. It should be noted that the Gibbs free energy is relatively constant as the temperature increases below the Krafft temperature, but it decreases above the Krafft temperature. The lower Gibbs free energy above the Krafft temperature indicates the more stable micelle.

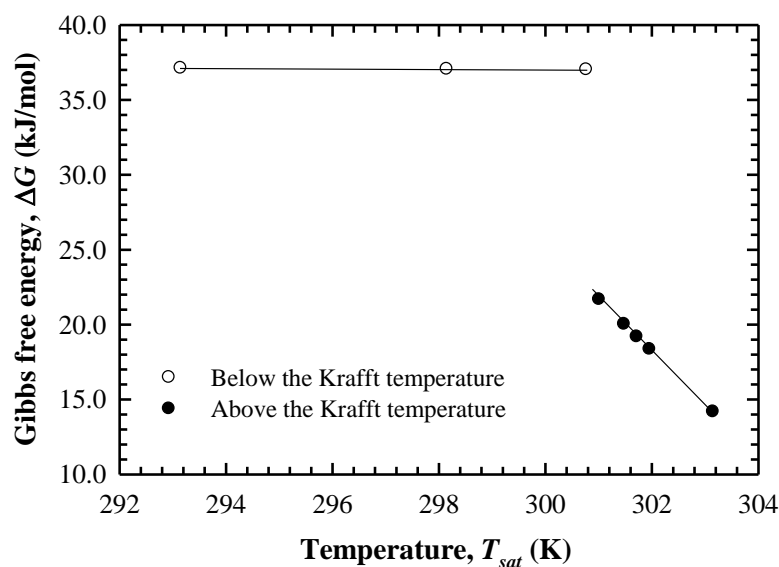


Figure 3.11 Gibbs free energy change for $\text{Ca}(\text{DeS})_2$ dissolution in water as a function of temperature.

3.5.1.3 Calcium Octylbenzenesulfonate

Unfortunately, it is quite difficult to investigate the solubility of Ca(OBS)_2 in aqueous solution as a function of temperature even though the solubility product of Ca(OBS)_2 is similar to Ca(DS)_2 at a specific temperature. The Krafft temperature and CMC are also not available in this work due to the limitation of the conductivity probe in the experiment, which cannot be used at high temperature. Consequently, the solubility product of Ca(OBS)_2 is only investigated at 30°C via the AAS technique. The solubility of Ca(OBS)_2 is reported in Table 3.3 and the K_{SP} of Ca(OBS)_2 is approximately 8.018×10^{-10} at 30°C .

Table 3.3 Total calcium ion concentration at saturation using the AAS technique for Ca(OBS)_2 in aqueous solution.

Sample #	Dilution ratio for AAS	Saturated concentration of calcium ion (mM)
1	1:10	1.3130
2	1:10	1.2490
3	1:10	1.3155
4	1:10	1.2370
5	1:10	1.2240
6	1:10	1.2780

Hence, it can be summarized that the solubility product of calcium surfactant salts in aqueous solution for Ca(DS)_2 and Ca(OBS)_2 are very similar to each other at the temperature studied in this work (30°C) while the solubility product of Ca(DeS)_2 in aqueous solution is higher than the other two calcium surfactant salts at the same temperature.

3.5.2 Precipitation Phase Boundary

3.5.2.1 Single Anionic Surfactant Precipitation Phase Boundary

The precipitation phase boundary for solutions of NaDS and CaCl_2 is shown in Figure 3.12 where the abscissa displays the total NaDS in the system and the ordinate plots the total calcium chloride (CaCl_2) concentration required to reach the phase boundary. As the concentration of NaDS increases in the system, the amount of CaCl_2 required to precipitate the $\text{Ca}(\text{DS})_2$ decreases until the minimum point, at the CMC of NaDS (also called the minimum hardness tolerance point).

Along the precipitation phase boundary and above the CMC, there is co-existence between monomers, micelles, and precipitate. In addition there are sodium ions due to the dissociation of NaDS, but NaDS is not found to precipitate at the levels of concentration and temperature studied in this work. Micellization causes the change of the slope in precipitation phase boundary above the CMC.

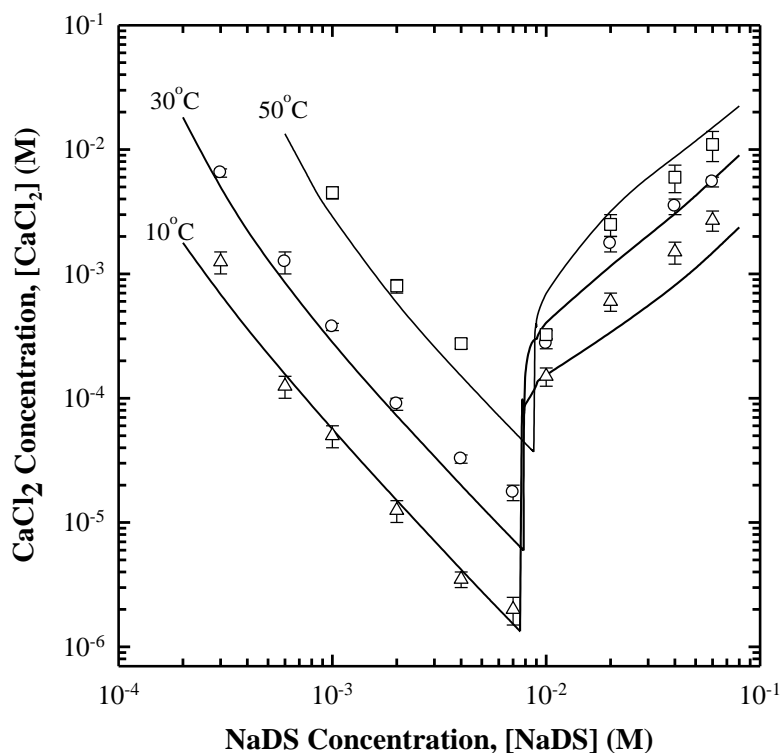


Figure 3.12 Theoretical precipitation phase boundaries estimated by the improved models for NaDS and CaCl_2 systems as a function of temperature corresponding with the experimental data.

The counterions (calcium and sodium ions) will partially bind to the negative charged surface of micelle; only the unbound counterions remain in the bulk solution. Thus, the total amount of calcium ions required to reach the phase boundary increases sharply above the CMC. Figure 3.12 also shows the model using the measured K_{SP} and other thermodynamic data is good, especially where the NaDS concentration is very low and in the region around the CMC. The model can be extended to cover the range 10 to 50°C (the range in which the K_{SP} has been measured) corresponding to the experimental data. The error bars shown in the figure indicate the uncertainty in determination of the precipitation phase boundary based on

the criteria to judge the saturated point, as described in experimental procedure (section 3.4.4)

The degree of supersaturation at the phase boundary is unity, or $S_0 = 1$, at the specific temperature studied. In order to satisfy equation (3.27) to be unity, the series of thermodynamic models of anionic surfactant precipitation described in Chapter 2 is employed in this work. The concentration of anionic surfactant monomers can be calculated by the Corrin-Harkins equation, and the concentration of unbound calcium ions can be calculated by the chemical equilibrium of counterion binding to the micelle. The directly measured K_{SP} value at a desired temperature is used in this equation. The activity coefficients are calculated by the use of the extended Debye-Hückel equation corresponding to the initial concentration of surfactant and CaCl_2 . The steps to calculate all precipitating species involved in equation (3.27) are demonstrated in detail in Appendix A.

The improvement of the models has been shown above the CMC where the counterion binding to the micelle is considered, while the previous models cannot well treat the activity of counterion binding to the micelle in the intermicellar solution, as can be seen by fitting the experimental data at other temperatures in Figure 3.13.

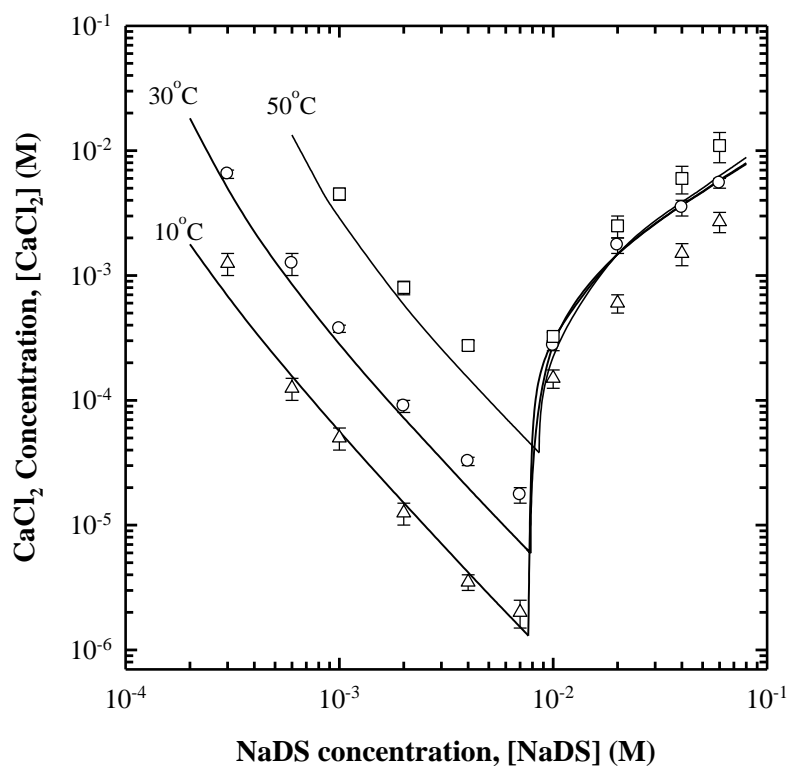


Figure 3.13 Theoretical precipitation phase boundaries estimated by the previous model (Stellner and Scamehorn, 1989a) for NaDS and CaCl_2 systems as a function of temperature corresponding with the experimental data.

The different results from the current and previous models shown in Figure 3.12 and 3.13, respectively, indicate that calcium ion partitioning on the micelle is not constant. The micellization model determines the concentration of monomers and the micelles in the bulk and they are dependent on temperature. The amount of micelles in the solution results in different levels of negated counterion on the micelle surface and thus, the calcium ion required to precipitate $\text{Ca}(\text{DS})_2$ changes. As can also be seen that the calcium ion required at precipitation phase boundaries above the CMC are separated as temperature changes.

However, it should be remarked that the modeling work for the precipitation phase boundary are improved above the CMC, but not yet perfect. The difficulty in modeling the phase boundary will be explained here. The counterion binding to the micelle based on chemical equilibrium of unbound and bound counterions binding to the micelle was assumed to be valid, and was employed throughout the range of temperature of 10 to 50°C, but the chemical equilibrium model was done with respect to the experimental data at only 30°C. The effect of temperature has only small on the counterion binding to the micelle for either pure ionic micelles (Zana, 1981) or mixed micelles (Rathman and Scamehorn, 1984). Also, the difference in the polar head group (sulfate and sulfonate) was also assumed not to have an effect on the counterion binding to the micelle. The previous study by Rathman and Scamehorn (1984) also showed constant total counterion binding in the mixtures containing different polar head groups on the micelles of sodium decyl sulfate (SO_4^-) mixed with sodium decyl sulfonate (SO_3^-). Although the temperature effect on the counterion binding to the micelle is claimed to have only a slight impact, it would be better to have the models of temperature dependence on the counterion binding to the micelle, rather than assuming it is constant for the temperatures studied. For many reasons, however, the experimental and modeling works of temperature effect on counterion binding to the micelle are performed only at 30°C, and as it can be observed that the precipitation phase boundary model at 30°C is the most accurate fit.

Another rationale is the estimation of activity coefficient by extended Debye-Hückel expression for the intermicellar solution. This work and elsewhere (Dharmawardana, Christian, Tucker, Taylor, and Scamehorn, 1993; Rodriguez, *et al.*, 2001; Soontravanich S., and Scamehorn, 2010; Stellner and Scamehorn, 1989a) assumed that the micelle is a separate phase, which will not contribute much to the ionic strength of the electrolyte solution and thus activity coefficient. But, it is probably due to accounting for micelle shielding factors, which is introduced to reduce the effect of the micellar charge on the ionic strength of the intermicellar solution, and results in very complex systems, with data only available for a few systems (Burchfield and Woolley, 1984). In this work, the ionic strength of the electrolyte solution was estimated by accounting for the counterion binding to the micelle effect as shown in Figure 3.14; however, this causes a worse prediction of the precipitation phase boundary, hence there is no accounting for counterion binding to the micelle in the calculation of ionic strength used in this work.

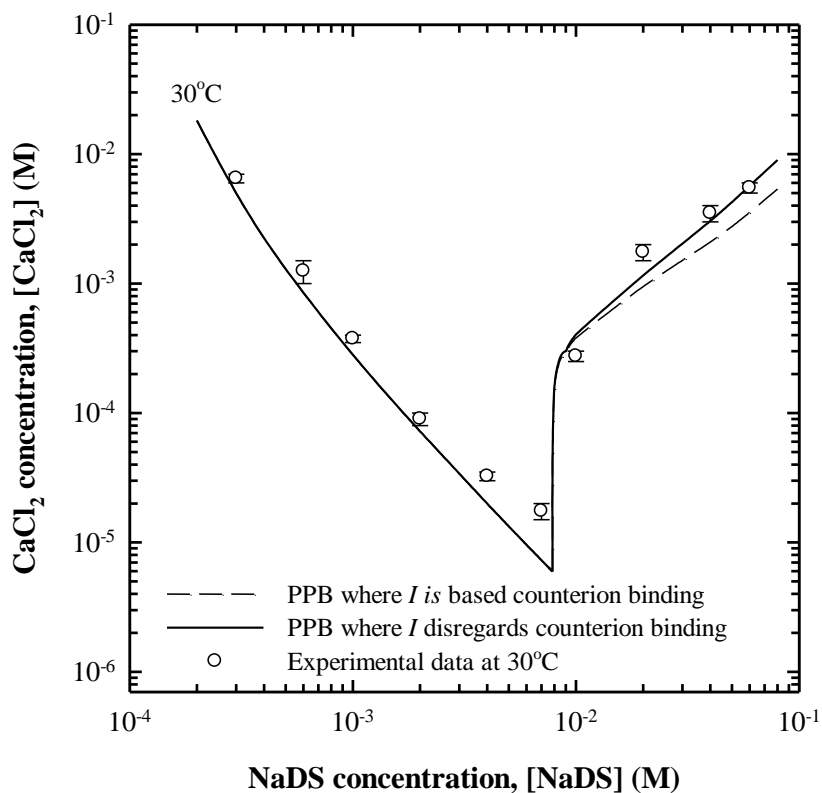


Figure 3.14 Comparison of prediction of the precipitation phase boundaries where the ionic strength, I , used in the Debye-Hückel equation is either based on, or discarding the counterion binding to the micelle effect for the NaDS and CaCl₂ systems, corresponding with the experimental data at 30°C.

3.5.2.2 Binary Mixed Anionic Surfactant Precipitation Phase

Boundary

It is interesting to study the precipitation of binary mixed anionic surfactant systems to determine how accurately the improved models predict the precipitation for the nonideal mixtures. An equimolar ratio of NaDS/NaOBS solution was studied to monitor the model accuracy. Figure 3.15 implies that pseudophase separation theory, regular solution model, and the proposed chemical equilibrium model of counterion binding to the micelle give a good prediction of the precipitation phase boundary.

As in single anionic surfactant precipitation, the degree of supersaturation at the phase boundary is unity, but based on the precipitating surfactant species at the specific temperature studied. In order to satisfy equation (3.27) to be unity, the series of thermodynamic models of mixed anionic surfactant precipitation described in Chapter 2 is employed in this work. The total concentration of anionic surfactant monomers can be calculated by the pseudophase separation theory and the regular solution model. The total concentration of mixed anionic surfactant will then be used in the chemical equilibrium model of bound and unbound counterions to quantify the amount of bound and unbound counterions. The measured K_{SP} of precipitating calcium salt at a desired temperature is used in this equation. The activity coefficients are calculated by the use of the extended Debye-Hückel equation corresponding to the initial total concentration of mixed anionic surfactant and CaCl_2 . The steps to calculate all precipitating species involved in equation (3.27) are demonstrated in details in Appendix B.

Theoretical phase boundaries for other molar ratios are also shown in Figure 3.15, but with no corresponding experimental data. The reason why only the equimolar ratio is studied is to monitor the precipitation of calcium surfactant salts for a similar type of anionic surfactant used, such as chemical structure, solubility product of their precipitates, and polar head group of their tails. The difference in surfactant tails (aliphatic and aromatic) is also less significant in the precipitation study; it may be due this being an ideal mixture as discussed in the previous chapter, but the investigation of the type of precipitating species is only based on solubility product value and experimental data fitting. More discussion of the precipitation of calcium surfactant salt in NaDS/NaOBS systems at an equimolar ratio is mentioned in the next chapter.

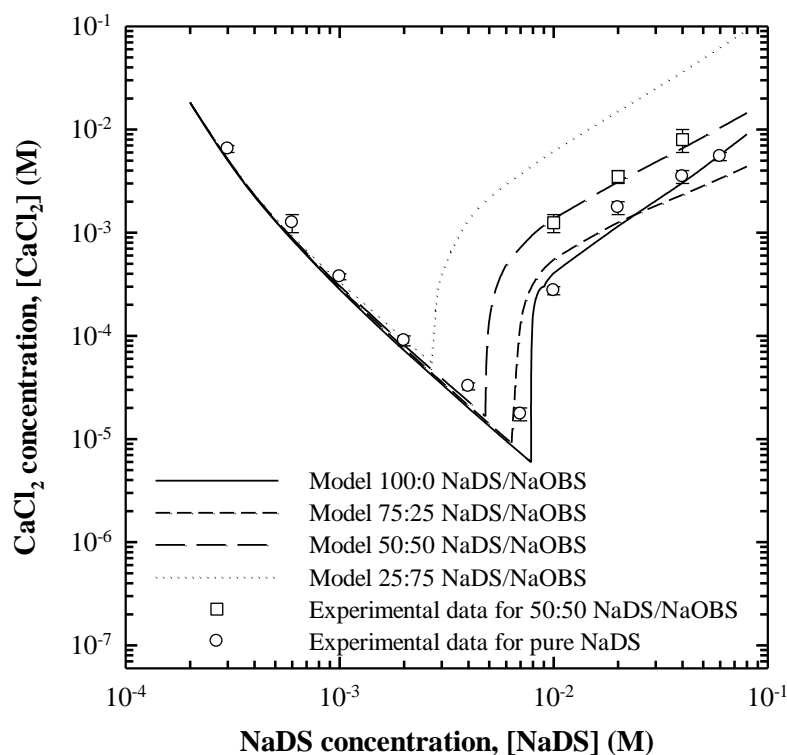


Figure 3.15 Theoretical precipitation phase boundaries from the improved models for binary mixed NaDS/NaOBS and CaCl_2 systems corresponding to the experimental data at pure NaDS and equimolar surfactant concentration at 30°C .

In the case that NaDS mixed with NaDeS is precipitated by CaCl_2 , theoretical precipitation phase boundaries are shown in Figure 3.16, with the corresponding experimental data. It is obvious that there is only $\text{Ca}(\text{DS})_2$ precipitating from binary mixed NaDS/NaDeS systems because the solubility product of $\text{Ca}(\text{DeS})_2$ is higher than $\text{Ca}(\text{DS})_2$, in the order of 10^{-5} as opposed to 10^{-10} , and the concentration of DeS^- in the solution is not sufficient to precipitate at the conditions employed in this work owing to the higher K_{SP} with calcium. The supersaturation ratio of the $\text{Ca}(\text{DeS})_2$ salt is below unity for all concentration levels studied here.

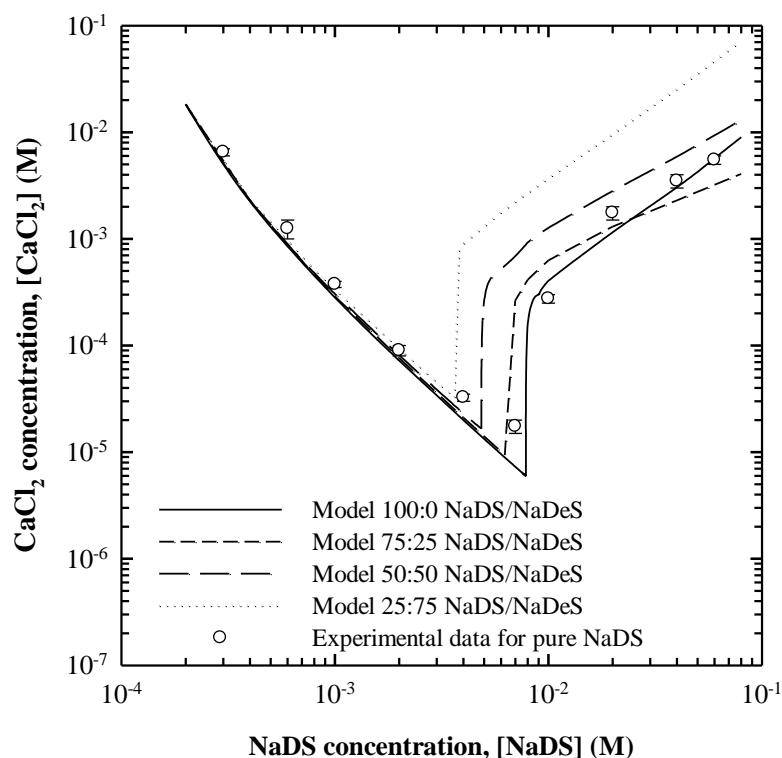


Figure 3.16 Theoretical precipitation phase boundaries from the improved models for binary mixed NaDS/NaDeS and CaCl_2 systems corresponding to the experimental data at pure NaDS systems at 30°C .

Moreover, a strange trend of the theoretical precipitation boundary is found in both Figure 3.15 and 3.16 at 75:25 molar ratios of binary mixed anionic surfactants. It may be due to the system reaching an ideal state as the fraction of NaDS increases in the solution. The switching of the treatment in thermodynamics of micellization to ideal solution theory may result in a better. In the lack of a better approach, however, the improved models will be also used in the next chapter of investigation of induction time.

3.6 Conclusions

The work has accurately measured the K_{SP} value of calcium dodecyl sulfate in aqueous solution over the temperature range of 10 to 55°C using two techniques; measuring the amount of $\text{Ca}(\text{DS})_2$ required to reach saturation at constant temperature with AAS and measuring the saturation temperature of constant composition solutions of $\text{Ca}(\text{DS})_2$ using conductivity measurements. The conductivity measurement is convenient and accurate for solutions whose solubility is in excess of the Krafft temperature, but has lower accuracy below the Krafft temperature. The solubility of $\text{Ca}(\text{DS})_2$ is very high at and above the Krafft temperature, and under these conditions the solutions require very high dilution ratios to enable measurement by AAS. This indicates that it is useful to use a combination of techniques in measurement of the solubility of surfactant systems, and the current study has shown that the two methods do give consistent results. The K_{SP} in this system exponentially increases with increasing temperature, resulting in the K_{SP} at 55°C being orders of magnitude larger than the value at 10°C. The work has also accurately measured the K_{SP} value of calcium decyl sulfate in aqueous solution over the temperature range of 20 to 30°C using two techniques and the current investigation has shown that the two methods do give consistent results for this species also. The K_{SP} of calcium 4-octylbenzenesulfonate in aqueous solution has been measured at only 30°C and the measurement technique by AAS results a highly consistent value of the solubility of $\text{Ca}(\text{OBS})_2$ in aqueous solution.

Thermodynamic properties of calcium surfactant salts dissolution in water such as, enthalpy, entropy, and Gibbs free energy are investigated in this work. The

calculated data shows the energy required to dissolve the calcium surfactant salts decreases as the temperature increases as the process is an endothermic process. The Gibbs free energy for the dissolution of calcium surfactant salts above the Krafft temperature indicates that the dissolved surfactant is more stable in the micellar form as there is a lower Gibbs free energy.

The precipitation phase boundary for $\text{Ca}(\text{DS})_2$ in solutions of NaDS and CaCl_2 , and binary mixed NaDS/NaOBS and NaDS/NaDeS systems can be predicted by the improved models that contain equations for the phase equilibrium between monomeric surfactant and unbound calcium ions, the K_{SP} as a function of temperature, the activity coefficients of the key species as a function of temperature and ionic strength, models that predict the micellization parameters, such as monomeric surfactant concentration as a function of temperature and ion concentrations, and also chemical equilibrium of counterions binding to the micelle. The fit of the model using a K_{SP} value determined from experiments of pure $\text{Ca}(\text{DS})_2$ in water gives a good fit to an experimental precipitation boundary studied in this work, but gives a slightly worse fit to an experimental precipitation boundary studied in previous work. This is to be expected since fundamentally measured parameters can never improve a fit to a model in comparison to models using parameters fitted to the data. The improved models better fit the data above the CMC in the system than earlier models, where the model for the micelle formation and counterion binding is dominant in determining the total amounts of NaDS and CaCl_2 present in the system required to form precipitates. Below the CMC the only modeling required is that for the K_{SP} value and the activity coefficients, and it is here that the model fitting is quite good. It may be noted that the K_{SP} value measured at 30°C is only 2.122×10^{-10} in

comparison to the value predicted from the phase boundary which is 5.02×10^{-10} . The current model fits dilute NaDS data quite well, but becomes less accurate as the system approaches the CMC value. There may be several reasons for this reduction in fitting ability as the NaDS concentration becomes higher, but perhaps the most likely reason is that the extended Debye-Hückel expression may be unable to accurately determine the effect of the ionic strength on the activity of the surfactant monomer ion. This has been suggested previously in sub-micellar solutions of sodium alkyl sulfates where deviations from the Debye-Hückel theory were noted, and possibly explained by variations in the hydrophobic hydration of the alkyl chains as the surfactant content increased. It may be necessary to determine more accurate models for activity coefficients for surfactants.

The precipitation phase boundary for $\text{Ca}(\text{DS})_2$ in solutions of equimolar ratio of binary mixed NaDS/NaOBS precipitating by CaCl_2 can be predicted by the improved models that contains equations of pseudophase separation assumption, regular solution theory, and also chemical equilibrium of counterions binding to the micelle. The models show a satisfactory prediction of precipitation phase boundary of $\text{Ca}(\text{DS})_2$ in the equimolar ratio of NaDS/NaOBS precipitating by CaCl_2 .

3.7 References

- Anuar, N., Daud, W. R. W., Roberts, K. J., Kamarudin, S. K., and Tasirin, S. M. (2009). An Examination of the Solution Chemistry, Nucleation Kinetics, Crystal Morphology, and Polymorphic Behavior of Aqueous phase Batch Crystallized l-Isoleucine at the 250 mL Scale Size. **Crystal Growth & Design** 9(6): 2853-2862.
- Atkins, P. and De Paula, J. (2009). **Elements of physical chemistry**. New York: W. H. Freeman & Company.
- Baviere, M., Bazin, B., and Aude, R. (1983). Calcium effect on the solubility of sodium dodecyl sulfate in sodium chloride solutions. **Journal of Colloid and Interface Science** 92(2): 580-583.
- Burchfield, T. E. and Woolley, E. M. (1984). Model for thermodynamics of ionic surfactant solutions. 1. Osmotic and activity coefficients. **The Journal of Physical Chemistry** 88(10): 2149-2155.
- Davies, C. W. and Shedlovsky, T. (1964). Ion association. **Journal of the Electrochemical Society** 111(3): 85-86.
- Dharmawardana, U. R., Christian, S. D., Tucker, E. E., Taylor, R. W., and Scamehorn, J. F. (1993). A surface tension method for determining binding constants for cyclodextrin inclusion complexes of ionic surfactants. **Langmuir** 9(9): 2258-2263.
- Dykstra, C. E. (1997). **Physical chemistry: A modern introduction**. New Jersey: Prentice-Hall.
- Frank, H. S. and Evans, M. W. (1945). Free Volume and Entropy in Condensed Systems III. Entropy in Binary Liquid Mixtures; Partial Molal Entropy in

- Dilute Solutions; Structure and Thermodynamics in Aqueous Electrolytes. **The Journal of Chemical Physics** 13(11): 507-532.
- Gale, W. W., Saunders, R. K., and Ashcraft Jr, T. L. (1976). **Oil recovery method using a surfactant**. US Patent no. 3,977,471.
- Gerbacia, W. E. F. (1983). Calcium dodecyl sulfate precipitation from solutions containing sodium chloride. **Journal of Colloid and Interface Science** 93(2): 556-559.
- Hollingsworth, M. (1978). Role of detergent builders in fabric washing formulations. **Journal of the American Oil Chemists' Society** 55(1): 49-51.
- Hrust, V., Skurić, M., Šošić, Z., and Kallay, N. (1999). Dissolution of anionic surfactants. Effect of cations on the change in heat capacity **Trends in Colloid and Interface Science XIII** (pp. 68-70): Springer Berlin / Heidelberg.
- Kallay, N., Pastuovic, M., and Matijevic, E. (1985). Solubility and enthalpy of precipitation of magnesium, calcium, strontium, and barium dodecyl sulfates. **Journal of Colloid and Interface Science** 106(2): 452-458.
- Klotz, I. M. and Rosenberg, R. M. (2008). **Chemical thermodynamics**. New Jersey: John Wiley & Sons.
- Lee, R. S. and Robb, I. D. (1979). Precipitation of calcium surfactants. Part 3. **Journal of the Chemical Society, Faraday Transactions** 1 75: 2126-2136.
- Li, F., Li, G.-Z., and Chen, J.-B. (1998). Synergism in mixed zwitterionic-anionic surfactant solutions and the aggregation numbers of the mixed micelles. **Colloids and Surfaces A: Physicochemical and Engineering Aspects** 145(1-3): 167-174.

- Lieser, K. H. (2003). Steps in precipitation reactions. **Angewandte Chemie International Edition in English** 8(3): 188-202.
- Mancera, R. L. and Buckingham, A. D. (1995). Molecular Properties of and Temperature Effects on the Hydrophobic Hydration of Ethane. **The Journal of Physical Chemistry** 99(40): 14632-14640.
- Moroi, Y., Oyama, T., and Matuura, R. (1977). Phase equilibria of anionic surfactant mixtures in aqueous solution. **Journal of Colloid and Interface Science** 60(1): 103-111.
- Mullin, J. W. (1992). **Crystallization**. Oxford: Butterworth-Heinemann.
- Myerson, A. S. (1993). **Handbook of industrial crystallization**. Boston: Butterworth-Heinemann.
- Nancollas, G. H. and Butler, J. N. (1967). Interactions in electrolyte solutions. **Journal of The Electrochemical Society** 114: 121C.
- Noïk, C., Bavière, M., and Defives, D. (1987). Anionic surfactant precipitation in hard water. **Journal of Colloid and Interface Science** 115(1): 36-45.
- Privalovl, P. and Gill, S. (1989). The hydrophobic effect: a reappraisal. **Pure & Applied Chemistry** 61(5): 1097-1104.
- Rathman, J. F. and Scamehorn, J. F. (1984). Counterion binding on mixed micelles. **The Journal of Physical Chemistry** 88(24): 5807-5816.
- Rodriguez, C. H., Lowery, L. H., Scamehorn, J. F., and Harwell, J. H. (2001). Kinetics of precipitation of surfactants. I. Anionic surfactants with calcium and with cationic surfactants. **Journal of Surfactants and Detergents** 4(1): 1-14.

- Rodriguez, C. H. and Scamehorn, J. F. (1999). Modification of Krafft temperature or solubility of surfactants using surfactant mixtures. **Journal of Surfactants and Detergents** 2: 17.
- Rodriguez, C. H. and Scamehorn, J. F. (2001). Kinetics of precipitation of surfactants. II. Anionic surfactant mixtures. **Journal of Surfactants and Detergents** 4(1): 15-26.
- Rosen, M. J. (1991). Synergism in mixtures containing zwitterionic surfactants. **Langmuir** 7(5): 885-888.
- Soontravanich, S., Munoz, J. A., Scamehorn, J. F., Harwell, J. H., and Sabatini, D. A. (2008). Interaction between an anionic and an amphoteric surfactant. Part I: Monomer–micelle equilibrium. **Journal of Surfactants and Detergents** 11(4): 251-261.
- Soontravanich, S. and Scamehorn, J. Relation of Supersaturation Ratio in Mixed Anionic Surfactant Solutions to Kinetics of Precipitation with Calcium. **Journal of Surfactants and Detergents** 13(1): 1-11.
- Soontravanich, S. and Scamehorn, J. F. (2010). Relation of supersaturation ratio in mixed anionic surfactant solutions to kinetics of precipitation with calcium. **Journal of Surfactants and Detergents** 13(1): 1-11.
- Stellner, K. L. and Scamehorn, J. F. (1989a). Hardness tolerance of anionic surfactant solutions. 1. Anionic surfactant with added monovalent electrolyte. **Langmuir** 5(1): 70-77.
- Stellner, K. L. and Scamehorn, J. F. (1989b). Hardness tolerance of anionic surfactant solutions. 2. Effect of added nonionic surfactant. **Langmuir** 5(1): 77-84.

- Tsujii, K., Saito, N., and Takeuchi, T. (1980). Krafft points of anionic surfactants and their mixtures with special attention to their applicability in hard water. **The Journal of Physical Chemistry** 84(18): 2287-2291.
- Vanjara, A. K. and Dixit, S. G. (1996). Recovery of cationic surfactant by using precipitation method. **Separations Technology** 6(1): 91-93.
- Wu, B., Christian, S., and Scamehorn, J. (1998). Recovery of surfactant from micellar-enhanced ultrafiltration using a precipitation process **Horizons 2000 – aspects of colloid and interface science at the turn of the millenium** (pp. 60-73).
- Zana, R. (1981). Effect of alcohols on the equilibrium properties and dynamics of micellar solutions. In D. O. Shah (Ed.), **Surface phenomena in enhanced oil recovery** (pp. 521-533). New York: Plenum.

CHAPTER IV

THE INDUCTION TIME OF BINARY MIXED ANIONIC SURFACTANT PRECIPITATION

4.1 Abstract

The precipitation of pure NaDS solution precipitated by CaCl_2 at a specific temperature depends only on the supersaturation ratio of the precipitating species in the bulk solution both below and above the CMC. The precipitation of calcium surfactant salts in binary mixed anionic surfactant systems can be summarized as following: for mixed NaDS/NaDeS precipitated by CaCl_2 systems, the induction time is only a function of the supersaturation ratio calculated based on $\text{Ca}(\text{DS})_2$. The experimental data shows the increase in the induction time is only due to the change in the concentration of the precipitating species (DS^-) because of changes in the molar ratio and thermodynamic changes due to mixed micellization. For the mixed NaDS/NaOBS precipitated by CaCl_2 , the precipitation of calcium surfactant salts can be considered based on $\text{Ca}(\text{DS})_2$ and $\text{Ca}(\text{OBS})_2$ due to their similar K_{SP} value. Precipitation of $\text{Ca}(\text{OBS})_2$ occurs in the systems of 25-50% NaDS molar ratio. At this range of molar ratio, the inhibition of precipitation is not found in the mixed NaDS/NaOBS systems. For precipitation of $\text{Ca}(\text{DS})_2$ in the systems of 50-75% molar ratio of NaDS/NaOBS mixtures, the induction time is essentially not a function of supersaturation ratio, which is calculated based on $\text{Ca}(\text{DS})_2$ as the different precipitation

trend can be observed when compared to the pure NaDS precipitated by CaCl_2 systems. In this case, the inhibition of precipitation is observed as the induction time appears larger than in the pure NaDS systems at the same degree of supersaturation with respect to $\text{Ca}(\text{DS})_2$. The inhibition is due to the change in precipitating species (DS^-) because of the molar ratio and thermodynamic change of mixed micellization. In this case, it is also predicted for the change in kinetics of precipitation.

The kinetics of precipitation of binary mixed anionic surfactants can be found at 50-75% NaDS/NaOBS systems, the interfacial energy estimated from the relationship of induction time and supersaturation ratio reveals that the time required precipitating the $\text{Ca}(\text{DS})_2$ in 50-75% NaDS/NaOBS systems is larger than the time required to precipitate $\text{Ca}(\text{DS})_2$ in pure NaDS aqueous solution. The other kinetic parameters such as nucleation rate, Gibbs free energy change of formation of critical nucleus, and the radius of critical nucleus are estimated, they also reveal that the inhibition of anionic surfactant precipitation is partly due to kinetic change.

4.2 Introduction

Precipitation of calcium surfactants is one of the problems for applications of anionic surfactants, in particular in laundry detergency. Much research has been directed towards avoiding anionic surfactant precipitation by counterions such as calcium and magnesium ions, or by cationic surfactants, and even precipitation of cationic surfactants, to avoid the formation of soap scum. There are at least three notable methods for tackling the detrimental effects of hardness ions in anionic surfactant applications. The first method uses considerable amounts of cosurfactants (e.g. fatty alcohols) to improve the solubility of the calcium surfactant below the Krafft temperature (Zapf, Beck, Platz, and Hoffmann, 2003). Another approach uses builders in order to enhance the surfactant's tolerance to calcium ions (Crutchfield, 1978; Hollingsworth, 1978). Zeolites, phosphates, or silicates act as the builder, which has a large affinity for calcium ions and prevents a decrease in active surfactant composition by binding to the calcium ions (Hollingsworth, 1978). The last method is the development of an anionic surfactant formulation which does not precipitate in the presence of calcium ions. It is well known that the use of mixed surfactant systems can decrease the Krafft temperature and increase hardness tolerance (Rodriguez and Scamehorn, 1999, 2001; Soontravanich S., and Scamehorn, 2010a; Stellner and Scamehorn, 1989a, 1989b). This chapter deals primarily with the third method, since practical applications of surfactants usually involve the use of mixtures of surfactants, while the use of builders can cause a serious environment problem as they can increase phosphorous concentrations in surface water, raising the growth of algae and duckweed. This phenomenon is commonly known as eutrophication.

There have been numerous thermodynamic studies on the equilibrium for precipitation of single anionic surfactants precipitated by divalent and cationic surfactants (Gerbacia, 1983; Kallay, Pastuovic, and Matijevic, 1985; Miyamoto, 1960; Noïk, Bavière, and Defives, 1987; Peacock and Matijevi, 1980; Rodriguez, Lowery, Scamehorn, and Harwell, 2001; Shinoda and Hirai, 1977) but few studies of the kinetics of precipitation of both single and mixed anionic surfactant systems (Rodriguez, *et al.*, 2001; Rodriguez and Scamehorn, 2001; Soontravanich S., and Scamehorn, 2010a). An investigation into the induction time of anionic surfactants precipitated by calcium ions is a key feature of kinetic studies in order to understand the inhibition of precipitation when a second anionic surfactant is present in the solution, however there are few such studies in the scientific literature. This is due to the complexity of the formation of the micelle in pure systems and/or the formation of the mixed micelle in the mixed system. The system is made more complex by the effects of counterion on the critical micelle concentration (CMC), and counterion binding on the charged micelle surface.

Consequently, this work aims to systematically investigate the inhibition of precipitation of mixed anionic surfactants by calcium ions. The work will elucidate the relationship between induction time and the degree of solution supersaturation in a wide range of solution molarity both below and above the CMC in order to extend the knowledge about the kinetics of precipitation of binary anionic surfactant mixtures. A series of improved models for anionic surfactant precipitation and the activity of counterion binding from previous chapters will be used here to calculate the amount of precipitating species in the intermicellar solution. This should improve understanding of the inhibition of anionic surfactants precipitated by hardness ions.

Moreover, important crystallization parameters will be estimated in order to model the behavior of calcium-induced precipitation of single and binary mixed anionic surfactants.

4.3. Theory

4.3.1 Surfactant Precipitation

In general, precipitation occurs when the ion product of soluble ionic species in solution is in excess of the equilibrium ion product, i.e. the solubility product (K_{SP}). Therefore, surfactant precipitation occurs when the activities of precipitating surfactant and counterion are such that the solubility product is satisfied. Below the CMC, all surfactant species are in the monomeric form together with dissociated monovalent counterion, and therefore counterions are not bound to the micelle. Thus, all species in the bulk solution can be found independently. For precipitating systems above the CMC, there are three phases coexisting together, monomeric, micellar, and precipitate phases. Surfactant species are in both the monomeric and micellar forms in solution, and monovalent and divalent counterion binding to the micelle surface also occurs. The solubility product relationship for precipitation of the anionic surfactants with calcium ions can be expressed as:

$$K_{SP} = [Ca^{2+}]_{unb} [S^-]_{mon}^2 f_{Ca^{2+}} f_{S^-}^2 \quad (4.1)$$

where K_{SP} is the activity-based solubility product of the precipitating anionic surfactant salt, $[Ca^{2+}]_{unb}$ is the concentration of unbound calcium ions, and $[S^-]_{mon}$ is the concentration of the precipitating surfactant ion in the monomeric form. The

activity coefficients of surfactant (f_S^-) and calcium ($f_{Ca^{2+}}$) can be estimated using an extended Debye-Hückel expression (Davies and Shedlovsky, 1964):

$$\log f_i = \frac{-A(z_i)^2 I^{0.5}}{1 + Ba_i I^{0.5}} - 0.3I \quad (4.2)$$

where A and B are constants depending on the solvent and solution temperature. The values of A and B for aqueous solution have been tabulated (Klotz and Rosenberg, 2008) and for 30°C, $A = 0.5239$ and $B = 3.279 \times 10^7$. The ion valence (z_i) for DS^- , DeS^- , and OBS^- is equal to -1, and for the calcium ion, z_i is equal to +2. The parameter a_i is an empirical value based on the ion diameter. It can be estimated based on the species: for NaDS NaDeS, and NaOBS, a_i is equal to $7 \times 10^{-8} \text{ cm}^{-1}$ (Robinson and Stokes, 1959; Rodriguez and Scamehorn, 2001) and a_i is equal to $6 \times 10^{-8} \text{ cm}^{-1}$ for the calcium ion (Klotz and Rosenberg, 2008). Assuming that only $CaCl_2$ and NaS are present in the system, the ionic strength of the solution (I) can be calculated using the following equation:

$$I = \sum 0.5c_i z_i^2 = [NaS] + 3[CaCl_2] \quad (4.3)$$

where c_i is the total concentration of ion i in solution; z_i is the valence of ion i ; $[NaS]$ is the total anionic surfactant concentration in solution and $[CaCl_2]$ is the total calcium chloride concentration in solution. However, thermodynamic parameters can be estimated by these equations regardless of the micellization and counterion binding phenomena since, it can be assumed that they do not contribute too much to the ionic strength, and do not have much effect on the monomer surfactant and unbound

calcium ions (Rodriguez, *et al.*, 2001; Rodriguez and Scamehorn, 2001; Soontravanich S., and Scamehorn, 2010a).

The induction time is a function of the supersaturation ratio (S_0); a number of articles have described investigations into the relationship between the induction time for precipitation and the degree of supersaturation for various crystal forms (Roelands, Jiang, Kitamura, ter Horst, Kramer, and Jansens, 2006; Roelands, Roestenberg, ter Horst, Kramer, and Jansens, 2004; Soontravanich S., and Scamehorn, 2010a; Teychené and Biscans, 2008). The supersaturation ratio is defined as the ion product of the precipitating surfactant salt (considering the activity of the surfactant in the monomer phase and the activity of the unbound calcium ions) divided by the solubility product, and to the inverse power of the sum of the stoichiometric coefficients of the reactants as shown in equation (4.4) (Stellner and Scamehorn, 1989b):

$$S_0 = \left(\frac{[Ca^{2+}]_{unb} [S^-]_{mon}^2 f_{Ca^{2+}} f_{S^-}^2}{K_{SP}} \right)^{1/3} \quad (4.4)$$

Micellization starts to occur at the CMC. As more anionic surfactant is added to a system above the CMC, the additional surfactant forms more micelles. This causes more unbound sodium ions to be dissociated from the surfactant salt, lowering the CMC because of the effect of unbound counterions on the CMC as described by the Corrin-Harkins relationship. Meanwhile, sodium and calcium ions tend to be bound at the micelle surface due to their opposite charge; hence, the unbound calcium ion concentration is reduced due to the binding phenomenon. The modeling of these phenomena in order to estimate surfactant monomer concentrations

and activity of counterions above the CMC can be performed by using a series of models developed in the previous two chapters.

Surfactant solutions containing mixed surfactants have longer induction times than systems having a single surfactant, and thus such mixtures appear to inhibit the precipitation for both anionic and nonionic surfactant systems (Soontravanich S., and Scamehorn, 2010b; Stellner and Scamehorn, 1989b) and mixtures of two different anionic surfactants (Rodriguez and Scamehorn, 2001; Soontravanich S., and Scamehorn, 2010b). However, the supersaturation ratio of each individual precipitating surfactant can be calculated for the binary mixed anionic surfactant systems even when a mixed micelle is formed. Consequently, the bulk solution systems are relatively more complex when mixing two different anionic surfactants even for similar surfactant structures, and it is probably better to treat the mixtures using a nonideal mixing model in order to obtain more an accurate value of supersaturation ratio.

The compositions of the precipitating species in each phase are estimated by using the Pseudophase Separation theory and the Regular Solution theory, as discussed in the previous chapters and elsewhere (Schulz, Rodríguez, Minardi, Sierra, and Morini, 2006; Soontravanich S., Munoz, Scamehorn, Harwell, and Sabatini, 2008). However, the counterion binding to the mixed micelles in binary mixed anionic surfactant systems is assumed to be the same as in single anionic surfactant systems (Rathman and Scamehorn, 1984, 1987) because the head groups (the polar part) are identical and the surfactant backbones (the nonpolar part) are alike. Consequently, it is assumed in this work that it is adequate to use the chemical equilibrium of bound and unbound mono- and divalent ions in the single anionic

surfactant system in order to quantify the amount of bound and unbound divalent ions. More details in calculating the precipitating anionic surfactant compositions in monomeric and micellar phases have been discussed in the previous chapters.

4.3.2 Induction Time to Precipitation

The nucleation rate (J) can be predicted based on the classical homogeneous nucleation model. The nucleation rate can be described as the number of nuclei formed per unit of time per volume, and can be expressed in the form of the Arrhenius reaction velocity equation commonly used for the rate of a thermally activated process (Mullin, 1992):

$$J = A \exp(-\Delta G / k_B T) \quad (4.5)$$

where A is the pre-exponential constant, k_B is the Boltzmann constant which is equal to 1.3805×10^{-23} J/K, and ΔG is the overall excess Gibbs free energy change of formation of nuclei in Joule. It can be defined as:

$$\Delta G = \frac{\beta \gamma^3 V_m^2 f(\theta)}{(2.303 k_B T \log S_0)^2} \quad (4.6)$$

where β is a geometric factor and is equal to $16\pi/3$ for a spherical nucleus, γ is the surface energy in J/m², V_m is the molecular volume and it is equal to 521.6 \AA^3 for Ca(DS)₂ and 502.8 \AA^3 for Ca(OBS)₂ as predicted by Chem3D Pro 11.0 software via the Connolly molecular volume method (Connolly, 1985). $f(\theta)$ is a correction factor; when homogeneous nucleation takes place $f(\theta) = 1$, and it is equal to 0.01 when heterogeneous nucleation takes place.

Induction time (t_{ind}) is one of the fundamental parameters in crystallization as it has frequently been used as a measure of the nucleation event, making the simplifying assumption that it can be considered to be inversely proportional to the rate of nucleation (Mullin, 1992).

$$t_{ind} \propto J^{-1} \quad (4.7)$$

Based on the classical homogeneous nucleation relationship, the induction time can be written with respect to the supersaturation ratio as the following expression (Mullin, 1992; Myerson, 1993):

$$\log t_{ind} \propto \left[\frac{\gamma^3}{T^3 (\log^2 S_0)} \right] \quad (4.8)$$

Anionic surfactant precipitation with hardness ions has been found to occur in a range of seconds to minutes (Soontravanich S., and Scamehorn, 2010a, 2010b). A study of nucleation rate is very difficult in a conventional laboratory. However, the nucleation rate can be approximated by using the relationship between the induction time and supersaturation ratios which can be used to approximate the interfacial energy of nuclei and free energy barrier. Equation (4.8) suggests that the plot between $(\log t_{ind})$ and the inverse of $(\log^2 S_0)$ at a specific temperature yields a linear function with slope which is related to homogeneous nucleation. It will allow evaluation of the amount of energy necessary to form the critical size of nuclei. The change in the nucleus formation results in the change in interfacial energy (Mullin, 1992; Myerson, 1993). The larger the energy required the larger the induction time

required to form a stable nucleus. The nucleation rate can be calculated approximately when the interfacial energy is known. However, the prediction using the above relationship has been suggested to be valid only for high supersaturation ratio (Randolph and Larson, 1988).

Furthermore, the behavior of a newly nucleated particle in a supersaturated solution depends on its size, which determines whether it will grow or redissolve; these processes should result in a change in the free energy of the particle. Hence, the radius of the critical nucleus (r_c) represents the minimum size of a stable nucleus. A nucleus smaller than r_c will dissolve because only in this way can the particle achieve a reduction in its free energy. Similarly, a nucleus larger than r_c will continue to grow. Based on the classical theory of nucleation, stemming from the work of Gibbs (1928) and discussed in detail in Mullin (1992), the radius of the critical nucleus can be calculated by the following equation (Mullin, 1992):

$$\Delta G_{crit} = \frac{4\pi\gamma r_c^2}{3} \quad (4.9)$$

where the critical Gibbs free energy (ΔG_{crit}) required to produce a stable nucleus can be calculated when the interfacial energy is known (Mullin, 1992):

$$\Delta G_{crit} = \frac{\beta\gamma^3 V_m^2}{(k_B T \ln S_0)^2} \quad (4.10)$$

4.4. Experimental Procedure

4.4.1 Materials

Sodium dodecyl sulfate (NaDS) was purchased from Carlo Erba with purity greater than 92%. Sodium 4-octylbenzene Sulfonate (NaOBS) was purchased from Aldrich with purity greater than 97%. These two anionic surfactants were further purified by recrystallizing twice using deionized water and methanol, respectively. They were dried over silica gel at room temperature for 24 hours. Sodium decyl sulfate (NaDeS) was purchased from Fluka with purity greater than 99% and was used as received without further purification. Calcium Chloride dihydrate ($\text{CaCl}_2 \cdot 2\text{H}_2\text{O}$), analytical reagent grade with purity greater than 98.0%, was purchased from Sigma-Aldrich and was used as received. Deionized water ($18 \text{ M}\Omega \cdot \text{cm}$) was used to prepare all aqueous samples through out the experiments.

4.4.2 Determination of Induction Time

Fresh stock solutions of NaDS both below and above the CMC was prepared to avoid the hydrolysis of NaDS. The induction time for precipitation of NaDS by CaCl_2 was investigated first to study the surfactant precipitation for the single anionic surfactant system and due to its precipitate (calcium dodecyl sulfate, $\text{Ca}(\text{DS})_2$) having the lowest solubility product (K_{SP}) of the three calcium surfactant salts. All experiments are performed over the precipitation phase boundary of NaDS with varying supersaturation ratios. For mixed (binary) anionic surfactant systems, fresh stock NaDS, NaDeS, and NaOBS solutions both below and above the critical micelle concentration of the mixture (CMC_M) were prepared to avoid the hydrolysis of anionic surfactants. The induction time of the two binary systems of NaDS/NaDeS and NaDS/NaOBS precipitated with CaCl_2 were investigated. The experiments are

performed with different molar ratios of surfactants and several supersaturation ratios by varying the total surfactant concentration and CaCl_2 concentration. A supersaturated solution can be prepared by mixing two reactants which will form a salt at a higher concentration than its equilibrium solubility. The supersaturation ratio in each system can be calculated from the equations described in the theoretical section (Section 4.3.1).

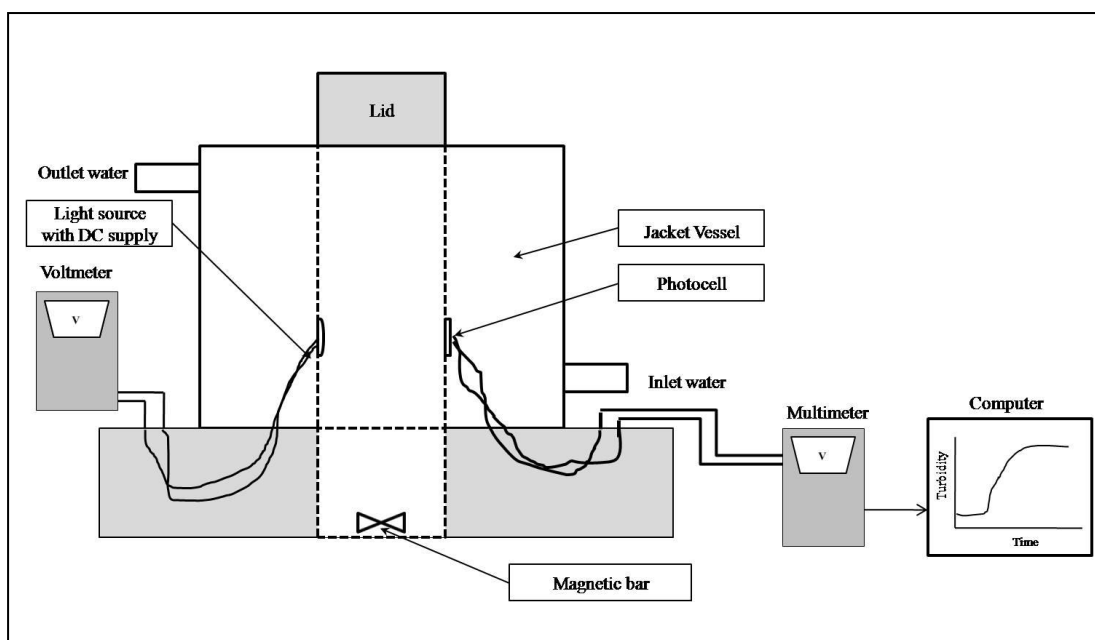


Figure 4.1 The design of a turbidity device to study the kinetics of anionic surfactant precipitation.

All experiments were carried out in an online turbidity device. The turbidity caused by the precipitation was measured using the apparatus shown in Figure 4.1. The transmitted light source was a green light diode (LED). The detector was a small photocell with a range of light resistance of 1-10 $\text{k}\Omega$, which depended on the light intensity. The reaction was held at 30°C by circulating water through the

jacket of the vessel. The temperature was monitored and maintained by a temperature-controlled water bath with constant agitation by a magnetic stirrer to ensure good mixing. The voltage signal was monitored and registered every second by a digital multimeter (Valleman DVM 345DI) with a PC interface. The response was converted to turbidity using the following equation (Soontravanich S., and Scamehorn, 2010a):

$$\tau = \frac{1}{L} \ln\left(\frac{I_0}{I}\right) = \frac{1}{L} \ln\left(\frac{V_0}{V}\right) \quad (4.11)$$

where τ is the turbidity with units of inverse length, L is the light path length, I is the intensity of light, and I_0 is the intensity of light detected with the isotropic sample (blank). The light intensity was measured by the resistance of the photocell, where the signal can be converted to voltage (V) as registered by the multimeter. V_0 is the voltage for isotropic sample.

The induction time was determined by finding the time difference between mixing and the point of the curve where there is the first small change in turbidity due to crystal nucleation. The induction time was determined at least three times for each batch to show reproducibility. For the fast precipitation, less than 10 seconds, the induction time was observed visually once again to confirm the device reliability.

4.5 Results and Discussion

4.5.1 Precipitation of Single Anionic Surfactant Systems by CaCl_2

NaDS is chosen as the surfactant to precipitate with calcium chloride in order to understand the single anionic surfactant precipitation system since NaDS has been widely used in various surfactant applications. Another reason for its choice is due to the solubility product (K_{SP}) of its precipitate, $\text{Ca}(\text{DS})_2$, is lower than the K_{SP} of the other two calcium salts ($\text{Ca}(\text{OBS})_2$ and $\text{Ca}(\text{DeS})_2$). The initial supersaturation ratio, S_0 , for NaDS precipitated with CaCl_2 based on the equations described in the theoretical section (section 4.3.1) are shown in Figure 4.2.

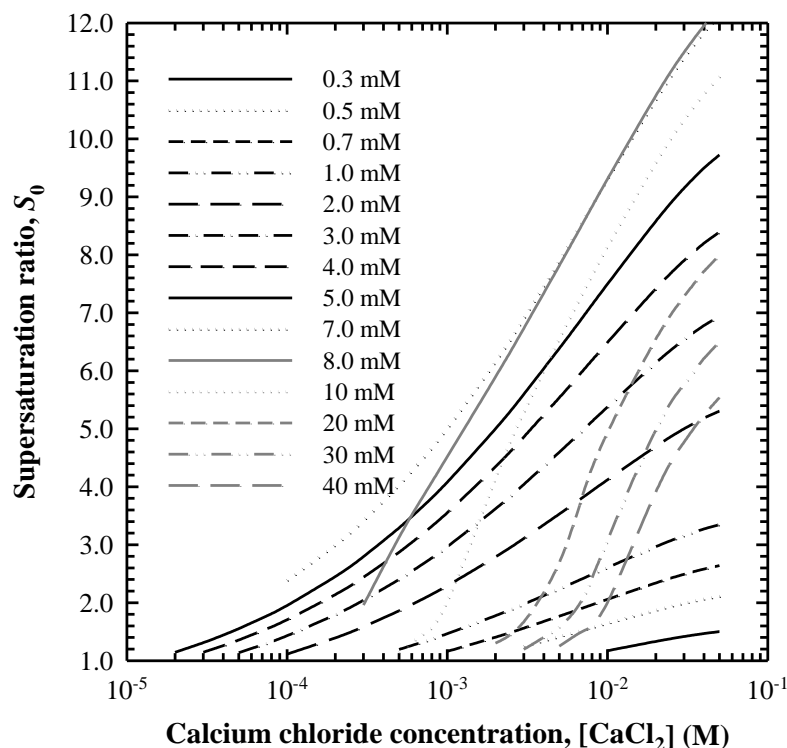


Figure 4.2 Supersaturation ratio curves as a function of CaCl_2 with varying NaDS concentration at 30°C below and above the CMC of NaDS.

The graph shows a range of supersaturation ratios corresponding to NaDS and CaCl₂ concentrations above the precipitation phase boundary of NaDS precipitating by CaCl₂. The supersaturation ratio increases as the concentrations of NaDS and CaCl₂ increase for systems below the CMC. At the CMC (approximately at 8 mM), all singly dispersed molecules are saturated and the micellization starts to occur. Above the CMC the surfactant monomer concentration is reduced due to the micelle formation and the effect of unbound sodium ions dissociated from NaDS molecules causes the change in the CMC value (Stellner and Scamehorn, 1989a). Consequently, the supersaturation ratio decreases as the NaDS concentration increases in systems above the CMC. The counterion binding to the micelle is reducing the amount of unbound calcium ions in the system above the CMC; if it is desired to spontaneously precipitate NaDS above the CMC for the single anionic surfactant precipitation system, an increase in the CaCl₂ concentration is required to force the supersaturation ratio equal to unity.

Furthermore, the region of supersaturation ratio above the precipitation phase boundary for precipitation of NaDS with CaCl₂ in Figure 4.2 can be demonstrated as shown in Figure 4.3. It is assumed that the effect of calcium ion on the CMC is negligible (Maneedaeng, Haller, Grady, and Flood, in press; Stellner and Scamehorn, 1989a). Figure 4.3 shows that far above the precipitation phase boundary of single anionic surfactant precipitating with calcium ions, the high supersaturation ratio causes fast precipitation as the driving force to precipitate increasing causes a reduction in induction time.

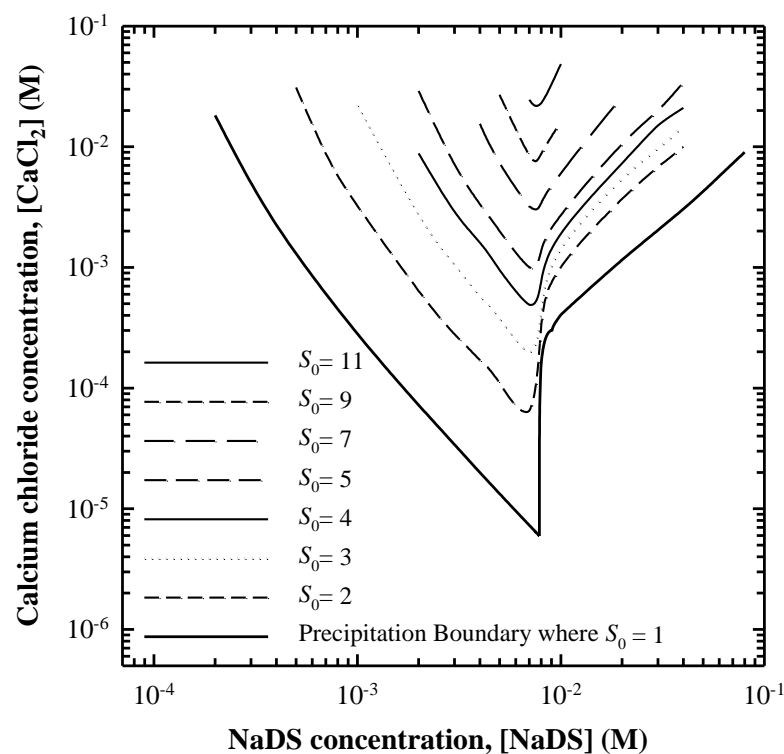


Figure 4.3 Supersaturation ratio regions over the theoretical precipitation phase boundary (PPB) for NaDS precipitating by CaCl_2 at 30°C .

Some selected experimental results from the online turbidity measurement are shown in Figures 4.4(a) and 4.4(b). These figures show some responses of the turbidity as NaDS is precipitated by CaCl_2 for both below and above the CMC. As can be seen from the experimental results in both cases, the induction time can be determined as the time elapsed between the mixing (zero seconds) and the appearance of the precipitate which results in a change in the slope of the turbidity curve.

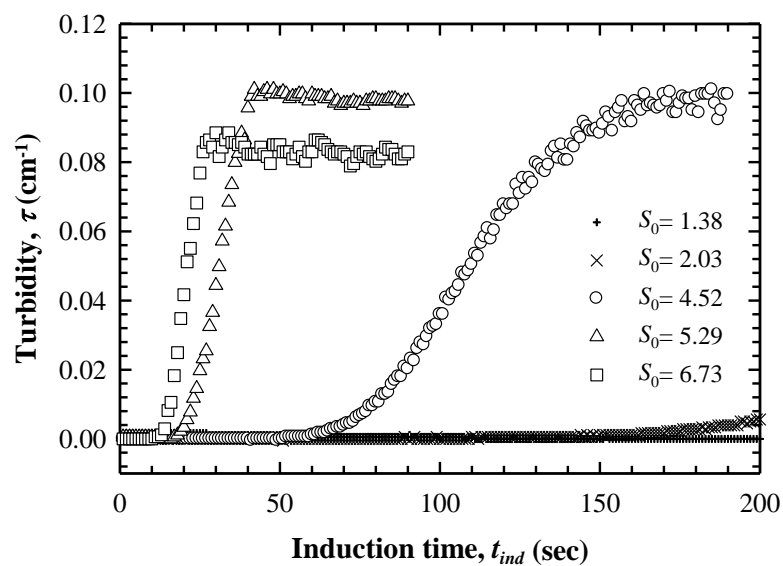
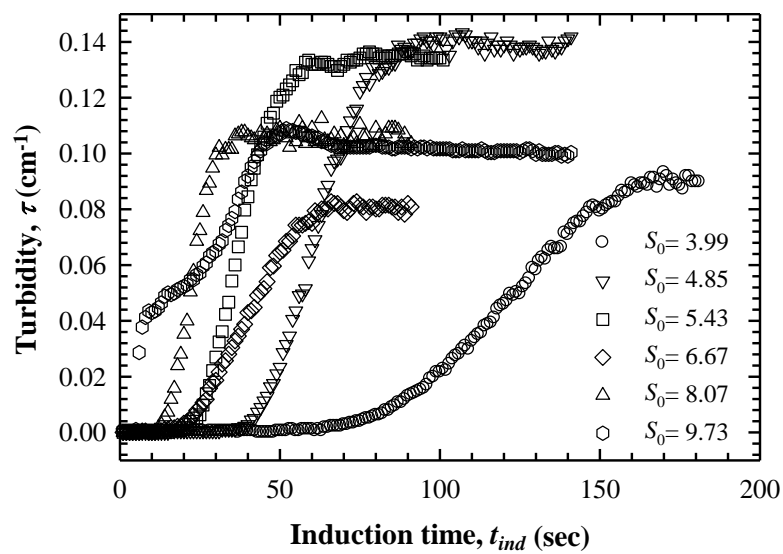


Figure 4.4 Some selected turbidity curves by precipitation of NaDS with CaCl_2 (a) below and (b) above the CMC at 30°C with varying supersaturation ratio, S_0 .

Both below and above the CMC the induction time increases as the supersaturation ratio decreases. However, it should be noticed that in precipitation systems above the CMC the induction time is much larger while the total surfactant concentration is higher by increasing the additional anionic surfactant above the CMC. This can be explained only by the reduction of the precipitating species (monomers) because of micellization, and the effect of salting out by dissociated sodium ions that increases the micelle concentration. The results for all systems studied in this work are shown in Table 4.1, and a plot of induction time against the supersaturation ratio for NaDS precipitation with CaCl_2 in Figure 4.5.

From Table 4.1 and Figure 4.5, it is clear that the precipitation of NaDS by CaCl_2 usually occurs within a minute or less. The time required to nucleate $\text{Ca}(\text{DS})_2$ approaches zero seconds when the supersaturation ratio approaches a high value (for instance when the supersaturation ratio is over 3) whether the system is below or above the CMC. The fact that the system gives the same result above and below the CMC can be understood as the micelles in solution are not acting as a template for nucleation of the precipitate. The result of the study also shows that the time required to precipitate $\text{Ca}(\text{DS})_2$ is a function of supersaturation ratio only with respect to the amount of dodecyl sulfate monomers ($[\text{DS}^-]_{\text{mon}}$) and unbound calcium ions ($[\text{Ca}^{2+}]_{\text{unb}}$) in the bulk solution.

Table 4.1 The summary of induction time of single NaDS systems precipitating by CaCl_2 corresponding to its supersaturation ratio at 30°C.

[NaDS], M	[CaCl ₂], M	[DS] _{mon} , M	[Ca ²⁺] _{unb} , M	S ₀	t _{ind} (sec)
0.003	0.0045	3.00×10 ⁻³	4.50×10 ⁻³	4.48	13.3
	0.012	3.00×10 ⁻³	1.20×10 ⁻²	5.58	12.0
	0.035	3.00×10 ⁻³	3.50×10 ⁻²	6.67	11.7
0.004	0.0045	4.00×10 ⁻³	4.50×10 ⁻³	5.39	13.3
	0.012	4.00×10 ⁻³	1.20×10 ⁻²	6.74	12.3
	0.035	4.00×10 ⁻³	3.50×10 ⁻²	8.07	11.0
0.005	0.00065	5.00×10 ⁻³	6.50×10 ⁻⁴	3.57	Large
	0.0018	5.00×10 ⁻³	1.80×10 ⁻³	4.85	32.0
	0.004	5.00×10 ⁻³	4.00×10 ⁻³	6.03	14.3
	0.0085	5.00×10 ⁻³	8.50×10 ⁻³	7.24	11.7
	0.05	5.00×10 ⁻³	5.00×10 ⁻²	9.73	5.0
0.006	0.00065	6.00×10 ⁻³	6.50×10 ⁻⁴	3.99	60.0
	0.0018	6.00×10 ⁻³	1.80×10 ⁻³	5.43	15.3
	0.004	6.00×10 ⁻³	4.00×10 ⁻³	6.77	12.3
	0.05	6.00×10 ⁻³	5.00×10 ⁻²	10.96	11.3
	0.1	6.00×10 ⁻³	1.00×10 ⁻¹	11.32	3.7
0.008	0.001	7.20×10 ⁻³	7.43×10 ⁻⁴	4.59	45.3
	0.002	7.20×10 ⁻³	1.74×10 ⁻³	5.95	19.7
	0.003	7.20×10 ⁻³	2.74×10 ⁻³	6.79	13.7
	0.01	7.20×10 ⁻³	9.74×10 ⁻³	9.37	11.3
0.010	0.001	6.47×10 ⁻³	8.85×10 ⁻⁵	2.07	110.0
	0.002	6.31×10 ⁻³	8.38×10 ⁻⁴	4.21	29.3
	0.003	6.29×10 ⁻³	1.81×10 ⁻³	5.34	16.3
	0.006	6.28×10 ⁻³	4.80×10 ⁻³	7.04	13.0
	0.01	6.28×10 ⁻³	8.80×10 ⁻³	8.21	12.7
0.020	0.003	4.73×10 ⁻³	1.16×10 ⁻⁴	1.68	165.0
	0.006	4.21×10 ⁻³	1.28×10 ⁻³	3.33	18.0
	0.01	4.13×10 ⁻³	4.96×10 ⁻³	4.96	15.0
0.030	0.003	4.22×10 ⁻³	6.04×10 ⁻⁵	1.20	Large
	0.006	3.64×10 ⁻³	3.06×10 ⁻⁴	1.81	68.7
	0.01	3.30×10 ⁻³	2.05×10 ⁻³	3.09	15.3
0.040	0.003	3.83×10 ⁻³	4.67×10 ⁻⁵	1.00	Large
	0.006	3.35×10 ⁻³	1.76×10 ⁻⁴	1.38	386.7
	0.01	2.94×10 ⁻³	7.72×10 ⁻⁴	2.01	27.7
0.050	0.003	3.52×10 ⁻³	4.05×10 ⁻⁵	0.87	Large
	0.006	3.12×10 ⁻³	1.32×10 ⁻⁴	1.17	Large
	0.01	2.75×10 ⁻³	4.41×10 ⁻⁴	1.55	94.7

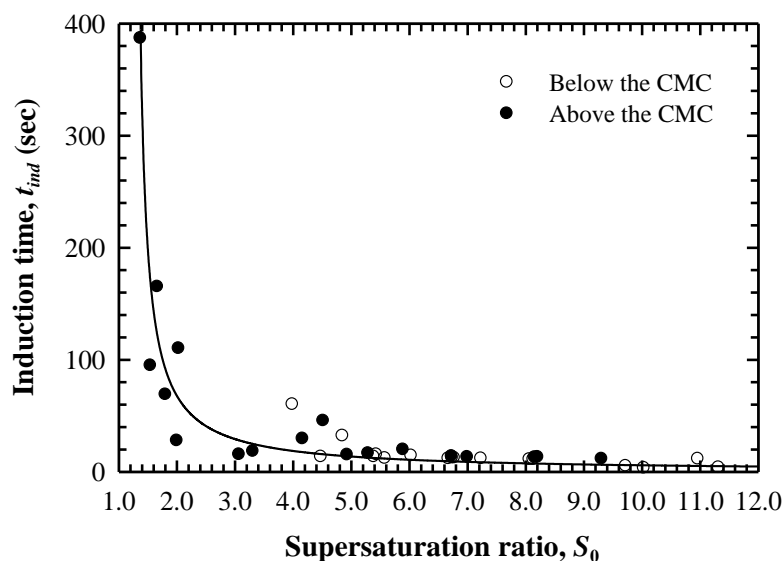


Figure 4.5 Dependence of the induction time on the supersaturation ratio for NaDS precipitating by CaCl_2 at 30°C .

As can be seen in Figure 4.6, the small induction time curves are far away from the equilibrium curve (where the supersaturation ratio, $S_0 = 1$). Figure 4.6 indicates that the induction time is the same function of the supersaturation ratio for both below and above the CMC even though induction time contours above the CMC have been shifted slightly higher compared to below the CMC. The shift of the induction time curves is the same as the shift in the constant S_0 curves. Rodriguez and Scamehorn (2001) suggested that the micellization affects the decreasing in the amount of surfactant monomers as the precipitating surfactant is more diluted in the micellar phase and this would shift the equilibrium toward the micelle so that larger induction times are evident as the reduction of surfactant monomers above the CMC.

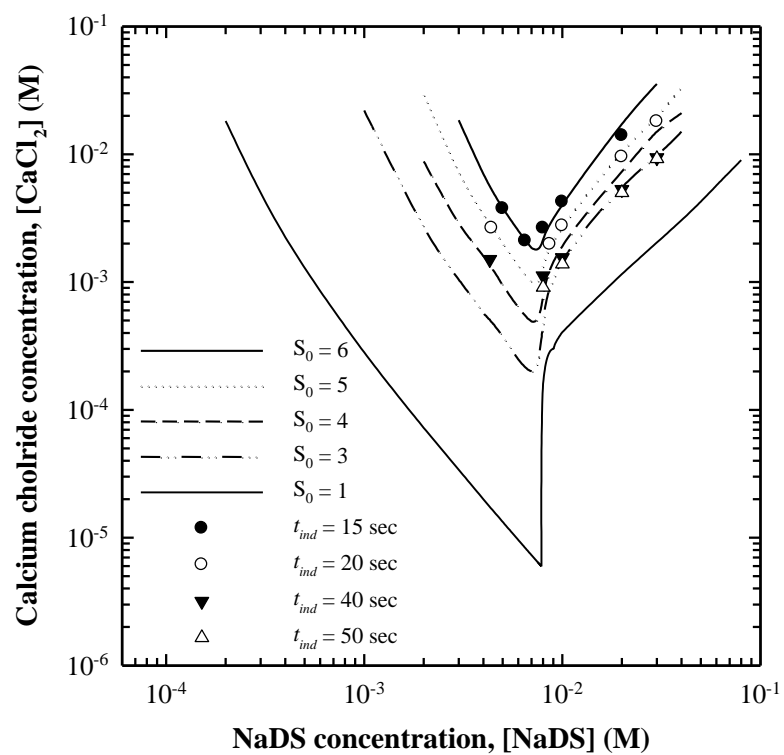


Figure 4.6 The theoretical precipitation phase boundary of NaDS precipitated by CaCl_2 and the corresponding induction time at 30°C .

4.5.2 Precipitation of Binary Mixed Anionic Surfactant Systems by CaCl_2

4.5.2.1 Binary Mixed NaDS/NaDeS Systems

The relationship between induction time and supersaturation ratio is shown in Figure 4.7 for the binary mixed NaDS/NaDeS systems precipitated by CaCl_2 . The precipitation trend is similar to the single anionic surfactant systems because there will be only $\text{Ca}(\text{DS})_2$ precipitating out from the mixtures. The reason that only $\text{Ca}(\text{DS})_2$ precipitates from any of the mixtures investigated is due to the large difference between the solubility products of $\text{Ca}(\text{DS})_2$ and $\text{Ca}(\text{DeS})_2$. All calculated supersaturation ratios for the NaDS/NaDeS system based on $\text{Ca}(\text{DeS})_2$ in this work are below their precipitation boundary (i.e. S_0 is below 1). Thus, supersaturation is shown only by supersaturation ratios with respect to $\text{Ca}(\text{DS})_2$ (as shown in Table 4.2 and Figure 4.7). Furthermore, the graph shows only one function of induction time with respect to supersaturation ratio for all NaDS/NaDeS molar ratios at the same value of supersaturation ratio. Thus the induction time is a function of supersaturation ratio only. This not only implies that the inhibition or disruption of mixed anionic surfactant precipitation due to the different tail length might be wrong, but also argues against some suggestions that the second surfactant monomers interfere with the surface of the $\text{Ca}(\text{DS})_2$ nucleus (Rodriguez and Scamehorn, 2001; Soontravanich S., and Scamehorn, 2010a).

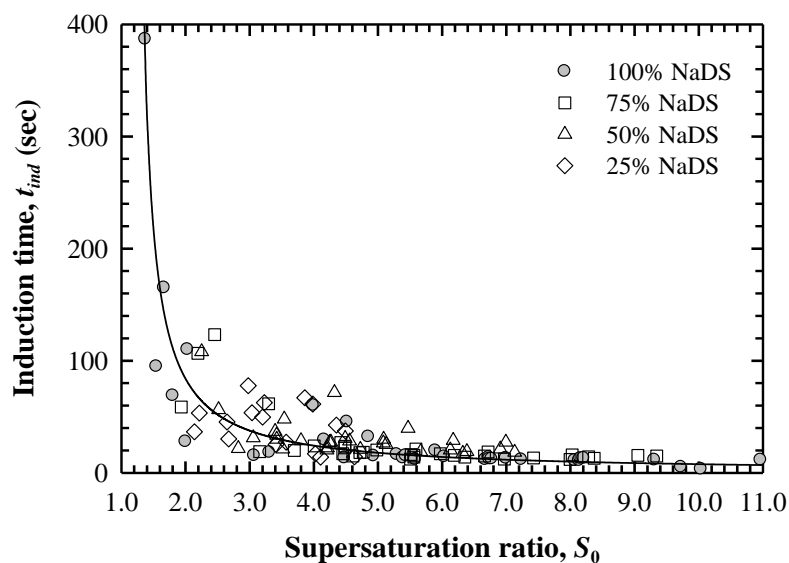


Figure 4.7 Dependence of the induction time on the supersaturation ratio for binary mixed NaDS/NaDeS systems precipitating by CaCl_2 at 30°C .

Thus, the induction time of binary mixed NaDS/NaDeS systems, precipitated with CaCl_2 is approximately equal to the induction time of single NaDS systems precipitated with CaCl_2 . This indicates that only $\text{Ca}(\text{DS})_2$ crystals precipitate rather than a combination of $\text{Ca}(\text{DeS})_2$ and $\text{Ca}(\text{DS})_2$ precipitating because the relationship between the supersaturation ratio of $\text{Ca}(\text{DS})_2$ and the induction time is the same for all results. The experimental data in the curve is scattered due to the stochastic nature of the nucleation mechanism, however it appears that the induction time of binary mixed NaDS/NaDeS systems precipitating with CaCl_2 follows the same function as seen in the single NaDS systems precipitated by CaCl_2 .

Table 4.2 Induction time vs. supersaturation ratio for binary mixed NaDS/NaDeS systems precipitated by CaCl₂ at 30°C.

[NaS], M	[CaCl ₂], M	100% NaDS		75% NaDS		50% NaDS		25% NaDS	
		S ₀	t _{ind} (s)						
0.003	0.0045	4.48	13.3	3.70	20.0	2.82	21.7	1.78	Large
	0.012	5.58	12.0	4.61	15.0	3.52	21.3	2.22	53.3
	0.035	6.67	11.7	5.51	12.3	4.20	20.3	2.65	45.3
0.005	0.00065	3.57	Large	2.95	Large	2.25	108.0	1.42	Large
	0.004	6.03	14.3	4.98	20.3	3.80	28.7	2.39	Large
	0.0085	7.24	11.7	5.97	17.0	4.56	28.3	2.87	Large
	0.05	9.73	5.0	8.03	16.0	6.13	20.3	3.86	67.0
	0.10	10.04	3.3	8.28	14.3	6.32	17.3	3.98	61.3
0.006	0.00065	3.99	60.0	3.30	61.7	2.51	56.3	1.58	Large
	0.0018	5.43	15.3	4.49	23.7	3.42	30.0	2.16	Large
	0.004	6.77	12.3	5.59	21.3	4.27	27.3	2.69	Large
	0.0085	8.14	11.0	6.72	18.7	5.13	25.3	3.23	62.7
	0.05	10.96	11.3	9.05	15.7	6.91	21.3	4.35	42.7
	0.10	11.32	3.7	9.34	15.0	7.13	18.3	4.49	37.3
0.008	0.001	4.59	45.3	4.48	22.3	3.42	33.7	2.15	Large
	0.002	5.95	19.7	5.52	16.3	4.21	22.3	2.65	Large
	0.003	6.79	13.7	6.19	15.7	4.72	21.0	2.98	77.7
	0.006	8.26	13.0	7.43	13.3	5.67	19.0	3.57	27.3
	0.01	9.37	11.3	8.37	13.0	6.39	19.0	4.02	17.0
0.010	0.001	2.07	110.0	3.16	19.0	3.54	48.0	2.46	Large
	0.002	4.21	29.3	4.72	18.0	4.49	30.7	3.04	53.7
	0.003	5.34	16.3	5.56	14.0	5.09	30.0	3.41	25.3
	0.006	7.04	13.0	6.97	12.3	6.17	29.0	4.10	14.0
	0.01	8.21	12.7	7.99	12.0	6.99	27.3	4.63	14.3
0.020	0.003	1.68	165.0	2.19	106.7	2.28	Large	2.46	Large
	0.006	3.33	18.0	4.77	18.3	4.32	71.7	3.73	Large
	0.01	4.96	15.0	6.35	14.0	5.47	39.7	4.52	Large
0.030	0.003	1.20	Large	1.32	Large	1.24	Large	1.47	Large
	0.006	1.81	68.7	2.45	123.3	2.52	Large	3.16	Large
	0.01	3.09	15.3	4.42	27.0	4.21	286.7	4.19	Large
0.040	0.003	1.00	Large	0.70	Large	1.00	Large	1.11	Large
	0.006	1.38	386.7	1.11	Large	1.64	Large	2.41	Large
	0.01	2.01	27.7	1.58	58.7	2.27	Large	3.77	Large

For most precipitation systems shown in Table 4.2, the induction time for precipitation of mixed NaDS/NaDeS systems by CaCl_2 is larger as the molar ratio of NaDS decreases compared to the pure NaDS system of the same total surfactant content. The reduction of the NaDS molar ratio causes a reduction in the supersaturation ratio resulting in a longer induction time. The induction time of binary mixed NaDS/NaDeS increases significantly when the molar ratio of NaDS/NaDeS is below 75% NaDS. As can be seen in the single anionic surfactant systems discussed previously, decreasing the concentration of the precipitating surfactant monomers by micellization and unbound monovalent counterions by counterion binding, are crucial factors in increasing in the induction time. The supersaturation ratio based on the precipitating surfactant (S_0 based on $\text{Ca}(\text{DS})_2$) decreases when the NaDeS molar ratio increases, and thus the induction time increases.

For the same total surfactant concentration ($[\text{NaS}]_{\text{total}}$) and total calcium chloride concentration ($[\text{CaCl}_2]_{\text{total}}$) in binary mixed NaDS/NaDeS systems precipitated by CaCl_2 as shown in Table 4.2, the supersaturation ratio required for nucleation at a particular induction time for pure NaDS systems below the CMC is larger than the supersaturation ratio of binary mixed NaDS/NaDeS systems, which is due to the concentration of precipitating surfactant being decreased when the molar ratio of NaDS/NaDeS with respect to NaDS is decreased. Consequently, the amount of precipitating surfactant, NaDS, is decreased resulting in a smaller supersaturation ratio and larger induction time.

Above the CMC (10-40 mM NaS, depending on the composition of the system) for same total surfactant concentration and total calcium chloride concentration, the supersaturation ratio of pure NaDS systems precipitated by CaCl_2 below the CMC is slightly lower than the supersaturation ratio of binary mixed NaDS/NaDeS systems, assuming the solutions contain the same total amount of calcium and total amount of surfactant (DS^- and DeS^-). The induction time of binary mixed NaDS/NaDeS systems precipitating by CaCl_2 is larger than the induction time of pure NaDS system precipitating by CaCl_2 for constant total concentration of surfactant and CaCl_2 . This is quite interesting because the delay in the precipitation is partly due to the total amount of precipitating surfactant and partly due to the change of the CMC of the binary anionic surfactant mixtures. Changing the molar ratio results in moving the precipitation phase boundary due to a lowering of the CMC with respect to NaDS, while the concentration of total calcium concentration present in the system is constant. For this reason, the supersaturation ratio of binary mixed NaDS/NaDeS systems precipitating by CaCl_2 above the CMCs is relatively higher than in single NaDS systems precipitating by CaCl_2 . Having the more soluble anionic surfactant in the systems will change the precipitation phase boundary as can be seen in the previous study by (Rodriguez and Scamehorn, 2001).

4.5.2.2 Binary Mixed NaDS/NaOBS Systems

Now, we consider the results for NaDS/NaOBS mixtures precipitated by CaCl_2 . The solubility products of these calcium surfactant salts are relatively close to each other at 30°C (in the same order of the magnitude, 10^{-10}) as well as their CMCs being similar 7.9 mM and 12.0 mM for NaDS and NaOBS solutions at 30°C , respectively. The mixed NaDS/NaOBS systems have been reported as an ideal mixture in this work and other (Soontravanich S., and Scamehorn, 2010a). Since either $\text{Ca}(\text{DS})_2$ or $\text{Ca}(\text{OBS})_2$ may have a large supersaturation ratio, the plot of induction time has been divided into 2 sets of data based on $\text{Ca}(\text{OBS})_2$ precipitation (Figure 4.8) and based on $\text{Ca}(\text{DS})_2$ precipitation (Figure 4.9) for the sake of clarity. Figure 4.8 and 4.9 demonstrate the relationship between induction time and supersaturation ratio for binary mixed NaDS/NaOBS systems precipitated by CaCl_2 for three different molar ratios and demonstrating a wide range of calcium chloride concentrations and a wide range of total surfactant concentrations below and above the CMCs.

Figure 4.8 shows the induction time of NaDS/NaOBS systems precipitated by CaCl_2 at a range of 25% NaDS and some data from the 50% NaDS system versus the supersaturation ratio calculated with respect to $\text{Ca}(\text{OBS})_2$. In this case, the induction time curve suggests that only $\text{Ca}(\text{OBS})_2$ precipitates out from these mixtures. The induction time of the mixed anionic surfactant precipitation at this range of 25% and some data from the 50% molar ratios of NaDS/NaOBS systems is very short compared to pure systems. This can be explained that NaDS and NaOBS have many similar physical and chemical properties hence; the precipitation behavior can be concluded to be similar.

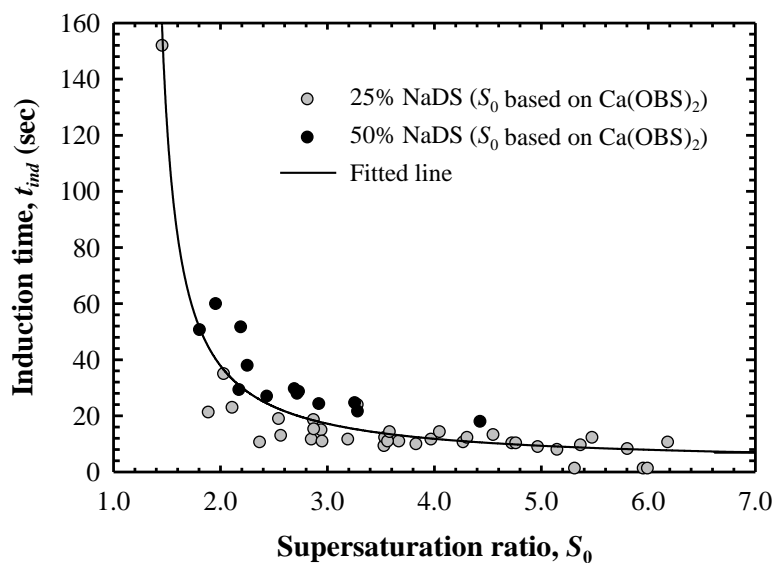


Figure 4.8 Dependence of the induction time on the supersaturation ratio for binary mixed NaDS/NaOBS systems precipitating by CaCl_2 for 25% and 50% NaDS molar ratios and supersaturation ratio based on $\text{Ca}(\text{OBS})_2$, at 30°C .

Figure 4.9 shows the induction time of NaDS/NaOBS systems precipitated by CaCl_2 at a range of 75% NaDS, with some data from the 50% NaDS system (where supersaturation ratios suggest the $\text{Ca}(\text{DS})_2$ salt should precipitate) versus the supersaturation ratio calculated with respect to $\text{Ca}(\text{DS})_2$. It is quite difficult to make a discussion on the dependence of induction time on supersaturation ratio, which is calculated based on $\text{Ca}(\text{DS})_2$ for the NaDS/NaOBS systems in this case. For clarity the induction time for pure NaDS precipitation is also plotted in Figure 4.9 in order to compare the precipitation behavior between pure and mixed systems. It can be observed that the induction time at this range of molar ratios of NaDS/NaOBS systems is larger than the induction time in pure NaDS systems even for the same supersaturation ratio value. Several points of experimental data are not plotted in the

figure because the induction time value is quite large, but they are tabulated in Table 4.3. Soontravanich S., and Scamehorn (2010a) showed that 60-65% NaDS molar ratio in the binary mixed NaDS/NaOBS systems is the range of optimal molar ratio that results in the maximum increase in the induction time. An increase in the induction time can be also noted in this work over a range of 50-75% NaDS molar ratio in the mixed NaDS/NaOBS systems. For clarity the supersaturation ratio of the individual surfactant species have been calculated separately to observe which surfactant salt is likely to be precipitating and all experimental data for all systems are tabulated in Table 4.3.

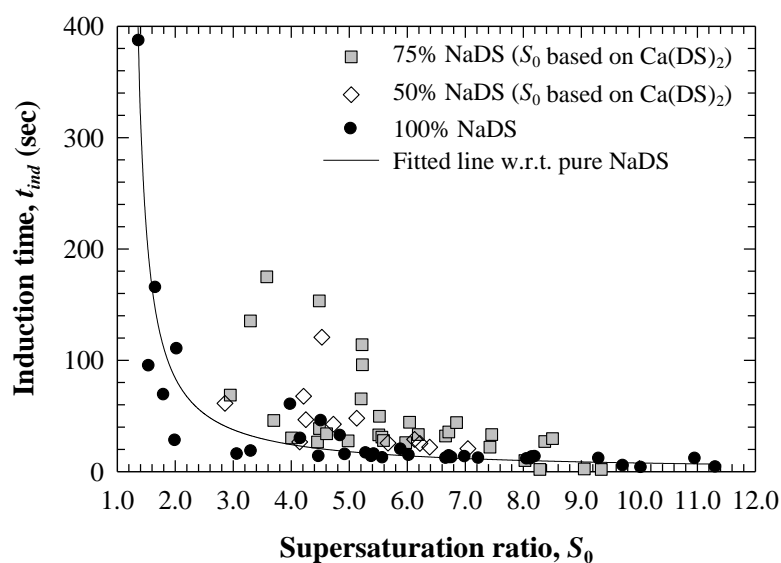


Figure 4.9 Dependence of the induction time on the supersaturation ratio for binary mixed NaDS/NaOBS systems precipitating by CaCl_2 for 50%, 75%, and 100% NaDS molar ratios, and supersaturation ratio based on $\text{Ca}(\text{DS})_2$, at 30°C .

Table 4.3 Induction time vs. supersaturation ratio for binary mixed NaDS/NaOBS

systems precipitating by CaCl_2 30°C. S_0 is given for both possible sodium salts.

[NaS], M	[CaCl ₂], M	75% NaDS			50% NaDS			25% NaDS		
		$S_{0(\text{DS})}$	$S_{0(\text{OBS})}$	t_{ind} (s)	$S_{0(\text{DS})}$	$S_{0(\text{OBS})}$	t_{ind} (s)	$S_{0(\text{DS})}$	$S_{0(\text{OBS})}$	t_{ind} (s)
0.003	0.0045	3.70	1.14	46.0	2.82	1.81	50.3	1.78	2.37	10.3
	0.012	4.61	1.42	34.0	3.52	2.26	37.7	2.22	2.96	10.7
	0.035	5.51	1.70	33.0	4.20	2.70	29.3	2.65	3.54	9.0
0.005	0.00065	2.95	0.91	68.7	2.25	1.44	Large	1.42	1.89	21.0
	0.0018	4.01	1.24	30.3	3.06	1.96	59.7	1.93	2.57	12.7
	0.004	4.98	1.54	27.7	3.80	2.44	29.0	2.39	3.20	11.3
	0.0085	5.97	1.84	26.0	4.56	2.93	24.0	2.87	3.83	9.7
	0.05	8.03	2.48	10.0	6.13	3.93	26.7	3.86	5.15	7.7
	0.10	8.28	2.56	2.0	6.32	4.06	2.0	3.98	5.32	1.0
0.006	0.00065	3.30	1.02	135.3	2.51	1.61	Large	1.58	2.12	22.7
	0.0018	4.49	1.38	38.7	3.42	2.20	51.3	2.16	2.88	15.0
	0.004	5.59	1.73	35.7	4.27	2.74	28.3	2.69	3.59	14.0
	0.0085	6.72	2.07	28.0	5.13	3.29	21.3	3.23	4.31	12.0
	0.05	9.05	2.79	2.3	6.91	4.43	16.3	4.35	5.81	8.0
	0.10	9.34	2.88	2.0	7.13	4.58	1.0	4.49	6.00	1.0
0.008	0.001	4.48	1.38	153.3	3.42	2.20	Large	2.15	2.88	18.3
	0.002	5.52	1.70	49.7	4.21	2.70	67.7	2.65	3.54	12.0
	0.003	6.19	1.91	33.3	4.72	3.03	42.7	2.98	3.97	11.3
	0.006	7.43	2.29	27.0	5.67	3.64	25.7	3.57	4.77	10.0
	0.01	8.37	2.58	22.0	6.39	4.10	22.0	4.02	5.37	9.3
0.010	0.001	3.83	1.27	Large	3.58	2.34	Large	2.46	3.29	23.7
	0.002	5.22	1.73	96.0	4.53	2.96	120.7	3.04	4.06	14.0
	0.003	6.04	2.00	44.3	5.13	3.36	48.0	3.41	4.56	13.0
	0.006	7.46	2.47	33.3	6.22	4.07	25.3	4.10	5.48	12.0
	0.01	8.50	2.81	29.7	7.04	4.61	20.7	4.63	6.19	10.3
0.020	0.003	2.46	1.02	Large	2.11	1.71	Large	1.56	2.55	18.7
	0.006	5.22	2.18	114.0	4.25	3.45	46.7	2.89	4.73	10.0
	0.01	6.85	2.85	44.0	5.47	4.43	17.7	3.64	5.96	1.0
0.030	0.003	1.55	0.72	Large	1.22	1.11	Large	0.79	1.46	151.7
	0.006	2.91	1.36	Large	2.38	2.16	243.3	1.60	2.95	14.7
	0.01	5.20	2.42	65.3	4.14	3.75	26.7	2.70	4.97	8.7
0.040	0.003	1.29	0.65	Large	1.00	0.97	Large	0.62	1.25	Large
	0.006	2.05	1.03	Large	1.61	1.57	Large	1.02	2.04	34.7
	0.01	3.58	1.79	175.0	2.86	2.79	61.3	1.84	3.68	10.7

At 25% NaDS (75% NaOBS), the supersaturation ratio with respect to Ca(OBS)_2 is significantly larger than the supersaturation ratio with respect to Ca(DS)_2 . This is due to the amount of precipitating OBS^- in the mixtures being significantly higher than the precipitating DS^- . Consequently, Ca(OBS)_2 will probably precipitate first from the mixtures even though the solubility product of the two surfactant salts is similar. The induction time for precipitation of Ca(OBS)_2 in 75% NaOBS molar ratio is quite short, the same as in the individual anionic surfactant systems. It can be explained that the amount of precipitating OBS^- is high enough to greatly exceed the solubility product of Ca(OBS)_2 . In this case, the inhibition of binary anionic surfactant mixtures has not been observed.

Due to similar solubility product and molecular structure of these two anionic surfactants, the precipitation of binary NaDS/NaOBS mixtures must be carefully considered at 50% NaDS molar ratio. In this case, the induction time appears to be larger than in pure anionic surfactant systems even though the supersaturation ratios with respect to both Ca(DS)_2 and Ca(OBS)_2 are higher than in pure systems. As can also be observed in Figure 4.10, the precipitation phase boundary for 50% NaDS/NaOBS molar ratio shows essentially the same precipitation behavior of these two anionic surfactants thus, it is difficult to say which precipitate is coming out primarily, but Ca(DS)_2 might precipitate first if we consider only the higher value of the supersaturation ratio.

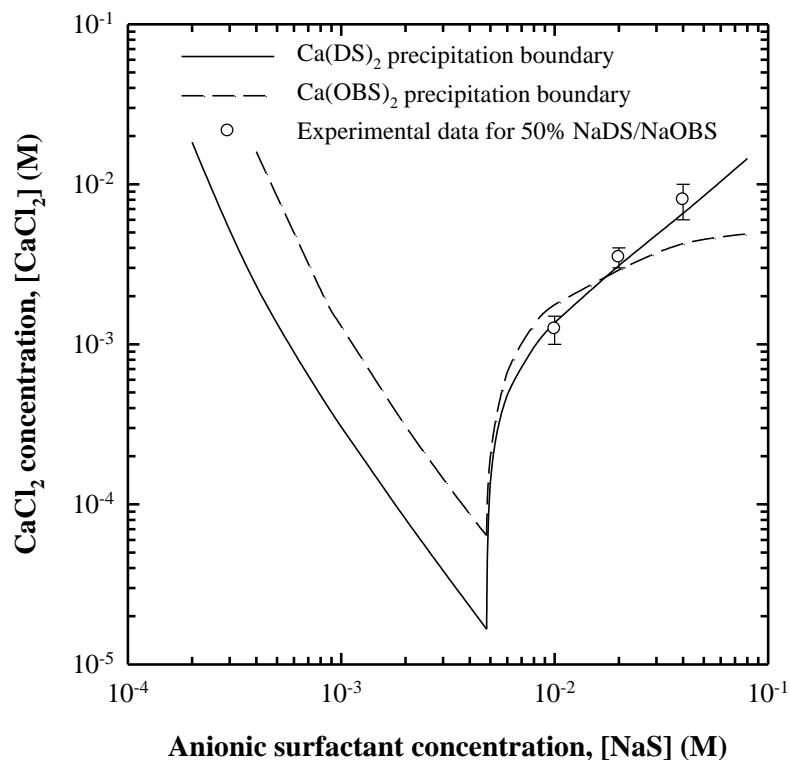


Figure 4.10 Precipitation phase boundaries for an equimolar ratio of NaDS/NaOBS mixtures precipitating by CaCl_2 at 30°C , and the experimental data corresponding to the precipitation system.

At 75% NaDS (25% NaOBS) the supersaturation ratio with respect to $\text{Ca}(\text{DS})_2$ is significantly larger than the supersaturation ratio with respect to $\text{Ca}(\text{OBS})_2$. In this case, the induction time is significantly higher than others even though supersaturation ratio with respect to $\text{Ca}(\text{DS})_2$ is large. The inhibition of binary anionic surfactant mixtures has been observed in most of the experimental data even though the supersaturation ratio with respect to $\text{Ca}(\text{DS})_2$ is relatively high. The precipitation behavior at 75% NaDS molar ratio is interesting with respect to what delays the precipitate forming, because the same behavior can not be observed in 75% NaOBS, even though both surfactants have a similar structure and solubility. It

should be noted that some data point of the precipitation system at 75% NaDS molar ratio are strongly scattered, probably due to the poor prediction of the models resulting in a worse prediction of theoretical precipitation phase boundary for 75:25 NaDS/NaOBS molar ratio as seen in Figure 3.15 in the previous chapter.

Furthermore, similar behavior can be observed in both binary mixed NaDS/NaDeS and NaDS/NaOBS systems above the CMCs (10-40 mM NaS) for the same total surfactant concentration and total calcium chloride concentration. Even though the calculated supersaturation ratio of the single NaDS systems below the CMC is slightly lower than the supersaturation ratio of the binary anionic surfactant mixtures, assuming the solutions contain the same total amount of calcium and total amount of surfactant, the induction time of binary mixed systems is still larger than the induction time of the single NaDS systems at a range of 50-75% with respect to NaDS. According to the previous chapter, we can explain what occurs when changing the molar ratio; this will slightly increase the precipitation phase boundary by lowering the CMC with respect to NaDS while the concentration of total calcium concentration present in the system remains constant. For this reason, the supersaturation ratio of binary mixed systems above the CMCs shows a higher value than that of the single NaDS systems.

4.5.3 The Estimation of Kinetic Parameters of Anionic Surfactant Precipitation

Figure 4.11 shows the relationship between induction time and supersaturation ratio based on equation (4.8) for mixed NaDS/NaDeS systems. The scattered experimental data is probably due to the stochastic nature of nucleation; however a relationship can still be observed from the data with 95% confidence intervals. The fitted line yields a slope of 0.0581 ± 0.031 with an intercept value of 1.234 ± 0.154 . From the slope of fitted line in Figure 4.11, the interfacial energy is calculated and is equal to $2.2 \pm 0.4 \text{ mJ/m}^2$. The interfacial energy (γ) of the systems can be calculated from the slope in order to estimate the kinetics of calcium surfactant salt precipitation.

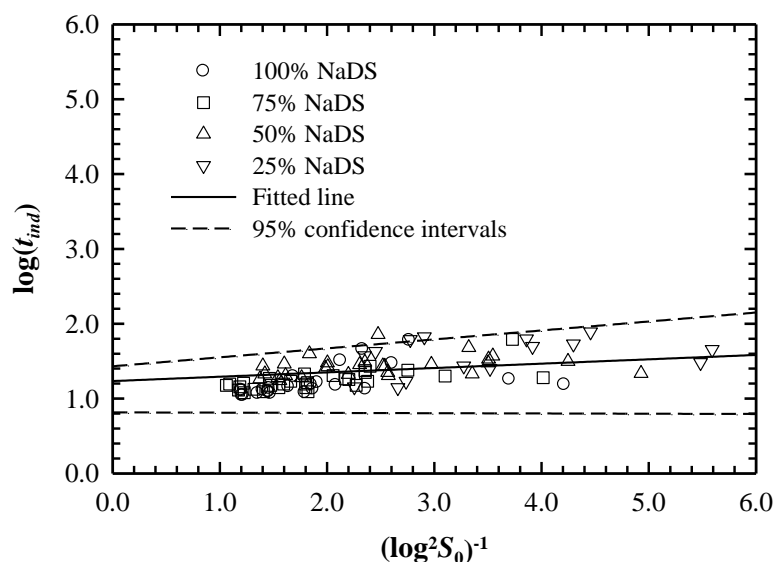


Figure 4.11 Variation in the induction time as a function of supersaturation ratio for the binary mixed NaDS/NaDeS systems precipitating by CaCl_2 at 30°C .

From Figure 4.12 and 4.13 for the binary mixed NaDS/NaOBS systems precipitating by CaCl_2 , the precipitation trends have been separated based on different calcium surfactant salts. Consider Figure 4.12 where the supersaturation ratio is based on Ca(OBS)_2 , the fitting lines which corresponding to 25% NaDS, gives the slope equals to 0.034 ± 0.006 with intercept value of 0.957 ± 0.046 and for 50% NaDS gives the slope equals to 0.041 ± 0.029 with intercept value of 1.34 ± 0.18 . Consider Figure 4.13 where the supersaturation ratio is based on Ca(DS)_2 , the fitted line which corresponding to 50% NaDS, gives the slope equals to 0.149 ± 0.055 with intercept value of 1.15 ± 0.16 and for 75% NaDS gives the slope equals to 0.196 ± 0.113 with intercept value of 1.23 ± 0.25 .

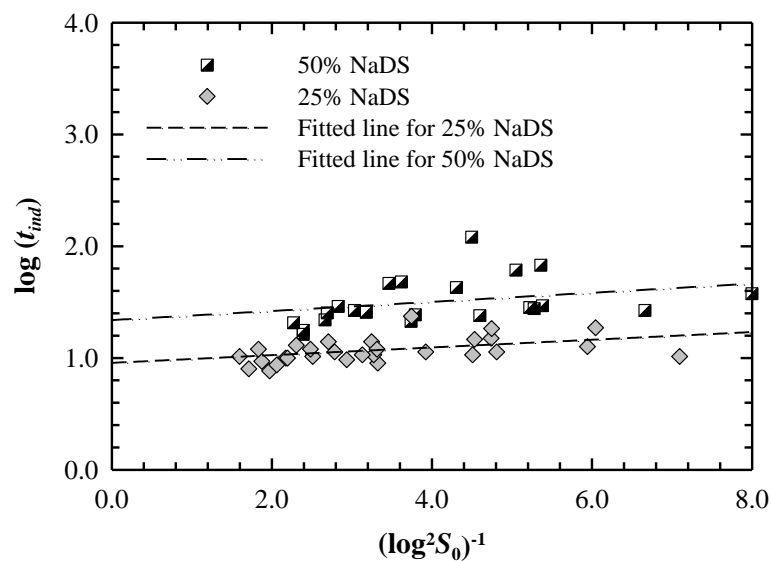


Figure 4.12 Variation in the induction time as a function of supersaturation ratio for the binary mixed NaDS/NaOBS systems precipitating by CaCl_2 at 30°C where S_0 is based on Ca(OBS)_2 .

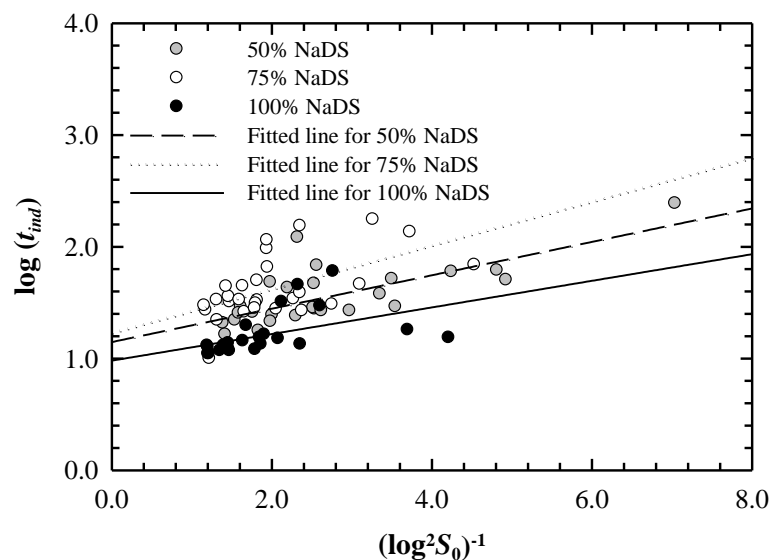


Figure 4.13 Variation in the induction time as a function of supersaturation ratio for the binary mixed NaDS/NaOBS systems precipitating by CaCl_2 at 30°C where S_0 is based on $\text{Ca}(\text{DS})_2$.

The interfacial energy for all systems can be calculated from the slope of the relationship between induction time and supersaturation ratio, and they are all tabulated in Table 4.4. It can be concluded that the large value of interfacial energy indicates a large time required precipitating the calcium surfactant salt. For instance, the energy required to form the nuclei of $\text{Ca}(\text{DS})_2$ in pure systems and in mixed NaDS/NaDeS is relatively close to each other when given the uncertainty to the interfacial energy value. As well, it can be observed that the energy required to form the nuclei of $\text{Ca}(\text{OBS})_2$ at 25% and 50% NaDS (but the supersaturation ratio is based on $\text{Ca}(\text{OBS})_2$) is close to each other. According to the interfacial energy value summarized above, the $\text{Ca}(\text{OBS})_2$ and $\text{Ca}(\text{DS})_2$ precipitation by CaCl_2 behaves the same trend and this may be due to the similar solubility product and structure.

Table 4.4 The interfacial energy required for calcium surfactant salt precipitation at 30°C.

System	Expected Precipitate	Interfacial Energy, γ (mJ m ⁻²)	Pre-exp. factor (A)
Pure NaDS solution	Ca(DS) ₂	1.842 ± 0.826	15.08
NaDS/NaDeS mixtures - For all molar ratios studied	Ca(DS) ₂	2.252 ± 0.826	17.13
NaDS/NaOBS mixtures - 25% NaDS (OBS ⁻ based)	Ca(OBS) ₂	1.872 ± 0.180	9.05
- 50% NaDS (OBS ⁻ based)	Ca(OBS) ₂	1.999 ± 0.180	21.84
- 50% NaDS (DS ⁻ based)	Ca(DS) ₂	3.084 ± 0.403	14.05
- 75% NaDS (DS ⁻ based)	Ca(DS) ₂	3.376 ± 0.403	16.87

It is interesting that the energy required to form the nuclei of Ca(DS)₂ from the 50-75% NaDS molar ratio systems is different compared to the interfacial energy value with respect to Ca(DS)₂ mentioned previously, and the value can imply the inhibition of precipitation of mixed NaDS/NaOBS mixtures. In this case, there is a change in kinetics of precipitation as the energy required to create the critical nuclei changes at these molar ratios of NaDS/NaOBS systems is much larger for same calcium surfactant salt (Ca(DS)₂). The larger interfacial energy required, the longer induction time, and the lower the nucleation rate.

In order to elucidate the kinetics and mechanism of mixed anionic surfactant precipitation by hardness ions, the estimated interfacial energy in this work will be used to estimate the nucleation rate and the excess Gibbs free energy change of formation of critical nuclei (r_c) corresponding to the solution supersaturation as shown in Figure 4.14. Considering only the mixed NaDS/NaOBS systems in

Figure 4.14, the nucleation rate of $\text{Ca}(\text{DS})_2$ and $\text{Ca}(\text{OBS})_2$ follows the same trend as DS^- and OBS^- tails have similar size; although the former is totally aliphatic while the latter has an aromatic portion and also the similar solubility product.

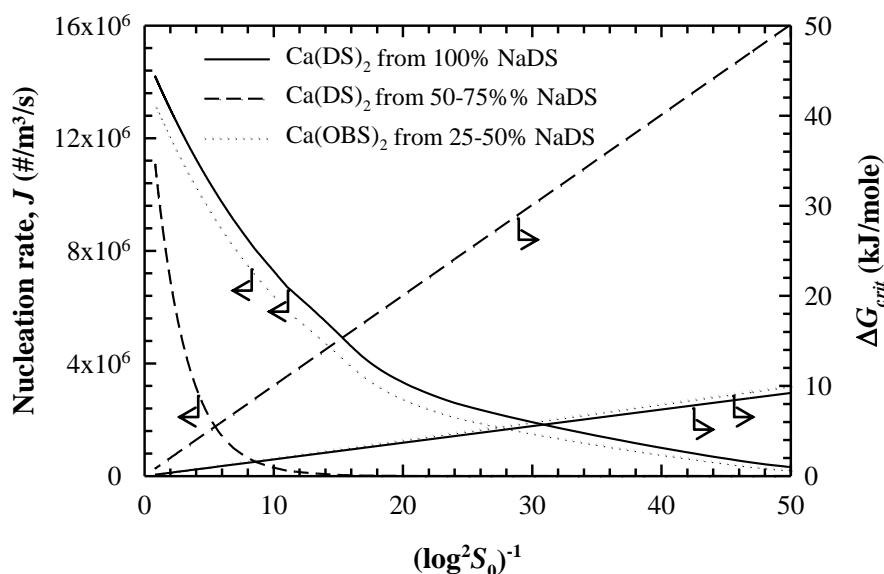


Figure 4.14 Dependence of the nucleation rate and the excess Gibbs free energy change of formation of critical nuclei as a function of degree of supersaturation for the binary mixed NaDS/NaOBS systems precipitating by CaCl_2 at 30°C .

The nucleation rate increases as the supersaturation ratio increases and also the Gibbs free energy change required for the critical nucleus decreases as supersaturation ratio increases. However, it can be observed that the kinetics of precipitation of $\text{Ca}(\text{DS})_2$ are changed when the molar ratio ranging between 50-75% NaDS/NaOBS with respect to NaDS. This indicates that the inhibition in binary mixed anionic surfactants precipitation is partly due to the kinetic change due to the interfacial energy change.

Moreover, the radius of the critical nucleus from different systems as a function of supersaturation ratio is shown in Figure 4.15, and it can be observed that $\text{Ca}(\text{DS})_2$ precipitating from 50-75% NaDS/NaOBS systems requires a much larger critical nucleus size than $\text{Ca}(\text{DS})_2$ precipitating from pure NaDS solution. The requirement for larger critical nucleus radius indicates that a larger induction time is required.

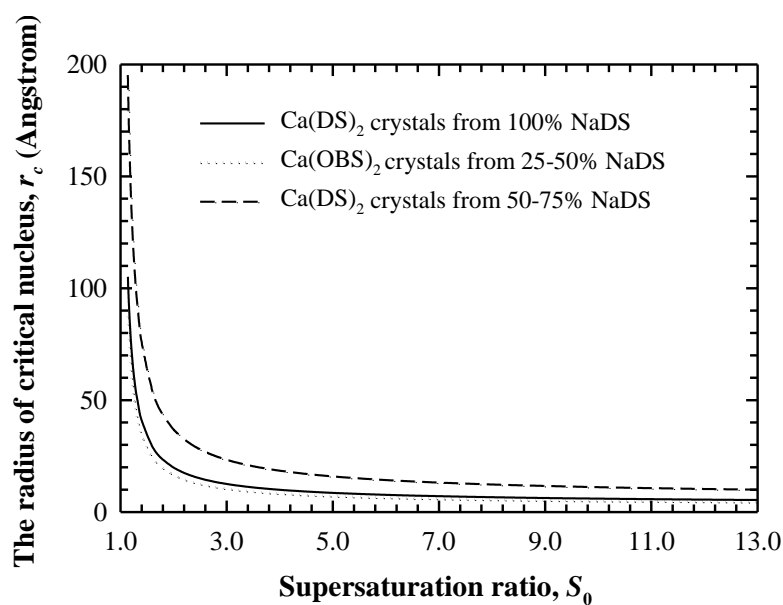


Figure 4.15 Variation of radius of critical nucleus of calcium surfactant salts as a function of supersaturation ratio at 30°C.

4.6 Conclusions

The precipitation of single anionic surfactant precipitated by CaCl_2 at a specific temperature depends only on the supersaturation of the precipitating species in the bulk solution both below and above the CMC as can be seen from the induction time being a function of supersaturation ratio. Above the CMC the concentration of the anionic surfactant monomers continuously decreases as the unbound sodium ion content increases due to dissociation from the surfactant molecule. A fraction of calcium ions are bound to the charged micelles reducing the amount of unbound calcium ions in the bulk solution.

The precipitation of calcium surfactant salts in binary mixed anionic surfactant systems can be summarized as following: for mixtures of NaDS and NaDeS precipitated by CaCl_2 the induction time is only a function of the supersaturation ratio calculated based on $\text{Ca}(\text{DS})_2$. At same supersaturation ratio value, the induction time from different molar ratios is not significantly different. From the relationship between the induction time and the supersaturation ratio it can be concluded that only $\text{Ca}(\text{DS})_2$ will precipitate out from the mixtures, and this is because the solubility product of $\text{Ca}(\text{DS})_2$ is much larger than the solubility product of $\text{Ca}(\text{DeS})_2$. In this case, the difference in the number of carbon atom in the surfactant backbone does not increase the induction time. From the experimental data, we can summarize that the increase in the induction time is only due to the change in precipitating species (DS^-) because of the molar ratio and thermodynamic change of mixed micellization.

For the mixed NaDS/NaOBS precipitating by CaCl_2 , the precipitation of calcium surfactant salts can be considered based on either $\text{Ca}(\text{DS})_2$ or $\text{Ca}(\text{OBS})_2$. For precipitation of $\text{Ca}(\text{OBS})_2$ occurs in the systems of 25-50% NaDS molar ratio it

should be noted that the data taken from some Ca(OBS)_2 precipitating in 50% NaDS molar ratio systems which the data are close to the pure Ca(OBS)_2 precipitation systems. At this range of molar ratio, the inhibition of precipitation is not found in the mixed NaDS/NaOBS systems.

For precipitation of Ca(DS)_2 in the systems of 50-75% molar ratio of NaDS/NaOBS mixtures, the induction time is not a function of supersaturation ratio, which is calculated based on Ca(DS)_2 but the different precipitation trend can be observed when compared to the pure NaDS precipitating by CaCl_2 systems. In this case, the inhibition of precipitation is observed as the induction time appears larger than in the pure systems at the same degree of supersaturation with respect to Ca(DS)_2 . The inhibition is due to the change in precipitating species (DS^-) because of the molar ratio and thermodynamic change of mixed micellization. In this case a change in kinetics of precipitation would also be predicted.

The kinetics of precipitation of binary mixed anionic surfactants can be found at 50-75% NaDS/NaOBS systems, the interfacial energy estimated from the relationship of induction time and supersaturation ratio reveals that the time required precipitating the Ca(DS)_2 in 50-75% NaDS/NaOBS systems is larger than the time required to precipitate in pure NaDS solution. The other kinetic parameters such as nucleation rate, Gibbs free energy change of formation of critical nucleus, and the radius of critical nucleus are estimated, they reveal that the inhibition of anionic surfactant precipitation is partly due to kinetic changes.

4.7 References

- Connolly, M. L. (1985). Computation of molecular volume. **Journal of the American Chemical Society** 107(5): 1118-1124.
- Crutchfield, M. M. (1978). Organic builders: A review of worldwide efforts to find organic replacements for detergent phosphates. **Journal of the American Oil Chemists' Society** 55(1): 58-65.
- Davies, C. W. and Shedlovsky, T. (1964). Ion association. **Journal of the Electrochemical Society** 111(3): 85-86.
- Gerbacia, W. E. F. (1983). Calcium dodecyl sulfate precipitation from solutions containing sodium chloride. **Journal of Colloid and Interface Science** 93(2): 556-559.
- Gibbs, J. W. (1928). **The collected works of JW Gibbs**. New York: Longmans.
- Hollingsworth, M. (1978). Role of detergent builders in fabric washing formulations. **Journal of the American Oil Chemists' Society** 55(1): 49-51.
- Kallay, N., Pastuovic, M., and Matijevic, E. (1985). Solubility and enthalpy of precipitation of magnesium, calcium, strontium, and barium dodecyl sulfates. **Journal of Colloid and Interface Science** 106(2): 452-458.
- Klotz, I. M. and Rosenberg, R. M. (2008). **Chemical thermodynamics**. New Jersey: John Wiley & Sons.
- Maneedaeng, A., Haller, K. J., Grady, B. P., and Flood, A. E. (in press). Measurement and modeling of thermodynamic parameters in binary anionic surfactant systems and the effect of counterion binding to the micelle. **Journal of Colloid and Interface Science**.

- Miyamoto, S. (1960). The effect of metallic ions on surface chemical phenomena. III. Solubility of various metal dodecyl sulfates in water. **Bulletin of the Chemical Society of Japan** 33(3): 371-375.
- Mullin, J. W. (1992). **Crystallization**. Oxford: Butterworth-Heinemann.
- Myerson, A. S. (1993). **Handbook of industrial crystallization**. Boston: Butterworth-Heinemann.
- Noïk, C., Bavière, M., and Defives, D. (1987). Anionic surfactant precipitation in hard water. **Journal of Colloid and Interface Science** 115(1): 36-45.
- Peacock, J. M. and Matijevi, E. (1980). Precipitation of alkylbenzene sulfonates with metal ions. **Journal of Colloid and Interface Science** 77(2): 548-554.
- Randolph, A. D. and Larson, M. A. (1988). **Theory of particulate processes: Analysis and techniques of continuous crystallization**. San Diego: Academic.
- Rathman, J. F. and Scamehorn, J. F. (1984). Counterion binding on mixed micelles. **The Journal of Physical Chemistry** 88(24): 5807-5816.
- Rathman, J. F. and Scamehorn, J. F. (1987). Counterion binding on mixed micelles: effect of surfactant structure. **Langmuir** 3(3): 372-377.
- Robinson, R. A. and Stokes, R. H. (1959). **Electrolyte solutions**. London: Butterworths.
- Rodriguez, C. H., Lowery, L. H., Scamehorn, J. F., and Harwell, J. H. (2001). Kinetics of precipitation of surfactants. I. Anionic surfactants with calcium and with cationic surfactants. **Journal of Surfactants and Detergents** 4(1): 1-14.

- Rodriguez, C. H. and Scamehorn, J. F. (1999). Modification of Krafft temperature or solubility of surfactants using surfactant mixtures. **Journal of Surfactants and Detergents** 2: 17.
- Rodriguez, C. H. and Scamehorn, J. F. (2001). Kinetics of precipitation of surfactants. II. Anionic surfactant mixtures. **Journal of Surfactants and Detergents** 4(1): 15-26.
- Roelands, C. P. M., *et al.* (2006). Antisolvent crystallization of the polymorphs of *i*-histidine as a function of supersaturation ratio and of solvent composition. **Crystal Growth & Design** 6(4): 955-963.
- Roelands, C. P. M., Roestenberg, R. R. W., ter Horst, J. H., Kramer, H. J. M., and Jansens, P. J. (2004). Development of an experimental method to measure nucleation rates in reactive precipitation. **Crystal Growth & Design** 4(5): 921-928.
- Schulz, P. C., Rodríguez, J. L., Minardi, R. M., Sierra, M. B., and Morini, M. A. (2006). Are the mixtures of homologous surfactants ideal? **Journal of Colloid and Interface Science** 303(1): 264-271.
- Shinoda, K. and Hirai, T. (1977). Ionic surfactants applicable in the presence of multivalent cations. Physicochemical properties. **The Journal of Physical Chemistry** 81(19): 1842-1845.
- Soontravanich, S., Munoz, J., Scamehorn, J., Harwell, J., and Sabatini, D. (2008). Interaction Between an Anionic and an Amphoteric Surfactant. Part I: Monomer–Micelle Equilibrium. **Journal of Surfactants and Detergents** 11(4): 251-261.

- Soontravanich, S. and Scamehorn, J. F. (2010a). Relation of supersaturation ratio in mixed anionic surfactant solutions to kinetics of precipitation with calcium. **Journal of Surfactants and Detergents** 13(1): 1-11.
- Soontravanich, S. and Scamehorn, J. F. (2010b). Use of a nonionic surfactant to inhibit precipitation of anionic surfactants by calcium. **Journal of Surfactants and Detergents** 13(1): 13-18.
- Stellner, K. L. and Scamehorn, J. F. (1989a). Hardness tolerance of anionic surfactant solutions. 1. Anionic surfactant with added monovalent electrolyte. **Langmuir** 5(1): 70-77.
- Stellner, K. L. and Scamehorn, J. F. (1989b). Hardness tolerance of anionic surfactant solutions. 2. Effect of added nonionic surfactant. **Langmuir** 5(1): 77-84.
- Teychené, S. and Biscans, B. (2008). Nucleation kinetics of polymorphs: Induction period and interfacial energy measurements. **Crystal Growth & Design** 8(4): 1133-1139.
- Zapf, A., Beck, R., Platz, G., and Hoffmann, H. (2003). Calcium surfactants: A review. **Advances in Colloid and Interface Science** 100: 349-380.

CHAPTER V

CONCLUSIONS AND RECOMMENDATIONS

8.1 Conclusions

Avoidance of precipitation of surfactants in the detergency industry is especially important for acceptable cleaning results. An important characteristic of anionic surfactants that is deleterious to their use in many detergency applications is their tendency to precipitate from solutions, especially when used in hard water, forming soap scum. The thermodynamic and kinetic parameters involved in the precipitation process of the soap scum, and in particular the precipitation boundary as the surfactant is mixed with hard water is still extremely important, but these are quite limited in scientific literature.

This research aims to extend the understanding of surfactant precipitation, both in aspects of thermodynamics and kinetics, since the use of surfactant mixtures reveals considerable manipulation of precipitation behavior. Surfactant mixtures can have synergistic advantages over the use of a single surfactant. Binary anionic surfactants were used to systematically investigate the synergistic effect to delay the induction time of anionic surfactants precipitated by divalent ions.

In order to achieve the research goal it is necessary to investigate the thermodynamic parameters of mixed micellization and the effect of counterion

binding to the micelle. Properties of the anionic surfactants sodium decyl sulfate (NaDeS), sodium dodecyl sulfate (NaDS), and sodium octylbenzene sulfonate (NaOBS) have been determined in both single and binary mixed surfactants in aqueous solution systems. Regular solution theory has been used to thermodynamically treat the micellization of mixed anionic surfactants. The model shows a satisfactory prediction of the critical micelle concentration (CMC) of surfactant mixtures together with providing equilibrium compositions in monomeric and micellar phases. The mixed micelle is ideal for the NaDS/NaOBS mixture; not surprising given the similarity in structure. The NaDS/NaDeS mixture is slightly nonideal (having attractive interactions in the micelle) with the nonideality probably being due to the difference in the number of carbon atoms in the backbone of the surfactant molecule. The effect of the counterion on the CMC of anionic surfactants has been measured for the pure surfactants. Experimentally, the CMC of the anionic surfactant depends on the concentration of the monovalent cations present in the solution, and can be described by the Corrin-Harkins relationship, while the dependence of the CMC on the concentration of divalent cations is far less significant. Moreover, the behavior of counterion binding to micelle of anionic surfactant system is investigated quantitatively. Experimentally, the counterion binding of sodium to the micelle is influenced by the calcium ion concentration, and vice versa. However the total degree of counterion binding is essentially constant at approximately 0.65 charge negation at the micelle's surface. The counterion binding coefficients can be quantitatively modeled using a simple equilibrium model relating concentrations of bound and unbound counterion.

Furthermore, general thermodynamic properties of calcium surfactant salts are required to better understand the anionic surfactant precipitation by counterions, for instance solubility data, Krafft temperature, CMC, and energy required for dissolution; however these are quite limited in the literature. These thermodynamic data will help to accurately predict the precipitation phase boundary of anionic surfactant used in this study when precipitated by CaCl_2 . Experimentally, the results reveal more accurately thermodynamic data from the experiments, which allows better thermodynamic modeling of the precipitation phase boundary of single and binary mixed anionic surfactant systems. The work has accurately measured the K_{SP} value of $\text{Ca}(\text{DS})_2$ in aqueous solution over the temperature range of 10 to 55°C. The K_{SP} in this system exponentially increases with increasing temperature, resulting in the K_{SP} at 55°C being orders of magnitude larger than the value at 10°C. In the same manner, the work has also accurately measured the K_{SP} value of $\text{Ca}(\text{DeS})_2$ in aqueous solution over the temperature range of 20 to 30°C. The K_{SP} of calcium 4-octylbenzenesulfonate in aqueous solution has been measured at only 30°C.

Thermodynamic properties of calcium surfactant salts dissolution in water such as, enthalpy, entropy, and Gibbs free energy are also investigated in this work. The calculated data shows the energy required to dissolve the calcium surfactant salts decreases as the temperature increases as the process is an endothermic process. The Gibbs free energy for the dissolution of calcium surfactant salts above the Krafft temperature indicates that the dissolved surfactant is more stable in micellar form as it has the lower Gibbs free energy.

The precipitation phase boundary for $\text{Ca}(\text{DS})_2$ in solutions of NaDS and CaCl_2 , and binary mixed NaDS/NaOBS and NaDS/NaDeS systems can be predicted by the improved models that contain equations for the phase equilibrium between monomeric surfactant and unbound calcium ions, the K_{SP} as a function of temperature, the activity coefficients of the key species as a function of temperature and ionic strength, and models that predict the micellization parameters, such as monomeric surfactant concentration as a function of temperature and ion concentrations, and also the chemical equilibrium model of counterion binding to the micelle. The fit of the model using a K_{SP} value determined from experiments of pure $\text{Ca}(\text{DS})_2$ in water gives a good fit to the experimentally determined precipitation boundary determined in this work, but gives a slightly worse fit to the experimental precipitation boundary studied in a previous work. This is to be expected since fundamentally measured parameters can never improve a fit to a model in comparison to models using parameters fitted to the data. The improved models better fit the data above the CMC in the system than earlier models, where the model for the micelle formation and counterion binding is dominant in determining the total amounts of NaDS and CaCl_2 present in the system required to form precipitates. Below the CMC the only modeling required is that for the K_{SP} value and the activity coefficients, and it is here that the model fitting is quite good. It may be noted that the K_{SP} value measured at 30°C is only 2.122×10^{-10} in comparison to the value predicted from the phase boundary which is 5.02×10^{-10} . The precipitation phase boundary for $\text{Ca}(\text{DS})_2$ in solutions of equimolar ratio of binary mixed NaDS/NaOBS precipitating by CaCl_2 can be predicted by the improved models that contains equations of pseudophase separation theory, regular solution theory, and also chemical equilibrium of

counterions binding to the micelle. The models show a satisfactory prediction of precipitation phase boundary of $\text{Ca}(\text{DS})_2$ in the equimolar ratio of NaDS/NaOBS precipitating by CaCl_2 .

The precipitation of single anionic surfactant precipitating by CaCl_2 at a specific temperature depends only on the supersaturation of the precipitating species in the bulk solution both below and above the CMC as can be seen from the induction time being a function of supersaturation ratio only. Above the CMC the concentration of the anionic surfactant monomers continuously decreases as the unbound sodium ion content increases which dissociated from surfactant molecule. The fraction of calcium ions are bound the charged micelles reducing the amount of unbound calcium ions in the bulk solution.

The precipitation of calcium surfactant salts in binary mixed anionic surfactant systems can be summarized as follows: for mixed NaDS/NaDeS precipitated by CaCl_2 , the induction time is only a function of the supersaturation ratio calculated based on $\text{Ca}(\text{DS})_2$. At same supersaturation ratio value, the induction time from different molar ratios is not significantly different. From the relationship between the induction time and the supersaturation ratio it can be concluded that only $\text{Ca}(\text{DS})_2$ will precipitate out from the mixtures, and this is because the solubility product of $\text{Ca}(\text{DeS})_2$ is much larger than the solubility product of $\text{Ca}(\text{DS})_2$. In this case, the difference in the number of carbon atom in the surfactant backbone does not increase the induction time. From the experimental data, we can summarize that the increase in the induction time is only due to the change in the concentration of the precipitating species (DS^-) because of the molar ratio and thermodynamic changes due to mixed micellization.

For the mixed NaDS/NaOBS precipitating by CaCl_2 , the precipitation of calcium surfactant salts can be considered based on $\text{Ca}(\text{DS})_2$ and $\text{Ca}(\text{OBS})_2$. Precipitation of $\text{Ca}(\text{OBS})_2$ occurs in the systems of 25-50% NaDS molar ratio. It should be remarked that $\text{Ca}(\text{OBS})_2$ precipitating in 50% NaDS molar ratio systems are collected from some precipitation systems where the data are similar to pure $\text{Ca}(\text{OBS})_2$ precipitation systems. At this range of molar ratio, the inhibition of precipitation is not found in the mixed NaDS/NaOBS systems.

For precipitation of $\text{Ca}(\text{DS})_2$ in the systems of 50-75% molar ratio of NaDS/NaOBS mixtures, the induction time is essentially not a function of supersaturation ratio calculated based on $\text{Ca}(\text{DS})_2$, as a different precipitation trend can be observed when compared to the pure NaDS systems precipitates by CaCl_2 . In this case, the inhibition of precipitation is observed as the induction time appears larger than in the pure systems at the same degree of supersaturation with respect to $\text{Ca}(\text{DS})_2$. The inhibition is due to the change in precipitating species (DS^-) because of the molar ratio and thermodynamic change of mixed micellization. In this case, it is also observed the change in kinetics of precipitation.

The kinetics of precipitation of binary mixed anionic surfactants can be found at 50-75% NaDS/NaOBS systems; the interfacial energy estimated from the relationship of induction time and supersaturation ratio reveals that the time required to begin precipitation of the $\text{Ca}(\text{DS})_2$ in 50-75% NaDS/NaOBS systems is larger than the time required to begin precipitation for pure NaDS solution. The other kinetic parameters such as nucleation rate, Gibbs free energy change of formation of critical nucleus, and the radius of critical nucleus are estimated. They reveal that the inhibition of anionic surfactant precipitation is partly due to kinetic change.

8.2 Recommendations

The current thermodynamic model fits dilute NaDS data quite well, but becomes less accurate as the system approaches the CMC value. There may be several reasons for this reduction in fitting ability as the NaDS concentration becomes higher, but perhaps the most likely reason is that the extended Debye-Hückel expression may be unable to accurately determine the effect of the ionic strength on the activity of the surfactant monomer ion. This has been suggested previously in submicellar solutions of sodium alkyl sulfates where deviations from the Debye-Hückel theory were noted, and possibly explained by variations in the hydrophobic hydration of the alkyl chains as the surfactant content increased. It may be necessary to determine more accurate models for activity coefficients for surfactants.

This work assumed that the micelle is a separate phase, which will not contribute much to the ionic strength of the electrolyte solution and thus activity coefficient. The ionic strength of the electrolyte solution was estimated by accounting the counterion binding to the micelle effect; however, this resulted in a worse prediction of precipitation phase boundary. Moreover, it should be noted that some data point of the precipitation system at 75% NaDS molar ratio are highly scattered; this is probably due to the poor prediction of the thermodynamic models of mixed micellization of regular solution theory resulting in a worse prediction of theoretical precipitation phase boundary for 75:25 NaDS/NaOBS molar ratio.

Furthermore, it may be necessary to confirm an accurate value of the calculated interfacial energy from the slope of the relationship between induction time and supersaturation ratio, because the value of interfacial energy indicates the time required for precipitation of the calcium surfactant salt. The estimated interfacial

energy in this work is used to estimate the nucleation rate of the related solution; hence, the experimental determination of nucleation rate as a function of supersaturation ratio is needed to confirm the calculated nucleation rate estimated from the relationship of interfacial energy based on classical homogeneous nucleation. This has not been performed in this work because of the lack of suitable instrument for an investigation of the nucleation process, which would occur at extremely large rates in these systems.

APPENDIX A

STEPS IN CALCULATION OF THE PRECIPITATING SPECIES

USING THE IMPROVED THERMODYNAMIC MODELS FOR

SINGLE ANIONIC SURFACTANT SYSTEMS

A.1 Single NaDS Precipitated by Calcium Chloride

A.1.1 Example of Calculation of the Supersaturation Ratio for the Precipitation of NaDS above the CMC

The total NaDS is 0.020 M mixed with 0.005 mM CaCl₂ aqueous solution at 30°C. The measured value of the K_{SP} of Ca(DS)₂ in aqueous solution is 2.122×10^{-10} at 30°C. We will use equation below to calculate the supersaturation ratio of this solution:

$$S_0 = \left(\frac{[Ca^{2+}]_{unb} [DS^-]_{mon}^2 f_{Ca^{2+}} f_{DS^-}^2}{K_{SP}} \right)^{1/3} \quad (A.1)$$

The amount of DS⁻ monomers can be quantified by the use of Corrin-Harkins relationship, and mass balances at 30°C as equation (A.1):

$$\ln[CMC] = -7.899 - 0.6142 \ln[Na^+]_{unb} \quad (A.2)$$

where $[DS^-] = [CMC]$ at the CMC and from the mass balance of sodium:

$$[NaDS] = [Na^+]_{unb} + [Na^+]_b \quad (A.3)$$

Equation (A.2) gives:

$$\ln[DS^-]_{mon} = -7.899 - 0.6142 \ln([NaDS] - [Na]_b) \quad (A.4)$$

The amount of unbound Ca^{2+} ion in equation (A.1) can be quantified by the use of chemical equilibrium of counterion binding to the micelle model with $K = 0.015$, and mass balances at $30^\circ C$ as follows:

$$\frac{[Na^+]_b}{[Na^+]_{unb} - [DS^-]_{mon}} = K \frac{[Ca^{2+}]_b}{[Ca^{2+}]_{unb}} \quad (A.5)$$

According to the mass balances of NaDS and $CaCl_2$:

$$[CaCl_2] = [Ca^{2+}]_{unb} + [Ca^{2+}]_b \quad (A.6)$$

$$[NaDS] = [DS^-]_{mon} + [DS^-]_{mic} \quad (A.7)$$

Equation (A.5) gives:

$$\frac{[Na^+]_b}{[NaDS] - [Na^+]_b - [DS^-]_{mon}} = 0.015 \frac{[Ca^{2+}]_b}{[CaCl_2] - [Ca^{2+}]_b} \quad (A.8)$$

From the definition of the degree of counterion binding to the micelle corresponding to the mono- and divalent cations present in the bulk solution:

$$\beta_{Na^+} = \frac{[NaDS] - [Na^+]_{unb}}{[NaDS] - [DS^-]_{mon}} = \frac{[Na^+]_b}{[DS^-]_{mic}} \quad (A.9)$$

$$\beta_{Ca^{2+}} = \frac{2([CaCl_2] - [Ca^{2+}]_{unb})}{[NaDS] - [DS^-]_{mon}} = \frac{2[Ca^{2+}]_b}{[DS^-]_{mic}} \quad (A.10)$$

Therefore, the above two equations give the total degree of total counterion binding:

$$\beta_T = \beta_{Na^+} + \beta_{Ca^{2+}} = \frac{[Na^+]_b + 2[Ca^{2+}]_b}{[DS^-]_{mic}} = 0.65 \quad (\text{A.11})$$

Solving equation (A.4), (A.8), and (A.11) simultaneously in Maple using the algorithm *fsolve*, when given $m = [CaCl_2]$, $n = [NaDS]$, $x = [Na^+]_b$, $y = [Ca^{2+}]_b$, and $z = [DS^-]_{mon}$. f , g , and h are the functions.

```
> m := 0.005;
> n := 0.020;
> f := (x + y)/(n - z) = 0.65;
> g := x/(n - x - z) - 0.015*y/(m - y) = 0;
> h := z - exp(-7.899 - 0.6142*ln(n - x)) = 0;
> fsolve({f, g, h}, {x, y, z}, {x=10-9..n - 10-9, y=10-10..m - 10-10, z=10-6..n - 10-10});
```

Solution:

$$\{x = 0.001471850161, y = 0.004366777681, z = 0.004299376118\}$$

The software gives the answer as follows:

$$[Na^+]_b = 0.00147 \text{ M}, [Ca^{2+}]_b = 0.00437 \text{ M}, \text{ and } [DS^-]_{mon} = 0.0043 \text{ M}$$

Therefore, from the mass balances:

$$[Na^+]_{unb} = 0.01853 \text{ M}, [Ca^{2+}]_{unb} = 0.00063 \text{ M}, \text{ and } [DS^-]_{mic} = 0.0157 \text{ M}$$

The activity coefficients in equation (A.1) can be calculated via the Debye-Hückel equation:

$$\log f_i = \frac{-A(z_i)^2 I^{1/2}}{1 + B a_i I^{1/2}} - 0.3I \quad (\text{A.12})$$

The parameters in the Debye-Hückel equation are discussed in Chapter 3, section 3.3.1.2, and the ionic strength can be determined from the following equation:

$$I = \frac{1}{2} \sum c_i z_i^2 \quad (\text{A.13})$$

From the given total concentration of NaDS and CaCl₂, the activity coefficients are:

$$f_{DS^-} = 0.8758$$

$$f_{Ca^{2+}} = 0.6002$$

Thus, the supersaturation ratio is:

$$S_0 = \left(\frac{(0.00063)(0.0043)^2 (0.6002)(0.8758)^2}{2.122 \times 10^{-10}} \right)^{1/3} = 2.93$$

In order to find the saturated point where $S_0 = 1$ for each NaDS concentration for both below and above the CMC, the CaCl₂ concentration will be varied until the solubility product is satisfied, and then the supersaturation ratio reaches unity as shown in Table A.1.

In Table A.1, the calculation starts at the surfactant concentration below the CMC which is 0.0079 M of NaDS aqueous solution. A new chemical equilibrium model that involving with sodium and calcium ions bound to the micelle is applied for the concentration above the CMC therefore, we known the concentration of bound and unbound counterions above the CMC corresponding to the system studies with varying NaDS and CaCl₂ concentration.

Table A.1 The results of calculation of saturated points (precipitation phase boundary) from the improved models of anionic surfactant precipitation.

[NaDS]	[CaCl] ₂	[DS] ⁻ _{mon}	[Ca ²⁺] _b	[Na ⁺] _b	[Na ⁺] _{unb}	[Ca ²⁺] _{unb}	[Cl ⁻]	<i>I</i>	<i>f</i> _{DS⁻}	<i>f</i> _{Ca²⁺}	<i>S</i> ₀
2.00×10 ⁻⁴	1.82×10 ⁻²	2.00×10 ⁻⁴	0.00	0.00	2.00×10 ⁻⁴	1.82×10 ⁻²	3.64×10 ⁻²	5.48×10 ⁻²	0.8044	0.4515	1.00
4.00×10 ⁻⁴	2.25×10 ⁻³	4.00×10 ⁻⁴	0.00	0.00	4.00×10 ⁻⁴	2.25×10 ⁻³	4.49×10 ⁻³	7.14×10 ⁻³	0.9152	0.7065	1.00
1.00×10 ⁻³	2.82×10 ⁻⁴	1.00×10 ⁻³	0.00	0.00	1.00×10 ⁻³	2.82×10 ⁻⁴	5.64×10 ⁻⁴	1.85×10 ⁻³	0.9536	0.8280	1.00
2.00×10 ⁻³	7.23×10 ⁻⁵	2.00×10 ⁻³	0.00	0.00	2.00×10 ⁻³	7.23×10 ⁻⁵	1.45×10 ⁻⁴	2.22×10 ⁻³	0.9495	0.8143	1.00
4.00×10 ⁻³	2.00×10 ⁻⁵	4.00×10 ⁻³	0.00	0.00	4.00×10 ⁻³	2.00×10 ⁻⁵	3.99×10 ⁻⁵	4.06×10 ⁻³	0.9338	0.7629	1.00
6.00×10 ⁻³	9.59×10 ⁻⁶	6.00×10 ⁻³	0.00	0.00	6.00×10 ⁻³	9.59×10 ⁻⁶	1.92×10 ⁻⁵	6.03×10 ⁻³	0.9212	0.7242	1.00
7.00×10 ⁻³	7.29×10 ⁻⁶	7.00×10 ⁻³	0.00	0.00	7.00×10 ⁻³	7.29×10 ⁻⁶	1.46×10 ⁻⁵	7.02×10 ⁻³	0.9158	0.7082	1.00
7.50×10 ⁻³	6.46×10 ⁻⁶	7.50×10 ⁻³	0.00	0.00	7.50×10 ⁻³	6.46×10 ⁻⁶	1.29×10 ⁻⁵	7.52×10 ⁻³	0.9133	0.7008	1.00
7.70×10 ⁻³	6.17×10 ⁻⁶	7.70×10 ⁻³	0.00	0.00	7.70×10 ⁻³	6.17×10 ⁻⁶	1.23×10 ⁻⁵	7.72×10 ⁻³	0.9123	0.6980	1.00
7.85×10 ⁻³	5.96×10 ⁻⁶	7.85×10 ⁻³	0.00	0.00	7.85×10 ⁻³	5.96×10 ⁻⁶	1.19×10 ⁻⁵	7.87×10 ⁻³	0.9116	0.6959	1.00
8.00×10 ⁻³	1.51×10 ⁻⁴	7.30×10 ⁻³	1.44×10 ⁻⁴	1.69×10 ⁻⁴	7.83×10 ⁻³	6.86×10 ⁻⁶	3.02×10 ⁻⁴	7.73×10 ⁻³	0.9123	0.6978	1.00
9.00×10 ⁻³	2.88×10 ⁻⁴	7.05×10 ⁻³	2.81×10 ⁻⁴	7.09×10 ⁻⁴	8.29×10 ⁻³	7.42×10 ⁻⁶	5.77×10 ⁻⁴	7.97×10 ⁻³	0.9111	0.6944	1.00
1.00×10 ⁻²	3.80×10 ⁻⁴	6.84×10 ⁻³	3.72×10 ⁻⁴	1.31×10 ⁻³	8.69×10 ⁻³	7.91×10 ⁻⁶	7.61×10 ⁻⁴	8.16×10 ⁻³	0.9102	0.6918	1.00
2.00×10 ⁻²	9.48×10 ⁻⁴	5.49×10 ⁻³	9.35×10 ⁻⁴	7.56×10 ⁻³	1.24×10 ⁻²	1.29×10 ⁻⁵	1.90×10 ⁻³	9.94×10 ⁻³	0.9023	0.6696	1.00
4.00×10 ⁻²	2.09×10 ⁻³	4.01×10 ⁻³	2.07×10 ⁻³	1.93×10 ⁻²	2.07×10 ⁻²	2.69×10 ⁻⁵	4.19×10 ⁻³	1.45×10 ⁻²	0.8855	0.6246	1.00
6.00×10 ⁻²	3.55×10 ⁻³	3.19×10 ⁻³	3.50×10 ⁻³	2.99×10 ⁻²	3.01×10 ⁻²	4.72×10 ⁻⁵	7.10×10 ⁻³	2.03×10 ⁻²	0.8686	0.5828	1.00
8.00×10 ⁻²	5.38×10 ⁻³	2.67×10 ⁻³	5.30×10 ⁻³	3.97×10 ⁻²	4.03×10 ⁻²	7.55×10 ⁻⁵	1.08×10 ⁻²	2.70×10 ⁻²	0.8524	0.5456	1.00

Remark: * The concentration is in the unit of molar (mole/L)

APPENDIX B

STEPS IN CALCULATION OF THE PRECIPITATING SPECIES

BY THE IMPROVED THERMODYNAMIC MODELS FOR

BINARY MIXED ANIONIC SURFACTANT SYSTEMS

B.1 Binary Mixed NaDS/NaDeS Precipitated by Calcium Chloride

B.1.1 Example of Calculation of the Supersaturation Ratio for the Precipitation of the equimolar ratio of NaDS/NaDeS system above the CMC

The total NaS is 0.012 M mixed with 0.010 M CaCl₂ aqueous solution at 30°C. The CMC of the binary NaDS/NaDeS mixtures (CMC_M) for an equimolar ratio is equal to 0.0098 M from the experimental measurement. For equimolar ratio, [NaS] = [NaDS] + [NaDeS] = 0.0060 + 0.0060 M. The measured value of K_{SP} of Ca(DS)₂ in aqueous solution is 2.122×10^{-10} while measured value of K_{SP} of Ca(DeS)₂ in aqueous solution is 2.677×10^{-5} at 30°C. Clearly, Ca(DS)₂ will precipitate out from the solution because of the lower K_{SP} . We will use equation below to calculate the supersaturation ratio of this solution:

$$S_0 = \left(\frac{[Ca^{2+}]_{unb} [DS^-]_{mon}^2 f_{Ca^{2+}} f_{S^-}^2}{K_{SP}} \right)^{1/3} \quad (B.1)$$

The amount of DS⁻ monomers can be quantified by the use of the regular solution theory and pseudophase separation theory, and mass balances at 30°C the series of equations discussed in Chapter 2, section 2.32. The results from the iterative calculation by regular solution theory are shown in Table B.1.

Therefore, we know the equilibrium composition of each species in binary mixed NaDS/NaDeS system by the regular solution theory as following:

$$[\text{NaDS}] = z_1[\text{NaS}] = (0.5)(12.0) = 6.0 \text{ mM}$$

$$[\text{S}^-]_{\text{mon}} = 10.3653 \text{ mM}$$

$$[\text{S}^-]_{\text{mic}} = 1.6347 \text{ mM}$$

$$[\text{DS}^-]_{\text{mon}} = \alpha_1[\text{S}^-]_{\text{mon}} = (0.4697)(10.3653) = 4.8686 \text{ mM}$$

and thus,

$$[\text{DeS}^-]_{\text{mon}} = 10.3653 - 4.8686 = 5.4967 \text{ mM}$$

$$[\text{DS}^-]_{\text{mic}} = X_1[\text{S}^-]_{\text{mic}} = (0.6920)(1.6347) = 1.1312 \text{ mM}$$

and thus,

$$[\text{DeS}^-]_{\text{mic}} = 1.6347 - 1.1312 = 0.5035 \text{ mM}$$

The amount of unbound Ca^{2+} ion in equation (B.1) can be quantified by the use of chemical equilibrium of counterion binding to the micelle model with $K = 0.015$ when the total anionic surfactant monomer concentration $[\text{S}^-]_{\text{mon}}$ is known from the regular solution theory, and mass balances at 30°C as follows:

$$\frac{[\text{Na}^+]_b}{[\text{Na}^+]_{\text{unb}} - [\text{S}^-]_{\text{mon}}} = 0.015 \frac{[\text{Ca}^{2+}]_b}{[\text{Ca}^{2+}]_{\text{unb}}} \quad (\text{B.2})$$

According to the mass balances of NaS and CaCl_2 :

$$[\text{CaCl}_2] = [\text{Ca}^{2+}]_{\text{unb}} + [\text{Ca}^{2+}]_b \quad (\text{B.3})$$

$$[NaS] = [Na^+]_{unb} + [Na^+]_b \quad (B.4)$$

$$[NaS] = [S^-]_{mon} + [S^-]_{mic} \quad (B.5)$$

Equation (B.2) gives:

$$\frac{[Na^+]_b}{[NaS] - [Na^+]_b - [S^-]_{mon}} = 0.015 \frac{[Ca^{2+}]_b}{[CaCl_2] - [Ca^{2+}]_b} \quad (B.6)$$

From the definition of the degree of counterion binding to the micelle corresponding to the mono- and divalent cations present in the bulk solution:

$$\beta_{Na^+} = \frac{[NaS] - [Na^+]_{unb}}{[NaS] - [S^-]_{mon}} = \frac{[Na^+]_b}{[S^-]_{mic}} \quad (B.7)$$

$$\beta_{Ca^{2+}} = \frac{2([CaCl_2] - [Ca^{2+}]_{unb})}{[NaS] - [S^-]_{mon}} = \frac{2[Ca^{2+}]_b}{[S^-]_{mic}} \quad (B.8)$$

Therefore, the above two equations give the total degree of total counterion binding:

$$\beta_T = \beta_{Na^+} + \beta_{Ca^{2+}} = \frac{[Na^+]_b + 2[Ca^{2+}]_b}{[S^-]_{mic}} = 0.65 \quad (B.9)$$

Solving equation (B.6) and (B.9) simultaneously in Maple by this algorithm using *fsolve* function when given $m = [CaCl_2]$, $n = [NaD]$, $x = [Na^+]_b$, $y = [Ca^{2+}]_b$. where $z = [S^-]_{mon} = 10.3653$ mM. f and g are the functions.

```

> m := 0.010;
> n := 0.012;
> z := 0.0103653;
> f := (x + y)/(n - z) = 0.65;
> g := x/(n - x - z) - 0.015·y/(m - y) = 0;
> fsolve({f, g}, {x, y}, {x = 10-9 .. n - 10-9, y = 10-10 .. m - 10-10});

```

Solution:

$$\{x = 0.000001372781940, y = 0.0005305911092\}$$

The software gives the answer as follows:

$$[Na^+]_b = 1.373 \times 10^{-6} \text{ M and } [Ca^{2+}]_b = 5.306 \times 10^{-4} \text{ M}$$

Therefore, from the mass balances:

$$[Na^+]_{umb} = 1.199 \times 10^{-2} \text{ M, } [Ca^{2+}]_{umb} = 9.469 \times 10^{-3} \text{ M}$$

The activity coefficients in equation (B.1) can be calculated via the Debye-Hückel equation:

$$\log f_i = \frac{-A(z_i)^2 I^{1/2}}{1 + B a_i I^{1/2}} - 0.3I \quad (\text{B.10})$$

The parameters in the Debye-Hückel equation are discussed in Chapter 3, section 3.3.1.2 and the ionic strength can be determined from this equation of ionic strength:

$$I = \frac{1}{2} \sum c_i z_i^2 \quad (\text{B.11})$$

From the given total concentration of NaDS and CaCl₂, the activity coefficients are:

$$f_{S^-} = 0.8239$$

$$f_{Ca^{2+}} = 0.4871$$

Thus, the supersaturation ratio based on Ca(DS)₂ is:

$$S_0 = \left(\frac{(9.47 \times 10^{-3})(4.87 \times 10^{-3})^2 (0.4871)(0.8239)^2}{2.122 \times 10^{-10}} \right)^{1/3} = 7.05$$

and the supersaturation ratio based on Ca(DeS)₂ at the same total concentration of NaS and CaCl₂ is:

$$S_0 = \left(\frac{(9.47 \times 10^{-3})(1.61 \times 10^{-2})^2 (0.4871)(0.8239)^2}{2.677 \times 10^{-5}} \right)^{1/3} = 0.15$$

In order to find the saturated point where $S_0 = 1$ for each NaS concentration in equimolar ratio system for both below and above the CMC_M, the CaCl₂ concentration will be varied until the solubility product of each calcium salts of surfactant is satisfied, and then the supersaturation ratio reaches the unity as shown in Table B.2.

Table B.2 The results of calculation of saturated points (precipitation phase boundary) from the improved models

Of binary mixed NaDS/NaDeS precipitation by CaCl₂.

[NaS]	[CaCl ₂]	[DS ⁻] _{tot}	[S ⁻] _{mon}	[S ⁻] _{mic}	[DS ⁻] _{mon}	[DeS ⁻] _{mon}	[Ca ²⁺] _b	[Na ⁺] _b	[Ca ²⁺] _{unb}	<i>I</i>	<i>f_s</i>	<i>f_{Ca²⁺}</i>	<i>S₀</i> (DS)	<i>S₀</i> (DeS)
4.00E-04	1.83E-02	2.00E-04	4.00E-04	0.00E+00	2.00E-04	2.00E-04	0.00E+00	0.00E+00	1.83E-02	5.53E-02	0.8036	0.4502	1.00	0.02
8.00E-04	2.32E-03	4.00E-04	8.00E-04	0.00E+00	4.00E-04	4.00E-04	0.00E+00	0.00E+00	2.32E-03	7.76E-03	0.9121	0.6974	1.00	0.02
1.60E-03	4.80E-04	8.00E-04	1.60E-03	0.00E+00	8.00E-04	8.00E-04	0.00E+00	0.00E+00	4.80E-04	3.04E-03	0.9418	0.7887	1.00	0.02
2.00E-03	3.05E-04	1.00E-03	2.00E-03	0.00E+00	1.00E-03	1.00E-03	0.00E+00	0.00E+00	3.05E-04	2.92E-03	0.9429	0.7922	1.00	0.02
4.00E-03	8.10E-05	2.00E-03	4.00E-03	0.00E+00	2.00E-03	2.00E-03	0.00E+00	0.00E+00	8.10E-05	4.24E-03	0.9325	0.7588	1.00	0.02
8.00E-03	2.30E-05	4.00E-03	8.00E-03	0.00E+00	4.00E-03	4.00E-03	0.00E+00	0.00E+00	2.30E-05	8.07E-03	0.9106	0.6931	1.00	0.02
9.70E-03	1.66E-05	4.85E-03	9.70E-03	0.00E+00	4.85E-03	4.85E-03	0.00E+00	0.00E+00	1.66E-05	9.75E-03	0.9031	0.6718	1.00	0.02
1.00E-02	2.55E-04	5.00E-03	8.97E-03	1.03E-03	5.00E-03	3.97E-03	2.40E-04	1.89E-04	1.59E-05	1.08E-02	0.8990	0.6604	1.00	0.02
1.20E-02	5.25E-04	6.00E-03	9.16E-03	2.84E-03	4.81E-03	4.36E-03	5.07E-04	8.31E-04	1.84E-05	1.36E-02	0.8887	0.6328	1.00	0.02
1.60E-02	9.25E-04	8.00E-03	9.55E-03	6.45E-03	4.52E-03	5.03E-03	9.02E-04	2.39E-03	2.30E-05	1.88E-02	0.8727	0.5926	1.00	0.02
2.00E-02	1.27E-03	1.00E-02	9.94E-03	1.01E-02	4.31E-03	5.63E-03	1.24E-03	4.06E-03	2.75E-05	2.38E-02	0.8598	0.5622	1.00	0.02
4.00E-02	2.81E-03	2.00E-02	1.17E-02	2.83E-02	3.71E-03	7.99E-03	2.76E-03	1.29E-02	4.97E-05	4.84E-02	0.8137	0.4680	1.00	0.03
8.00E-02	5.92E-03	4.00E-02	1.45E-02	6.55E-02	3.20E-03	1.13E-02	5.82E-03	3.09E-02	9.75E-05	9.77E-02	0.7540	0.3746	1.00	0.05
1.60E-01	1.30E-02	8.00E-02	1.88E-02	1.41E-01	2.75E-03	1.61E-02	1.28E-02	6.61E-02	2.18E-04	1.99E-01	0.6719	0.2838	1.00	0.06

Remark: * The concentration is in the unit of molar (mole/L)

APPENDIX C

RAW DATA OF INDUCTION TIME

Table C.1 The induction time of single NaDS systems precipitating by CaCl_2 for the systems *below* the CMC of NaDS (7.9 mM) corresponding to its supersaturation ratio at 30°C.

[NaDS], M	[CaCl ₂], M	S_0	t_1	t_2	t_3	$t_{ind}(\text{avg})$
0.003	0.0045	4.48	14.00	15.00	11.00	13.33
	0.012	5.58	12.00	12.00	12.00	12.00
	0.035	6.67	11.00	12.00	12.00	11.67
0.004	0.0045	5.39	13.00	13.00	14.00	13.33
	0.012	6.74	13.00	12.00	12.00	12.33
	0.035	8.07	10.00	11.00	12.00	11.00
0.005	0.00065	3.57	Large	Large	Large	Large
	0.0018	4.85	34.00	32.00	30.00	32.00
	0.004	6.03	14.00	16.00	13.00	14.33
	0.0085	7.24	13.00	11.00	11.00	11.67
	0.05	9.73	5.00	5.00	5.00	5.00
	0.1	10.04	3.00	3.00	4.00	3.33
0.006	0.00065	3.99	56.00	60.00	64.00	60.00
	0.0018	5.43	15.00	16.00	15.00	15.33
	0.004	6.77	13.00	12.00	12.00	12.33
	0.0085	8.14	11.00	11.00	11.00	11.00
	0.05	10.96	10.00	12.00	12.00	11.33
	0.1	11.32	3.00	4.00	4.00	3.67

Remark: Time (t_1 , t_2 , t_3 , and t_{ind}) in a unit of second.

Table C.2 The induction time of single NaDS systems precipitating by CaCl_2 for the systems *above* the CMC of NaDS (7.9 mM) corresponding to its supersaturation ratio at 30°C.

[NaDS], M	[CaCl ₂], M	S_0	t_1	t_2	t_3	t_{ind} (avg)
0.008	0.001	4.52	42.00	50.00	44.00	45.33
	0.002	5.89	21.00	18.00	20.00	19.67
	0.003	6.73	13.00	16.00	12.00	13.67
	0.006	8.21	12.00	14.00	13.00	13.00
	0.01	9.31	11.00	13.00	10.00	11.33
0.01	0.001	2.03	110.00	110.00	110.00	110.00
	0.002	4.16	32.00	26.00	30.00	29.33
	0.003	5.29	17.00	16.00	16.00	16.33
	0.006	7.00	13.00	13.00	13.00	13.00
	0.01	8.16	12.00	12.00	14.00	12.67
0.02	0.003	1.67	160.00	170.00	165.00	165.00
	0.006	3.31	17.00	20.00	17.00	18.00
	0.01	4.93	16.00	13.00	16.00	15.00
0.03	0.003	1.19	Large	Large	Large	Large
	0.006	1.81	64.00	76.00	66.00	68.67
	0.01	3.07	16.00	15.00	15.00	15.33
0.04	0.003	0.99	Large	Large	Large	Large
	0.006	1.38	400.00	360.00	400.00	386.67
	0.01	2.00	28.00	29.00	26.00	27.67
0.05	0.003	0.87	Large	Large	Large	Large
	0.006	1.16	Large	Large	Large	Large
	0.01	1.55	100.00	86.00	98.00	94.67

Remark: Time (t_1 , t_2 , t_3 , and t_{ind}) in a unit of second.

Table C.3 The induction time of 75:25 NaDS/NaDeS molar ratio systems precipitating by CaCl_2 for the systems *below* the CMC_M of NaDS/NaDeS mixtures (8.4 mM) corresponding to its supersaturation ratio at 30°C.

[NaS], M	[CaCl ₂], M	S_0 (DS)	S_0 (DeS)	t_1	t_2	t_3	t_{ind} (avg)
0.003	0.0045	3.70	0.06	20	20	20	20.00
	0.012	4.61	0.09	16	14	15	15.00
	0.035	5.51	0.13	12	12	13	12.33
0.004	0.0045	4.45	0.08	17	16	18	17.00
	0.012	5.56	0.12	16	16	15	15.67
	0.035	6.66	0.17	14	16	15	15.00
0.005	0.00065	2.95	0.05	Large	Large	Large	Large
	0.0018	4.01	0.07	24	25	23	24.00
	0.004	4.98	0.10	19	22	20	20.33
	0.0085	5.97	0.13	17	15	19	17.00
	0.05	8.03	0.23	15	17	16	16.00
	0.10	8.28	0.26	15	14	14	14.33
0.006	0.00065	3.30	0.05	64	62	59	61.67
	0.0018	4.49	0.08	22	24	25	23.67
	0.004	5.59	0.11	22	21	21	21.33
	0.0085	6.72	0.15	19	18	19	18.67
	0.05	9.05	0.27	16	16	15	15.67
	0.10	9.34	0.31	14	15	16	15.00
0.008	0.001	4.48	0.08	24	21	22	22.33
	0.002	5.52	0.11	17	17	15	16.33
	0.003	6.19	0.13	14	17	16	15.67
	0.006	7.43	0.17	13	13	14	13.33
	0.01	8.37	0.21	13	13	13	13.00

Remark: Time (t_1 , t_2 , t_3 , and t_{ind}) in a unit of second.

Table C.4 The induction time of 75:25 NaDS/NaDeS molar ratio systems precipitating by CaCl_2 for the systems *above* the CMC_M of NaDS/NaDeS mixtures (8.4 mM) corresponding to its supersaturation ratio at 30°C.

[NaS], M	[CaCl ₂], M	S_0 (DS)	S_0 (DeS)	t_1	t_2	t_3	t_{ind} (avg)
0.01	0.001	3.16	0.06	19	19	19	19.00
	0.002	4.72	0.10	16	18	20	18.00
	0.003	5.56	0.12	15	13	14	14.00
	0.006	6.97	0.17	12	12	13	12.33
	0.01	7.99	0.21	11	12	13	12.00
0.02	0.003	2.19	0.05	105	95	120	106.67
	0.006	4.77	0.14	18	18	19	18.33
	0.01	6.35	0.21	14	14	14	14.00
0.03	0.003	1.32	0.03	Large	Large	Large	Large
	0.006	2.45	0.08	125	125	120	123.33
	0.01	4.42	0.18	29	24	28	27.00
0.04	0.003	0.70	0.03	Large	Large	Large	Large
	0.006	1.11	0.07	Large	Large	Large	Large
	0.01	1.58	0.11	60	58	58	58.67

Remark: Time (t_1 , t_2 , t_3 , and t_{ind}) in a unit of second.

Table C.5 The induction time of 50:50 NaDS/NaDeS molar ratio systems precipitating by CaCl_2 for the systems *below* the CMC_M of NaDS/NaDeS mixtures (9.8 mM) corresponding to its supersaturation ratio at 30°C.

[NaS], M	[CaCl ₂], M	S_0 (DS)	S_0 (DeS)	t_1	t_2	t_3	t_{ind} (avg)
0.003	0.0045	2.82	0.06	23	21	21	21.67
	0.012	3.52	0.07	22	21	21	21.33
	0.035	4.20	0.08	21	19	21	20.33
0.004	0.0045	3.40	0.07	26	27	28	37.00
	0.012	4.24	0.08	27	26	27	27.00
	0.035	5.08	0.10	36	36	39	26.67
0.005	0.00065	2.25	0.04	112	92	120	108.00
	0.0018	3.06	0.06	27	29	29	31.33
	0.004	3.80	0.08	21	19	21	28.67
	0.0085	4.56	0.09	30	27	29	28.33
	0.05	6.13	0.12	32	31	31	20.33
	0.10	6.32	0.13	18	17	17	17.33
0.006	0.00065	2.51	0.05	56	56	57	56.33
	0.0018	3.42	0.07	27	26	29	30.00
	0.004	4.27	0.09	18	20	17	27.33
	0.0085	5.13	0.10	20	21	23	25.33
	0.05	6.91	0.14	25	25	26	21.33
	0.10	7.13	0.14	28	30	32	18.33
0.008	0.001	3.42	0.07	34	33	34	33.67
	0.002	4.21	0.08	22	21	20	22.33
	0.003	4.72	0.09	19	19	19	21.00
	0.006	5.67	0.11	19	19	19	19.00
	0.01	6.39	0.13	24	22	21	19.00

Remark: Time (t_1 , t_2 , t_3 , and t_{ind}) in a unit of second.

Table C.6 The induction time of 50:50 NaDS/NaDeS molar ratio systems precipitating by CaCl_2 for the systems *above* the CMC_M of NaDS/NaDeS mixtures (9.8 mM) corresponding to its supersaturation ratio at 30°C.

[NaS], M	[CaCl ₂], M	S_0 (DS)	S_0 (DeS)	t_1	t_2	t_3	t_{ind} (avg)
0.01	0.001	3.54	0.07	46	49	49	48.00
	0.002	4.49	0.09	32	29	31	30.67
	0.003	5.09	0.10	28	27	27	30.00
	0.006	6.17	0.13	28	29	30	29.00
	0.01	6.99	0.14	30	29	31	27.33
0.02	0.003	2.28	0.06	Large	Large	Large	Large
	0.006	4.32	0.12	60	70	85	71.67
	0.01	5.47	0.15	40	35	44	39.67
0.03	0.003	1.24	0.04	Large	Large	Large	Large
	0.006	2.52	0.08	Large	Large	Large	Large
	0.01	4.21	0.14	240	380	240	286.67
0.04	0.003	1.00	0.04	Large	Large	Large	Large
	0.006	1.64	0.06	Large	Large	Large	Large
	0.01	2.27	0.08	1000	1000	1000	1000.00

Remark: Time (t_1 , t_2 , t_3 , and t_{ind}) in a unit of second.

Table C.7 The induction time of 25:75 NaDS/NaDeS molar ratio systems precipitating by CaCl_2 for the systems *below* the CMC_M of NaDS/NaDeS mixtures (14.5 mM) corresponding to its supersaturation ratio at 30°C.

[NaS], M	[CaCl ₂], M	S_0 (DS)	S_0 (DeS)	t_1	t_2	t_3	t_{ind} (avg)
0.003	0.0045	1.78	0.07	Large	Large	Large	Large
	0.012	2.22	0.09	54	51	55	53.33
	0.035	2.65	0.11	43	44	49	45.33
0.004	0.0045	2.14	0.09	49	50	50	49.67
	0.012	2.67	0.11	29	34	28	30.33
	0.035	3.20	0.13	40	32	38	36.67
0.005	0.00065	1.42	0.06	Large	Large	Large	Large
	0.0018	1.93	0.08	Large	Large	Large	Large
	0.004	2.39	0.10	Large	Large	Large	Large
	0.0085	2.87	0.12	Large	Large	Large	Large
	0.05	3.86	0.16	72	65	64	67.00
	0.10	3.98	0.17	60	60	64	61.33
0.006	0.00065	1.58	0.07	Large	Large	Large	Large
	0.0018	2.16	0.09	Large	Large	Large	Large
	0.004	2.69	0.11	Large	Large	Large	Large
	0.0085	3.23	0.13	60	68	60	62.67
	0.05	4.35	0.18	44	42	42	42.67
	0.10	4.49	0.19	40	32	40	37.33
0.008	0.001	2.15	0.09	Large	Large	Large	Large
	0.002	2.65	0.11	Large	Large	Large	Large
	0.003	2.98	0.12	80	73	80	77.67
	0.006	3.57	0.15	28	30	24	27.33
	0.01	4.02	0.17	17	17	17	17.00
0.01	0.001	2.46	0.10	Large	Large	Large	Large
	0.002	3.04	0.13	56	52	53	53.67
	0.003	3.41	0.14	26	25	25	25.33
	0.006	4.10	0.17	15	14	13	14.00
	0.01	4.63	0.19	13	15	15	14.33

Remark: Time (t_1 , t_2 , t_3 , and t_{ind}) in a unit of second.

Table C.8 The induction time of 25:75 NaDS/NaDeS molar ratio systems precipitating by CaCl_2 for the systems *above* the CMC_M of NaDS/NaDeS mixtures (14.5 mM) corresponding to its supersaturation ratio at 30°C.

[NaS], M	[CaCl ₂], M	S_0 (DS)	S_0 (DeS)	t_1	t_2	t_3	t_{ind} (avg)
0.02	0.003	2.46	0.12	Large	Large	Large	Large
	0.006	3.73	0.18	Large	Large	Large	Large
	0.01	4.52	0.22	Large	Large	Large	Large
0.03	0.003	1.47	0.09	Large	Large	Large	Large
	0.006	3.16	0.19	Large	Large	Large	Large
	0.01	4.19	0.25	Large	Large	Large	Large
0.04	0.003	1.11	0.08	Large	Large	Large	Large
	0.006	2.41	0.17	Large	Large	Large	Large
	0.01	3.77	0.27	Large	Large	Large	Large

Remark: Time (t_1 , t_2 , t_3 , and t_{ind}) in a unit of second.

Table C.9 The induction time of 75:25 NaDS/NaOBS molar ratio systems precipitating by CaCl_2 for the systems *below* the CMC_M of NaDS/NaOBS mixtures (8.5 mM) corresponding to its supersaturation ratio at 30°C.

[NaS], M	[CaCl ₂], M	S_0 (DS)	S_0 (OBS)	t_1	t_2	t_3	t_{ind} (avg)
0.003	0.0045	3.70	1.14	48	48	42	46.00
	0.012	4.61	1.42	34	36	32	34.00
	0.035	5.51	1.70	35	32	32	33.00
0.004	0.0045	4.45	1.37	32	32	32	32.00
	0.012	5.56	1.72	31	29	33	31.00
	0.035	6.66	2.06	28	26	26	26.67
0.005	0.00065	2.95	0.91	65	69	72	68.67
	0.0018	4.01	1.24	29	32	30	30.33
	0.004	4.98	1.54	27	27	29	27.67
	0.0085	5.97	1.84	26	26	26	26.00
	0.05	8.03	2.48	10	10	10	10.00
	0.10	8.28	2.56	2	2	2	2.00
0.006	0.00065	3.30	1.02	140	138	128	135.33
	0.0018	4.49	1.38	41	38	37	38.67
	0.004	5.59	1.73	36	35	36	35.67
	0.0085	6.72	2.07	29	28	27	28.00
	0.05	9.05	2.79	2	3	2	2.33
	0.10	9.34	2.88	2	2	2	2.00
0.008	0.001	4.48	1.38	158	160	142	153.33
	0.002	5.52	1.70	45	52	52	49.67
	0.003	6.19	1.91	33	33	34	33.33
	0.006	7.43	2.29	27	24	30	27.00
	0.01	8.37	2.58	22	21	23	22.00

Remark: Time (t_1 , t_2 , t_3 , and t_{ind}) in a unit of second.

Table C.10 The induction time of 75:25 NaDS/NaOBS molar ratio systems precipitating by CaCl_2 for the systems *above* the CMC_M of NaDS/NaOBS mixtures (8.5 mM) corresponding to its supersaturation ratio at 30°C.

[NaS], M	[CaCl ₂], M	S_0 (DS)	S_0 (OBS)	t_1	t_2	t_3	t_{ind} (avg)
0.01	0.001	3.83	1.27	Large	Large	Large	Large
	0.002	5.22	1.73	96	98	94	96.00
	0.003	6.04	2.00	44	44	45	44.33
	0.006	7.46	2.47	32	35	33	33.33
	0.01	8.50	2.81	31	30	28	29.67
0.02	0.003	2.46	1.02	Large	Large	Large	Large
	0.006	5.22	2.18	116	106	120	114.00
	0.01	6.85	2.85	42	45	45	44.00
0.03	0.003	1.55	0.72	Large	Large	Large	Large
	0.006	2.91	1.36	Large	Large	Large	Large
	0.01	5.20	2.42	67	62	67	65.33
0.04	0.003	1.29	0.65	Large	Large	Large	Large
	0.006	2.05	1.03	Large	Large	Large	Large
	0.01	3.58	1.79	165	180	180	175.00

Remark: Time (t_1 , t_2 , t_3 , and t_{ind}) in a unit of second.

Table C.11 The induction time of 50:50 NaDS/NaOBS molar ratio systems precipitating by CaCl_2 for the systems *below* the CMC_M of NaDS/NaOBS mixtures (10.0 mM) corresponding to its supersaturation ratio at 30°C.

[NaS], M	[CaCl ₂], M	S_0 (DS)	S_0 (OBS)	t_1	t_2	t_3	t_{ind} (avg)
0.003	0.0045	2.82	1.81	47	53	51	50.33
	0.012	3.52	2.26	40	38	35	37.67
	0.035	4.20	2.70	29	29	30	29.33
0.004	0.0045	3.40	2.18	31	29	27	29.00
	0.012	4.24	2.72	30	28	25	27.67
	0.035	5.08	3.26	23	25	25	24.33
0.005	0.00065	2.25	1.44	Large	Large	Large	Large
	0.0018	3.06	1.96	55	67	57	59.67
	0.004	3.80	2.44	31	30	26	29.00
	0.0085	4.56	2.93	24	22	26	24.00
	0.05	6.13	3.93	28	26	26	26.67
	0.10	6.32	4.06	2	2	2	2.00
0.006	0.00065	2.51	1.61	Large	Large	Large	Large
	0.0018	3.42	2.20	48	55	51	51.33
	0.004	4.27	2.74	27	29	29	28.33
	0.0085	5.13	3.29	21	21	22	21.33
	0.05	6.91	4.43	19	15	15	16.33
	0.10	7.13	4.58	1	1	1	1.00
0.008	0.001	3.42	2.20	Large	Large	Large	Large
	0.002	4.21	2.70	73	65	65	67.67
	0.003	4.72	3.03	43	45	40	42.67
	0.006	5.67	3.64	22	29	26	25.67
	0.01	6.39	4.10	23	21	22	22.00

Remark: Time (t_1 , t_2 , t_3 , and t_{ind}) in a unit of second.

Table C.12 The induction time of 50:50 NaDS/NaOBS molar ratio systems precipitating by CaCl_2 for the systems *above* the CMC_M of NaDS/NaOBS mixtures (10.0 mM) corresponding to its supersaturation ratio at 30°C.

[NaS], M	[CaCl ₂], M	S_0 (DS)	S_0 (OBS)	t_1	t_2	t_3	t_{ind} (avg)
0.01	0.001	3.58	2.34	Large	Large	Large	Large
	0.002	4.53	2.96	118	122	122	120.67
	0.003	5.13	3.36	48	51	45	48.00
	0.006	6.22	4.07	26	24	26	25.33
	0.01	7.04	4.61	20	21	21	20.67
0.02	0.003	2.11	1.71	Large	Large	Large	Large
	0.006	4.25	3.45	45	47	48	46.67
	0.01	5.47	4.43	15	18	20	17.67
0.03	0.003	1.22	1.11	Large	Large	Large	Large
	0.006	2.38	2.16	240	240	250	243.33
	0.01	4.14	3.75	28	26	26	26.67
0.04	0.003	1.00	0.97	Large	Large	Large	Large
	0.006	1.61	1.57	Large	Large	Large	Large
	0.01	2.86	2.79	62	64	58	61.33

Remark: Time (t_1 , t_2 , t_3 , and t_{ind}) in a unit of second.

Table C.13 The induction time of 25:75 NaDS/NaOBS molar ratio systems precipitating by CaCl_2 for the systems *below* the CMC_M of NaDS/NaOBS mixtures (11.4 mM) corresponding to its supersaturation ratio at 30°C.

[NaS], M	[CaCl ₂], M	S_0 (DS)	S_0 (OBS)	t_1	t_2	t_3	t_{ind} (avg)
0.003	0.0045	1.78	2.37	11	10	10	10.33
	0.012	2.22	2.96	10	11	11	10.67
	0.035	2.65	3.54	9	10	8	9.00
0.004	0.0045	2.14	2.86	10	11	10	11.33
	0.012	2.67	3.57	13	11	10	10.67
	0.035	3.20	4.28	10	12	10	10.33
0.005	0.00065	1.42	1.89	23	20	20	21.00
	0.0018	1.93	2.57	11	11	12	12.67
	0.004	2.39	3.20	9	10	10	11.33
	0.0085	2.87	3.83	13	13	12	9.67
	0.05	3.86	5.15	7	8	8	7.67
	0.10	3.98	5.32	1	1	1	1.00
0.006	0.00065	1.58	2.12	22	23	23	22.67
	0.0018	2.16	2.88	14	13	15	15.00
	0.004	2.69	3.59	12	12	12	14.00
	0.0085	3.23	4.31	16	14	15	12.00
	0.05	4.35	5.81	7	8	9	8.00
	0.10	4.49	6.00	1	1	1	1.00
0.008	0.001	2.15	2.88	19	17	19	18.33
	0.002	2.65	3.54	11	11	12	12.00
	0.003	2.98	3.97	11	9	10	11.33
	0.006	3.57	4.77	10	10	8	10.00
	0.01	4.02	5.37	11	13	12	9.33
0.01	0.001	2.46	3.29	25	22	24	23.67
	0.002	3.04	4.06	14	13	15	14.00
	0.003	3.41	4.56	13	12	11	13.00
	0.006	4.10	5.48	10	11	10	12.00
	0.01	4.63	6.19	14	12	13	10.33

Remark: Time (t_1 , t_2 , t_3 , and t_{ind}) in a unit of second.

Table C.14 The induction time of 25:75 NaDS/NaOBS molar ratio systems precipitating by CaCl_2 for the systems *above* the CMC_M of NaDS/NaOBS mixtures (11.4 mM) corresponding to its supersaturation ratio at 30°C.

[NaS], M	[CaCl ₂], M	S_0 (DS)	S_0 (OBS)	t_1	t_2	t_3	t_{ind} (avg)
0.02	0.003	1.56	2.55	19	17	20	18.67
	0.006	2.89	4.73	10	9	11	10.00
	0.01	3.64	5.96	1	1	1	1.00
0.03	0.003	0.79	1.46	160	145	150	151.67
	0.006	1.60	2.95	13	16	15	14.67
	0.01	2.70	4.97	9	8	9	8.67
0.04	0.003	0.62	1.25	Large	Large	Large	Large
	0.006	1.02	2.04	33	38	33	34.67
	0.01	1.84	3.68	11	11	10	10.67

Remark: Time (t_1 , t_2 , t_3 , and t_{ind}) in a unit of second.

APPENDIX D
LIST OF PUBLICATIONS
AND CONFERENCE PROCEEDINGS

Peer Reviewed Publication in Progress

Maneedaeng A., Haller K. J., Grady B. P., and Flood A. E., **Measurement and modeling of thermodynamic parameters in binary anionic surfactant systems and the effect of counterion binding to the micelle**, Journal of Colloid and Interface Science, in press.

Conference Proceedings

Maneedaeng A., Haller K. J., Grady B. P., and Flood A. E., **Modeling of induction time for the calcium salts of surfactants in pure and mixed surfactant system**, International Workshop on Industrial crystallization (BIWIC) 2010, Halle (Saale), Germany.

Maneedaeng A., Haller K. J., Grady B. P., and Flood A. E., **An explanation for the increased induction time when anionic surfactants are precipitated from mixed-surfactant solutions**, 9th International Workshop on Crystal Growth of Organic Materials (CGOM9) 2010, Singapore.

Maneedaeng A., Haller K. J., Grady B. P., and Flood A. E., **Precipitation of calcium dodecyl sulfate in hard water**, 17th International Symposium on Industrial Crystallization (ISIC17) 2008, Maastricht, The Netherlands.

Maneedaeng A., Flood A. E., Haller K. J., and Scamehorn J. F., **Temperature dependence of the solubility product of calcium dodecyl sulfate and modeling of the phase boundary**, International Workshop on Industrial crystallization (BIWIC) 2007, Cape Town, South Africa.

Maneedaeng A. and Flood A. E., **Measurement and modeling of the solubility of calcium dodecyl sulfate in aqueous solution**, 17th TIChE Meeting 2007, Chiang-Mai, Thailand.

Conference Abstracts

Maneedaeng A., Haller K. J., Grady B. P., and Flood A. E., **An investigation into inhibition of precipitation of mixed anionic surfactant systems**, 101st AOCS Annual Meeting & Expo 2010, Phoenix, Arizona, USA.

Maneedaeng A., Haller K. J., Grady B. P., and Flood A. E., **Measurement and modeling of thermodynamic parameters in binary anionic surfactant systems and the effect of counterion binding to the micelle**, RGJ Congress XI 2010, Chonburi, Thailand.

Maneedaeng A., Haller K. J., Grady B. P., and Flood A. E., **Precipitation of calcium dodecyl sulfate under the influence of sodium decyl sulfate in binary anionic surfactant systems**, 100th AIChE Annual Meeting 2008, Philadelphia, Pennsylvania, USA.

Maneedaeng A. and Flood A. E., **Measurement and modeling of the solubility of calcium dodecyl sulfate**, RGJ Congress VIII, 2007, Chonburi, Thailand.

9th International Workshop on Crystal Growth of Organic Materials (CGOM9)

Preferred field of presentation: Crystal science fundamentals

Prefer mode of presentation: Oral

An explanation for the increased induction time when anionic surfactants are precipitated from mixed-surfactant solutions

Atthaphon Maneedaeng¹, Kenneth J. Haller², Brian P. Grady³, and Adrian E. Flood¹

¹*School of Chemical Engineering, Suranaree University of Technology, Nakhon Ratchasima, 30000 Thailand.* ²*School of Chemistry, Suranaree University of Technology, Nakhon Ratchasima, 30000 Thailand.* ³*School of Chemical, Biological, and Materials Engineering, University of Oklahoma, Norman, Oklahoma, 73019 USA. adrainfl@sut.ac.th*

Precipitation of the calcium form of anionic surfactants is a significant problem when these surfactants are used in hard waters. It is well known that the use of mixed surfactant solutions can decrease the Krafft temperature and increase the hardness tolerance. Previous studies have shown that the apparent increase in hardness tolerance is partly due to a larger induction time in mixed-surfactant systems when compared to pure surfactant systems of the same total surfactant content. The current work has measured induction times (via turbidity measurement) for pure and mixed-surfactant systems involving sodium dodecylsulfate (NaDS), sodium decylsulfate (NaDeS), and sodium octylbenzene sulfonate (NaOBS) precipitated by calcium solutions. Activity based supersaturation ratios have been evaluated using a combination of thermodynamic models, including the solubility product of the calcium surfactants, regular solution theory for the critical micelle concentration (CMC) and composition of the micelle, and a new chemical equilibrium model for the extent of sodium and calcium counterion binding to the micelle. The results of the study show that the dependence of the induction time on the supersaturation ratio is the same both below and above the CMC, suggesting that the micelles do not have a role in the mechanism of nucleation. It is also seen that the dependence of the induction time on the supersaturation ratio is the same for all surfactant compositions (ratios of the precipitating surfactant to the co-surfactant) assuming that the same surfactant species is precipitating. Therefore, the increase in the induction time in mixed-surfactant systems is due to a decrease in the supersaturation ratio of these systems. However the decrease in the supersaturation ratio cannot be estimated only by considering the reduced concentration of the precipitating surfactant in the mixed system. When the surfactant composition changes many other features of the system also change, including the CMC, the micelle composition, and the amount of counterions (including calcium) bound to the micelle. All these parameters have a strong effect on the supersaturation ratio.

Keyword: Induction time, mixed surfactants, mixed micelles, counterion binding

Precipitation of Calcium Dodecyl Sulfate in Hard Water

A. Maneedaeng¹, Assoc. Prof. K. J. Haller², Prof. B. P. Grady³ and Assoc. Prof. A. E. Flood¹

¹School of Chemical Engineering, Suranaree University of Technology, Nakhon Ratchasima, 30000, Thailand. ²School of Chemistry, Suranaree University of Technology, Nakhon Ratchasima, 30000, Thailand. ³School of Chemical, Biological and Materials Engineering, The University of Oklahoma, Norman, Oklahoma 73019-1004, USA.

adrianfl@sut.ac.th

Surfactants precipitate with divalent cations in hard waters to form scum that inhibits the cleaning action and perception of washing effectiveness. It has been previously determined that using mixed surfactant systems inhibits precipitation of surfactant, but it is currently not known whether this inhibition is due to a change in the thermodynamics of the system, inhibition of nuclei formation, or inhibition of crystal growth. A previous study has modeled the precipitation phase boundary for CaDS_2 from 10 to 50°C using a model involving the equilibrium between precipitate, micelles, and individual species in solution. The induction time for nucleation has been determined for CaDS_2 , and it can be seen that the induction time is far smaller for solutions with a surfactant concentration above the critical micelle composition (CMC) than for solutions below this point. This can be understood as the micelles in solution, which contain both a high concentration of surfactant molecules in a structured form and bound calcium ions in significant amounts, acting as a template for nucleation of the precipitate. Precipitation rates for CaDS_2 demonstrate that the key kinetic feature of the precipitation is the induction time for nucleation: nucleation rates at the point of induction are sufficiently high that the crystal growth kinetics do not play a significant role in the overall time required for complete precipitation. Finally, induction times for mixed surfactant systems demonstrate that the mechanism of inhibition appears to be related to the reduced influence of the mixed-micelle (as compared to the pure micelle in the single surfactant system). The mixed micelle contains species of both surfactants, present in solution at mole fractions determined via the regular solution theory, and therefore the mixed micelles appear to be less effective as nucleation inhibitors.

1. Introduction

Anionic surfactants are widely used in detergency applications, but may have problems in hard water due to precipitation caused by multivalent cations. If a single anionic surfactant is added to hard water the calcium salt of the surfactant will precipitate rapidly, reaching equilibrium within a few minutes, a property which is certainly undesirable in detergency applications. It has been found that mixtures of surfactants containing a similar or even greater level of total surfactant can remain un-precipitated for substantial periods of time. Although this property is widely used in industrial applications, quantified reasons for the behavior are not found in the scientific literature, and the mechanism for the behavior is not well understood. For this reason, detergent manufacturers find it necessary to add binders to commercial detergents, which allow them to be used in hard waters: a better understanding of the inhibition of precipitation in mixed surfactant systems could allow a reduction in the amount of binder added or improved detergent formulations.

It could be hypothesized that the inhibition of precipitation of mixtures of anionic surfactants (in comparison to a pure surfactant mixture at the same total surfactant content) may be due to one or more of four mechanisms: (1) The state of the less soluble surfactant has been changed to less than its saturation point due to a relative reduction in its concentration, while the more soluble surfactant has not been added in sufficient amounts to reach its saturation point; (2) The state of the less soluble surfactant has been changed to less than

its saturation point due to a change in solution properties of the surfactant mixture (in particular the value of the critical micelle concentration CMC), while the more soluble surfactant has not been added in sufficient amounts to reach its saturation point; (3) Nucleation of the less soluble surfactant has been inhibited by the presence of the second surfactant, either due to adsorption of an impurity onto pre-nuclei clusters, or due to the properties of the mixed micelle (if the system is above the CMC); (4) Inhibition of crystal growth due to adsorption of the more soluble surfactant onto the crystal surface of the less soluble surfactant, such that surfactant crystals nucleate but do not grow large enough to be detected in the solution for extended periods of time. The current study is an attempt to clarify the mechanisms of the inhibition of precipitation in mixed-anionic surfactant systems and, if multiple mechanisms exist, to quantify the significance of each of the mechanisms.

To understand the kinetics in a precipitation system it is first necessary to be able to quantify the precipitation phase boundaries. The phase boundaries in systems involving surfactants is more complex than in typical precipitation systems due to the presence of micelles in the solution when the surfactant concentration is above the CMC. Below the CMC, all ions will be in the unbound state and the phase boundary can be accurately modeled using the activity based solubility product (K_{SP}) and the extended Debye-Hückel activity coefficient model.

$$K_{SP} = [S^-]^2 \gamma_s^2 [Ca^{2+}] \gamma_{Ca}$$

Above the CMC, some fraction of the surfactant is in the form of micelles and is thus not available for the precipitation. In addition, the micelle binds to its surface not only sodium ions added with the surfactant, but also some of the calcium ions in solution, thus also removing these ions from participation in the precipitation. In this case the model for the solubility product must account for only the surfactant in monomer form in solution, and the calcium ions which are not bound to the micelle. Thus

$$K_{SP} = [S_{mon}^-]^2 \gamma_s^2 [Ca_{unb}^{2+}] \gamma_{Ca}$$

The extended Debye-Hückel model used is

$$\log \gamma = \frac{-A(z)^2 \sqrt{I}}{1 + Ba\sqrt{I}} - 0.3I$$

With A, B, and a being temperature, solvent, and species dependent constants, and the ionic strength depending on the ion concentrations and valences by

$$I = 0.5 \sum_i c_i z_i^2$$

In order to calculate the concentration of monomeric surfactant it is necessary to know the CMC, which may be calculated from the equation below if the unbound calcium ion concentration is small enough as to not affect the CMC.

$$\ln [DS^-]_{mon} = -K_1 - K_g \ln [Na_{unb}^+]$$

K_1 may be determined from the CMC of pure SDS in water, since at the CMC the unbound sodium ion concentration is equal to the concentration of the monomeric surfactant. The CMC of SDS has been measured by da Silva *et al.* [DAS04]. The counterion binding coefficients are defined as

$$\beta_{Ca^{2+}} = 2 [Ca_b^{2+}] / [DS_{mic}^-]$$

$$\beta_{Na^+} = [Na_b^+] / [DS_{mic}^-]$$

An earlier study [STE89] gave these values as 0.2 and 0.45 respectively. If there is more than one anionic surfactant in solution then the micelles will contain some proportion of both surfactants, and it is necessary to model the mixed micelles to accurately predict the concentration of the monomer surfactants in the solution. The regular solution theory is able to accurately predict the composition of the micelles in mixed micelle systems if the types of surfactant present do not differ to a great extent. In such a system, precipitation will occur when the solubility product of the least soluble surfactant is exceeded. In most systems the solubility of the two surfactants differs appreciably, and therefore there is no mixed precipitate formed. Examples of the ability of the model to fit experimentally determined precipitation boundaries are given in [ROD01]. Further discussion of, and extensions to this model are given in a series of articles from the group of Scamehorn, for instance [ROD98].

2. Experimental Section

Analytical Reagent (AR) grade surfactants (sodium dodecylsulfate [SDS], sodium decylsulfate [SDeS], and sodium octylbenzenesulfonic acid [SOBS]) were purchased and used without further purification for induction time measurements. Structures (in the sodium form) of the surfactants used are shown in Figure 1.

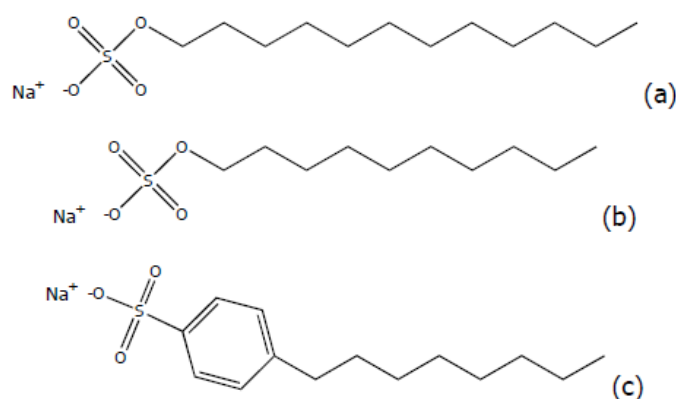


Figure 1: Chemical structures of the surfactants used: (a) sodium dodecylsulfate (SDS); (b) sodium decylsulfate (SDeS); (c) sodium octylbenzenesulfonate (SOBS).

For measurements of K_{SP} the surfactants were three times recrystallized into the calcium form of the surfactant, which is the species precipitating in the system, before being used to measure the equilibrium state from both above and below the equilibrium. Concentrations were measured using atomic absorption spectroscopy (AAS) and induced coupled plasma optical emission spectroscopy (ICP-OES).

Induction time experiments were performed by mixing stock solutions of the surfactants and CaCl_2 , and measuring the time at which nucleation could be detected by visual observation. Nucleation was observed between minutes and hours after mixing of the stock solutions, and the onset of nucleation could be easily observed visually. Modeling of the phase boundary and prediction of the supersaturation ratio was performed using the models shown in the Introduction section and the papers cited therein.

3. Results and Discussion

The study is designed to investigate the effect of using both similar mixed surfactants (SDS and SDeS, which have both similar head groups and tail groups, with a difference in chain length of two carbons), and different types of mixed surfactant (SDS and SOBS, which differ both in their head groups, sulfate vs sulfonate, and their tails, since SOBS is not a straight chain) in order to increase the induction time for precipitation, or to increase the hardness tolerance.

The solubility product for SDS has been measured from below 10°C to above 50°C, and this can be used with thermodynamic data on the micellization of the surfactant and the extended Debye-Hückel activity coefficient model to predict phase boundaries for the aqueous SDS-CaCl₂ system, as shown in Figure 2. This type of diagram is often called a hardness tolerance, because it shows the degree of water hardness that a surfactant mixture can tolerate before it would form a precipitate under equilibrium conditions. As a second anionic surfactant (such as SDeS or SOBS) is added to the system in small amounts the precipitation phase boundary for SDS moves up slightly (i.e. a particular SDS concentration can tolerate higher concentrations of Ca²⁺ without precipitating), but this change is initially very small. As the amount of the second surfactant increases significantly (for instance becoming larger than the amount of SDS) then the amount of Ca²⁺ that SDS can tolerate becomes very large (principally because the CMC of the solution decreases). However at some point the higher content of the second surfactant means that it approaches or exceeds its own precipitation phase boundary, and thus it will precipitate. Thus, the phase boundary of both surfactants in the mixture must be known, and where one of the surfactants has a supersaturation ratio greater than one, this surfactant will precipitate if the system is left long enough to reach equilibrium. Whether the system precipitates within a finite period of time, for instance within the period required for detergency and before the surfactant is removed from the application depends on the induction time for the precipitation, and this becomes a key point for the system.

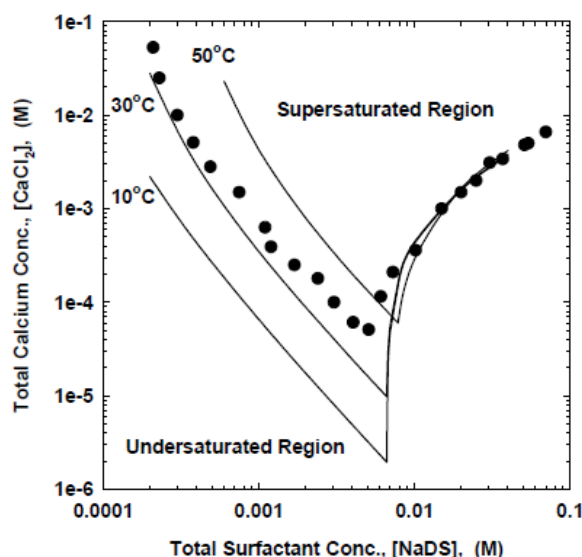


Figure 2: The precipitation phase boundary for SDS in aqueous solutions of CaCl₂ at 30°C (●), and predicted precipitation phase boundaries at 10, 30, and 50°C.

Induction times for the precipitation of various binary mixtures of surfactants (SDS+SDeS, SDS+SOBS, in addition to pure SDS) in solutions containing CaCl_2 were measured through visual observation of the time required between mixing and nucleation. Results are shown in Figure 3.

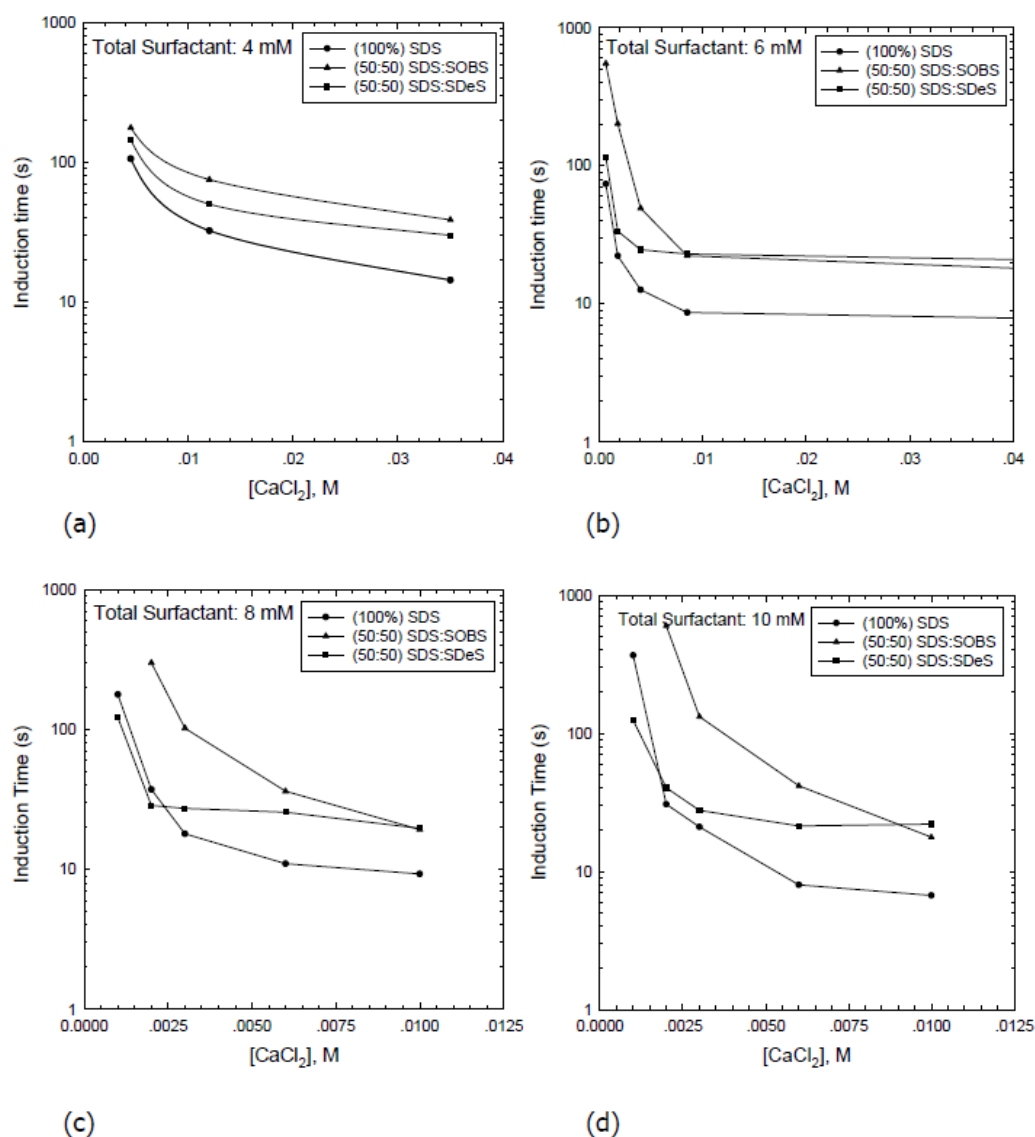


Figure 3: Induction times for various mixed surfactant systems: SDS, SDS+SDeS, and SDS+SOBS. Total surfactant content equal to (a) 4 mM; (b) 6 mM; (c) 8 mM; and (d) 10 mM. Values of extremely high induction times or large calcium content have been excluded in order to present the data more clearly.

The four plots relating the induction time to the calcium content each have a constant total amount of surfactant, from 4 mM, which is below the CMC for the pure dodecylsulfate

system, to 10 mM which is above the CMC for the pure dodecylsulfate system. The induction times for constant surfactant content are strongly dependent on the hardness of the water, as high calcium contents lead to higher values of the supersaturation ratio. The measured induction times are over three orders of magnitude: at very low levels of the supersaturation ratio the induction times are in the order of one hour, where at high levels of supersaturation the induction times are of the order of one second.

The results show a clear effect of both whether the surfactant is pure or a mixture of surfactants, and the surfactants present in the mixture for the mixed systems. The induction times for the pure SDS systems is the lowest for essentially all hardness values and total surfactant contents, as was expected based on previous experience. The similar surfactant SDeS inhibited the nucleation of SDS to some extent, but the largest induction times were found in the system of SDS+SOBS. Since the crystallization is very rapid in these systems, it is likely that the tail groups in the precipitate are not fully crystalline. This may allow SDS and SDeS to form essentially solid solutions in the crystal phase since the head groups are identical and the tail groups are very similar. In this case it may be expected that SDeS may have a weaker inhibition of the precipitation of SDS. It also can not be excluded that SDeS causes a small change in the CMC of the SDS, leading to lower supersaturation for the same total surfactant content. The inhibition exists both above and below the CMC of the pure dodecylsulfate system, so it is clear that the effect is not solely due to the effect of the mixed micelles on the nucleation of the precipitate.

It is also necessary to model the differences in the phase boundary as the second surfactant is added into the system. This is a relatively complex behaviour because it is not only necessary to model the effect of the additional ions on the ionic strength and the activity coefficients, it is also necessary to model how the added surfactant changes the CMC of the precipitating surfactant, how the counterion binding on the micelle changes, and what the composition of the micelle is. Because of the similarity in the molecules, the mixed micelles of SDS and SDeS will be almost ideal: the composition of the micelle will be very close to the composition of the liquid phase it is in equilibrium with. This is not true for the SDS+SOBS, which will have a larger nonideality in the micelle phase, and therefore removes surfactant monomers from the liquid phase at a different composition than the bulk. It can be noted that the behaviour of the SDS+SDeS system is quite different from the pure SDS and the SDS+SOBS systems at 8 and 10 mM total surfactant, with the induction time decreasing rapidly before becoming essentially constant at a low hardness value. This may be due to a change in the CMC of the system due to the addition of the SDeS, but this has not yet been verified.

4. Conclusions

The current work is an initial work to understand the mechanism by which the use of mixed anionic surfactants inhibits the precipitation of the surfactant in hard waters. It is possible to model the complex equilibria in the system, which has equilibria between the crystal, solution, and micelle phases. Induction time measurements have indicated that the use of mixed surfactants can increase the induction time substantially, and that the largest increase appears to occur where the surfactants used in the mixture have substantially different features. Further research will use both measurements and models of the precipitation phase boundary in the mixed surfactant systems to predict the dependence of the induction time on the supersaturation ratio for various surfactant compositions in order to further elucidate the mechanism of the inhibition. A complete understanding of this behaviour will assist in determining optimum surfactant formulations for detergency applications in hard waters.

5. Nomenclature

A	Parameter in the extended Debye-Huckel activity coefficient model
a	Ion size parameter in the extended Debye-Huckel activity coefficient model
B	Parameter in the extended Debye-Huckel activity coefficient model
c	Total molar concentration of a species, [M]
I	Ionic strength in the liquid phase, [M]
K_1	Parameter in the model of the CMC
K_g	Parameter determining the effect of the unbound sodium content on the CMC
K_{sp}	Activity based solubility product of a crystalline species
$[X]$	Concentration of species X in solution, [M]
z	Valence of an ion, [-]

Greek

β	Coefficient for the binding of ions onto the micelle, [-]
γ	Activity coefficient of a species, [-]

Subscripts

(aq)	Aqueous phase species
(s)	Crystalline phase species
b	Ion bound to the micelle
mic	Surfactant molecule in the micellar phase
mon	Monomeric surfactant molecule in the liquid phase
unb	Ion that is not bound to a micelle

6. References

[DAS04] da Silva, R.C., Loh, W., Olofsson, G. Calorimetric investigation of temperature effect on the interaction between poly(ethylene oxide) and sodium dodecylsulfate in water. *Thermochimica Acta* (2004) 417, 295-300

[ROD01] Rodriguez, C.H., Scamehorn, J.F. Kinetics of precipitation of surfactants. II. Anionic surfactant mixtures. *J. Surf. Det.* (2001) 4, 15-26

[ROD98] Rodriguez, C.H., Chintanasathien, C., Scamehorn, J.F., Saiwan, C., Chavadej, S. Precipitation in solutions containing mixtures of synthetic anionic surfactant and soap. I. Effect of sodium octanoate on hardness tolerance of sodium dodecyl sulfate. *J. Surf. Det.* (1998) 1, 321-328

[STE89] Stellner, K.L., Scamehorn, J.F. Hardness tolerance of anionic surfactant solutions. I. Anionic surfactant with added monovalent electrolytes. *Langmuir* (1989) 5, 70-77

Acknowledgements

The authors acknowledge the support of the Thailand Research Fund through the Royal Golden Jubilee Ph.D. program, grant no. 1.C.TS/47/B.1.

Temperature Dependence of the Solubility Product of Calcium Dodecyl Sulfate and Modeling of the Phase Boundary

A. Maneedaeng¹, A. E. Flood^{1*}, K. J. Haller², J. F. Scamehorn³

¹School of Chemical Engineering, Suranaree University of Technology, Nakhon Ratchasima 30000, Thailand, ²School of Chemistry, Suranaree University of Technology, Nakhon Ratchasima 30000, Thailand, ³Institute for Applied Surfactant Research, University of Oklahoma, Norman, Oklahoma 73019, USA
adrianfl@sut.ac.th

In hard water, dodecyl sulfate (DS) tends to precipitate with the counterions, Ca^{2+} and Mg^{2+} forming soap scum, and is thus no longer available to participate in the cleaning action. The scum formed from the precipitation is also a problem in that it causes graying of the fabric. Solubility data of the precipitated calcium dodecyl sulfate (CDS) crystals remains quite limited. Consequently, this work has investigated the activity-based solubility product of CDS in aqueous solutions as a function of temperature, with modeling between 10°C and 55°C. Two techniques of measuring the solubility were used. Below the Krafft temperature, approximately 50°C for CDS, the solutions were saturated at fixed temperatures and then analyzed using Atomic-Absorption Spectroscopy. Above the Krafft temperature a conductivity technique was used. Plotting the conductivity of a fixed concentration solution against temperature allows the solubility to be found from a discontinuity in the derivative. The activity-based solubility product, K_{SP} , was calculated from the experimental data based on modeling of the micellar phase in solutions for the samples which were above the critical micelle concentration. Both techniques for measuring the solubility of CDS yield consistent values of the solubility product, which can be used to model the phase boundary of CDS precipitation in solutions of sodium dodecyl sulfate (SDS) and calcium chloride as a function of temperature.

1. Introduction

Sodium dodecyl sulfate is one of the most commonly used anionic surfactants, and is present in a wide variety of household products and detergents. Anionic surfactants have a tendency to precipitate in aqueous solution, particularly if they are used in hard water (water containing multivalent cations such as Ca^{2+} or Mg^{2+}), forming soap scum. Precipitation of soap scum reduces the amount of surfactant available for cleaning and causes discoloration of the material being cleaned. Manufacturers of detergents generally add builders to their products in order to reduce the water hardness by either chelating or adsorbing the multivalent cations. However the thermodynamic and kinetic parameters involved in the precipitation process of the soap scum, and in particular the precipitation boundary as the surfactant is mixed with hard water is still extremely important. Despite this, data on the precipitation boundaries for surfactants is limited, particularly in relation to the effect of temperature. The objective of the current work is to extend knowledge of the precipitation boundaries for CDS through accurate measurement of the K_{SP} value for CDS over the range 10 to 55°C, and to use the model of Stellner and Scamehorn [1] to predict the precipitation boundary of CDS in solutions of SDS and CaCl_2 .

2. Theory

The material presented here is a concise summary of theory already presented in papers such as Stellner and Scamehorn [1] and Rodriguez *et al.* [2]. Surfactants in a liquid phase may appear as monomeric surfactant or as aggregates known as micelles. Below the critical

micelle concentration (CMC) only the monomeric form will be evident, and thus the precipitate is in equilibrium with monomeric surfactant molecules and free calcium ions. Above the CMC there is an equilibrium between the monomeric surfactant and micelles, with the concentration of monomeric surfactant being equal to the CMC. Since the surfactant molecules in an anionic surfactant micelle are negatively charged, cations will be bound to the hydrophilic surface of the micelle in order to partially negate the negative charge at the surface. Therefore in a solution above the CMC the precipitate is in equilibrium both with the micelles and with the monomeric surfactant and the unbound calcium ions. The precipitation reaction is represented by



Only the unbound calcium ions and the monomeric surfactant molecules take part in the precipitation reaction so that the activity based solubility product is given by

$$K_{SP} = [\text{Ca}^{2+}]_{\text{unb}} [\text{DS}^{-}]_{\text{mon}}^2 \gamma_{\text{Ca}^{2+}} \gamma_{\text{DS}^{-}}^2 \quad (2)$$

In order to calculate the concentration of monomeric surfactant it is necessary to know the CMC, which may be calculated from equation (3) if the unbound calcium ion concentration is small enough as to not affect the CMC.

$$\ln [\text{DS}^{-}]_{\text{mon}} = -K_1 - K_g \ln [\text{Na}^{+}]_{\text{unb}} \quad (3)$$

K_1 may be determined from the CMC of pure SDS in water, since at the CMC the unbound sodium ion concentration is equal to the concentration of the monomeric surfactant. The CMC of SDS has been measured by da Silva *et al.* [3]. The data for the CMC of SDS in water and the parameter K_1 are shown in Figure 1.

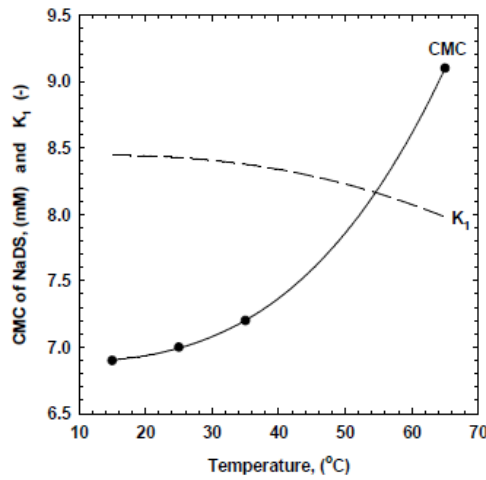


Fig. 1: The CMC [3] and parameter K_1 for SDS in water.

In the absence of other species (apart from SDS and CaCl_2) we may perform balances on the surfactant, and sodium and calcium ions to obtain

$$[\text{NaDS}] = [\text{DS}^{-}]_{\text{mon}} + [\text{DS}^{-}]_{\text{mic}} \quad (4)$$

$$[\text{NaDS}] = [\text{Na}^{+}]_{\text{unb}} + [\text{Na}^{+}]_{\text{b}} \quad (5)$$

$$[\text{CaCl}_2] = [\text{Ca}^{2+}]_{\text{unb}} + [\text{Ca}^{2+}]_{\text{b}} \quad (6)$$

The concentrations of the bound sodium and calcium concentrations can be calculated from the micelle binding coefficients

$$\beta_{\text{Ca}^{2+}} = 2[\text{Ca}^{2+}]_{\text{b}} / [\text{DS}^{-}]_{\text{mic}} \quad (7)$$

$$\beta_{\text{Na}^{+}} = [\text{Na}^{+}]_{\text{b}} / [\text{DS}^{-}]_{\text{mic}} \quad (8)$$

An earlier study [1] gave these values as 0.2 and 0.45 respectively.

The previous equations must be solved simultaneously since the monomer concentration is determined via the CMC value, which depends on the concentration of unbound sodium ions. The concentration of unbound sodium ions depends on the amount of ions bound to the micelles, which depends on the concentration of surfactant present in micelles, which in turn depends on the CMC value.

The remaining equations required are to predict the activity coefficients of the ions present in the crystal phase. These may be predicted by the extended Debye-Huckel model [4]

$$\log \gamma = \frac{-A(z)^2 \sqrt{I}}{1 + Ba\sqrt{I}} - 0.3I \quad (9)$$

which is able to determine the activity coefficient of either ion. The constants A and B depend on the temperature and the solvent while the parameter a depends on the diameter of the ion. These values can be found in standard texts [4]. The ionic strength, I , is determined from

$$I = \sum_i c_i z_i^2 = [\text{NaDS}] + 3[\text{CaCl}_2]$$

Further discussion of, and extensions to this model are given in a series of articles from the group of Scamehorn [1], [2], [5], [6].

3. Materials and Methods

Crystal Preparation. CDS was prepared from the precipitation of sodium dodecyl sulfate with calcium chloride. The crystals were separated by a 0.45 μm cellulose nitrate membrane and rinsed with deionized water. After drying by silica gel under room temperature overnight, CDS was then recrystallized in water. The pure CDS was separated by filtration and dried at room temperature with silica gel. Dry CDS crystals were used to prepare a number of solutions in deionized water.

Solubility Measurements. CDS behaves like a conventional anionic surfactant which leads to two techniques of measuring the solubility, measuring concentrations (by AAS) for saturated solutions at fixed temperatures, or measuring the conductivity of fixed concentration solutions as the temperature is varied to search for the saturation temperature. Which method is more convenient depends on whether the system is above or below the Krafft temperature, the minimum temperature at which surfactants form micelles. The Krafft temperature of CDS is 50°C [7].

The AAS method was used below the Krafft temperature. A series of CDS solutions were prepared at varying saturation temperatures ranging from from 10 to 50°C. Additional solutions at 51, 53, and 55°C were prepared to verify the consistency of the two techniques. AAS was used to measure the concentration of calcium ions in the solutions; the total amount of surfactant can be estimated using the stoichiometric ratio of calcium ion to surfactant monomer. Solubilities were reported at the saturation temperature. The concentration was determined three times for each batch and three batches were performed per saturation temperature. The replicates show that the experimental data are highly reproducible.

Conductometry was used to measure the solubility above the Krafft temperature by determining the saturation temperature of known concentration solutions at 0.5, 3, 4, 6, 8, and 10 mM. The equilibrium temperature was determined by measuring the conductivity of a surfactant solution as a function of temperature. The concentration at the point that the slope is discontinuous is the saturation temperature for the concentration measured.

4. Results and Discussion

The results of the solubility study using AAS to measure saturation concentrations at fixed temperature are shown in Table 1. Further experiments were performed on solutions from 0.5 to 10 mM CDS to determine the saturation temperature using measurements of conductivity. The K_{SP} values as a function of temperature were calculated using the results of the two methods, and the results are shown in Figure 2. The agreement between the two techniques is excellent except for one value predicted using the conductivity technique at 42°C. At this point (which is well below the Krafft temperature) the change in the slope at the saturation point is very small, and therefore the relative error is quite large. The main improvements to the knowledge of the system gained from this study are that (a) it can be seen that two totally independent measurements can give consistent results for the K_{SP} ; (b) the K_{SP} value is now

known over a wide range of temperature; (c) the K_{SP} value has been measured in pure CDS solutions where the effects of other ions have been removed (which will lower the ionic strength of the solution and therefore increase the accuracy of the activity coefficient model); (d) the K_{SP} predicted here is a measured property rather than a property determined by fitting to a boundary.

Table 1. Total calcium ion concentration at saturation using the AAS technique.

Temperature (°C)	Dilution for AAS	Concentration of Ca^{2+} (mM)
10.0	1:10	0.2529
15.0	1:10	0.2554
20.0	1:10	0.3184
25	1:10	0.3520
30	1:10	0.4411
35	1:10	0.5233
40	1:25	0.5760
45	1:25	0.7122
50	1:25	0.9217
51	1:25	1.0794
53	1:25	1.1290
55	1:2000	19.4620

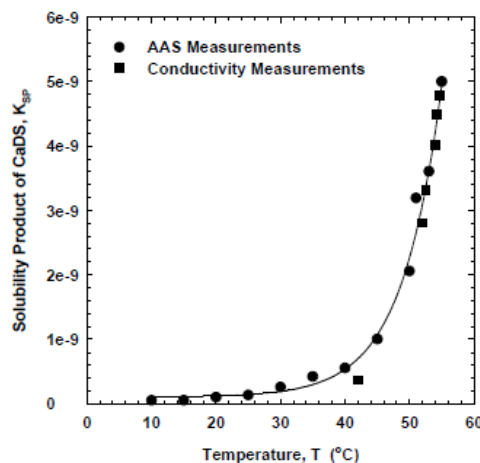


Fig. 2: Solubility product of CDS as a function of temperature.

The data in Figure 2 gives the solubility product, K_{SP} , as a function of temperature, which can be used with the model discussed in the theory section to model the precipitation phase boundary for solutions containing SDS and CaCl_2 . This calculation has already been performed at 30°C [1], however in this previous study the K_{SP} value was determined by regression over all of the data below the CMC in order to minimize the error between the experimental precipitation boundary and the model. While this is a reasonable approach to obtain an accurate empirical model of the system, it is useful to determine the most accurate possible value of K_{SP} to determine the fundamental accuracy of the model, and this can be achieved conveniently through determination of the solubility of pure CDS in water, as described above.

Figure 3 shows the precipitation phase boundary for solutions of SDS and CaCl_2 , where the abscissa displays the *total* SDS in the system and the ordinate plots the *total* calcium ion concentration required to reach the phase boundary. Although the model using the measured value of K_{SP} does not fit the measured phase boundary (re-plotted from data in [1]) as well as the model with the fitted K_{SP} , the fit is acceptable, especially where the SDS concentration is very low and in the region above the CMC. The difference is a clear consequence of comparing a partially fitted model to one that is not fitted. The model can be extended to cover the range of 10 to 55°C (the range in which the K_{SP} has been measured) and the result is shown in Figure 4.

As mentioned previously [1] below the CMC the system displays typical behavior for precipitation of an electrolyte: as the concentration of one of the ions increases, the concentration of the other ion required to reach the precipitation boundary decreases. However, above the CMC the amount of CaCl_2 required to reach the phase boundary increases even as the total concentration of SDS increases. This is due to the formation of micelles, which has several effects on the 'free' ions in the system.

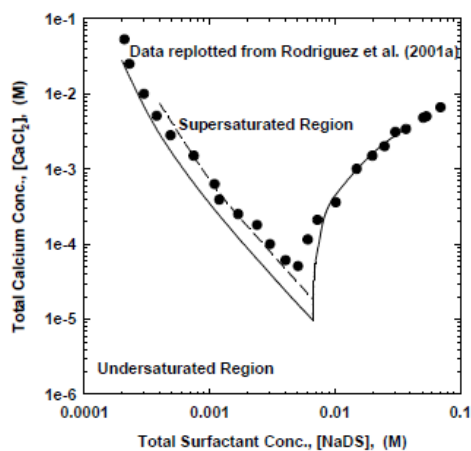


Fig. 3: Precipitation boundary for CDS at 30°C, including the model of the boundary. The dashed line is the model from [1].

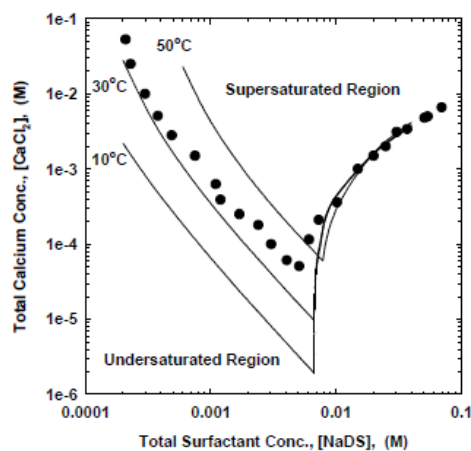


Fig. 4: Precipitation boundary for CDS at 10, 30, and 50°C predicted from the K_{SP} and micellization model.

At the CMC the concentration of monomeric DS^- in the system stops increasing with increasing SDS since the additional surfactant forms micellar aggregates. As additional sodium ions are added to the system the CMC decreases (see equation 3) which results in a decreased concentration of DS^- monomers. As the concentration of micelles increases the amount of cations bound to the micelles also increases. An increase in the micelle concentration results in the concentration of unbound sodium ions not increasing as rapidly with increasing SDS content as below the CMC, and more significantly the concentration of unbound calcium ions (required in the precipitation) decreasing rapidly due to counterion binding onto the micelles. Results of the model predictions of the concentrations of the significant ions are shown in Figure 5 for total $CaCl_2$ concentrations of 0.001 (a) and 0.0001 M (b).

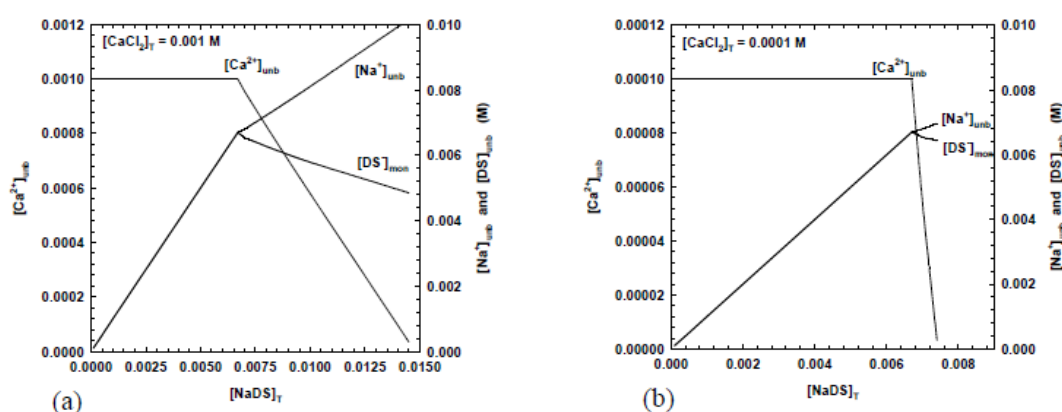


Fig. 5: Concentrations of the key species in the precipitation of CDS as a function of the total SDS concentration at 30°C. (a) 0.001 M $CaCl_2$; (b) 0.0001 M $CaCl_2$.

When the total $CaCl_2$ concentration is relatively high, for instance 1 mM (Figure 5a) then the concentration of unbound calcium ions decreases relative slowly as the SDS concentration

increases because a significant concentration of micelles is necessary to bind a significant fraction of the large number of ions present. The unbound calcium ion concentration stays relatively high over a range of SDS concentrations above the CMC, and the monomeric surfactant ion concentration also decreases relatively slowly, so the system is above the precipitation boundary for a large range of SDS concentrations from well below the CMC to far above the CMC for 1 mM CaCl_2 , which is evident in Figure 3.

When the CaCl_2 concentration is low, for instance 0.1 mM (Figure 5b) the concentration of unbound calcium ions decreases very rapidly as the system moves above the CMC, and thus the system will rapidly move out of the supersaturated region as the SDS concentration is increased above the CMC. At the CMC the concentration of surfactant molecules is almost two orders of magnitude larger than the concentration of calcium ions, and thus even for a small increase in SDS above the CMC the concentration of the surfactant in the micelles will be ten times the concentration of the calcium ions in solution. At this point the concentration of free calcium ions will be zero since the binding coefficient for the calcium ions is 0.2, representing one Ca^{2+} ion bound for every ten DS^- molecules in the micelle, a charge negation fraction of 0.2. Thus, very small increases in SDS concentration above the CMC result in soaking up the unbound calcium ions required in the precipitation reaction, and the system quickly moves out of the supersaturated region, as demonstrated in Figure 3.

5. Conclusions

The research has accurately measured the K_{SP} value of calcium dodecyl sulfate over the temperature range of 10 to 55°C using two techniques, measuring the amount of CDS required to reach saturation at constant temperature with AAS and measuring the saturation temperature of constant composition solutions of CDS using conductivity measurements. The conductivity measurement is convenient and accurate for solutions whose solubility is in excess of the Krafft temperature, but has lower accuracy below the Krafft temperature because the point of discontinuity in the slope of the conductivity curve is more difficult to accurately determine under these conditions. The solubility of CDS is very high at and above the Krafft temperature, and under these conditions the solutions require very high dilution ratios to enable measurement by AAS. This indicates that it is useful to use a combination of techniques in measurement of the solubility of surfactant systems, and the current study has shown that the two methods do give consistent results. The K_{SP} in this system exponentially increases with increasing temperature, resulting in the K_{SP} at 55°C being orders of magnitude than the value at 10°C.

The precipitation phase boundary for CDS in solutions of SDS and CaCl_2 can be predicted by a model that contains equations for the phase equilibrium between monomeric surfactant and unbound calcium ions, essentially the K_{SP} as a function of temperature, the activity coefficients of the key species as a function of temperature and ionic strength, and models that predict the micellization parameters, such as monomeric surfactant concentration as a function of temperature and ion concentrations, and also ion binding to the micelle. The constant relating to the temperature effect on the concentration of monomer surfactant (K_1) is known over the temperature range of interest, however the constant reflecting the effect of the unbound sodium ion concentration has been measured at 30°C only. It is reasonable to assume that this parameter is not significantly altered by a 20°C change in temperature, in which case the model is completely characterized over the temperature range of interest.

The fit of the model using a K_{SP} value determined from experiments of pure CDS in water gives a slightly worse fit to an experimental precipitation boundary compared to an earlier model where the K_{SP} value was predicted *a-posteriori* from the precipitation phase boundary of CDS in solutions containing SDS and CaCl_2 . This is to be expected since fundamentally measured parameters can never improve a fit to a model in comparison to models using parameters fitted to the data. The two models fit the data equally above the CMC in the

system, where the model for the micelle formation and counterion binding is dominant in determining the total amounts of SDS and CaCl_2 present in the system required to form precipitates. Below the CMC the only modeling required is that for the K_{SP} value and the activity coefficients, and it is here that the model fitting is not as good. It may be noted that the K_{SP} value measured at 30°C is only 2.60×10^{-10} in comparison to the value predicted from the phase boundary which is 5.02×10^{-10} . The current model fits dilute SDS data quite well, but becomes less accurate as the system approaches the CMC value, and becomes more concentrated in SDS. There may be several reasons for this reduction in fitting ability as the SDS concentration becomes higher, but perhaps the most likely reason is that the extended Debye-Huckel model may be unable to accurately determine the effect of the ionic strength on the activity of the surfactant monomer ion. This has been suggested previously [8] in sub-micellar solutions of sodium alkyl sulfates where deviations from the Debye-Huckel theory were noted, and possibly explained by variations in the hydrophobic hydration of the alkyl chains as the surfactant content increased. It may be necessary to determine more accurate models for activity coefficients for surfactants.

6. Nomenclature

A	Parameter in the extended Debye-Huckel activity coefficient model
a	Ion size parameter in the extended Debye-Huckel activity coefficient model
B	Parameter in the extended Debye-Huckel activity coefficient model
c	Total molar concentration of a species, [M]
I	Ionic strength in the liquid phase, [M]
K_1	Parameter in the model of the CMC
K_g	Parameter determining the effect of the unbound sodium content on the CMC
K_{SP}	Activity based solubility product of a crystalline species
[X]	Concentration of species X in solution, [M]
z	Valence of an ion, [-]

Greek

β	Coefficient for the binding of ions onto the micelle, [-]
γ	Activity coefficient of a species, [-]

Subscripts

(aq)	Aqueous phase species
(s)	Crystalline phase species
b	Ion bound to the micelle
mic	Surfactant molecule in the micellar phase
mon	Monomeric surfactant molecule in the liquid phase
unb	Ion that is not bound to a micelle

7. References

- [1] Stellner, K. L. and Scamehorn, J. F. Hardness Tolerance of Anionic Surfactant Solutions. 1. Anionic Surfactant with Added Monovalent Electrolyte. *Langmuir* **5** (1989) 70-77.
- [2] Rodriguez, C. H., Lowery, L. H., Scamehorn, J. F. and Harwell, J. H. Kinetics of Precipitation of Surfactants. 1. Anionic Surfactants with Calcium and with Cationic Surfactants. *J. Surfact. Deterg.* **4**(1) (2001) 1-14.
- [3] da Silva, R. C., Loh, W. and Olofsson, G. Calorimetric Investigation of Temperature Effect on the Interaction between Poly(ethylene oxide) and Sodium Dodecylsulfate in water. *Thermochimica Acta* **417** (2004) 295-300.

- [4] Klotz, I. R. and Rosenberg, R. M. *Chemical Thermodynamics: Basic Theory and Methods*. 6th Edition. John Wiley and Sons, New York, USA, 2000.
- [5] Stellner, K. L. and Scamehorn, J. F. Hardness Tolerance of Anionic Surfactant Solutions. 2. Effect of Added Nonionic Surfactant. *Langmuir* **5** (1989) 77-84.
- [6] Rodriguez, C. H. and Scamehorn, J. F. Kinetics of Precipitation of Surfactants. 2. Anionic Surfactant Mixtures. *J. Surfact. Deterg.* **4**(1) (2001) 15-26.
- [7] Lee, R. S., and Robb, I. D. Precipitation of Calcium Surfactants: Part 2. *J. Chem. Soc., Faraday Trans. 1* **75** (1979) 2116-2125.
- [8] Birch, B. J. and Hall, D. G. Heats of Dilution of Sub-Micellar Aqueous Surfactant Solutions. *J. Chem. Soc., Faraday Trans. 1* **68** (1972) 2350-2355.

Acknowledgements

The authors acknowledge the support of the Thailand Research Fund through the Royal Golden Jubilee Ph.D. program, grant no. 1.C.TS/47/B.1.

Measurement and Modeling of the Solubility of Calcium Dodecyl Sulfate in Aqueous Solution

Attaphon Maneedaeng* and Adrian E. Flood

School of Chemical Engineering, Institute of Engineering, Suranaree University of Technology 30000, Thailand

1. Introduction and Objective

In hard water, sodium dodecyl sulfate (SDS) tends to precipitate with the counterions Ca^{2+} and Mg^{2+} , and the SDS is thus no longer available to participate in the cleaning action. The scum formed from the precipitation is also a problem, however the solubility data of precipitated crystals remains limited, and consequently this work aims to investigate the solubility of precipitated crystals of calcium dodecyl sulfate (CDS) in aqueous solutions as a function of temperature with thermodynamic modeling between 10 and 55°C. The activity-based solubility products (K_{sp}) determined here could be used with previously determined data on micellization to model the phase boundary of SDS precipitated with calcium chloride at any specific temperature.

2. Materials and Experimental Procedure

2.1 Materials

The anionic surfactant used in this study was sodium dodecyl sulfate, obtained from Carlo Erba with a purity of 98%. Reagent-grade dihydrate calcium chloride was obtained from Carlo Erba. Both were used as received. Deionized water was used in the preparation of the CDS crystals used in the solubility measurements.

2.2 Experimental Procedure

2.2.1 Crystal Preparation

Calcium dodecyl sulfate (CDS) was prepared by precipitation upon reacting sodium dodecyl sulfate with calcium chloride. The crystals were separated by a 0.45 μm cellulose nitrate membrane and rinsed with deionized water. After drying by silica gel at room temperature overnight, they were then recrystallized in water. The pure CDS was separated by filter paper and dried by silica gel at room temperature overnight. Dried CDS crystals were used to prepare a number of solutions in deionized water.

2.2.2 Solubility Measurements

The critical micelle concentration (CMC) is the concentration at which surfactant molecules start to form spherical micelles; in this case the CMC of CDS is approximately at 2.4 mM (Hoffmann, 2002). However, CDS still behaves like a conventional anionic surfactant. Due to micellization, both atomic-absorption spec-

troscopy (AAS) and conductometry were used to measure the solubility. The Krafft temperature (micellization temperature), the minimum temperature at which surfactants form micelles, of CDS was at 50°C (Lee et al, 1979).

The AAS technique was not used for all temperatures since at just above the Krafft temperature the solubility dramatically increases with temperature, leading to laborious preparation of the sample solutions of varying temperature. Conductometry is another technique providing a powerful tool for investigating anionic surfactant systems. This technique was used here at and above the Krafft temperature.

Below the Krafft temperature

A series of CDS solutions were prepared at different equilibrium saturation temperature ranging from 10 to 50°C. Additional saturation solutions at 51, 53, and 55°C were prepared to verify the consistency of the two measurement techniques. AAS was used to measure the amount of calcium ions in the solutions; the total amount of surfactant can be estimated using the stoichiometric ratio of calcium ion to the surfactant monomer. The mass solubilities were reported at the known saturation temperature. The mass solubility was reported three times for each batch and there were three batches per saturation temperature. Replicates showed that the experimental data were highly reproducible.

Above the Krafft temperature

Conductometry was used to measure the solubility by determining the equilibrium saturation temperature of known concentration solutions at 0.5, 3, 4, 6, 8, and 10 mM. The equilibrium temperature was determined by measuring the conductivity of a surfactant solution as a function of temperature. The concentration at the discontinuity is the solubility at the saturation temperature.

2.2.3 The Calculation of the Solubility Product

Case I: Below the CMC

All disassociated surfactants are only in the monomeric form and calcium ions freely dissolve in the solution, so the expression will not change due to the micellar effect. The activity-based solubility product can be expressed as

$$K_{sp} = [\text{Ca}^{2+}][\text{DS}]^2 f_{\text{Ca}^{2+}} f_{\text{DS}^{2-}}^2 \quad (1)$$

* Corresponding author; E-mail: attaphonm@hotmail.com

FUPI2_2

Where $[DS]$ is the total surfactant concentration, $[Ca^{2+}]$ is the total calcium concentration in solution. The parameter f_{DS} and $f_{Ca^{2+}}$ are the activity coefficients of the surfactant and calcium, respectively.

Case II: Above the CMC

The solubility product relationship that describes surfactant precipitation above the CMC is shown in Equation 2:

$$K_{sp} = [Ca^{2+}]_{in} [DS]_{mon}^2 f_{Ca^{2+}} f_{DS}^{-2} \quad (2)$$

Where $[DS]_{mon}$ is the monomeric concentration of the precipitating surfactant and $[Ca^{2+}]_{in}$ is the concentration of calcium ions that are not bound to micelles. The activity coefficients for insertion into Equations 1 and 2 are found using an extended Debye-Hückel expression (Klotz, et al, 2000):

$$\log f = -A(z)^2 I^{0.5} / (1 + Ba I^{0.5}) - 0.3I \quad (3)$$

The constants A and B are dependent on the solvent and the temperature of solution. The parameter z is the ion valence and the parameter a is an empirical value based on the diameter of the ion. I represents the ionic strength. Data to calculate the binding of calcium ions onto DS micelles has been reported (Stellner et al, 1988).

3. Results and Discussion

3.1 Below the Krafft temperature

Table 1 The total amount of Ca^{2+} ions in CDS solution at various saturation temperatures determined from the AAS technique.

Temperature(°C)	Avg. Conc (mg/L)	Molar Conc (mM)
10	10.1367	0.2529
20	12.7600	0.3184
30	17.6767	0.4411
40	23.0833	0.5760
50	36.9417	0.9217

3.2 Above the Krafft temperature

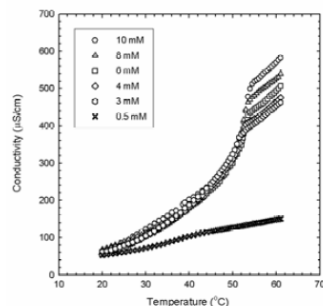


Figure 1 Evolution of conductivity as a function of temperature for different concentrations of CDS in aqueous solution.

The experimental results are shown in Table 1 and Figure 1. Discontinuity points show the equilibrium saturation temperature for each concentration and can be used to calculate K_{sp} using Equations 1 and 2.

3.3 Solubility Product Curve for CDS

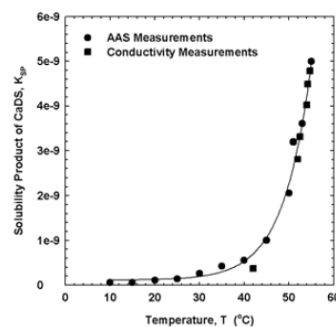


Figure 2 Solubility product of CDS in aqueous solution as function of temperature for different methods of measurements

The calculated solubility product is plotted against temperature in Figure 2. The solubility of CDS dramatically increases above the Krafft temperature. The plotted data indicate the consistency between the techniques. An exponential growth function as a function of temperature ($T, ^\circ C$) was assumed to fit the data, with $R^2 = 1.0000$ as:

$$K_{sp} = (1.9369 \times 10^{-10}) + (2.1101 \times 10^{-14}) \exp(0.2289 T) \quad (4)$$

The solubility products have been used to model the phase boundary of SDS precipitated with $CaCl_2$ at 10 and $50^\circ C$. However, this work is not shown here due to the space limitation of the extended abstract.

4. Conclusion

Both techniques for measuring the solubility of CDS yield consistent values of K_{sp} . The solubility of CDS in aqueous solution grows exponentially as a function of temperature. The calculated activity-based solubility product can be used to model the precipitation phase boundary of SDS and $CaCl_2$ as well.

5. Acknowledgment

AM and AEF would like to acknowledge the support of the Thailand Research Fund through the Royal Golden Jubilee Ph.D. program, grant no. 1.C.TS/47/B.1.

6. Selected Reference

Stellner, K.L., and J.F. Scamehorn (1988), *Hardness Tolerance of Anionic Surfactant Solutions: 1. Anionic Surfactant with Added Monovalent Electrolyte*, Langmuir, 5, 70-77.

An Investigation into Inhibition of Precipitation of Mixed Anionic Surfactant Systems

A. Maneedaeng^{1,*}, K. J. Haller², B. P. Grady³, and A. E. Flood¹

¹School of Chemical Engineering, Suranaree University of Technology, Nakhon Ratchasima, 30000 Thailand, ²School of Chemistry, Suranaree University of Technology, Nakhon Ratchasima, 30000 Thailand, ³School of Chemical, Biological, and Materials Engineering, University of Oklahoma, Norman, Oklahoma, 73019 USA

Binary anionic surfactant was used to investigate the synergism on the increase in the induction time for nucleation of anionic surfactants precipitated by divalent ions forming soap scum. The induction time was investigated via an online turbidity device for two binary systems; NaDS/NaOBS and NaDS/NaDeS, with various degrees of supersaturation, in order to monitor the increase in the induction time. The Regular Solution and Pseudophase Separation theories were employed to quantify surfactant concentrations in micellar and monomeric phases. The results show that the NaDS/NaOBS system is ideal while the NaDS/NaDeS is not ideal due to the difference in the molecular size. The degree of counterion binding to the micelle was monitored by activity measurement using an ion-specific electrode. The chemical equilibrium of unbound and bound counterions during the micellization can be used to model the fraction of counterion binding to the micelle relatively well. The results show that the inhibition of anionic surfactant precipitation is due partly to the thermodynamic change and is also partly due to a change in the energy required to create the surface of the critical nuclei, as shown by mixed systems having a different nucleation time dependence on supersaturation than the related pure system.

Measurement and Modeling of Thermodynamic Parameters in Binary Anionic Surfactants Systems and the Effect of Counterion Binding to the Micelle

Attaphon Maneedaeng,^a Kenneth J. Haller,^b Brian P. Grady,^c and Adrian E. Flood^a

^a School of Chemical Engineering, Suranaree University of Technology, Nakhon Ratchasima, 30000 Thailand

^b School of Chemistry, Suranaree University of Technology, Nakhon Ratchasima, 30000 Thailand

^c School of Chemical, Biological, and Materials Engineering, University of Oklahoma, Norman, OK 73019 USA

Introduction and Objective

Binary anionic surfactant mixtures show an excellent ability to increase the induction time of anionic surfactant precipitated by divalent ions. The binary system, however, is relatively complex due to the mixed micellization and counterion binding to the micelle. Hence, this work aims to investigate the thermodynamic parameters and surface properties of binary anionic surfactant mixtures by Regular Solution Theory (RST) together with an investigation of the fraction of counterion binding to the micelle.

Methods

Sodium dodecyl sulfate (NaDS) was mixed with sodium octylbenzene sulfonate (NaOBS) and with sodium decyl sulfate (NaDeS). The surface tension of various molar ratios of the two binary anionic surfactant solutions was measured by a tensiometer at 30°C in order to determine the Critical Micelle Concentration of the surfactant mixture (CMC_M). RST was employed to quantify the surfactant concentration in monomeric and micellar phases. The thermodynamic parameters and surface properties were determined from RST and Gibbs adsorption isotherm, respectively. The counterion binding to the micelle was investigated by activity measurement using an ion-specific electrode (ISE). Na-ISE and Ca-ISE were used to monitor the response during micellization at 30°C. The electrode potential can be converted to activity by Nernst equation, and unbound and bound counterion concentrations were obtained. The chemical equilibrium of unbound and bound counterion during the micellization was used to model the fraction of counterion binding to the micelle.

Results

The experimental results show the NaDS/NaOBS system is ideal while the NaDS/NaDeS system is not ideal due to the difference in the size of the molecules. RST can be applied to binary anionic surfactant systems relatively well. The counterion binding to the micelle is not constant at the commencement of micellization due to the competitiveness of the monovalent and divalent cation binding to the micelle but, the overall fraction of counterion binding can be assumed to be constant. The chemical equilibrium of unbound and bound counterion can be used to model the fraction of counterion binding to the micelle very well.

Conclusion

RST can model the CMC_M relatively well and thermodynamic parameters for the system studied are obtained. The fraction of counterion binding to the micelle can be modeled by chemical equilibrium. All modeling works are in good agreement with experimental data.

Keywords: mixed anionic surfactants, regular solution theory, counterion binding

Selected References

1. Sasaki, T., Hattori, M., Sasaki, J., Nukina, K. *Bull Chem Soc Jpn* 1975; 48(5): 1397-1403.
2. Holland, P., Rubingh, D. *J. Phys Chem* 1983; 8(11): 1984-1990.
3. Vora, S., Geoge, A., Desai, H., Bahadur, P. *J Surf Det* 1999; 2(2): 213-221.

Precipitation of Calcium Dodecyl Sulfate under the Influence of Sodium Decyl Sulfate in the Binary Anionic Surfactant Systems

Atthaphon Maneedaeng¹, Kenneth J. Haller², Brian P. Grady³ and Adrian E. Flood⁴

^{1,4}*School of Chemical Engineering, Suranaree University of Technology, Nakhon Ratchasima 30000 Thailand.*

²*School of Chemistry, Suranaree University of Technology, Nakhon Ratchasima 30000 Thailand*

³*School of Chemical, Biological and Materials Engineering, University of Oklahoma, Norman OK 73019 USA*

Precipitation of Anionic surfactants by counterions contained in hard water has been a problem in detergent industry. This is because of scum forming that readily inhibits cleaning action yielding the unacceptable cleaning result. It has been previously known that the use of mixed surfactant systems can prolong the induction time of surfactant precipitation compared to the single anionic surfactant systems in hard water, however, it is currently not known whether this inhibition is due to a change in the thermodynamics of the system, inhibition of nuclei formation, or inhibition of crystal growth. In this study, the induction time for calcium dodecyl sulfate has been investigated with several supersaturation ratios via the visual observation both in single and mixed surfactant systems: sodium dodecyl sulfate is used to mix with sodium decyl sulfate precipitated with calcium chloride. The results can show that the single surfactant systems that the induction time is far smaller for solutions with a surfactant concentration above the critical micelle concentration than for solutions below this point. Besides, the results imply that micelles probably act as a template for nucleation. The mechanism of inhibition appears to be related to the decreased influence of the mixed micelle as compared to the micelle in the single surfactant system. The mixed micelle contains species of both surfactants, present in solution at mole fractions determined by the use of the regular solution theory, and therefore the mixed micelles appear to be less effective as nucleation inhibitors and the prolongation in induction time has been visually observed. Precipitation rates for calcium dodecyl sulfate reveal that the key kinetic feature of the precipitation is the induction time for nucleation while the nucleation rates at the point of induction are sufficiently high that means the crystal growth kinetics do not play a significant role in the overall time required for complete precipitation.

Measurement and Modeling of the Solubility of Calcium Dodecyl Sulfate

Atthaphon Maneedaeng and Adrian E. Flood

School of Chemical Engineering, Suranaree University of Technology, Nakhon Ratchasima 30000, Thailand.

Introduction and Objective

In hard water, sodium dodecyl sulfate (SDS) tends to precipitate with the counterions, Ca^{2+} and Mg^{2+} , and the SDS is thus no longer available to participate in the cleaning action. The scum formed from the precipitation is also a problem in the cleaning. The solubility data of those precipitated crystals remains quite limited. Consequently, this work aims to investigate the solubility product of those precipitated crystals in aqueous solutions as a function of temperature with modeling between 10°C to 55°C.

Methods

Calcium dodecyl sulfate (CDS) was obtained from the precipitation of sodium dodecyl sulfate with calcium. The dry crystals were used to prepare a number of solutions of varying concentration in deionized water. The CDS behaves like a conventional anionic surfactant which leads to two techniques of measuring the solubility. The solutions were prepared at an 'equilibrium' saturation temperature from 10-50°C below the Krafft temperature, approximately 50°C for CDS (1) and the solutions were analyzed using the Atomic-Absorption Spectroscopy as the first technique; the mass solubility were reported at the known saturation temperature. Conductometry is another technique providing a powerful tool for investigating the systems (2). This technique was used due to the fact that at just above the Krafft temperature the solubility dramatically increases with temperature, leading to laborious preparation of the samples. The saturation temperature of a known concentration can be determined as a break in a curve of the conductivity plotted against temperature. The activity-based solubility product, K_{SP} , was calculated from the experimental data based on modeling of the present of micellar phase in solutions for the samples which is above the critical micelle concentration or CMC (3).

Results

The solubility product of CDS from the two techniques can be determined including with modeling. The solubility below the Krafft temperature slightly increases with temperature while above the Krafft temperature the solubility strongly increases with temperature. It is clear that both two techniques will yield the same value of K_{SP} . The exponential growth was assumed to fit the data resulting as $K_{\text{SP}} = 1.7149 \times 10^{-15} e^{0.2863T}$ with $R_{\text{sq}} = 0.9701$.

Conclusion

Both two techniques for measuring the solubility of CDS yield the consistent values of solubility product. The solubility behavior of CDS in aqueous solution can be predicted by the exponential growth as a function temperature.

Keywords: Solubility, Calcium Dodecyl Sulfate, Surfactant, Precipitation

Selected References:

1. Moroi, Y., Oyama, T. Matuura, R. *J. Colloid Interface Sci.* 1977; 60(1): 103.
2. Fergoug, T., Bendedouch, D., Aicart, E. *J. Colloids Surf. A* 2004; 237: 95-103.
3. Stellner, K.L., Scamehorn, J.F. *Langmuir* 1989; 5(1): 70-77.

BIOGRAPHY

Atthaphon Maneedaeng was born on March 22, 1982 in Bangkok. He earned his B.Eng. degree (first class honors) in Chemical Engineering in 2005 from Suranaree University of Technology, Nakhon Ratchasima. During the pursuit of his Ph.D. Atthaphon received a full scholarship provided by the Thailand Research Fund (TRF) through the Royal Golden Jubilee (RGJ) Ph.D. program from the beginning of his study in 2005. He has also had additional laboratory experience as an exchange scholar at the Institute of Applied Surfactant Research at the University of Oklahoma, Norman, USA, in 2008. Previously, he was an occupational trainee in Chemical Engineering at Well Services Division, Subsurface Department, Unocal (Thailand) Co., Ltd. during his Cooperative Education Program in 2004. His research interests cover the area of reactive crystallization and surfactant precipitation through the investigation of relevant thermodynamic and kinetic properties of mixtures of surfactants.